DEVELOPMENT OF A TSUNAMI FORECAST MODEL FOR

KIHEI, HAWAI‘I, USA

Edison Gica

Sept 15, 2011

Table of Contents

List of Tables 2
List of Figures 3
Abstract 24
1.0 Background and Objectives 24
2.0 Forecast Methodology 25
3. Model Development 26
3.1 Forecast area 26
3.2 Historical events and data 27
3.3 Model setup 27
4. Results and Discussion 28
4.1 Model validation 28
4.2 Model stability and reliability 28
4.3 Results of tested events 29
5. Summary and Conclusion 31
6.0 Acknowledgments 32
7.0 References 32
Appendix A 208

List of Tables

Table 1. MOST setup parameters for reference and forecast models for Kihei, Maui, Hawai'i..... 34

Table 2. Historical events with recorded run-up at Kihei, Maui, Hawai'i..... 35

Table 3. Historical events simulated for Kihei, Maui, Hawai'i. 36

Table 4. Synthetic mega-tsunamis tested for Kihei, Maui, Hawai'i..... 38

Table 5. Synthetic tsunamis with Mw = 7.5 and 0 (1 case) tested for Kihei, Hawai'i. 40

List of Figures

Figure 1. Location of Kihei, Maui, Hawai'i. 41

Figure 2. Plot of forecast model grid developed; a) Grid A, b) Grid B and c) Grid C. 42

Figure 3. Plot of reference model grid developed; a) Grid A, b) Grid B and c) Grid C. 42

Figure 4. Plot of Kahului DEM. 43

Figure 5. Location of Kihei, Maui, Hawai'i relative to historical events simulated. 44

Figure 6. Location of Kihei, Maui, Hawai'i relative to synthetic events simulated. 44

Figure 7. Plot of maximum tsunami wave amplitude distribution and tsunami time series at the warning point for 1946 Unimak tsunami with forecast model, a) A-grid, b) B-grid and c) C-grid. 45

Figure 8. Plot of maximum tsunami wave amplitude distribution and tsunami time series at the warning point for 1946 Unimak tsunami with reference model, a) A-grid, b) B-grid and c) C-grid. 45

Figure 9. Plot of maximum tsunami wave amplitude distribution and tsunami time series at the warning point for 1957 Andreanov tsunami with forecast model, a) A-grid, b) B-grid and c) C-grid. 46

Figure 10. Plot of maximum tsunami wave amplitude distribution and tsunami time series at the warning point for 1957 Andreanov tsunami with reference model, a) A-grid, b) B-grid and c) C-grid. 46

Figure 11. Plot of maximum tsunami wave amplitude distribution and tsunami time series at the warning point for 1960 Chile tsunami with forecast model, a) A-grid, b) B-grid and c) C-grid. .. 47

Figure 12. Plot of maximum tsunami wave amplitude distribution and tsunami time series at the warning point for 1960 Chile tsunami, a) A-grid, b) B-grid and c) C-grid. 47

Figure 13. Plot of maximum tsunami wave amplitude distribution and tsunami time series at the warning point for 1994 East Kuril tsunami with forecast model, a) A-grid, b) B-grid and c) C-grid. 48

Figure 14. Plot of maximum tsunami wave amplitude distribution and tsunami time series at the warning point for 1994 East Kuril tsunami with reference model, a) A-grid, b) B-grid and c) C-grid. 48

Figure 15. Plot of maximum tsunami wave amplitude distribution and tsunami time series at the warning point for 2003 Rat Island tsunami with forecast model, a) A-grid, b) B-grid and c) C-grid. 49

Figure 16. Plot of maximum tsunami wave amplitude distribution and tsunami time series at the warning point for 2003 Rat Island tsunami with reference model, a) A-grid, b) B-grid and c) C-grid. 49

Figure 17. Plot of maximum tsunami wave amplitude distribution and tsunami time series at the warning point for 2006 Tonga tsunami with forecast model, a) A-grid, b) B-grid and c) C-grid.. 50

Figure 18. Plot of maximum tsunami wave amplitude distribution and tsunami time series at the warning point for 2006 Tonga tsunami with reference model, a) A-grid, b) B-grid and c) C-grid. 50

Figure 19. Plot of maximum tsunami wave amplitude distribution and tsunami time series at the warning point for 2006 Kuril Island tsunami with forecast model, a) A-grid, b) B-grid and c) C-grid. 51

Figure 20. Plot of maximum tsunami wave amplitude distribution and tsunami time series at the warning point for 2006 Kuril Island tsunami with t reference model, a) A-grid, b) B-grid and c) C-grid. 51

Figure 21. Plot of maximum tsunami wave amplitude distribution and tsunami time series at the warning point for 2007 Kuril Island tsunami with forecast model, a) A-grid, b) B-grid and c) C-grid. 52

Figure 22. Plot of maximum tsunami wave amplitude distribution and tsunami time series at the warning point for 2007 Kuril Island tsunami with reference model, a) A-grid, b) B-grid and c) C-grid. 52

Figure 23. Plot of maximum tsunami wave amplitude distribution and tsunami time series at the warning point for 2007 Solomon tsunami with forecast model, a) A-grid, b) B-grid and c) C-grid. 53

Figure 24. Plot of maximum tsunami wave amplitude distribution and tsunami time series at the warning point for 2007 Solomon tsunami with reference model, a) A-grid, b) B-grid and c) C-grid. 53

Figure 25. Plot of maximum tsunami wave amplitude distribution and tsunami time series at the warning point for 2007 Peru tsunami with forecast model, a) A-grid, b) B-grid and c) C-grid. . . . 54

Figure 26. Plot of maximum tsunami wave amplitude distribution and tsunami time series at the warning point for 2007 Peru tsunami with reference model, a) A-grid, b) B-grid and c) C-grid. . 54

Figure 27. Plot of maximum tsunami wave amplitude distribution and tsunami time series at the warning point for 2009 Samoa tsunami with forecast model, a) A-grid, b) B-grid and c) C-grid. 55

Figure 28. Plot of maximum tsunami wave amplitude distribution and tsunami time series at the warning point for 2009 Samoa tsunami with reference model, a) A-grid, b) B-grid and c) C-grid. 55

Figure 29. Plot of maximum tsunami wave amplitude distribution and tsunami time series at the warning point for 2010 Chile tsunami with forecast model, a) A-grid, b) B-grid and c) C-grid. .. 56

Figure 30. Plot of maximum tsunami wave amplitude distribution and tsunami time series at the warning point for 2010 Chile tsunami with reference model, a) A-grid, b) B-grid and c) C-grid.. 56

Figure 31. Plot of maximum tsunami wave amplitude distribution and tsunami time series at the warning point for 2011 Honshu tsunami with forecast model, a) A-grid, b) B-grid and c) C-grid.57

Figure 32. Plot of maximum tsunami wave amplitude distribution and tsunami time series at the warning point for 2011 Honshu tsunami with reference model, a) A-grid, b) B-grid and c) C-grid. 57

Figure 33. Comparative plot of maximum/minimum tsunami wave amplitude distribution and tsunami time series at the warning point for the 1946 Unimak tsunami between forecast and reference models. The red circle indicates the location of historical run-up while the blue square is the location of simulated run-up..... 58

Figure 34. Comparative plot of maximum/minimum tsunami wave amplitude distribution and tsunami time series at the warning point for 1957 Andreanov tsunami between forecast and reference models. The red circle indicates the location of historical run-up while the blue square is the location of simulated run-up..... 59

Figure 35. Comparative plot of maximum/minimum tsunami wave amplitude distribution and tsunami time series at the warning point for 1960 Chile tsunami between forecast and reference models. The red circle indicates the location of historical run-up while the blue square is the location of simulated run-up. 60

Figure 36. Comparative plot of maximum/minimum tsunami wave amplitude distribution and tsunami time series at the warning point for 1994 East Kuril tsunami between forecast and reference models..... 61

Figure 37. Comparative plot of maximum/minimum tsunami wave amplitude distribution and tsunami time series at the warning point for 2003 Rat Island tsunami between forecast and reference models. 62

Figure 38. Comparative plot of maximum/minimum tsunami wave amplitude distribution and tsunami time series at the warning point for 2006 Tonga tsunami between forecast and reference models. 63

Figure 39. Comparative plot of maximum/minimum tsunami wave amplitude distribution and tsunami time series at the warning point for 2006 Kuril tsunami between forecast and reference models. 64

Figure 40. Comparative plot of maximum/minimum tsunami wave amplitude distribution and tsunami time series at the warning point for 2007 Kuril tsunami between forecast and reference models. 65

Figure 41. Comparative plot of maximum/minimum tsunami wave amplitude distribution and tsunami time series at the warning point for 2007 Solomon tsunami between forecast and reference models. 66

Figure 42. Comparative plot of maximum/minimum tsunami wave amplitude distribution and tsunami time series at the warning point for 2007 Peru tsunami between forecast and reference models. 67

Figure 43. Comparative plot of maximum/minimum tsunami wave amplitude distribution and tsunami time series at at the warning point for 2009 Samoa tsunami between forecast and reference models. 68

Figure 44. Comparative plot of maximum/minimum tsunami wave amplitude distribution and tsunami time series at the warning point for 2010 Chile tsunami between forecast and reference models. 69

Figure 45. Comparative plot of maximum/minimum tsunami wave amplitude distribution and tsunami time series at the warning point for 2011 Honshu tsunami between forecast and reference models. 70

Figure 46. Comparative plot of maximum current speed distribution, current speed and directionality at the warning point for 1946 Unimak tsunami between forecast and reference models. 71

Figure 47. Comparative plot of maximum current speed distribution, current speed and directionality at the warning point for 1957 Andreanov tsunami between forecast and reference models. 72

Figure 48. Comparative plot of maximum current speed distribution, current speed and directionality at the warning point at C-grid level for 1960 Chile tsunami between forecast reference models..... 73

Figure 49. Comparative plot of maximum current speed distribution, current speed and directionality at the warning point at C-grid level for 1994 East Kuril tsunami between forecast reference models..... 74

Figure 50. Comparative plot of maximum current speed distribution, current speed and directionality at the warning point at C-grid level for 2003 Rat Island tsunami between forecast reference models..... 75

Figure 51. Comparative plot of maximum current speed distribution, current speed and directionality at the warning point at C-grid level for 2006 Tonga tsunami between forecast reference models..... 76

Figure 52. Comparative plot of maximum current speed distribution, current speed and directionality at the warning point at C-grid level for 2006 Kuril tsunami between forecast reference models..... 77

Figure 53. Comparative plot of maximum current speed distribution, current speed and directionality at the warning point at C-grid level for 2007 Kuril tsunami between forecast reference models..... 78

Figure 54. Comparative plot of maximum current speed distribution, current speed and directionality at the warning point at C-grid level for 2007 Solomon tsunami between forecast reference models..... 79

Figure 55. Comparative plot of maximum current speed distribution, current speed and directionality at the warning point at C-grid level for 2007 Peru tsunami between forecast reference models..... 80

Figure 56. Comparative plot of maximum current speed distribution, current speed and directionality at the warning point at C-grid level for 2009 Samoa tsunami between forecast reference models..... 81

Figure 57. Comparative plot of maximum current speed distribution, current speed and directionality at the warning point at C-grid level for 2010 Chile tsunami between forecast reference models..... 82

Figure 58. Comparative plot of maximum current speed distribution, current speed and directionality at the warning point at C-grid level for 2011 Honshu tsunami between forecast reference models..... 83

Figure 59. Plot of maximum tsunami wave amplitude distribution for Grids A, B and C and tsunami time series at the warning point for synthetic case AC01-10 with forecast model. 84

Figure 60. Plot of maximum tsunami wave amplitude distribution for Grids A, B and C and tsunami time series at the warning point for synthetic case AC01-10 with reference model..... 84

Figure 61. Plot of maximum tsunami wave amplitude distribution for Grids A, B and C and tsunami time series at the warning point for synthetic case AC11-20 with forecast model. White areas on land indicate non-inundated sections. 85

Figure 62. Plot of maximum tsunami wave amplitude distribution for Grids A, B and C and tsunami time series at the warning point for synthetic case AC11-20 with reference model. White areas on land indicate non-inundated sections. 85

Figure 63. Plot of maximum tsunami wave amplitude distribution for Grids A, B and C and tsunami time series at the warning point for synthetic case AC21-30 with forecast model. White areas on land indicate non-inundated sections. 86

Figure 64. Plot of maximum tsunami wave amplitude distribution for Grids A, B and C and tsunami time series at the warning point for synthetic case AC21-30 with reference model. White areas on land indicate non-inundated sections. 86

Figure 65. Plot of maximum tsunami wave amplitude distribution for Grids A, B and C and tsunami time series at the warning point for synthetic case AC31-40 with forecast model. 87

Figure 66. Plot of maximum tsunami wave amplitude distribution for Grids A, B and C and tsunami time series at the warning point for synthetic case AC31-40 with reference model..... 87

Figure 67. Plot of maximum tsunami wave amplitude distribution for Grids A, B and C and tsunami time series at the warning point for synthetic case AC41-50 with forecast model. White areas on land indicate non-inundated sections. 88

Figure 68. Plot of maximum tsunami wave amplitude distribution for Grids A, B and C and tsunami time series at the warning point for synthetic case AC41-50 with reference model. White areas on land indicate non-inundated sections. 88

Figure 69. Plot of maximum tsunami wave amplitude distribution for Grids A, B and C and tsunami time series at the warning point for synthetic case AC46-55 with forecast model. White areas on land indicate non-inundated sections. 89

Figure 70. Plot of maximum tsunami wave amplitude distribution for Grids A, B and C and tsunami time series at the warning point for synthetic case AC46-55 with reference model. White areas on land indicate non-inundated sections. 89

Figure 71. Plot of maximum tsunami wave amplitude distribution for Grids A, B and C and tsunami time series at the warning point for synthetic case AC56-65 with forecast model. 90

Figure 72. Plot of maximum tsunami wave amplitude distribution for Grids A, B and C and tsunami time series at the warning point for synthetic case AC56-65 with reference model..... 90

Figure 73. Plot of maximum tsunami wave amplitude distribution for Grids A, B and C and tsunami time series at the warning point for synthetic case CS01-10 with forecast model..... 91

Figure 74. Plot of maximum tsunami wave amplitude distribution for Grids A, B and C and tsunami time series at the warning point for synthetic case CS01-10 with reference model..... 91

Figure 75. Plot of maximum tsunami wave amplitude distribution for Grids A, B and C and tsunami time series at the warning point for synthetic case CS11-20 with forecast model..... 92

Figure 76. Plot of maximum tsunami wave amplitude distribution for Grids A, B and C and tsunami time series at the warning point for synthetic case CS11-20 with reference model..... 92

Figure 77. Plot of maximum tsunami wave amplitude distribution for Grids A, B and C and tsunami time series at the warning point for synthetic case CS21-30 with forecast model..... 93

Figure 78. Plot of maximum tsunami wave amplitude distribution for Grids A, B and C and tsunami time series at the warning point for synthetic case CS21-30 with reference model..... 93

Figure 79. Plot of maximum tsunami wave amplitude distribution for Grids A, B and C and tsunami time series at the warning point for synthetic case CS31-40 with forecast model..... 94

Figure 80. Plot of maximum tsunami wave amplitude distribution for Grids A, B and C and tsunami time series at the warning point for synthetic case CS31-40 with reference model..... 94

Figure 81. Plot of maximum tsunami wave amplitude distribution for Grids A, B and C and tsunami time series at the warning point for synthetic case CS41-50 with forecast model..... 95

Figure 82. Plot of maximum tsunami wave amplitude distribution for Grids A, B and C and tsunami time series at the warning point for synthetic case CS41-50 with reference model..... 95

Figure 83. Plot of maximum tsunami wave amplitude distribution for Grids A, B and C and tsunami time series at the warning point for synthetic case CS51-60 with forecast model..... 96

Figure 84. Plot of maximum tsunami wave amplitude distribution for Grids A, B and C and tsunami time series at the warning point for synthetic case CS51-60 with reference model..... 96

Figure 85. Plot of maximum tsunami wave amplitude distribution for Grids A, B and C and tsunami time series at the warning point for synthetic case CSSZ 61-70 with forecast model.... 97

Figure 86. Plot of maximum tsunami wave amplitude distribution for Grids A, B and C and tsunami time series at the warning point for synthetic case CSSZ 61-70 with reference model.. 97

Figure 87. Plot of maximum tsunami wave amplitude distribution for Grids A, B and C and tsunami time series at the warning point for synthetic case CSSZ 71-80 with forecast model.... 98

Figure 88. Plot of maximum tsunami wave amplitude distribution for Grids A, B and C and tsunami time series at the warning point for synthetic case CSSZ 71-80 with reference model.. 98

Figure 89. Plot of maximum tsunami wave amplitude distribution for Grids A, B and C and tsunami time series at the warning point for synthetic case CSSZ 81-90 with forecast model. White areas on land indicate non-inundated sections. 99

Figure 90. Plot of maximum tsunami wave amplitude distribution for Grids A, B and C and tsunami time series at the warning point for synthetic case CSSZ 81-90 with reference model. White areas on land indicate non-inundated sections. 99

Figure 91. Plot of maximum tsunami wave amplitude distribution for Grids A, B and C and tsunami time series at the warning point for synthetic case CSSZ 91-100 with forecast model. White areas on land indicate non-inundated sections. 100

Figure 92. Plot of maximum tsunami wave amplitude distribution for Grids A, B and C and tsunami time series at the warning point for synthetic case CSSZ 91-100 with reference model. White areas on land indicate non-inundated sections. 100

Figure 93. Plot of maximum tsunami wave amplitude distribution for Grids A, B and C and tsunami time series at the warning point for synthetic case CSSZ 101-110 with forecast model. 101

Figure 94. Plot of maximum tsunami wave amplitude distribution for Grids A, B and C and tsunami time series at the warning point for synthetic case CSSZ 101-110 with reference model. 101

Figure 95. Plot of maximum tsunami wave amplitude distribution for Grids A, B and C and tsunami time series at the warning point for synthetic case CSSZ 106-115 with forecast model. White areas on land indicate non-inundated sections. 102

Figure 96. Plot of maximum tsunami wave amplitude distribution for Grids A, B and C and tsunami time series at the warning point for synthetic case CSSZ 106-115 with reference model. White areas on land indicate non-inundated sections. 102

Figure 97. Plot of maximum tsunami wave amplitude distribution for Grids A, B and C and tsunami time series at the warning point for synthetic case EPSZ 01-10 with forecast model. White areas on land indicate non-inundated sections. 103

Figure 98. Plot of maximum tsunami wave amplitude distribution for Grids A, B and C and tsunami time series at the warning point for synthetic case EPSZ 01-10 with reference model. White areas on land indicate non-inundated sections. 103

Figure 99. Plot of maximum tsunami wave amplitude distribution for Grids A, B and C and tsunami time series at the warning point for synthetic case EPSZ 09-18 with forecast model. White areas on land indicate non-inundated sections. 104

Figure 100. Plot of maximum tsunami wave amplitude distribution for Grids A, B and C and tsunami time series at the warning point for synthetic case EPSZ 09-18 with reference model. White areas on land indicate non-inundated sections. 104

Figure 101. Plot of maximum tsunami wave amplitude distribution for Grids A, B and C and tsunami time series at the warning point for synthetic case KISZ 01-10 with forecast model. White areas on land indicate non-inundated sections. 105

Figure 102. Plot of maximum tsunami wave amplitude distribution for Grids A, B and C and tsunami time series at the warning point for synthetic case KISZ 01-10 with reference model. White areas on land indicate non-inundated sections. 105

Figure 103. Plot of maximum tsunami wave amplitude distribution for Grids A, B and C and tsunami time series at the warning point for synthetic case KISZ 11-20 with forecast model. White areas on land indicate non-inundated sections. 106

Figure 104. Plot of maximum tsunami wave amplitude distribution for Grids A, B and C and tsunami time series at the warning point for synthetic case KISZ 11-20 with reference model. White areas on land indicate non-inundated sections. 106

Figure 105. Plot of maximum tsunami wave amplitude distribution for Grids A, B and C and tsunami time series at the warning point for synthetic case KISZ 32-41 with forecast model. White areas on land indicate non-inundated sections. 107

Figure 106. Plot of maximum tsunami wave amplitude distribution for Grids A, B and C and tsunami time series at the warning point for synthetic case KISZ 32-41 with reference model. White areas on land indicate non-inundated sections. 107

Figure 107. Plot of maximum tsunami wave amplitude distribution for Grids A, B and C and tsunami time series at the warning point for synthetic case KISZ421-51 with forecast model. White areas on land indicate non-inundated sections. 108

Figure 108. Plot of maximum tsunami wave amplitude distribution for Grids A, B and C and tsunami time series at the warning point for synthetic case KISZ 42-51 with reference model. White areas on land indicate non-inundated sections. 108

Figure 109. Plot of maximum tsunami wave amplitude distribution for Grids A, B and C and tsunami time series at the warning point for synthetic case KISZ52-61 with forecast model. White areas on land indicate non-inundated sections. 109

Figure 110. Plot of maximum tsunami wave amplitude distribution for Grids A, B and C and tsunami time series at the warning point for synthetic case KISZ 52-61 with reference model. White areas on land indicate non-inundated sections. 109

Figure 111. Plot of maximum tsunami wave amplitude distribution for Grids A, B and C and tsunami time series at the warning point for synthetic case KISZ56-65 with forecast model. White areas on land indicate non-inundated sections. 110

Figure 112. Plot of maximum tsunami wave amplitude distribution for Grids A, B and C and tsunami time series at the warning point for synthetic case KISZ 56-65 with reference model. White areas on land indicate non-inundated sections. 110

Figure 113. Plot of maximum tsunami wave amplitude distribution for Grids A, B and C and tsunami time series at the warning point for synthetic case KISZ66-75 with forecast model. White areas on land indicate non-inundated sections. 111

Figure 114. Plot of maximum tsunami wave amplitude distribution for Grids A, B and C and tsunami time series at the warning point for synthetic case KISZ66-75 with reference model. White areas on land indicate non-inundated sections. 111

Figure 115. Plot of maximum tsunami wave amplitude distribution for Grids A, B and C and tsunami time series at the warning point for synthetic case MOSZ01-10 with forecast model. White areas on land indicate non-inundated sections. 112

Figure 116. Plot of maximum tsunami wave amplitude distribution for Grids A, B and C and tsunami time series at the warning point for synthetic case MOSZ01-10 with reference model. White areas on land indicate non-inundated sections. 112

Figure 117. Plot of maximum tsunami wave amplitude distribution for Grids A, B and C and tsunami time series at the warning point for synthetic case MOSZ08-17 with forecast model.. 113

Figure 118. Plot of maximum tsunami wave amplitude distribution for Grids A, B and C and tsunami time series at the warning point for synthetic case MOSZ08-17 with reference model. 113

Figure 119. Plot of maximum tsunami wave amplitude distribution for Grids A, B and C and tsunami time series at the warning point for synthetic case NGSZ01-10 with forecast model. . 114

Figure 120. Plot of maximum tsunami wave amplitude distribution for Grids A, B and C and tsunami time series at the warning point for synthetic case NGSZ01-10 with reference model. 114

Figure 121. Plot of maximum tsunami wave amplitude distribution for Grids A, B and C and tsunami time series at the warning point for synthetic case NGSZ06-15 with forecast model. . 115

Figure 122. Plot of maximum tsunami wave amplitude distribution for Grids A, B and C and tsunami time series at the warning point for synthetic case NGSZ06-15 with reference model. 115

Figure 123. Plot of maximum tsunami wave amplitude distribution for Grids A, B and C and tsunami time series at the warning point for synthetic case NTSZ01-10 with forecast model. . 116

Figure 124. Plot of maximum tsunami wave amplitude distribution for Grids A, B and C and tsunami time series at the warning point for synthetic case NTSZ01-10 with reference model. 116

Figure 125. Plot of maximum tsunami wave amplitude distribution for Grids A, B and C and tsunami time series at the warning point for synthetic case NTSZ11-20 with forecast model. . 117

Figure 126. Plot of maximum tsunami wave amplitude distribution for Grids A, B and C and tsunami time series at the warning point for synthetic case NTSZ11-20 with reference model. 117

Figure 127. Plot of maximum tsunami wave amplitude distribution for Grids A, B and C and tsunami time series at the warning point for synthetic case NTSZ21-30 with forecast model. . 118

Figure 128. Plot of maximum tsunami wave amplitude distribution for Grids A, B and C and tsunami time series at the warning point for synthetic case NTSZ21-30 with reference model. 118

Figure 129. Plot of maximum tsunami wave amplitude distribution for Grids A, B and C and tsunami time series at the warning point for synthetic case NTSZ30-39 with forecast model. . 119

Figure 130. Plot of maximum tsunami wave amplitude distribution for Grids A, B and C and tsunami time series at the warning point for synthetic case NTSZ30-39 with reference model. 119

Figure 131. Plot of maximum tsunami wave amplitude distribution for Grids A, B and C and tsunami time series at the warning point for synthetic case NVSZ01-10 with forecast model. . 120

Figure 132. Plot of maximum tsunami wave amplitude distribution for Grids A, B and C and tsunami time series at the warning point for synthetic case NVSZ01-10 with reference model. 120

Figure 133. Plot of maximum tsunami wave amplitude distribution for Grids A, B and C and tsunami time series at the warning point for synthetic case NVSZ11-20 with forecast model. . 121

Figure 134. Plot of maximum tsunami wave amplitude distribution for Grids A, B and C and tsunami time series at the warning point for synthetic case NVSZ11-20 with reference model. 121

Figure 135. Plot of maximum tsunami wave amplitude distribution for Grids A, B and C and tsunami time series at the warning point for synthetic case NVSZ28-37 with forecast model. White areas on land indicate non-inundated sections. 122

Figure 136. Plot of maximum tsunami wave amplitude distribution for Grids A, B and C and tsunami time series at the warning point for synthetic case NVSZ28-37 with reference model. White areas on land indicate non-inundated sections. 122

Figure 137. Plot of maximum tsunami wave amplitude distribution for Grids A, B and C and tsunami time series at the warning point for synthetic case RNSZ01-10 with forecast model. . 123

Figure 138. Plot of maximum tsunami wave amplitude distribution for Grids A, B and C and tsunami time series at the warning point for synthetic case RNSZ01-10 with reference model. 123

Figure 139. Plot of maximum tsunami wave amplitude distribution for Grids A, B and C and tsunami time series at the warning point for synthetic case RNSZ13-22 with forecast model. White areas on land indicate non-inundated sections. 124

Figure 140. Plot of maximum tsunami wave amplitude distribution for Grids A, B and C and tsunami time series at the warning point for synthetic case RNSZ13-22 with reference model. White areas on land indicate non-inundated sections. 124

Figure 141. Comparative plot of maximum/minimum tsunami wave amplitude distribution and tsunami time series at C-grid level for synthetic case ACSZ01-10 between forecast and reference models. White areas on land for the top two figures indicate non-inundated sections..... 125

Figure 142. Comparative plot of maximum/minimum tsunami wave amplitude distribution and tsunami time series at C-grid level for synthetic case AC11-20 between forecast and reference models. White areas on land for the top two figures indicate non-inundated sections..... 126

Figure 143. Comparative plot of maximum/minimum tsunami wave amplitude distribution and tsunami time series at C-grid level for synthetic case AC21-30 between forecast and reference models. White areas on land for the top two figures indicate non-inundated sections..... 127

Figure 144. Comparative plot of maximum/minimum tsunami wave amplitude distribution and tsunami time series at C-grid level for synthetic case AC31-40 between forecast and reference models. 128

Figure 145. Comparative plot of maximum/minimum tsunami wave amplitude distribution and tsunami time series at C-grid level for synthetic case AC41-50 between forecast and reference models. White areas on land for the top two figures indicate non-inundated sections..... 129

Figure 146. Comparative plot of maximum/minimum tsunami wave amplitude distribution and tsunami time series at C-grid level for synthetic case AC46-55 between forecast and reference models. White areas on land for the top two figures indicate non-inundated sections..... 130

Figure 147. Comparative plot of maximum/minimum tsunami wave amplitude distribution and tsunami time series at C-grid level for synthetic case AC56-65 between forecast and reference models. White areas on land for the top two figures indicate non-inundated sections..... 131

Figure 148. Comparative plot of maximum/minimum tsunami wave amplitude distribution and tsunami time series at C-grid level for synthetic case CS01-10 between forecast and reference models. 132

Figure 149. Comparative plot of maximum/minimum tsunami wave amplitude distribution and tsunami time series at C-grid level for synthetic case CS11-20 between forecast and reference models. 133

Figure 150. Comparative plot of maximum/minimum tsunami wave amplitude distribution and tsunami time series at C-grid level for synthetic case CS21-30 between forecast and reference models. 134

Figure 151. Comparative plot of maximum/minimum tsunami wave amplitude distribution and tsunami time series at C-grid level for synthetic case CS31-40 between forecast and reference models. 135

Figure 152. Comparative plot of maximum/minimum tsunami wave amplitude distribution and tsunami time series at C-grid level for synthetic case CS41-50 between forecast and reference models. 136

Figure 153. Comparative plot of maximum/minimum tsunami wave amplitude distribution and tsunami time series at C-grid level for synthetic case CS51-60 between forecast and reference models. 137

Figure 154. Comparative plot of maximum/minimum tsunami wave amplitude distribution and tsunami time series at C-grid level for synthetic case CSSZ 61-70 between forecast and reference models. 138

Figure 155. Comparative plot of maximum/minimum tsunami wave amplitude distribution and tsunami time series at C-grid level for synthetic case CSSZ 71-80 between forecast and reference models. 139

Figure 156. Comparative plot of maximum/minimum tsunami wave amplitude distribution and tsunami time series at C-grid level for synthetic case CSSZ 81-90 between forecast and reference models. White areas on land for the top two figures indicate non-inundated sections..... 140

Figure 157. Comparative plot of maximum/minimum tsunami wave amplitude distribution and tsunami time series at C-grid level for synthetic case CSSZ 91-100 between forecast and reference models. White areas on land for the top two figures indicate non-inundated sections. 141

Figure 158. Comparative plot of maximum/minimum tsunami wave amplitude distribution and tsunami time series at C-grid level for synthetic case CSSZ 101-110 between forecast and reference models. White areas on land for the top two figures indicate non-inundated sections. 142

Figure 159. Comparative plot of maximum/minimum tsunami wave amplitude distribution and tsunami time series at C-grid level for synthetic case CSSZ 106-115 between forecast and reference models. White areas on land for the top two figures indicate non-inundated sections. 143

Figure 160. Comparative plot of maximum/minimum tsunami wave amplitude distribution and tsunami time series at C-grid level for synthetic case EPSZ 01-10 between forecast and reference models. White areas on land for the top two figures indicate non-inundated sections..... 144

Figure 161. Comparative plot of maximum/minimum tsunami wave amplitude distribution and tsunami time series at C-grid level for synthetic case EPSZ 09-18 between forecast and reference models. White areas on land for the top two figures indicate non-inundated sections..... 145

Figure 162. Comparative plot of maximum/minimum tsunami wave amplitude distribution and tsunami time series at C-grid level at the warning point for synthetic case KISZ 01-10 between forecast and reference models. White areas on land for the top two figures indicate non-inundated sections..... 146

Figure 163. Comparative plot of maximum/minimum tsunami wave amplitude distribution and tsunami time series at C-grid level for synthetic case KISZ 11-20 between forecast and reference models. White areas on land for the top two figures indicate non-inundated sections..... 147

Figure 164. Comparative plot of maximum/minimum tsunami wave amplitude distribution and tsunami time series at C-grid level for synthetic case KISZ 32-41 between forecast and reference models. White areas on land for the top two figures indicate non-inundated sections..... 148

Figure 165. Comparative plot of maximum/minimum tsunami wave amplitude distribution and tsunami time series at C-grid level for synthetic case KISZ421-51 between forecast and reference models. White areas on land for the top two figures indicate non-inundated sections..... 149

Figure 166. Comparative plot of maximum/minimum tsunami wave amplitude distribution and tsunami time series at C-grid level for synthetic case KISZ52-61 between forecast and reference models. White areas on land for the top two figures indicate non-inundated sections..... 150

Figure 167. Comparative plot of maximum/minimum tsunami wave amplitude distribution and tsunami time series at C-grid level for synthetic case KISZ56-65 between forecast and reference models. White areas on land for the top two figures indicate non-inundated sections..... 151

Figure 168. Comparative plot of maximum/minimum tsunami wave amplitude distribution and tsunami time series at C-grid level for synthetic case KISZ66-75 between forecast and reference models. White areas on land for the top two figures indicate non-inundated sections..... 152

Figure 169. Comparative plot of maximum/minimum tsunami wave amplitude distribution and tsunami time series at C-grid level for synthetic case MOSZ01-10 between forecast and reference models. White areas on land for the top two figures indicate non-inundated sections..... 153

Figure 170. Comparative plot of maximum/minimum tsunami wave amplitude distribution and tsunami time series at C-grid level for synthetic case MOSZ08-17 between forecast and reference models. 154

Figure 171. Comparative plot of maximum/minimum tsunami wave amplitude distribution and tsunami time series at C-grid level for synthetic case NGSZ01-10 between forecast and reference models. 155

Figure 172. Comparative plot of maximum/minimum tsunami wave amplitude distribution and tsunami time series at C-grid level for synthetic case NGSZ06-15 between forecast and reference models. 156

Figure 173. Comparative plot of maximum/minimum tsunami wave amplitude distribution and tsunami time series at C-grid level for synthetic case NTSZ01-10 between forecast and reference models. White areas on land for the top two figures indicate non-inundated sections..... 157

Figure 174. Comparative plot of maximum/minimum tsunami wave amplitude distribution and tsunami time series at C-grid level for synthetic case NTSZ11-20 between forecast and reference models. 158

Figure 175. Comparative plot of maximum/minimum tsunami wave amplitude distribution and tsunami time series at C-grid level for synthetic case NTSZ21-30 between forecast and reference models. 159

Figure 176. Comparative plot of maximum/minimum tsunami wave amplitude distribution and tsunami time series at C-grid level for synthetic case NTSZ30-39 between forecast and reference models. 160

Figure 177. Comparative plot of maximum/minimum tsunami wave amplitude distribution and tsunami time series at C-grid level for synthetic case NVSZ01-10 between forecast and reference models. 161

Figure 178. Comparative plot of maximum/minimum tsunami wave amplitude distribution and tsunami time series at C-grid level for synthetic case NVSZ11-20 between forecast and reference models. 162

Figure 179. Comparative plot of maximum/minimum tsunami wave amplitude distribution and tsunami time series at C-grid level for synthetic case NVSZ28-37 between forecast and reference models. White areas on land for the top two figures indicate non-inundated sections..... 163

Figure 180. Comparative plot of maximum/minimum tsunami wave amplitude distribution and tsunami time series at C-grid level for synthetic case RNSZ01-10 between forecast and reference models. 164

Figure 181. Comparative plot of maximum/minimum tsunami wave amplitude distribution and tsunami time series at C-grid level for synthetic case RNSZ13-22 between forecast and reference models. White areas on land for the top two figures indicate non-inundated sections..... 165

Figure 182. Comparative plot of maximum current distribution, current speed and directionality at the warning point at C-grid level for synthetic case ACSZ01-10 between forecast and reference models. White areas on land for the top two figures indicate non-inundated sections..... 166

Figure 183. Comparative plot of maximum current distribution, current speed and directionality at the warning point at C-grid level for synthetic case AC11-20 between forecast and reference models. White areas on land for the top two figures indicate non-inundated sections..... 167

Figure 184. Plot of maximum tsunami wave amplitude distribution for Grids A, B and C and tsunami time series at the warning point for synthetic case AC21-30 between forecast and reference models. White areas on land for the top two figures indicate non-inundated sections. 168

Figure 185. Comparative plot of maximum current distribution, current speed and directionality at the warning point at C-grid level for synthetic case AC31-40 between forecast and reference models. 169

Figure 186. Comparative plot of maximum current distribution, current speed and directionality at the warning point at C-grid level for synthetic case AC41-50 between forecast and reference models. White areas on land for the top two figures indicate non-inundated sections..... 170

Figure 187. Comparative plot of maximum current distribution, current speed and directionality at the warning point at C-grid level for synthetic case AC46-55 between forecast and reference models. White areas on land for the top two figures indicate non-inundated sections..... 171

Figure 188. Comparative plot of maximum current distribution, current speed and directionality at the warning point at C-grid level for synthetic case AC56-65 between forecast and reference models. White areas on land for the top two figures indicate non-inundated sections..... 172

Figure 189. Comparative plot of maximum current distribution, current speed and directionality at the warning point at C-grid level for synthetic case CS01-10 between forecast and reference models. 173

Figure 190. Comparative plot of maximum current distribution, current speed and directionality at the warning point at C-grid level for synthetic case CS11-20 between forecast and reference models. 174

Figure 191. Comparative plot of maximum current distribution, current speed and directionality at the warning point at C-grid level for synthetic case CS21-30 between forecast and reference models. 175

Figure 192. Comparative plot of maximum current distribution, current speed and directionality at the warning point at C-grid level for synthetic case CS31-40 between forecast and reference models. 176

Figure 193. Comparative plot of maximum current distribution, current speed and directionality at the warning point at C-grid level for synthetic case CS41-50 between forecast and reference models. 177

Figure 194. Comparative plot of maximum current distribution, current speed and directionality at the warning point at C-grid level for synthetic case CS51-60 between forecast and reference models. 178

Figure 195. Comparative plot of maximum current distribution, current speed and directionality at the warning point at C-grid level for synthetic case CSSZ 61-70 between forecast and reference models..... 179

Figure 196. Comparative plot of maximum current distribution, current speed and directionality at the warning point at C-grid level for synthetic case CSSZ 71-80 between forecast and reference models..... 180

Figure 197. Comparative plot of maximum current distribution, current speed and directionality at the warning point at C-grid level for synthetic case CSSZ 81-90 between forecast and reference models. White areas on land for the top two figures indicate non-inundated sections. 181

Figure 198. Comparative plot of maximum current distribution, current speed and directionality at the warning point at C-grid level for synthetic case CSSZ 91-100 between forecast and reference models. White areas on land for the top two figures indicate non-inundated sections. 182

Figure 199. Comparative plot of maximum current distribution, current speed and directionality at the warning point at C-grid level for synthetic case CSSZ 101-110 between forecast and reference models. White areas on land for the top two figures indicate non-inundated sections. 183

Figure 200. Comparative plot of maximum current distribution, current speed and directionality at the warning point at C-grid level for synthetic case CSSZ 106-115 between forecast and reference models. White areas on land for the top two figures indicate non-inundated sections. 184

Figure 201. Comparative plot of maximum current distribution, current speed and directionality at the warning point at C-grid level point for synthetic case EPSZ 01-10 between forecast and reference models. White areas on land for the top two figures indicate non-inundated sections. 185

Figure 202. Comparative plot of maximum current distribution, current speed and directionality at the warning point at C-grid level for synthetic case EPSZ 09-18 between forecast and reference models..... 186

Figure 203. Comparative plot of maximum current distribution, current speed and directionality at the warning point at C-grid level for synthetic case KISZ 01-10 between forecast and reference models. White areas on land for the top two figures indicate non-inundated sections..... 187

Figure 204. Comparative plot of maximum current distribution, current speed and directionality at the warning point at C-grid level for synthetic case KISZ 11-20 between forecast and reference models. White areas on land for the top two figures indicate non-inundated sections..... 188

Figure 205. Comparative plot of maximum current distribution, current speed and directionality at the warning point at C-grid level for synthetic case KISZ 32-41 between forecast and reference models. White areas on land for the top two figures indicate non-inundated sections..... 189

Figure 206. Comparative plot of maximum current distribution, current speed and directionality at the warning point at C-grid level for synthetic case KISZ421-51 between forecast and reference models. White areas on land for the top two figures indicate non-inundated sections. 190

Figure 207. Comparative plot of maximum current distribution, current speed and directionality at the warning point at C-grid level for synthetic case KISZ52-61 between forecast and reference models. White areas on land for the top two figures indicate non-inundated sections..... 191

Figure 208. Comparative plot of maximum current distribution, current speed and directionality at the warning point at C-grid level t for synthetic case KISZ56-65 between forecast and reference models. White areas on land for the top two figures indicate non-inundated sections. 192

Figure 209. Comparative plot of maximum current distribution, current speed and directionality at the warning point at C-grid level for synthetic case KISZ66-75 between forecast and reference models. White areas on land for the top two figures indicate non-inundated sections..... 193

Figure 210. Comparative plot of maximum current distribution, current speed and directionality at the warning point at C-grid level for synthetic case MOSZ01-10 between forecast and reference models. White areas on land for the top two figures indicate non-inundated sections. 194

Figure 211. Comparative plot of maximum current distribution, current speed and directionality at the warning point at C-grid level for synthetic case MOSZ08-17 between forecast and reference models..... 195

Figure 212. Comparative plot of maximum current distribution, current speed and directionality at the warning point at C-grid level for synthetic case NGSZ01-10 between forecast and reference models. 196

Figure 213. Comparative plot of maximum current distribution, current speed and directionality at the warning point at C-grid level for synthetic case NGSZ06-15 between forecast and reference models. 197

Figure 214. Comparative plot of maximum current distribution, current speed and directionality at the warning point at C-grid level for synthetic case NTSZ01-10 between forecast and reference models. White areas on land for the top two figures indicate non-inundated sections..... 198

Figure 215. Comparative plot of maximum current distribution, current speed and directionality at the warning point at C-grid level for synthetic case NTSZ11-20 between forecast and reference models. 199

Figure 216. Comparative plot of maximum current distribution, current speed and directionality at the warning point at C-grid level for synthetic case NTSZ21-30 between forecast and reference models. 200

Figure 217. Comparative plot of maximum current distribution, current speed and directionality at the warning point at C-grid level for synthetic case NTSZ30-39 between forecast and reference models. 201

Figure 218. Comparative plot of maximum current distribution, current speed and directionality at the warning point at C-grid level for synthetic case NVSZ01-10 between forecast and reference models. 202

Figure 219. Comparative plot of maximum current distribution, current speed and directionality at the warning point at C-grid level for synthetic case NVSZ11-20 between forecast and reference models. 203

Figure 220. Comparative plot of maximum current distribution, current speed and directionality at the warning point at C-grid level for synthetic case NVSZ28-37 between forecast and reference models. White areas on land for the top two figures indicate non-inundated sections..... 204

Figure 221. Comparative plot of maximum current distribution, current speed and directionality at the warning point at C-grid level for synthetic case RNSZ01-10 between forecast and reference models. 205

Figure 222. Comparative plot of maximum current distribution, current speed and directionality at the warning point at C-grid level for synthetic case RNSZ13-22 between forecast and reference models. White areas on land for the top two figures indicate non-inundated sections..... 206

Figure 223. Location of Kihei, Maui, Hawai'i relative to simulated synthetic mega-events that generated low coastal impact. 207

Figure 224. Location of Kihei, Maui, Hawai'i relative to simulated synthetic mega-events that generated extreme coastal impact. 207

Development of a Tsunami Forecast Model for Kihei, Hawai‘i, USA

Edison Gica

Abstract

The National Oceanic and Atmospheric Administration has developed a tsunami forecast model for Kihei, Hawai'i, as part of an effort to provide tsunami forecasts for United States coastal communities. Development, validation, and stability testing of the tsunami forecast model has been conducted to ensure model robustness and stability. The Kihei, Hawai'i tsunami forecast model employs the Method of Splitting Tsunami numerical code. The forecast model was validated with three historical tsunamis and the stability and reliability was tested by simulating artificial tsunamis from different source regions. A total of 13 historical cases and 41 synthetic mega tsunami (M_w =9.4) events, 20 M_w = 7.5 and 1 M_w = 0 were simulated and the forecast model was stable for 24 hours. The Kihei, Hawai'i forecast model can generate 4 hours of tsunami wave characteristics in approximately 13.22 minutes of CPU time.

1.0 Background and Objectives

The National Oceanic and Atmospheric Administration (NOAA) Center for Tsunami Research (NCTR) at the NOAA Pacific Marine Environmental Laboratory (PMEL) has developed a tsunami forecasting capability for operational use by NOAA's two Tsunami Warning Centers located in Hawai'i and Alaska (Titov *et al.*, 2005). The system is designed to efficiently provide basin-wide warning of approaching tsunami waves accurately and quickly. The system, termed Short-term Inundation Forecast of Tsunamis (SIFT), combines real-time tsunami event data with numerical models to produce estimates of tsunami wave arrival times and amplitudes at a coastal community of interest. The SIFT system integrates several key components: deep-ocean observations of tsunamis in real time, a basin-wide pre-computed propagation database of water level and flow velocities based on potential seismic unit sources, an inversion algorithm to refine the tsunami source based on deep-ocean observations during an event, and high-resolution tsunami forecast models termed Forecast Models.

The town of Kihei is located on the southern coast (southwest of Haaleakalā) of Maui, Hawai'i (Figure 1). It faces the Pacific Ocean and is partially blocked by the islands of Lanai and Kahoolawe (Figure 1). With less than 13 inches of annual rain, it was referred to as "Kama'ole", meaning 'barren', by the Hawaiians. In the early 1900's, there was an effort to establish a sugar plantation but failed. With not so much to attract people to live there, the population was only 350 in 1930. Between the years 1932 to 1950, land was being sold by the government at a very low price to attract businesses and people ($0.05 per square foot for the residential areas). Even with such an attractive price, nobody wanted to live and work in Kihei. However the situation changed between 1970 to 1980 since water from Central and West Maui was piped into the town (www.about.com).

The town's population increased from 16,749 in year 2000 (mapzones.org) to 20,881 in year 2010 (Census, 2010). In 2000, it was ranked as the 10th most populous area in Hawai'i (mapzones.org). With a census designation land area of 10.16 square miles (26.31 km^2), its current population density would be 2,055.2 people per square mile (793.6/km^2). Kihei has a great weather with an average of 276 sunny days (due to its very low annual rainfall) and temperatures ranging from 53°F (in January) to 74°F (July). The current median home cost is $486,200 with home appreciation of -1.4% in 2010. The average household income is $61,112 with an unemployment rate of 7.8% and a current job growth of -1.69%. The population's occupation ranges from management, business and financial operations, professional and related occupations, service, sales, farming, fishing, forestry, construction, production, transportation and material moving. The majority of the population, 26.52%, is in the service occupation with the lowest (0.44%) in farming, fishing and forestry (BestPlaces). Higher education is available from Kapiolani Community College, Leeward Community College, Honolulu Community College and Brigham Young University – Hawaii Campus (CityTownInfo). The Maui High Performance

Computing Center which is the US Department of Defense supercomputing resource center and corporations like High Technology Development Corporation (www.htdc.org) are located in Kihei. With lots of condominiums, timeshares, rentals ranging from inexpensive to moderate rates, it has become a popular attraction for tourist to enjoy Maui (www.about.com).

This report details the development of a tsunami forecast model for Kihei, Maui, Hawai'i. Development includes construction of a digital elevation model based on available bathymetric and topographic data, model validation with historic events, and stability tests of the model with a suite of mega tsunami events the originating from subduction zones in the Pacific Ocean.

2.0 Forecast Methodology

A high-resolution inundation model was used as the basis for development of a tsunami forecast model to operationally provide an estimate of wave arrival time, wave height, and inundation at Kihei, Hawai'i following tsunami generation. All tsunami forecast models are run in real time while a tsunami is propagating across the open ocean. The Kihei, Maui, Hawai'i model was designed and tested to perform under stringent time constraints given that time is generally the single limiting factor in saving lives and property. The goal of this work is to maximize the length of time that the community of Kihei, Hawai'i has to react to a tsunami threat by providing accurate information quickly to emergency managers and other officials responsible for the community and infrastructure.

The general tsunami forecast model, based on the Method of Splitting Tsunami (MOST), is used in the tsunami inundation and forecasting system to provide real-time tsunami forecasts at selected coastal communities. The model runs in minutes while employing high-resolution grids constructed by the National Geophysical Data Center. The Method of Splitting Tsunami (MOST) is a suite of numerical simulation codes capable of simulating three processes of tsunami evolution: earthquake, transoceanic propagation, and inundation of dry land. The MOST model has been extensively tested against a number of laboratory experiments and benchmarks (Synolakis *et al.*, 2008) and was successfully used for simulations of many historical tsunami events. The main objective of a forecast model is to provide an accurate, yet rapid, estimate of wave arrival time, wave height, and inundation in the minutes following a tsunami event. Titov and González (1997) describe the technical aspects of forecast model development, stability, testing, and robustness, and Tang *et al.*, 2009 provide detailed forecast methodology

A basin-wide database of pre-computed water elevations and flow velocities for unit sources covering worldwide subduction zones has been generated to expedite forecasts (Gica *et al.*, 2008). As the tsunami wave propagates across the ocean and successively reaches tsunameter observation sites, recorded sea level is ingested into the tsunami forecast application in near real-time and incorporated into an inversion algorithm to produce an improved estimate of the tsunami source. A linear combination of the pre-computed database is then performed based on this tsunami source, now reflecting the transfer of energy to the fluid body, to produce synthetic boundary conditions of water elevation and flow velocities to initiate the forecast model computation.

Accurate forecasting of the tsunami impact on a coastal community largely relies on the accuracies of bathymetry and topography and the numerical computation. The high spatial and temporal grid resolution necessary for modeling accuracy poses a challenge in the run-time requirement for real-time forecasts. Each forecast model consists of three telescoped grids with increasing spatial resolution in the finest grid, and temporal resolution for simulation of wave inundation onto dry land. The forecast model utilizes the most recent bathymetry and topography available to reproduce the correct wave dynamics during the inundation computation. Forecast models, including the Kihei, Hawai'i model, are constructed for at-risk populous coastal

communities in the Pacific and Atlantic Oceans. Previous and present development of forecast models in the Pacific (Titov *et al.*, 2005; Titov, 2009; Tang *et al.*, 2008; Wei *et al.*, 2008) have validated the accuracy and efficiency of each forecast model currently implemented in the real-time tsunami forecast system. Models are tested when the opportunity arises and are used for scientific research. Tang *et al.*, 2009 provide forecast methodology details.

3. Model Development

The general methodology for modeling at-risk coastal communities is to develop a set of three nested grids, referred to as A, B, and C-grids, each of which becomes successively finer in resolution as they telescope into the population and economic center of the community of interest. The offshore area is covered by the largest and lowest resolution A-grid while the near-shore details are resolved within the finest scale C-grid to the point that tide gauge observations recorded during historical tsunamis are resolved within expected accuracy limits. The procedure is to begin development with large spatial extent merged bathymetric topographic grids at high resolution, and then optimize these grids by sub-sampling to coarsen the resolution and reduce the overall grid dimensions to achieve a 4 to 10 hr simulation of modeled tsunami waves within the required time period of 10 min of wall-clock time. The basis for these grids is a high-resolution digital elevation model constructed by the National Geophysical Data Center and NCTR using all available bathymetric, topographic, and shoreline data to reproduce the wave dynamics during the inundation computation for an at-risk community. For each community, data are compiled from a variety of sources to produce a digital elevation model referenced to Mean High Water in the vertical and to the World Geodetic System 1984 in the horizontal (NGDC). From these digital elevation models, a set of three high-resolution, "reference" elevation grids are constructed for development of a high-resolution reference model from which an 'optimized' model is constructed to run in an operationally specified period of time. The operationally developed model is referred to as the optimized tsunami forecast model or forecast model for brevity.

Development of an optimized tsunami forecast model for Kihei, Maui, Hawai'i began with the spatial extent merged bathymetric-topographic grids shown in Figure 1. Grid dimension extension and additional information were updated as needed and appropriate. A significant portion of the modeled tsunami waves, 24 hrs of modeled tsunami time for Kihei, Hawai'i, pass through the model domain without appreciable signal degradation. Table 1 provides specific details of both reference model and forecast model grids, including extents, and complete input parameter information for the model runs is provided in **Appendix A**.

3.1 Forecast area

The town of Kihei has a census designated area of 10.16 square miles (26.31 km^2) with a population of 20,881 (Census, 2010). It is located on the southern coast of Maui, Hawaii or southwest of Haaleakalā. South Kihei Road and Piilani Highway (Highway 31) are the two main roads that run roughly parallel to the coastline (Figure 1). South Kihei road runs along the coast and cuts through the town while Piilani Highway is further east. Highway 31 is roughly within 1 to 1.5 kilometers from the coastline with the highest elevation of approximately 22 meters mean sea level (MSL). As can be seen in Figure 1, majority of the town is located west of Highway 31.

Figures 2c and 3c show the contour of the coastal area where a large portion is at an elevation 5 meters or below and roughly 1 to 1.5 kilometers from the coastline providing a mild slope region. This is the area where businesses and population are located. The elevation then slowly increases (in most areas) another 5 meters eastward and then quickly slopes toward the hills. A portion of the occupied area is located northeastern end of the Highway 31 (Figure 1) and has an

approximate elevation of 40 meters MSL. The Maui High Performance Computing Center is located on the central east side of Piilani Highway but on a much higher elevation of 50 meters MSL (Figure 1).

A large portion of the coast has a small coastal shelf where the water depth slowly increases to 5 meters depth (Figures 2c and 3c) and then quickly drops another 5 meters then encounters another mild slope. Further offshore, the bathymetry gets complicated with deeper depths clustered in concentrated areas. These areas are clearly seen on the southwest areas of Figures 2c and 3c. Similar clusters are also found between 20.75°N and 20.76°N along 203.26°E. Another feature that can be noticed is along 20.76°N where there is a c-shape formed in the 10 meter contour line. The effects of this feature will be seen in the maximum current speed distribution and discussed in later sections.

3.2 Historical events and data

The Hawaiian Islands is located such that it is along the path of any tsunamis generated in the Pacific Ocean. With active subduction zone in the Pacific Basin, the potential for tsunamigenic earthquakes is high (Nishenko 1991). The Hawaiian Islands had been hit by numerous tsunamis where a few (e.g. 1946 Unimak, 1952 Kamchatka, 1957 Aleutian Islands, 1960 Chile and 1975 Big Island tsunamis) have caused millions of dollars in damage and human lives. Although historical records (Table 2) show tsunami run-up in Kihei for the 1946 Unimak, 1957 Aleutian Islands and 1960 Chilean tsunamis; there are no records of significant damage (NGDC). Although only 3 historical tsunamis were recorded, simulations will be conducted with other historical events (Table 3) to determine how it would have affected the community of Kihei.

Historical tide gauge record is not available since no gauge has been installed. The closest tide gauge is located in Kahului Harbor on the other side of the island of Maui. The selected warning point for Kihei is at 203.540277°E, 20.747685°N with a depth of 1.74 meters (Figures 2c and 3c). Historically Kihei had not experienced significant tsunami damages, one possible reason for which could be its location. Located on the southern part of Maui, it is partially blocked by the islands of Lanai and Kahoolawe (Figure 1). Depending on the location of the tsunami source, the island blocking might not hold true all the time. This will be tested by running synthetic mega-events in the Pacific region. The more recent 2011 Honshu tsunami did cause minor flooding along the coast of Kihei.

3.3 Model setup

Normally, the high-resolution digital elevation model is constructed by the National Geophysical Data Center and NCTR using all available bathymetric, topographic, and shoreline data. For Kihei, Maui, Hawai‘i, the high resolution Digital Elevation Model (DEM) was developed in-house by Chris Chamberlin (2007) with a grid resolution of 1/3 arc-seconds, coverage extent of 156.55°W, 20.65°N to 156.2°W, 21.05°N (Figure 4) and using a horizontal datum of WGS84 decimal degrees and a vertical datum of mean high water in meters. Sources of the data are from SHOALS Lidar, National Ocean Service, US Army Corps of Engineers, USGS Seafloor Mapping, NOAA CSC ifSAR and Digitized NOS charts. Both reference and forecast models consist of three nested grid where the outer most grid (Grid A) covers the deep ocean region so as to capture the tsunami characteristics as it propagates in the deep ocean while the inner most grid (Grid C) covers the area outside the coral reef to capture the tsunami wave transformations in shallow water. The A and B grids for Kihei, Maui, Hawai‘i are from those developed by Tang et al. (2010) to be consistent with the other inundation models developed in Hawai‘i. While the C-grid is extracted from the 1/3 arc-second DEM developed in-house.

The coverage extent of the C-grid for both reference inundation model and forecast model are same. Table 1 shows the details of the nested grid (Grids A, B and C) including the modeling parameters used. The plots of the nested grids are shown in Figures 2 and 3 for the forecast model and reference model, respectively. Since there is no tide gauge in Kihei, a warning point was arbitrarily selected and is shown in Figures 2c and 3c which has a coordinate of 20.747685°N, 203.540277°E and a depth of 1.74 meters.

Although the digital elevation model used for the forecast and reference models are derived from the same source, the forecast model is an optimized version of the reference model designed to provide a quick tsunami forecast. The use of different grid resolution sometimes requires modification on the digital elevation model to make a stable and reliable run. The difference in the digital elevation model used between the forecast and reference model is shown in Figures 2c and 3c. Figure 3c, which is the reference grid, shows a complicated bathymetry in the deeper region (lower left area along 203.26°E) while it is much smoother in the forecast model (Figure 2c).

The forecast model, which is used for tsunami forecast during an event, is an optimized version of the high resolution inundation model. It is designed so that it can quickly provide 4 hours of simulated tsunami wave characteristics which includes time series at the tide gauge. For the town of Kihei, Maui, Hawai‘i, the forecast model can simulate the tsunami wave characteristics in approximately 13.22 minutes (Table 1). The high resolution inundation model on the other hand takes about 22.68 hours to complete a simulated run of 4 hours. Both the high resolution inundation model and forecast model were validated with historical events to check for accuracy.

4. Results and Discussion

4.1 Model validation

The development of the DEM for the high resolution reference inundation model and forecast model requires that it be validated to determine the accuracy of the simulated tsunami characteristics as it hits the coastal areas of Kihei, Maui, Hawai‘i. Historically, lots of tsunamis had occurred in the Pacific Basin (Table 2 lists tsunamis with recorded runup) and most likely have impacted Kihei, Maui, Hawai‘i considering that it is located along the path of any tsunamis generated in the Basin. Unfortunately, no tide gauge has been established on the southern part of Maui. The closest tide gauge is located in Kahului Habor, Hawai‘i which is on the other side of the island of Maui. The wave characteristics at Kahului Harbor would be completely different from that at Kihei, Hawai’i, thus Kahului gauge cannot be used for model-to-data comparison at Kihei. However, historical records (NGDC) indicated tsunami run-up at Kihei, Hawaii for three tsunamis; 1 April 1946 Unimak Island, Alaska, 9 March 1957 Andreanov Islands, Alaska and 22 May 1960 Chilean tsunamis. The historical data of these three events will be used to validate the forecast model. Other historical events are also simulated to determine how it affects the coastal areas of Kihei (Table 3). The locations of these historical events relative to Kihei are plotted in Figure 5.

4.2 Model stability and reliability

The development of the forecast model also requires that the model provides a reliable forecast and should be stable enough to simulate several hours of the tsunami event. A set of reliability and stability tests was conducted by simulating synthetic events (Table 4) emanating from different regions and using different earthquake magnitudes (Mw= 9.4, 7.5 and 0). Since each tsunami event is unique, tests using different earthquake

magnitudes and source location would indicate if the model grid developed will generate instabilities that need to be corrected. This set of tests is not exhaustive however, representative cases from select sources should be sufficient. A total of forty-one artificial mega-tsunamis (Mw=9.4) were generated from twenty unit sources with a slip value of thirty meters for each unit source. Twenty cases of Mw=7.5 uses one unit source with a slip of one meter and once case of Mw=0 is to tests the model for a no wave condition. The unit sources are from the propagation database developed at NCTR (Gica et al., 2008). Tests were conducted for a total of 24 hours simulation. The list of sources used are indicated in Table 4 and 5 for the artificial mega-tsunamis and Mw=7.5 and Mw=0, respectively. The location of the synthetic mega-events (Table 4) relative to Kihei, Maui, Hawai‘i is shown in Figure 6.

4.3 Results of tested events

Results of the tested events (historical and synthetic) are shown by plotting the maximum/minimum tsunami wave amplitude distribution, inundation, tsunami time series, maximum tsunami current speed distribution, current speed and directionality. All the plots show both the forecast model and reference models. The simulated tsunami time series, current speed and directionality are recorded at the selected warning point (Figures 2c and 3c). Plots showing the maximum tsunami wave amplitude distribution for grids A, B and C and tsunami time series at the warning point are shown in Figures 7 to 32 and Figures 59 to 140 for historical events and synthetic mega-events (Table 4), respectively. Comparison of the maximum/minimum tsunami amplitude distribution and tsunami time series at C-grid level is shown in Figures 33 to 45 (historical events) and Figures 141 to 181 (synthetic mega-events, Table 4). These sets of plots will show whether the coastal areas of Kihei will be inundated or not, as well as the tsunami amplitude. Plots of the maximum tsunami current speed distribution, current speed and directionality at the warning point (Figures 2c and 3c) are shown in Figures 46 to 58 (historical events) and Figures 182 to 222 (synthetic mega-events, Table 4). These set would show the maximum current speed both on sea and land as inundation occurs and its directionality (at the warning point) as it hits the coastline. These set of figures are divided into three parts; the upper figure shows the maximum tsunami current speed distribution, the middle figure is the tsunami current speed while the bottom figure indicates the directionality of the current. Both middle and bottom figure are at the warning point selected (Figures 2c and 3c). The direction of the current is subdivided into four regions; West to North, South to West, East to South and North to East. Relative to the coastline, this would indicate whether the incoming tsunami wave is advancing or retreating from the shore or moving in the along-shore direction.

A total of 13 historical cases were simulated for validation of the Kihei forecast and reference models. Since Kihei does not have a tide gauge, tsunami time series comparison are done only between the forecast and reference model with exception for a few historical events where records of tsunami run-up are available (Table 2). The maximum tsunami wave amplitude distribution (Grids A, B and C) and tsunami time series at the warning point for historical events for forecast and reference models are shown in Figures 7 to 32. Comparison of maximum/minimum tsunami wave amplitude distribution and tsunami time series (at the warning point) at C-grid level between the forecast and reference models are shown in Figures 33 to 45. The comparisons of maximum current speed distribution, current speed and directionality are plotted in Figures 46 to 58. In all historical cases, the maximum tsunami wave amplitude for the reference model is higher than the forecast model as seen in the tsunami time series at the warning point. The first tsunami wave matches really well between the reference inundation model and forecast model for all historical cases. The succeeding waves though are much higher for the reference model but matches well in phase. Similarly, the current speed at the warning point is much higher for the reference model. Finer wave patterns are also seen in the reference models which are not present in the forecast model. Another aspect that can be noticed is in the maximum current speed distribution plot (Figures 46 to 58). The southwest area of the C-grid

shows slightly different maximum current speed distribution for the reference model when compared to the forecast model. This is attributed to the complex bathymetry in that region that needed modification in the forecast model to generate a stable run (Figures 2c and 3c). Overall, both maximum/minimum tsunami wave amplitude distribution and maximum current speed distribution are similar between the forecast and reference models. Inundation extent was either none or minor for all the 13 historical cases simulated.

From the historical cases simulated, National Geophysical Data Center (NGDC) has data of eyewitness accounts of run-up for three cases (Table 2). For the 1946 Unimak Island tsunami, the record indicated a run-up height of 2.7 meters. The simulated result for this specific event produced a run-up of approximately 1.78 meters for the forecast model and 1.82 meters for the reference model (Figure 33) near the historical recorded run-up. The distance from the simulated run-up to the historical recoded run-up is approximately 71 meters for the forecast model and 63 meters for the reference model. As for the 1957 Andreanov tsunami, historical run-up indicated 2.1 meters while the forecast model indicated 1.56 meters and 1.68 meters (Figure 34) for the reference model. Location of the simulated maximum run-up is approximately 71 meters (forecast model) and 63 meters (reference model) away from the recorded run-up location. For the 1960 Chile event, the run-up recorded is 2.4 meters. A run-up of 2.4 meters is recorded for the 1960 Chile tsunami (NGDC) while the forecast model simulated a 2.07 meters (Figure 35) and approximately 71 meters away from the recorded data while the reference model simulated 2.36 meters and is 94 meters away from the recorded data.

The comparison of the simulated run-up values with historical records for all three events (Table 2) showed that the historical records have a higher run-up as compared to the simulation. The simulated historical events were approximately 0.33 meter to 0.9 meter below that of the historical record and approximately 63 meters to 94 meters away. One possible reason for this discrepancy could be that the tsunami source used in the simulation is still not well-defined. For the more recent 2011 Honshu event, several videos have been posted in youtube (www.youtube.com) which showed minor flooding in Kihei. The simulated result also indicated minor flooding along the coast (Figure 45). Tsunami survey in the state of Hawaii was conducted for the 2011 Honshu event. Field measurement data of inundation and run-up can be used to validate the Kihei forecast model. However, NCTR has not yet gotten hold of surveyed data at the time when this report was written. For the remaining historical events where historical data is not available, the forecast model is compared with the reference model.

The synthetic events simulated for the forecast model showed that it is both stable and reliable. Although the mega-tsunami (Mw = 9.4, Table 4) tests is not exhaustive, the results can indicate which tsunami source regions would pose a threat to Kihei, Maui, Hawai‘i. The maximum tsunami wave amplitude distribution for grids A, B and C and tsunami time series at the selected warning point are shown in Figures 59 to 140 for the forecast and reference models. Figures 141 to 181 compares the maximum/minimum tsunami wave amplitude distribution and time series at C-grid level between the forecast and reference model and would also indicate the extent of inundation.

Of the 41 synthetic mega-tsunami (Mw=9.4, Table 4), only 19 sources produced very minor inundation along the coast of Kihei based on the forecast model and 15 sources based on the reference model. Figure 223 shows the locations of these low coastal impact synthetic mega-events relative to Kihei which clearly indicate that the main tsunami energy is directed away from Kihei. Tsunami sources that have extreme coastal impact emanates from EPSZ09-18 (Figure 161), KISZ01-10 (Figure 162), KISZ11-20 (Figure 163), KISZ42-51 (Figure 165) and MOSZ01-10 (Figure 169). The inundation extent for these tsunami sources occupies a significant portion of the coastal town. The location of these extreme tsunami sources relative to Kihei is shown in Figure 224. The remaining 17 synthetic mega-events still produce significant tsunami impact and depending on the tsunami source location relative to Kihei, for the same event, some areas are not that extensive.

The plots showing both the maximum and minimum tsunami amplitude distribution does not clearly show how the incoming tsunami waves interact with the coastal shelf in Kihei. This interaction is clearly seen in the maximum tsunami current speed distribution plots (Figures 46 to 58 for historical events and Figures 182 to 222 for synthetic mega-events). The current speed is high as the incoming tsunami waves encounter the 5 meter offshore contour line of the coastal shelf. Its strength diminishes as it passes thru the coastal shelf. However depending on where the tsunami source is located relative to Kihei, the incoming waves could either produce no inundation to extreme inundation with high current speed as it inundates the coastal areas. For synthetic mega-events (Table 4), the current speed on land is at least 5 meters/second with an extreme case of around 10 meters/second for EPSZ09-18 source. The plot of the current directionality shows a complex pattern, the tsunami waves not only approaches and recedes from the shore but also generates cross-currents.

5. Summary and Conclusion

A set of reference and forecast inundation models has been prepared for Kihei, Maui, Hawai‘i. During the development of the forecast model, instabilities occurred in the deeper region of the C-grid due to its complex bathymetry (Figures 2c and 3c). The locations that caused instability were corrected by adjusting the depth of the node so that it will have a mild slope with its surrounding area or manually or smoothing a cluster of nodes if the single node causing the instability is not located. Although there were corrections made to the DEM both models were found to be reliable and the comparison of the maximum/minimum tsunami wave amplitude distribution, maximum tsunami current speed, tsunami time series, current speed and directionality at the warning point were relatively good.

Reliability of the reference and forecast inundation models were validated with three historical events. The National Geophysical Data Center has 3 records of historical run-up due to tsunami in Kihei which are due to 1 April 1946 Unimak Island, 9 March 1957 Andreanov and 22 May 1960 Chilean tsunamis. Comparison with the historical records show that the simulated run-up (forecast and reference models) was on average 0.52 meters less than the record and 72 meters (on average) away. This discrepancy could indicate that the source used by NCTR is still not well-defined. For the 2011 Honshu event, both reference and forecast (Figure 45) models indicated minor flooding along the coast. Comparison with surveyed data has not been done since NCTR have not received the data at the time when this inundation model was developed and when the report was written.

The stability tests showed that both the forecast and reference models are stable for a 24-hour simulation for both historical cases and synthetic sources (Tables 4 and 5) with different earthquake magnitudes (i.e. Mw = 9.4, 7.5, and 0) emanating from different source regions. A total of 41 Mw =9.4, 20 Mw =7.5 and 20 Mw=0 were simulated. Testing with mega-tsunami events not only checks the stability of the forecast model, it can also provide information on which source region is Kihei, Maui, Hawai‘i more susceptible to tsunamis. From the limited test of synthetic scenarios conducted, 19 source scenarios based on forecast model (15 for reference model) out of the 41 tested produce minor inundation along the coast. Significant inundation was from 17 source scenarios and 5 extreme cases that inundated a significant portion of the coastal town.

Other than the tsunami time series at the selected warning point and distribution of the maximum and minimum tsunami wave amplitude, plots of the maximum current speed distribution and current directionality at the selected warning point are also presented. Results from the synthetic mega-events showed that the current speed on land can reach at least 5 meters/second and as high as 10 meters/second from source region EPSZ09-18. The current direction at the selected warning point also indicates the complex pattern of the tsunami waves.

The tsunami waves not only approach and retreat from the shore but also generate cross-current along the coast.

Since the main objective of developing the Kihei, Maui, Hawai'i forecast model is for tsunami forecast, the DEM has been optimized to simulate 4 hours of tsunami wave characteristics in approximately 13.22 minutes. As presented in this report, the Kihei, Maui, Hawai'i forecast model should be able to provide a reliable forecast during an event and is stable for a 24 hours simulation. Other than being used as a forecast model in real-time events, the developed grids can also be used for hazard assessment to assist the local community in developing an evacuation plan.

6.0 Acknowledgments

This publication is contribution XXX from NOAA/Pacific Marine Environmental Laboratory and funded by the Joint Institute for the Study of the Atmosphere and Ocean (JISAO) at the University of Washington under NOAA Cooperative Agreement No. NA17RJ1232, JISAO contribution XXX. The author would also like to thank Lt. Lindsey Wright, NOAA Corps (for retrieving historical tide gauge data) and Sandra Bigley (for comments, edits and formatting of this report).

7.0 References

About.com

www.about.com, http://gohawaii.about.com/od/maui/p/kihei_maui.htm, accessed 23 August 2011.

Best Places
http://www.bestplaces.net/city/hawaii/kihei, accessed 6 September 2011.

Chamberlin, C (2007), 1/3s digital elevation model for Kahului, Maui, Hawaii, NCTR. April 27 2007, http://new-nctrd.pmel.noaa.gov/atlas/grid/Kahului%201_3s/

CityTownInfo, http://www.citytowninfo.com/places/hawaii/kihei, accessed 23 August 2011.

Gica, Edison, M.C. Spillane, V.V. Titov, C.D. Chamberlin and J.C. Newman (2008): Development of the forecast propagation database for NOAA's Short-term Inundation Forecast for Tsunamis (SIFT), NOAA Tech. Memo OAR PMEL139, NOAA/Pacific Marine Environmental Laboratory, Seattle, WA, 89pp.

High Technology Development Corporation
http://www.htdc.org/programsservices/incubation_techcenter_mrtcdirections.html, accessed 23 August 2011

Nishenko, Stuart P. (1991): Circum-Pacific Seismic Potential: 1989-1999, Pure and Applied Geophysics, Vol. 135, No. 2, pp 169-259.

MapZones

mapzones.org, http://mapzones.org/Kihei_Cdp_Hawaii.html, accessed 23 August 2011.

National Geodetic and Data Center
http://ngdc.noaa.gov/mgg/inundation/tsunami/inundation.html, accessed 1 June 2011.

Tang, L., V.V. Titov, and C.D. Chamberlin (2009): Development, testing, and applications of site-specific tsunami inundation models for real-time forecasting. *J. Geophys. Res.*, 6, doi: 10.1029/2009JC005476, in press.

Synolakis, C.E., E.N. Bernard, V.V. Titov, U. Kânoğlu and F.I. González (2008): Validation and verification of tsunami numerical models. *Pure and Applied Geophysics* 165(11-12), 2197-2228.

Tang, L., Chamberlin, C.D. and Titov, V.V. (2010): A tsunami forecast model for Hilo, Hawai'i, NOAA OAR Special Report, PMEL Tsunami Forecast Series: Vol. 1, 94 pp.
Titov, V.V. and F.I. Gonzalez (1997): Implementation and testing of Method of Splitting Tsunami (MOST) model. NOAA Tech. Memo. ERL PMEL-112 (PB98-122773), NOAA/Pacific Marine Environmental Laboratory, Seattle, WA, 11pp.
Titov, V.V., F.I. Gonzalez, E.N. Bernard, M.C. Eble, H.O. Mofjeld, J.C. Newman and A.J. Venturato (2005): Real-time tsunami forecasting: Challenges and solutions. Natural Hazards, 35, 41-58.
Titov, V.V. (2009): Tsunami forecasting. In *The Sea*, Vol. 15, Chapter 12, Harvard University Press, Cambridge, MA, and London, England, 371–400.

Wei, Y., E. Bernard, L. Tang, R. Weiss, V. Titov, C. Moore, M. Spillane, M. Hopkins, and U. Kânoglu (2008): Real-time experimental forecast of the Peruvian tsunami of August 2007 for U.S. coastlines. *Geophys. Res. Lett.*, *35*, L04609, doi: 10.1029/2007GL032250.

Youtube videos, www.youtube.com, accessed May 2011.

Table 1. MOST setup parameters for reference and forecast models for Kihei, Maui, Hawai‘i.

		Reference Model				Forecast Model			
Grid	Region	Coverage Lat. [ºN] Lon. [ºW]	Cell Size [“]	nx x ny	Time Step [sec]	Coverage Lat. [ºN] Lon. [ºW]	Cell Size [“]	nx x ny	Time Step [sec]
A	Hawaiian Islands	18.0083-22.9983 199.0000-205.9799	36	699 x 500	3.6	18.0317-22.9983 199.0000-205.9667	120	210 x 150	10.0
B	Maui	20.4000-21.3933 202.5717-204.0983	6	917 x 597	0.6	20.4017-21.2550 202.8967-204.0967	12	361 x 257	1.0
C	Kihei	20.7167-20.7907 203.5275-203.5638	1/3	393 x 800	0.3	20.7168-20.7907 203.5278-203.5636	1	131 x 267	1.0
Minimum offshore depth [m]				1.0			1.0		
Water depth for dry land [m]				0.1			0.1		
Friction coefficient [n^2]				0.00009			0.0009		
CPU time for 4-hr simulation				22.68 hours			13.22 minutes		

Computations were performed on a dual Hex-core Intel Xeon E5670 processor at 2.936 GHz each 12M cache, Dell PowerEdge R510.

Table 2. Historical events with recorded run-up at Kihei, Maui, Hawai'i.

Event	Earthquake Date Time (UTC)	Lat. (°)	Lon. (°)	Seismic Moment Magnitude (Mw)	Tsunami Runup Location[1]		Runup height (m)[1]
					Lat. (°)	Lon. (°)	
1946 Unimak	1946-04-01 12:28:56	52.75N	163.500 W	8.5[2]	20.785N	156.467W	2.70
1957 Andreanov[3]	1957-03-09 14:22:31.9	38.29N	175.39W	8.6[3]	20.785N	156.467W	2.10
1960 Chile[3]	1960-05-22 19:11:17	38.29S	73.05W	9.5[4]	20.785N	156.467W	2.40

[1] National Geophysical Data Center (NGDC)

[2] López and Okal (2006)

[3] United States Geological Survey (USGS)

[4] Kanamori and Cipar (1974)

Table 3. Historical events simulated for Kihei, Maui, Hawai'i.

Event	Earthquake Date Time (UTC)	Lat. (°)	Lon. (°)	Subduction Zone	Seismic Moment Magnitude (Mw)	Tsunami Magnitude[1]	Model Tsunami Source
1946 Unimak	1946-04-01 12:28:56	52.75N	163.50W	Aleutian-Alaska-Cascadia (ACSZ)	8.5[2]	8.5	7.5 x b23 + 19.7 x b24 + 3.7 x b25
1957 Andreanov	1957-03-09 14:22:31	51.56N	175.39W	Aleutian-Alaska-Cascadia (ACSZ)	8.6[3]	8.7	31.4 x a15 + 10.6 x a16 + 12.2 x a17
1960 Chile	1960-05-22 19:11:14	38.29S	73.050W	Central-South America (CSSZ)	9.5[5]		Kanamori & Cipar (1974)
1994 East Kuril	1994-10-04 13:22:58	43.73N	147.321 E	Kamchatka-Kuril-Japan-Izu-Marian-Yap (KISZ)	8.3[3]	8.1	9.0 x a20
2003 Rat Island	2003-11-17 06:43:31.0	51.14N	177.86E	Aleutian-Alaska-Cascadia (ACSZ)	7.7[3]	7.8	2.81 x b11
2006 Tonga	2006-05-03 15:27:03.7	20.39S	173.47W	New Zealand-Kermadec-Tonga (NTSZ)	8.3[3]	8.1	4 x a12 + 0.5 x b12 + 2 x a13 + 1.5 x b13
2006 Kuril	2006-11-15 11:15:08.0	46.71N	154.33E	Kamchatka-Kuril-Japan-Izu-Marian-Yap (KISZ)	8.3[3]	8.1	4 x a12 + 0.5 x b12 + 2 x a13 + 1.5 x b13
2007 Kuril	2007-01-13 04:23:48.1	46.17N	154.80E	Kamchatka-Kuril-Japan-Izu-Marian-Yap (KISZ)	8.1[3]	7.9	-3.64 x b13
2007 Solomon	2007-04-01 20:39:56	8.481S	156.978 E	New Britain-Solomons-Vanuatu (NVSZ)	8.1[4]	8.2	12.0 x b10
2007 Peru	2007-08-15 23:40:57	13.345 S	76.509W	Central-South America (CSSZ)	8.0[3]	8.1	0.9 x a61 + 1.25*b61+ 5.6 x a62

							+ 6.97 x b62 + 3.5 x z62
2009 Samoa	2009-09-29 17:48:10	15.509 S	172.034 W	New Zealand-Kermadec-Tonga (NTSZ)	8.1[3]	8.1	3.96 x a34 + 3.96 x b34
2010 Chile	2010-02-27 06:35:15.4	35.950 S	73.150W	Central-South America (CSSZ)	8.8[3]	8.8	17.24 x a88 + 8.82 x a90 + 11.86 x b88 + 18.39 x b89 + 16.75 x b90 + 20.79 x z88 + 7.06 x z90
2011 Honshu	2011-03-11 05:46:00	38.322 N	142.369 E	Kamchatka-Kuril-Japan-Izu-Marian-Yap (KISZ)	9.0[2]	8.8	4.66 x b24 + 12.23 x b25 + 26.31 x a26 + 21.27 x b26 + 22.75 x a27 + 4.98 x b27

[1]Preliminary source – derived from source and deep-ocean observations [2]López and Okal (2006) [2]Centroid Moment Tensor [4]United States Geological Survey (USGS) [5]Kanamori and Cipar (1974)

Table 4. Synthetic mega-tsunamis tested for Kihei, Maui, Hawai'i.

Scenario Name	Subduction Zone	Tsunami Source
ACSZ 01-10	Aleutian-Alaska-Cascadia	A01-10, B01-10
ACSZ 11-20	Aleutian-Alaska-Cascadia	A11-20, B11-20
ACSZ 21-30	Aleutian-Alaska-Cascadia	A21-30, B21-30
ACSZ 31-40	Aleutian-Alaska-Cascadia	A31-40, B31-40
ACSZ 41-50	Aleutian-Alaska-Cascadia	A41-50, B41-50
ACSZ 51-60	Aleutian-Alaska-Cascadia	A51-60, B51-60
ACSZ 56-65	Aleutian-Alaska-Cascadia	A56-65, B56-65
CSSZ 01-10	Central-South America	A01-10, B01-10
CSSZ 11-20	Central-South America	A11-20, B11-20
CSSZ 21-30	Central-South America	A21-30, B21-30
CSSZ 31-40	Central-South America	A31-40, B31-40
CSSZ 41-50	Central-South America	A41-50, B41-50
CSSZ 51-60	Central-South America	A51-60, B51-60
CSSZ 61-70	Central-South America	A61-70, B61-70
CSSZ 71-80	Central-South America	A71-80, B71-80
CSSZ 81-90	Central-South America	A81-90, B81-90
CSSZ 91-100	Central-South America	A91-100, B91-100
CSSZ 101-110	Central-South America	A101-110, B101-110
CSSZ 106-115	Central-South America	A106-115, B106-115
EPSZ 01-10	East Philippines	A01-10, B01-10
EPSZ 06-15	East Philippines	A06-15, B06-15
KISZ 01-10	Kamchatka-Yap-Mariana-Izu-Bonin	A01-10, B01-10
KISZ 32-41	Kamchatka-Yap-Mariana-Izu-Bonin	A32-41, B32-41
KISZ 32-41	Kamchatka-Yap-Mariana-Izu-Bonin	A32-41, B32-41
KISZ42-51	Kamchatka-Yap-Mariana-Izu-Bonin	A42-52, B42-51
KISZ52-61	Kamchatka-Yap-Mariana-Izu-Bonin	A52-61, B52-61
KISZ56-65	Kamchatka-Yap-Mariana-Izu-Bonin	A56-65, B56-65
KISZ 66-75	Kamchatka-Yap-Mariana-Izu-Bonin	A66-75, B66-75

MOSZ 01-10	Manus OCB	A01-10, B10-10
MOSZ 08-17	Manus OCB	A08-17, B08-17
NGSZ 01-10	North New Guinea	A01-10, B01-10
NGSZ 06-15	North New Guinea	A06-15, B06-15
NTSZ 01-10	New Zealand-Kermadec-Tonga	A01-10, B01-10
NTSZ 11-20	New Zealand-Kermadec-Tonga	A11-20,B11-20
NTSZ 21-30	New Zealand-Kermadec-Tonga	A21-30, B21-30
NTSZ 30-39	New Zealand-Kermadec-Tonga	A30-39, B30-39
NVSZ 01-10	New Britain-Solomons-Vanuatu	A01-10, B01-10
NVSZ 11-20	New Britain-Solomons-Vanuatu	A11-20, B11-20
NVSZ 28-37	New Britain-Solomons-Vanuatu	A28-37, B28-37
RNSZ 01-10	Ryukus-Kyushu-Nankai	A01-10, B01-10
RNSZ 13-22	Ryukus-Kyushu-Nankai	A13-22, B13-22

Table 5. Synthetic tsunamis with Mw = 7.5 and 0 (1 case) tested for Kihei, Hawai'i.

Scenario Name	Subduction Zone	Tsunami Source
ACSZ 9	Aleutian-Alaska-Cascadia	B9
ACSZ 18[1]	Aleutian-Alaska-Cascadia	B18
ACSZ 30	Aleutian-Alaska-Cascadia	B18
ACSZ 50	Aleutian-Alaska-Cascadia	B50
ACSZ 65	Aleutian-Alaska-Cascadia	B65
CSSZ 2	Central-South America	B2
CSSZ 22	Central-South America	B22
CSSZ 49	Central-South America	B49
CSZ 59	Central-South America	B59
CSSZ 84	Central-South America	B84
EPSZ 10	East Philippines	B10
KISZ 8	Kamchatka-Yap-Mariana-Izu-Bonin	B8
KISZ 15	Kamchatka-Yap-Mariana-Izu-Bonin	B15
KISZ 27	Kamchatka-Yap-Mariana-Izu-Bonin	B27
KISZ 53	Kamchatka-Yap-Mariana-Izu-Bonin	B53
MOSZ 9	Manus OCB	B9
NTSZ 19	New Zealand-Kermadec-Tonga	B19
NTSZ 36	New Zealand-Kermadec-Tonga	B36
NVSZ 23	New Britain-Solomons-Vanuatu	B23
RNSZ 11	Ryukus-Kyushu-Nankai	B11

[1] simulated an M_w=0 case

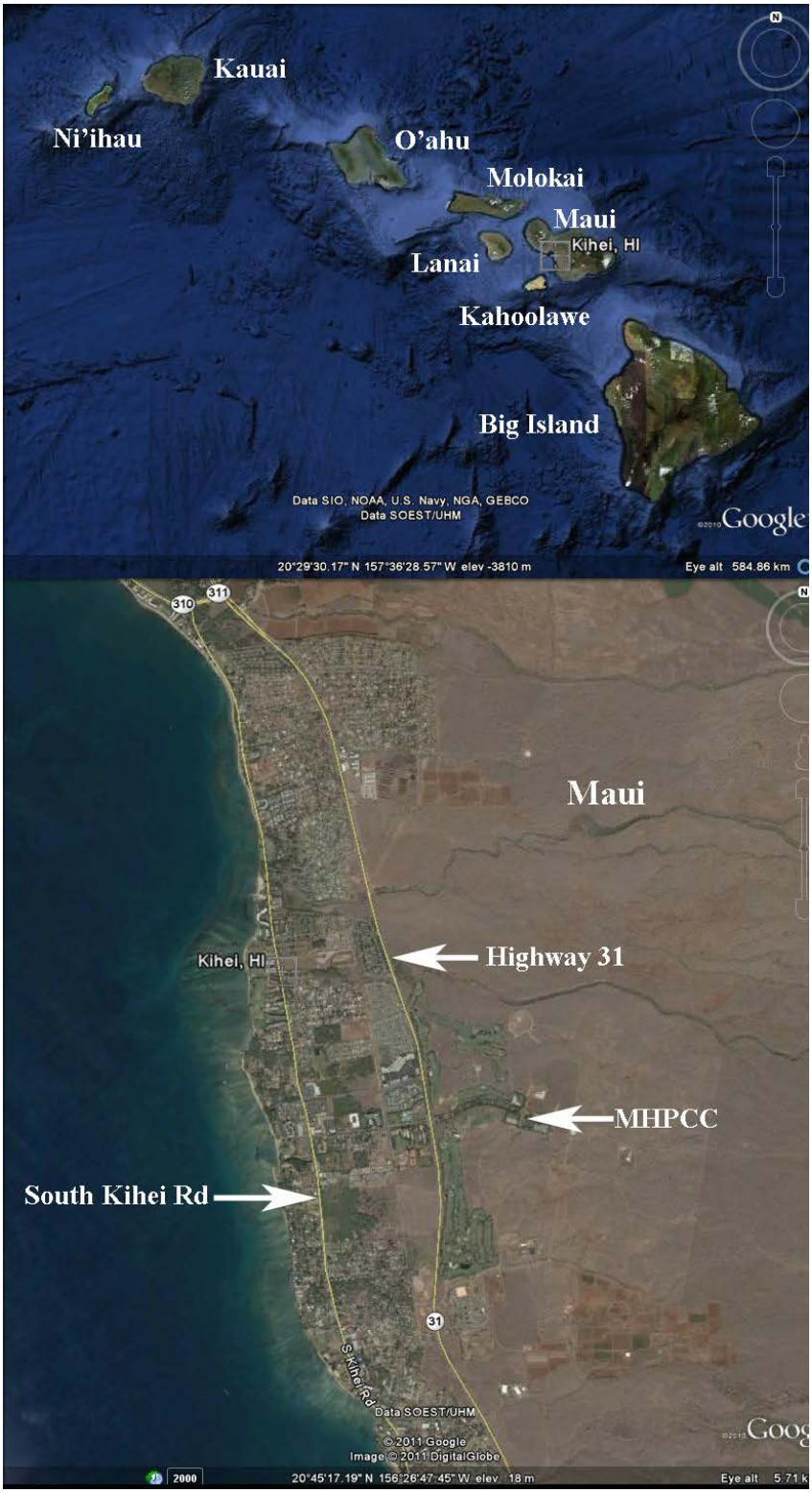

Figure 1. Location of Kihei, Maui, Hawai'i.

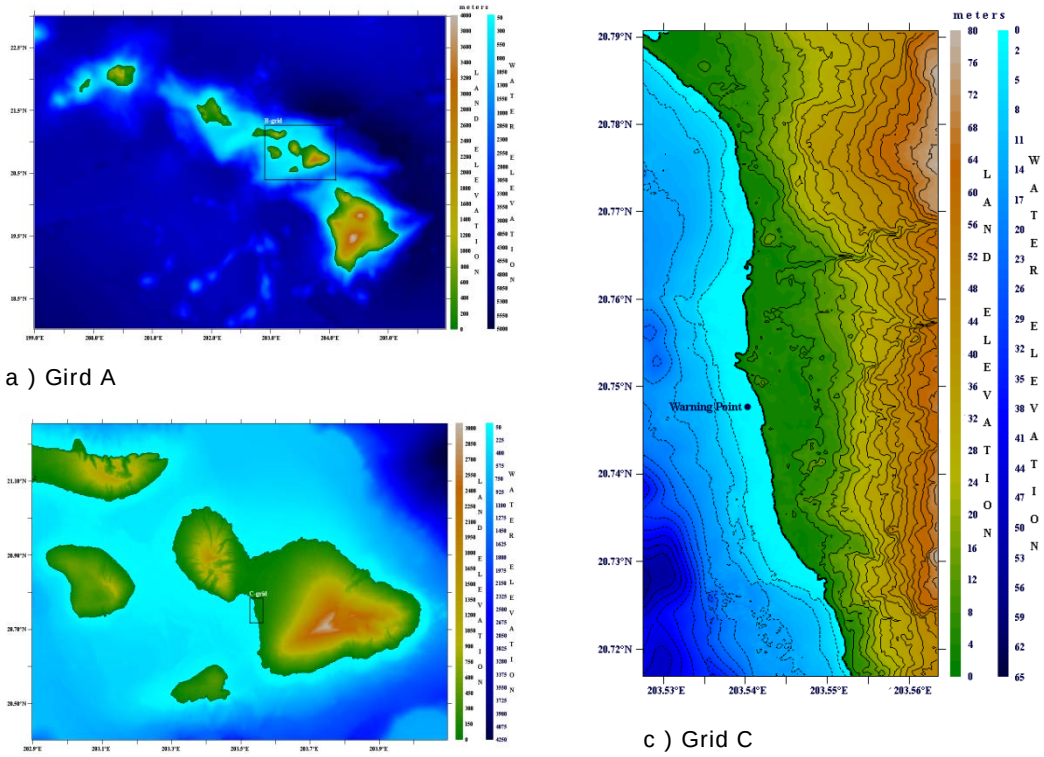

a) Gird A

b) Grid B

c) Grid C

Figure 2. Plot of forecast model grid developed; a) Grid A, b) Grid B and c) Grid C.

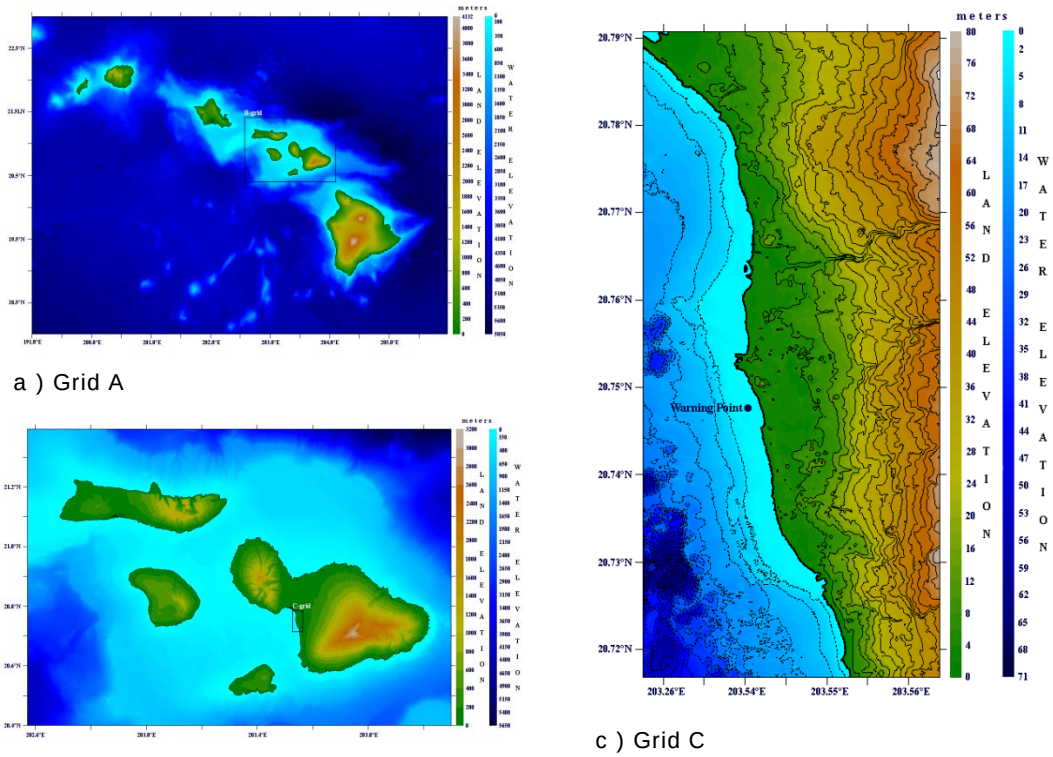

a) Grid A

b) Grid B

c) Grid C

Figure 3. Plot of reference model grid developed; a) Grid A, b) Grid B and c) Grid C.

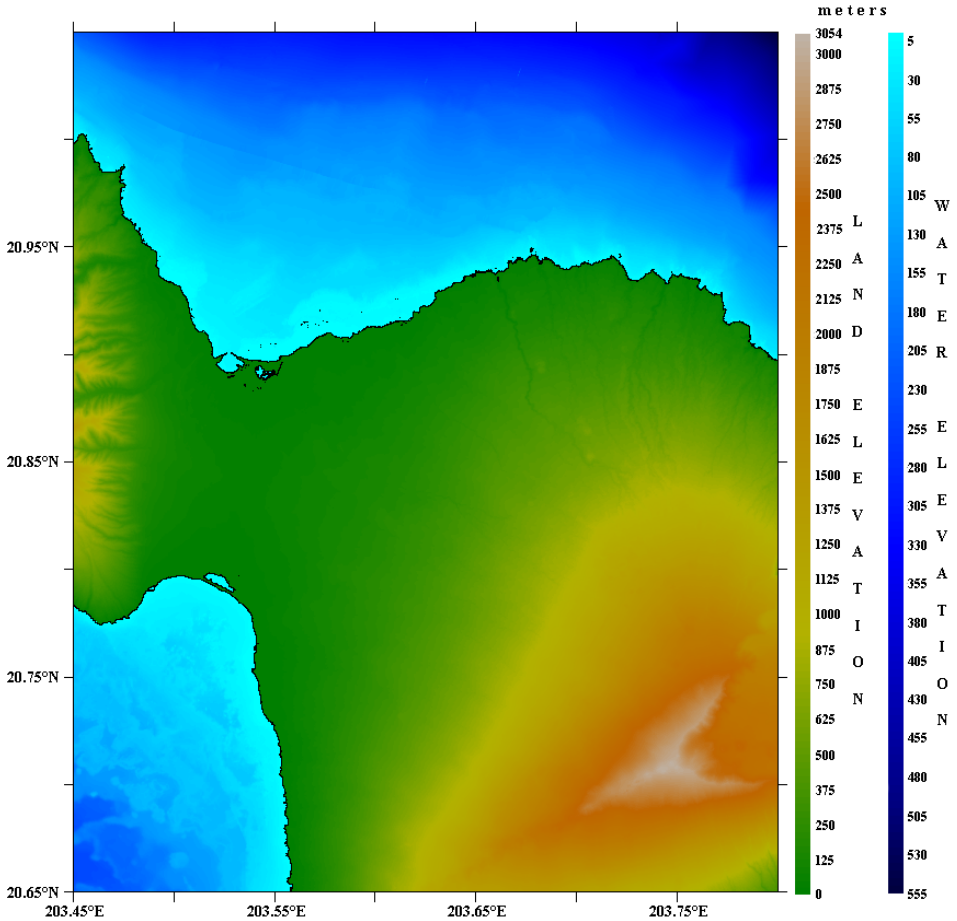

Figure 4. Plot of Kahului DEM.

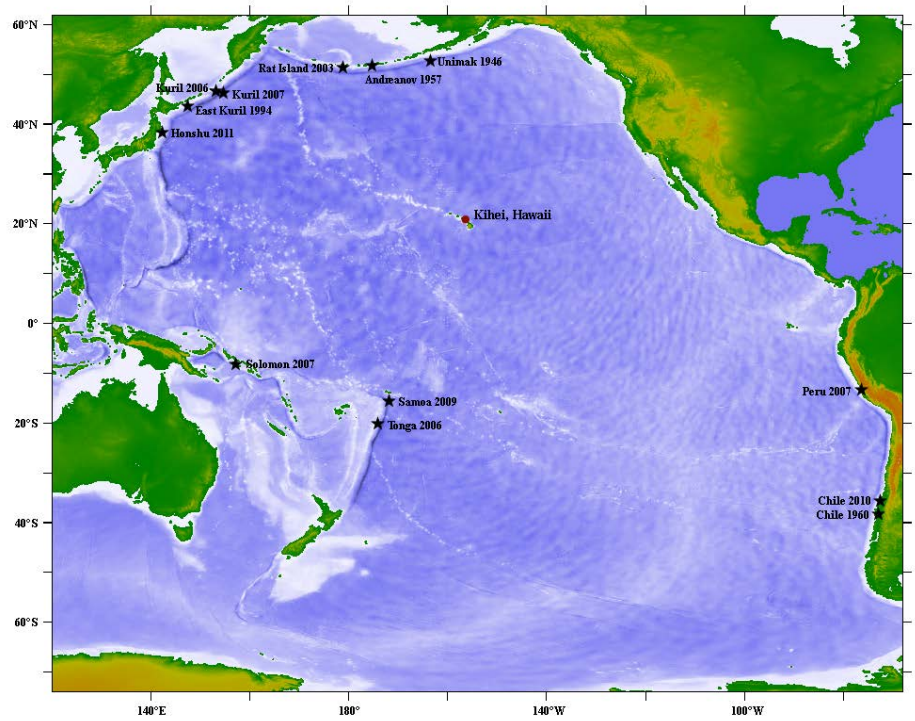

Figure 5. Location of Kihei, Maui, Hawai‘i relative to historical events simulated.

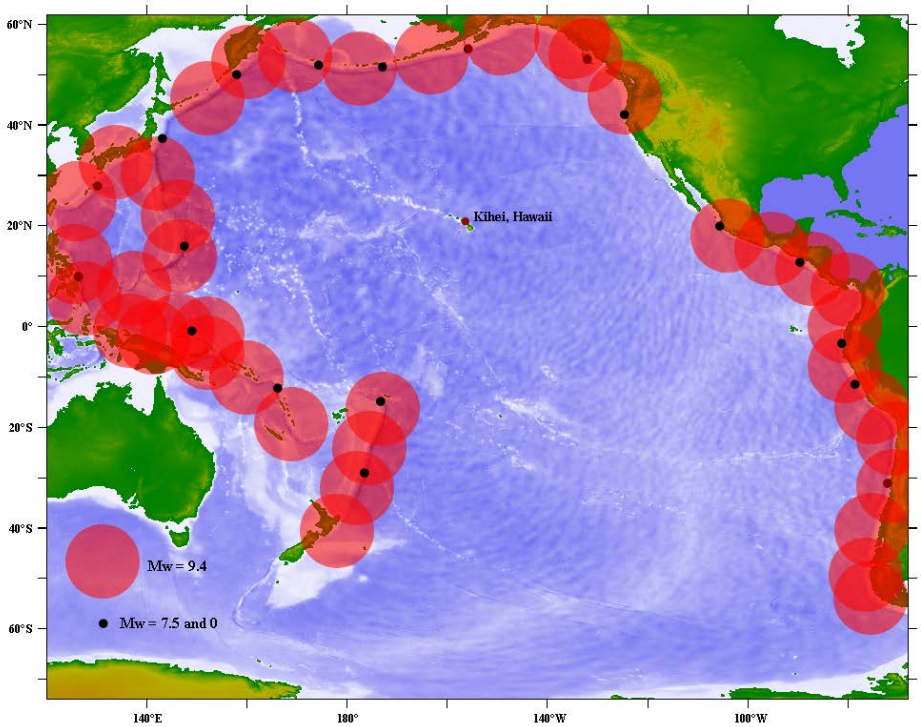

Figure 6. Location of Kihei, Maui, Hawai’i relative to synthetic events simulated.

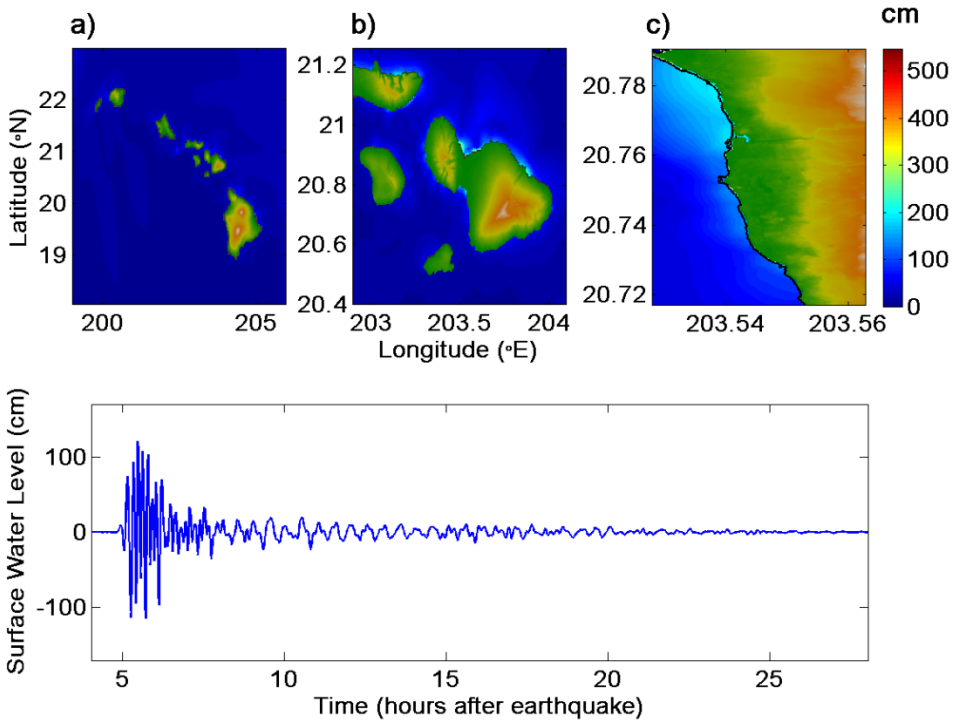

Figure 7. Plot of maximum tsunami wave amplitude distribution and tsunami time series at the warning point for 1946 Unimak tsunami with forecast model, a) A-grid, b) B-grid and c) C-grid.

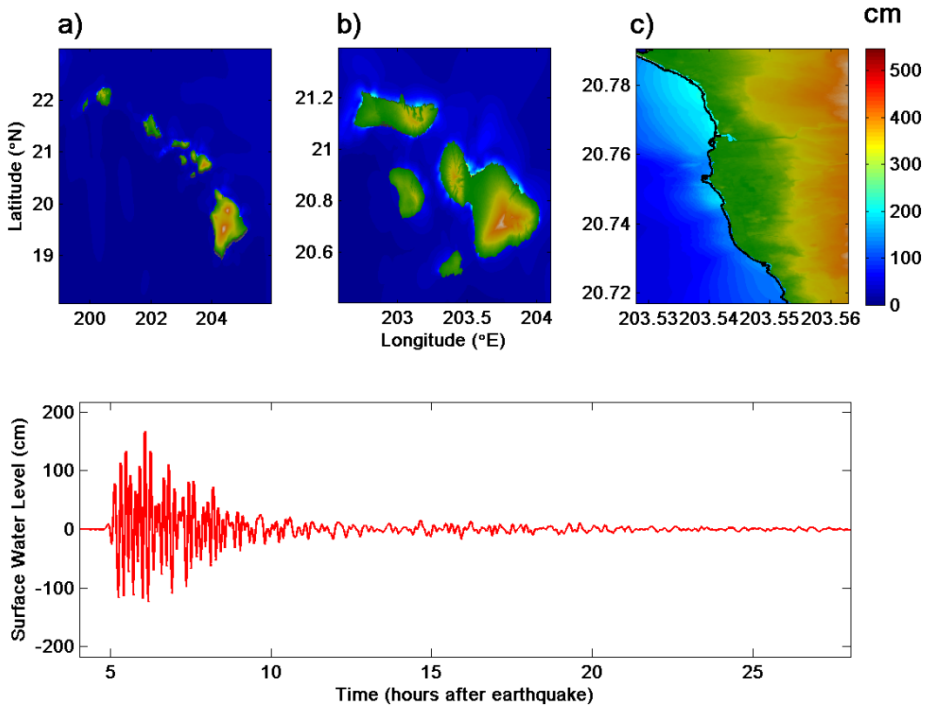

Figure 8. Plot of maximum tsunami wave amplitude distribution and tsunami time series at the warning point for 1946 Unimak tsunami with reference model, a) A-grid, b) B-grid and c) C-grid.

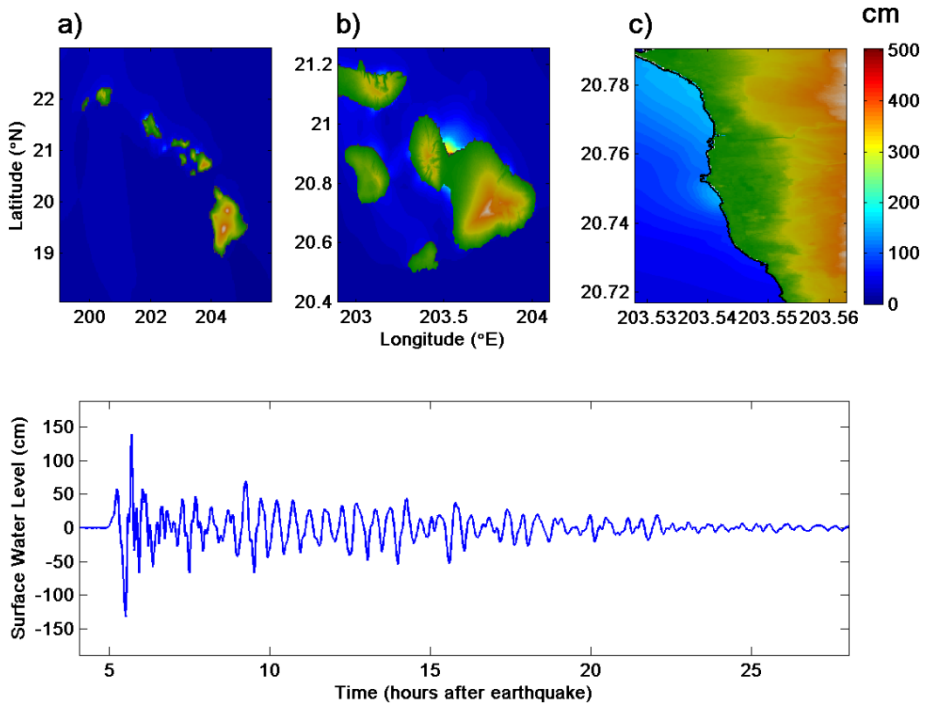

Figure 9. Plot of maximum tsunami wave amplitude distribution and tsunami time series at the warning point for 1957 Andreanov tsunami with forecast model, a) A-grid, b) B-grid and c) C-grid.

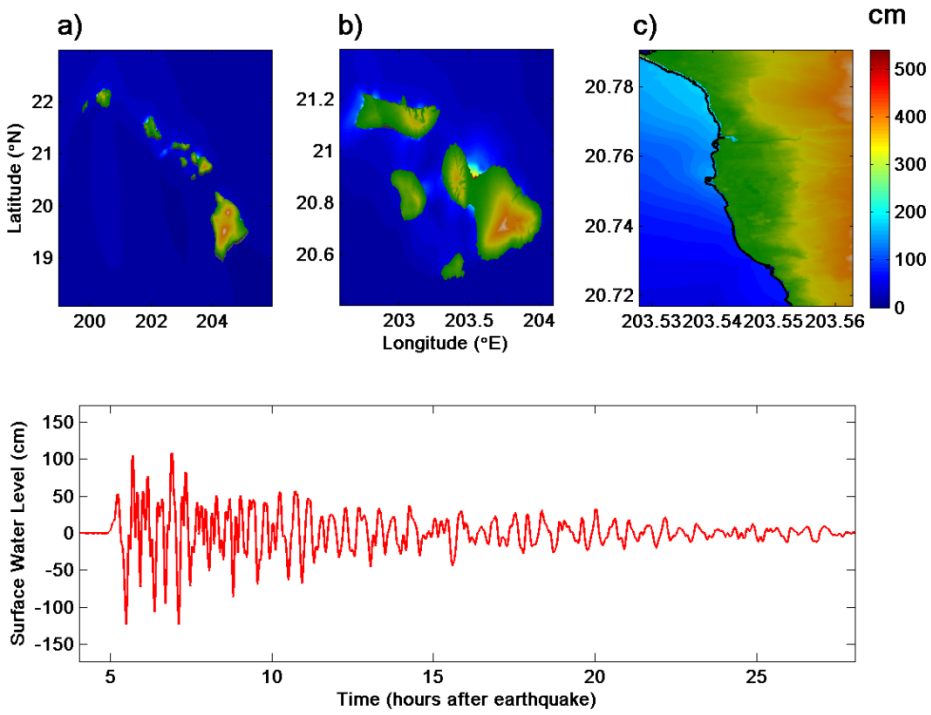

Figure 10. Plot of maximum tsunami wave amplitude distribution and tsunami time series at the warning point for 1957 Andreanov tsunami with reference model, a) A-grid, b) B-grid and c) C-grid.

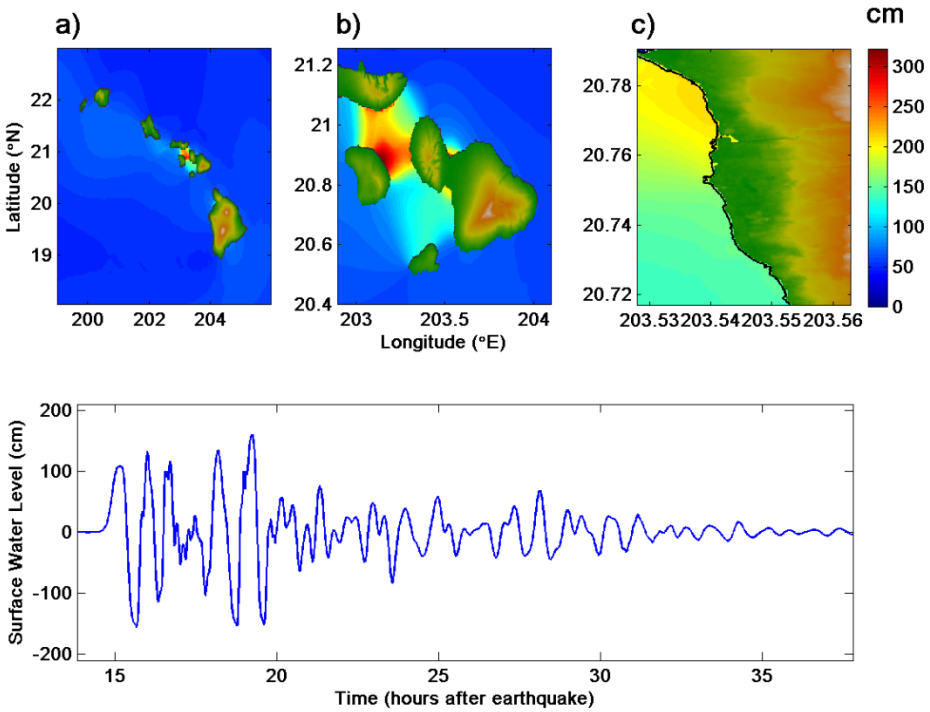

Figure 11. Plot of maximum tsunami wave amplitude distribution and tsunami time series at the warning point for 1960 Chile tsunami with forecast model, a) A-grid, b) B-grid and c) C-grid.

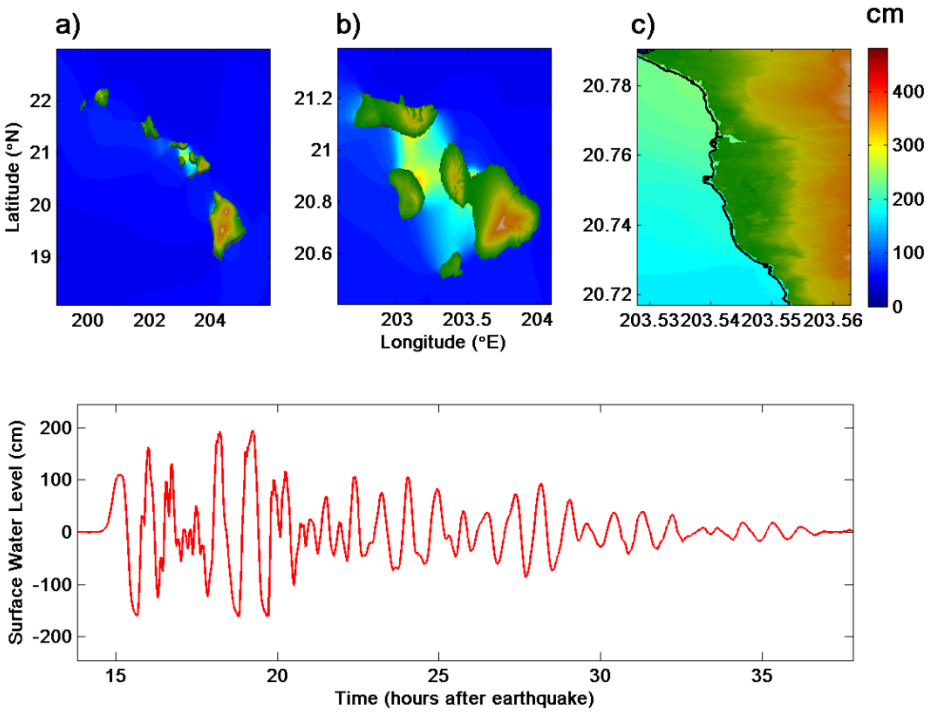

Figure 12. Plot of maximum tsunami wave amplitude distribution and tsunami time series at the warning point for 1960 Chile tsunami, a) A-grid, b) B-grid and c) C-grid.

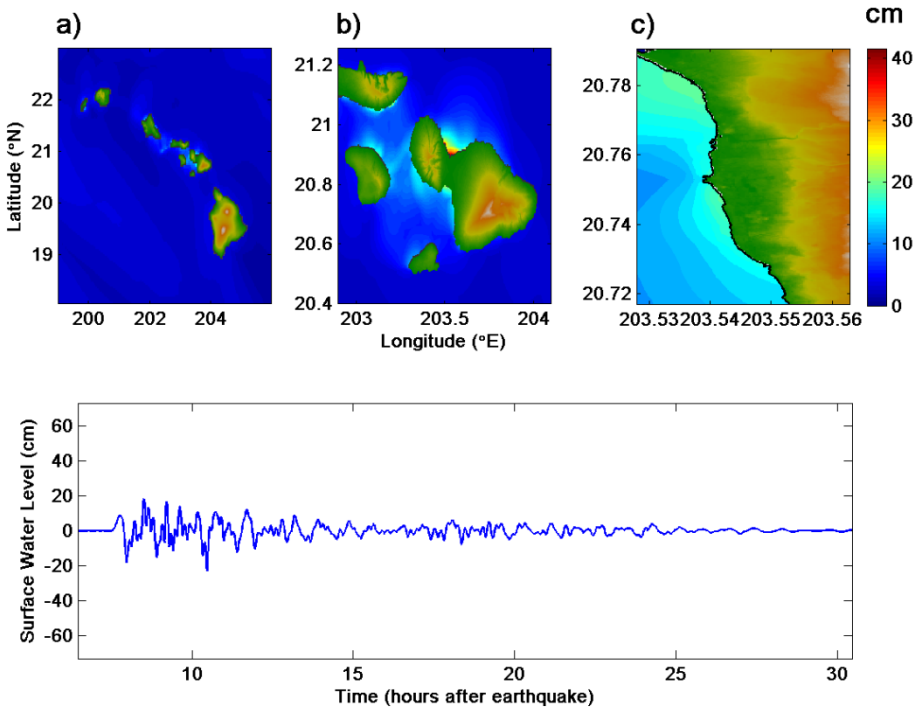

Figure 13. Plot of maximum tsunami wave amplitude distribution and tsunami time series at the warning point for 1994 East Kuril tsunami with forecast model, a) A-grid, b) B-grid and c) C-grid.

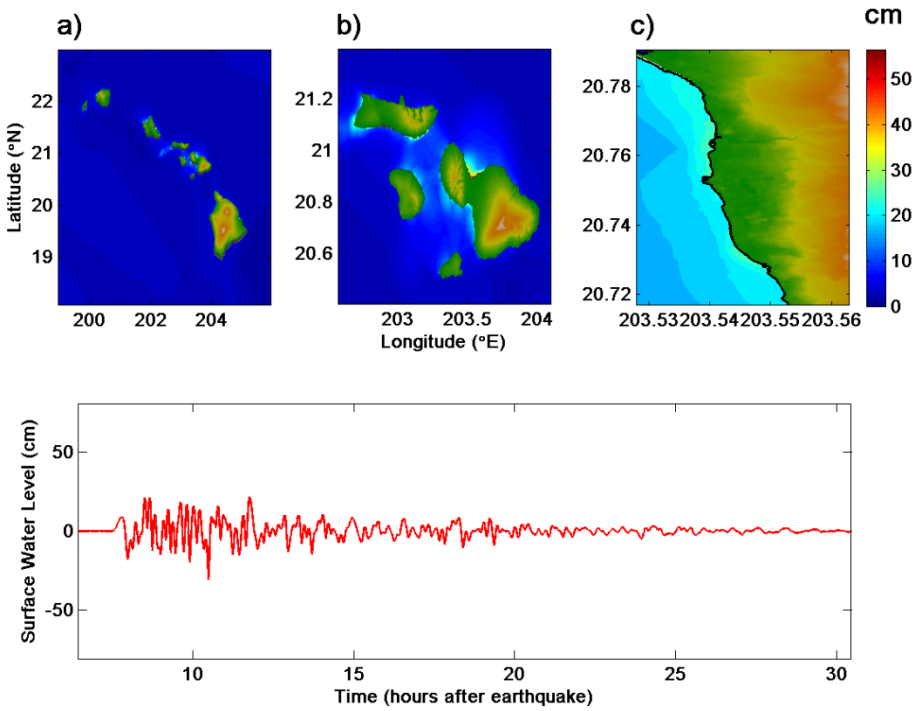

Figure 14. Plot of maximum tsunami wave amplitude distribution and tsunami time series at the warning point for 1994 East Kuril tsunami with reference model, a) A-grid, b) B-grid and c) C-grid.

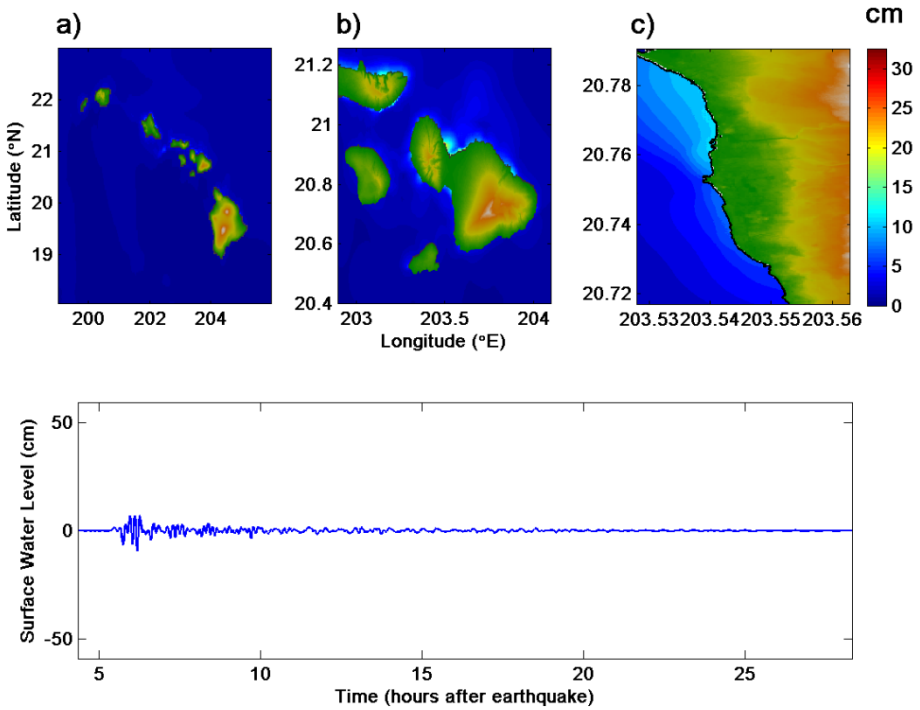

Figure 15. Plot of maximum tsunami wave amplitude distribution and tsunami time series at the warning point for 2003 Rat Island tsunami with forecast model, a) A-grid, b) B-grid and c) C-grid.

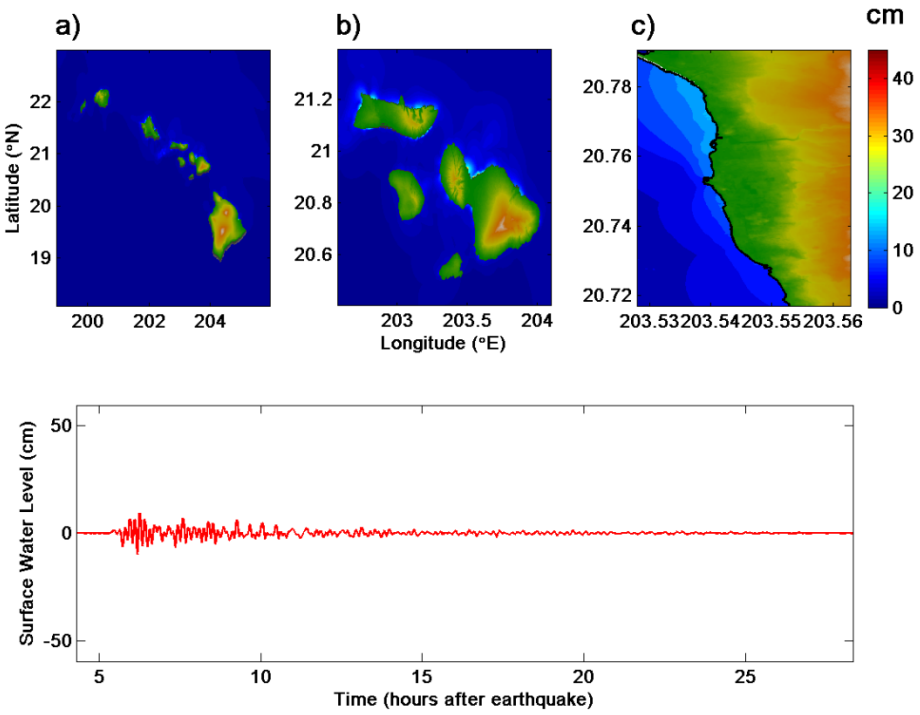

Figure 16. Plot of maximum tsunami wave amplitude distribution and tsunami time series at the warning point for 2003 Rat Island tsunami with reference model, a) A-grid, b) B-grid and c) C-grid.

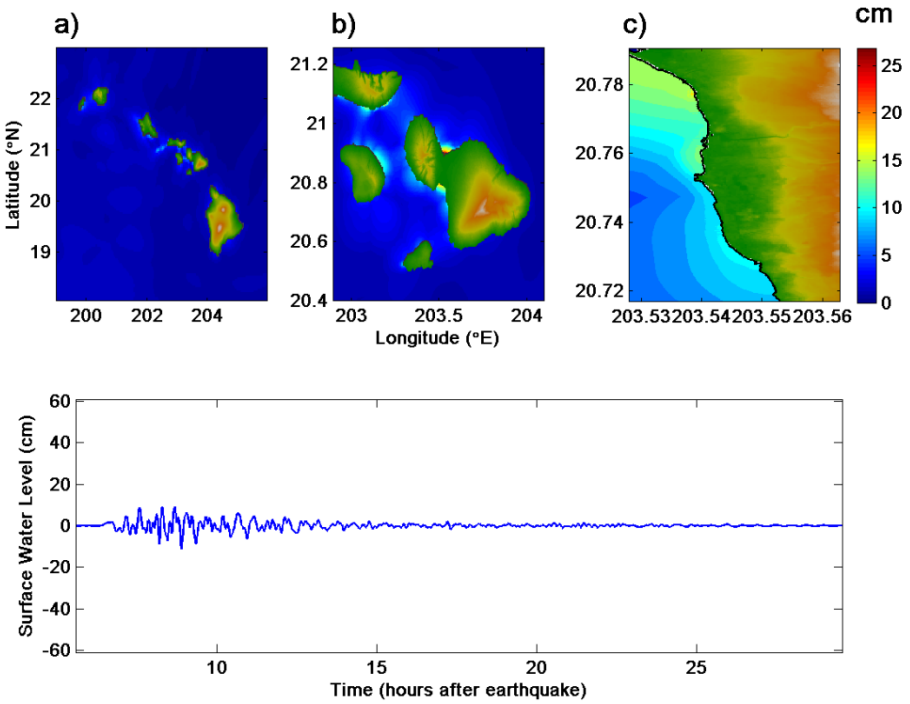

Figure 17. Plot of maximum tsunami wave amplitude distribution and tsunami time series at the warning point for 2006 Tonga tsunami with forecast model, a) A-grid, b) B-grid and c) C-grid.

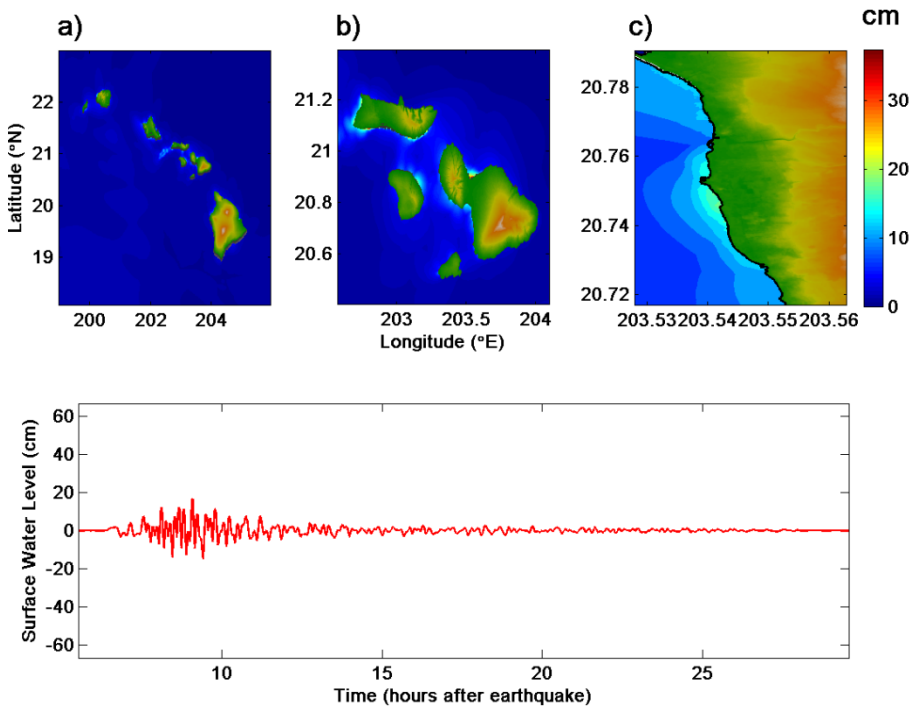

Figure 18. Plot of maximum tsunami wave amplitude distribution and tsunami time series at the warning point for 2006 Tonga tsunami with reference model, a) A-grid, b) B-grid and c) C-grid.

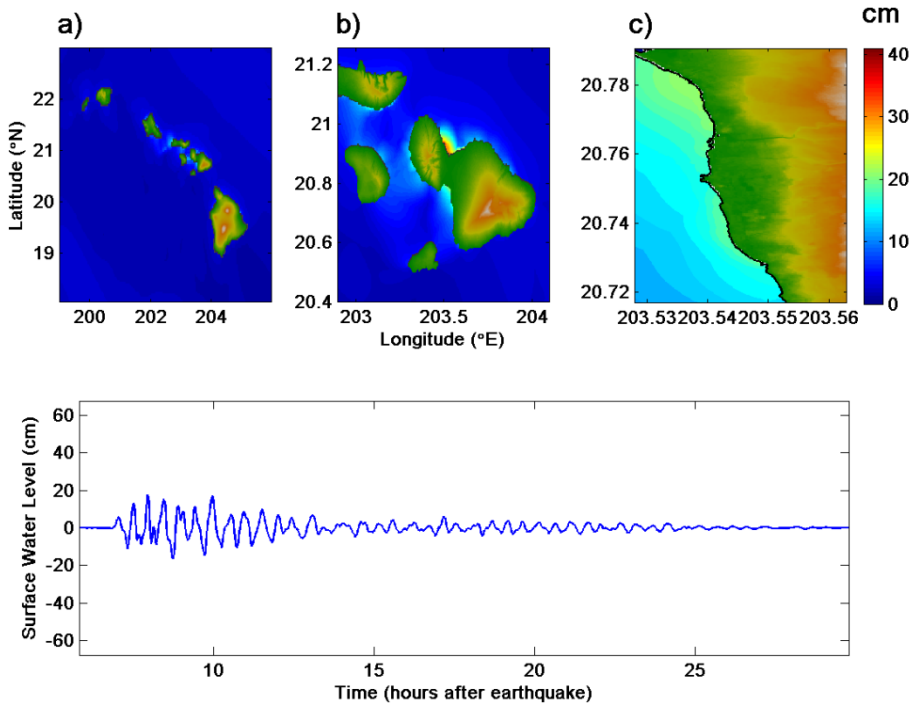

Figure 19. Plot of maximum tsunami wave amplitude distribution and tsunami time series at the warning point for 2006 Kuril Island tsunami with forecast model, a) A-grid, b) B-grid and c) C-grid.

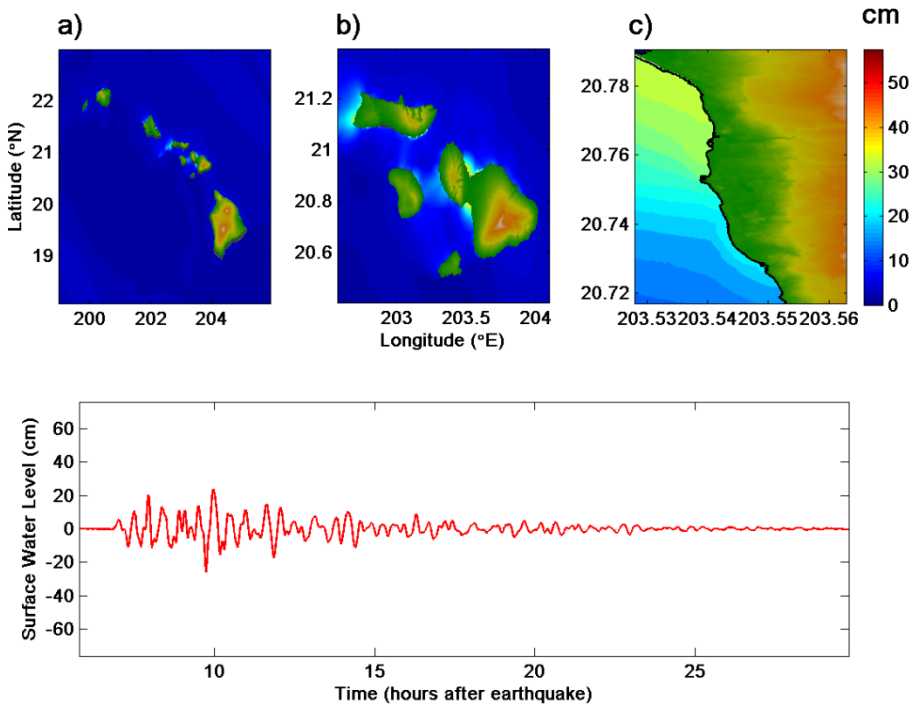

Figure 20. Plot of maximum tsunami wave amplitude distribution and tsunami time series at the warning point for 2006 Kuril Island tsunami with t reference model, a) A-grid, b) B-grid and c) C-grid.

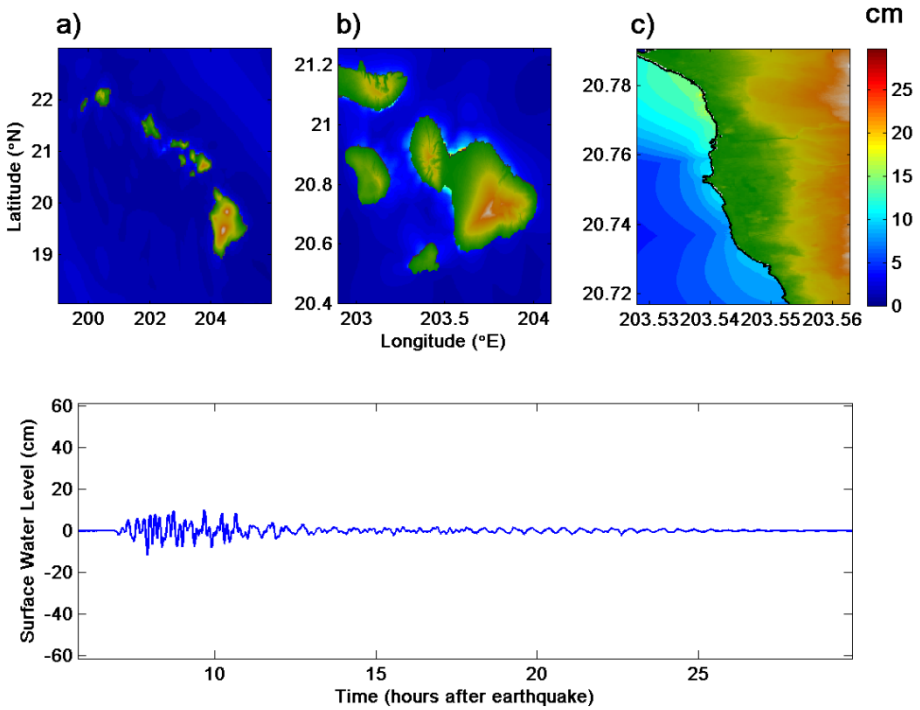

Figure 21. Plot of maximum tsunami wave amplitude distribution and tsunami time series at the warning point for 2007 Kuril Island tsunami with forecast model, a) A-grid, b) B-grid and c) C-grid.

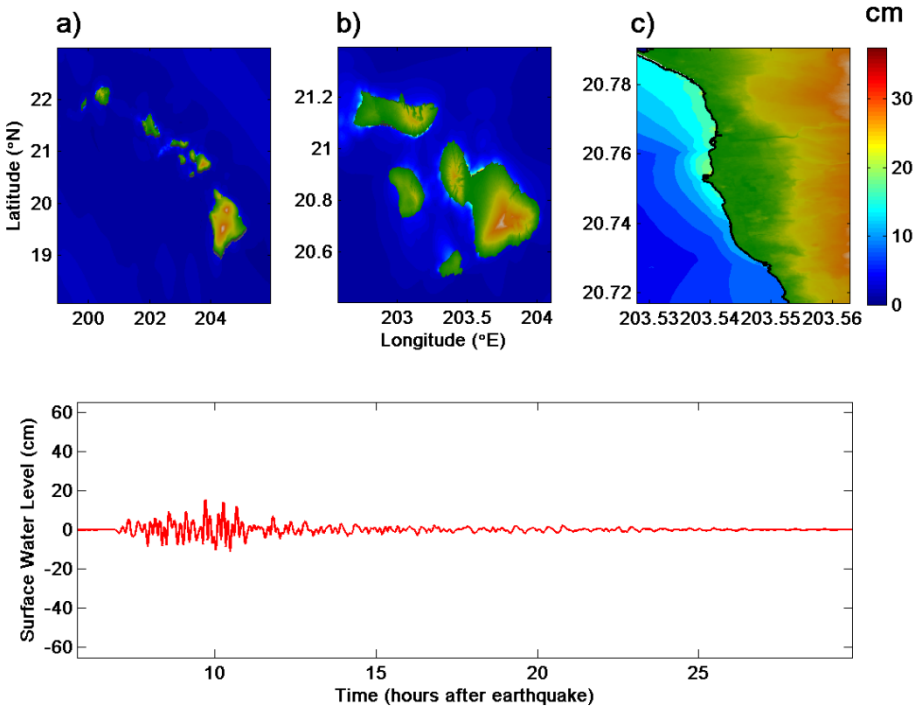

Figure 22. Plot of maximum tsunami wave amplitude distribution and tsunami time series at the warning point for 2007 Kuril Island tsunami with reference model, a) A-grid, b) B-grid and c) C-grid.

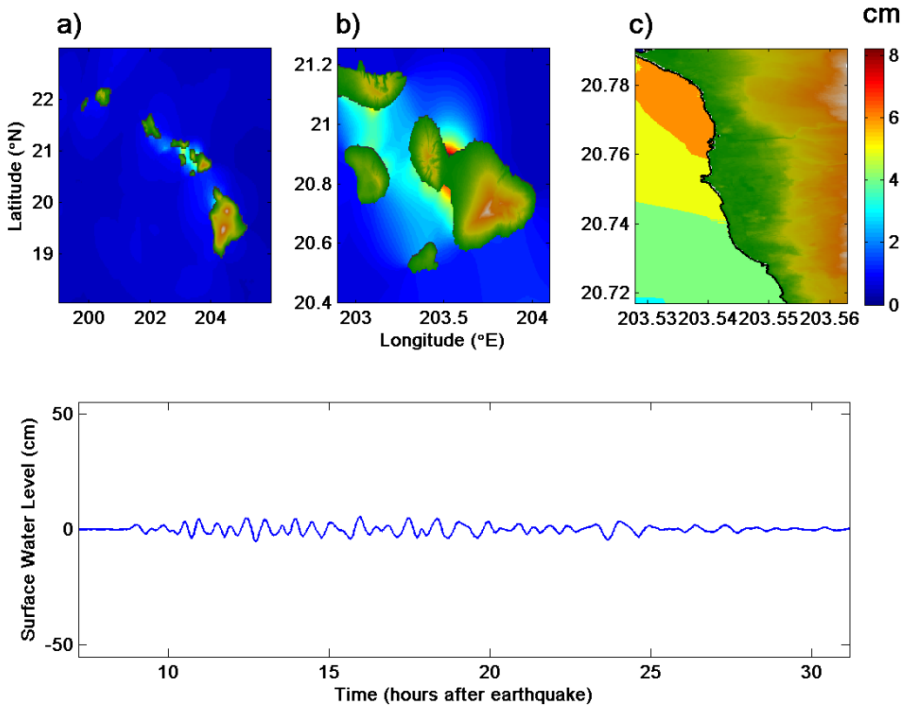

Figure 23. Plot of maximum tsunami wave amplitude distribution and tsunami time series at the warning point for 2007 Solomon tsunami with forecast model, a) A-grid, b) B-grid and c) C-grid.

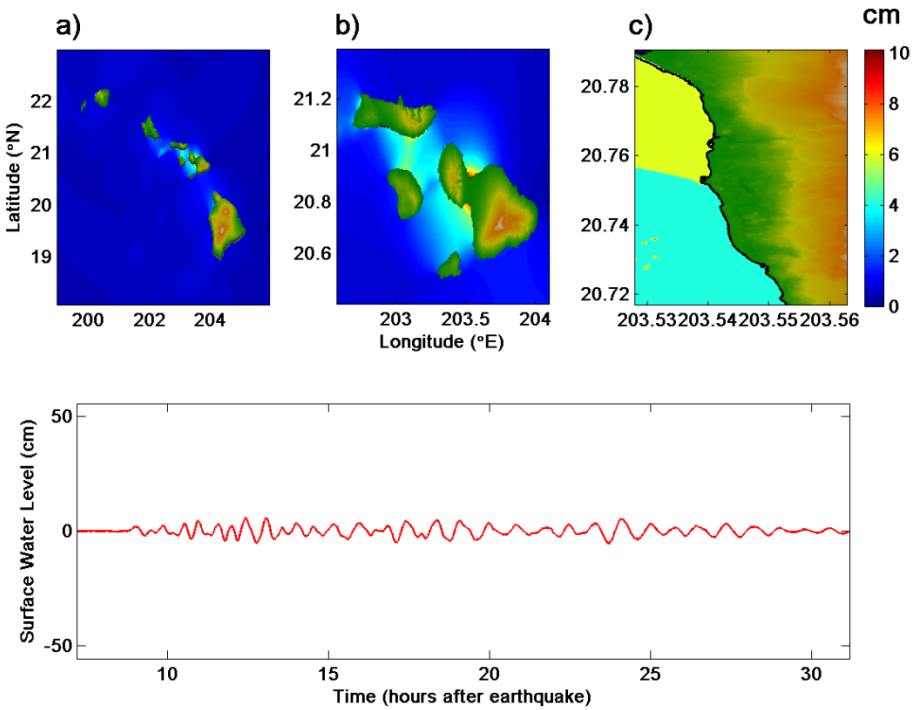

Figure 24. Plot of maximum tsunami wave amplitude distribution and tsunami time series at the warning point for 2007 Solomon tsunami with reference model, a) A-grid, b) B-grid and c) C-grid.

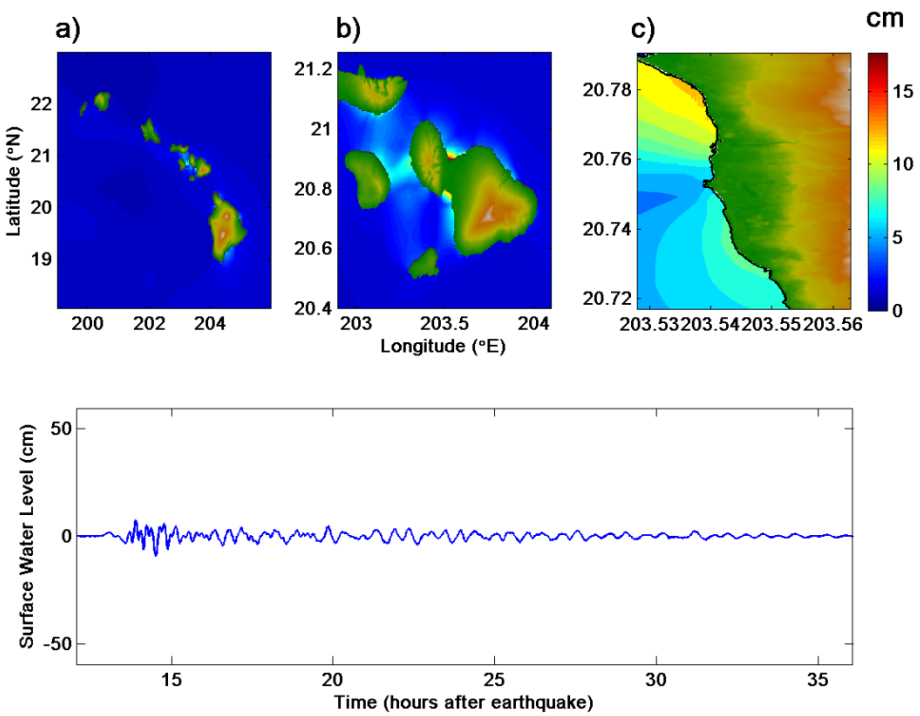

Figure 25. Plot of maximum tsunami wave amplitude distribution and tsunami time series at the warning point for 2007 Peru tsunami with forecast model, a) A-grid, b) B-grid and c) C-grid.

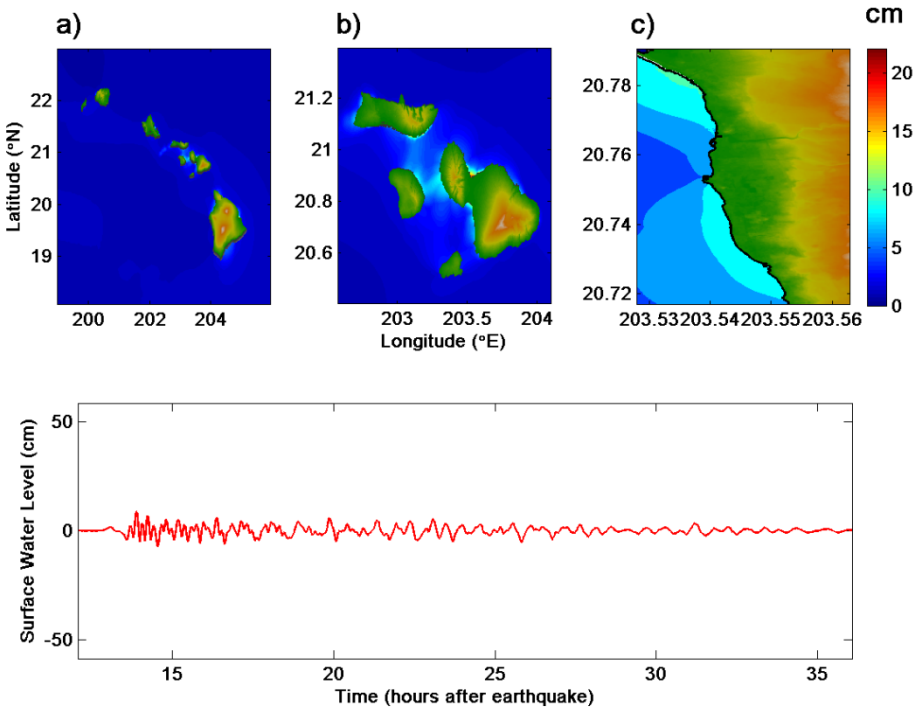

Figure 26. Plot of maximum tsunami wave amplitude distribution and tsunami time series at the warning point for 2007 Peru tsunami with reference model, a) A-grid, b) B-grid and c) C-grid.

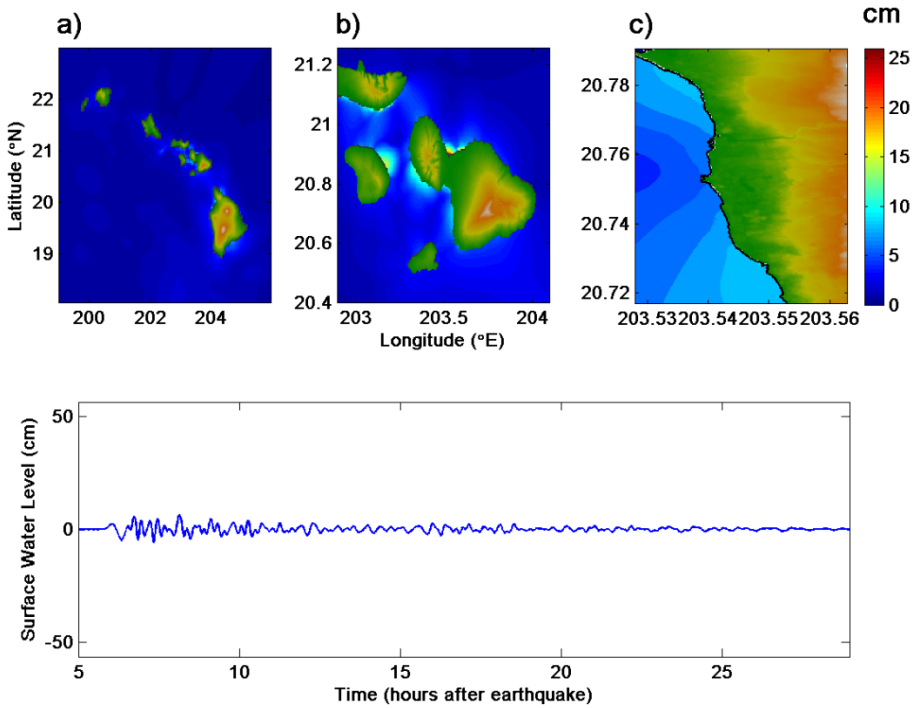

Figure 27. Plot of maximum tsunami wave amplitude distribution and tsunami time series at the warning point for 2009 Samoa tsunami with forecast model, a) A-grid, b) B-grid and c) C-grid.

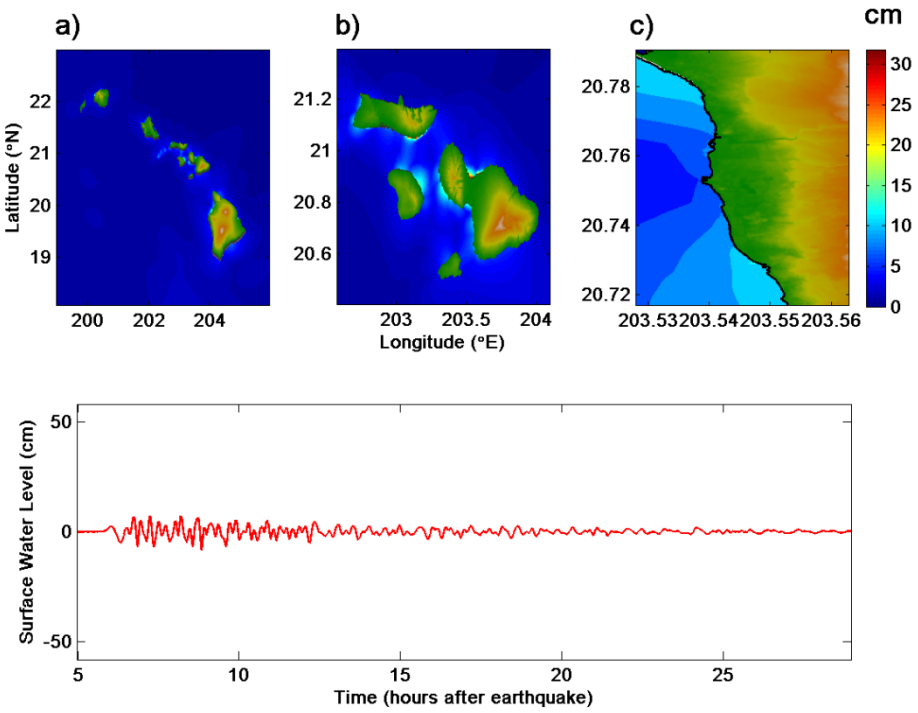

Figure 28. Plot of maximum tsunami wave amplitude distribution and tsunami time series at the warning point for 2009 Samoa tsunami with reference model, a) A-grid, b) B-grid and c) C-grid.

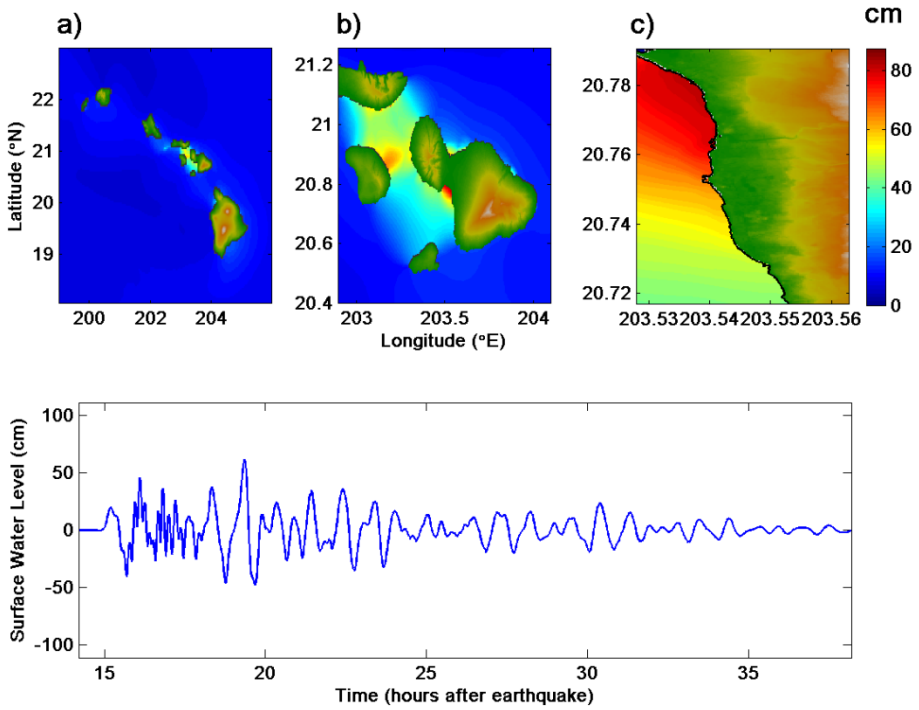

Figure 29. Plot of maximum tsunami wave amplitude distribution and tsunami time series at the warning point for 2010 Chile tsunami with forecast model, a) A-grid, b) B-grid and c) C-grid.

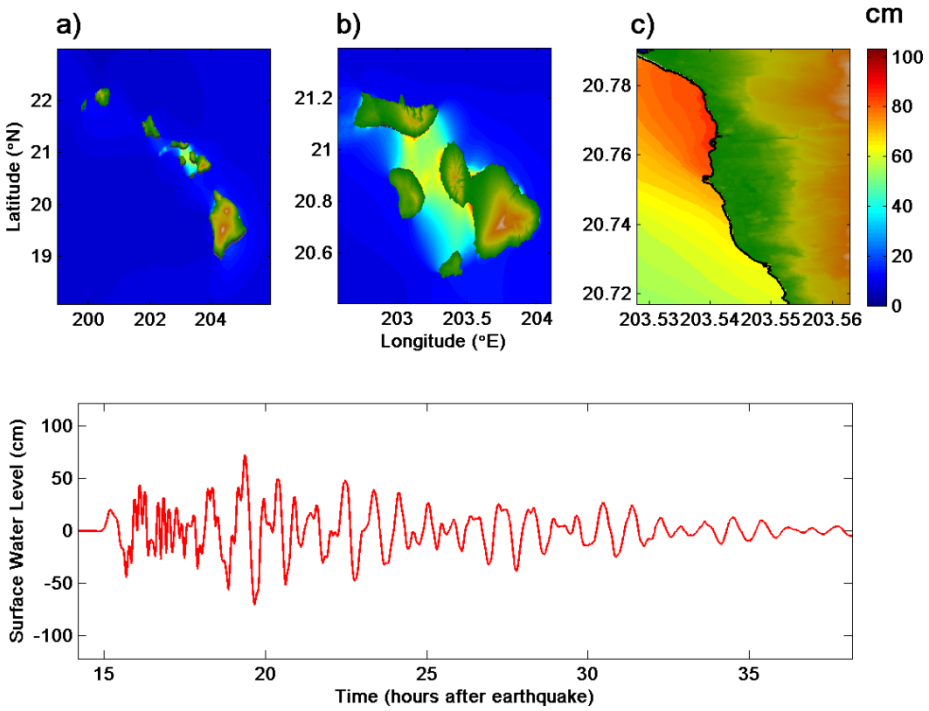

Figure 30. Plot of maximum tsunami wave amplitude distribution and tsunami time series at the warning point for 2010 Chile tsunami with reference model, a) A-grid, b) B-grid and c) C-grid.

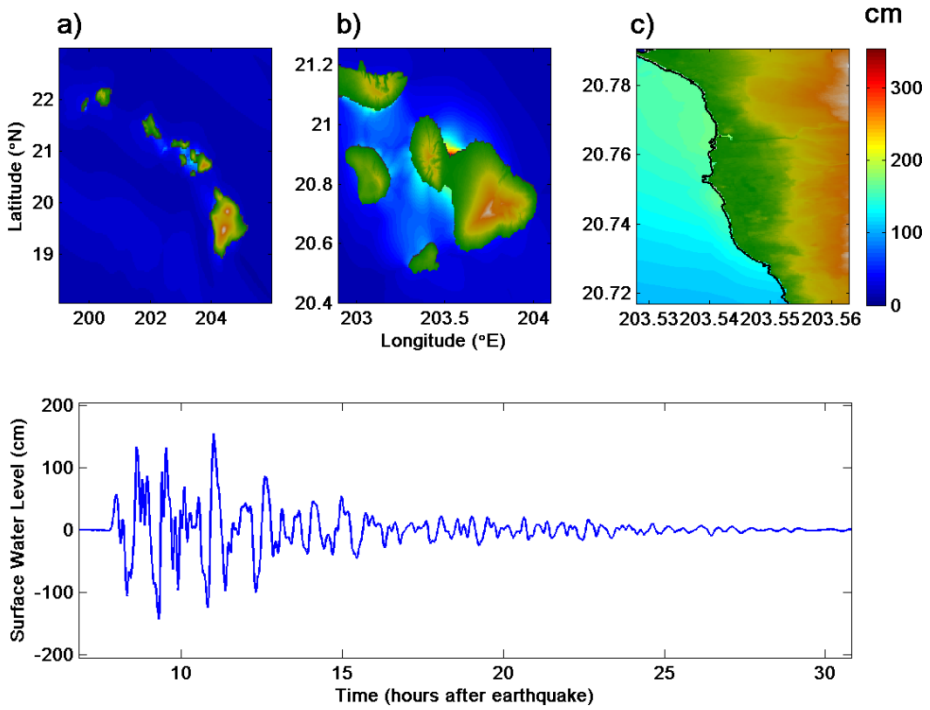

Figure 31. Plot of maximum tsunami wave amplitude distribution and tsunami time series at the warning point for 2011 Honshu tsunami with forecast model, a) A-grid, b) B-grid and c) C-grid.

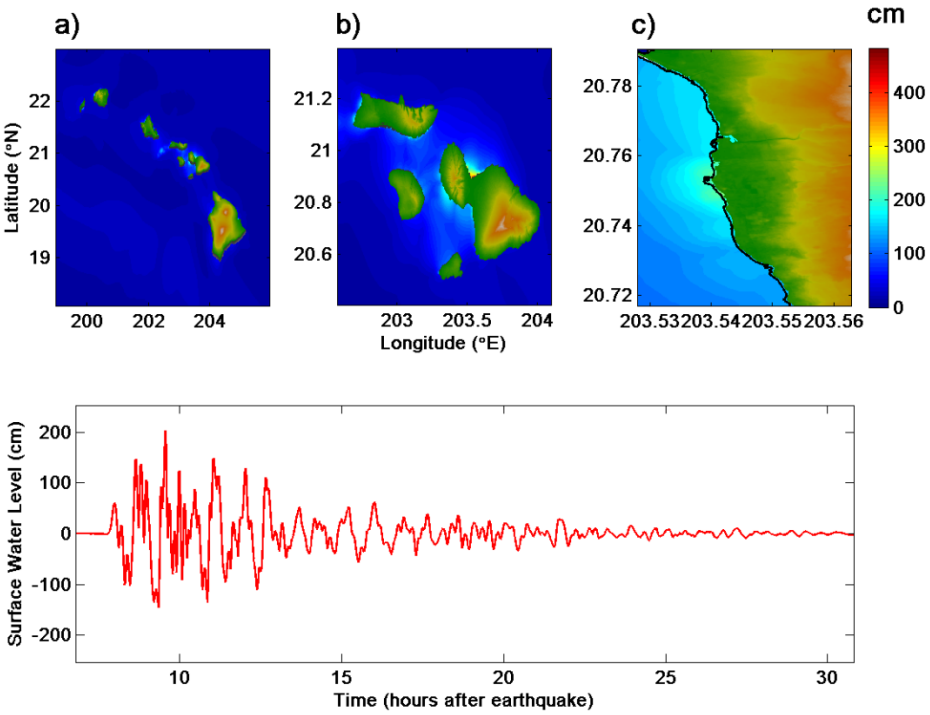

Figure 32. Plot of maximum tsunami wave amplitude distribution and tsunami time series at the warning point for 2011 Honshu tsunami with reference model, a) A-grid, b) B-grid and c) C-grid.

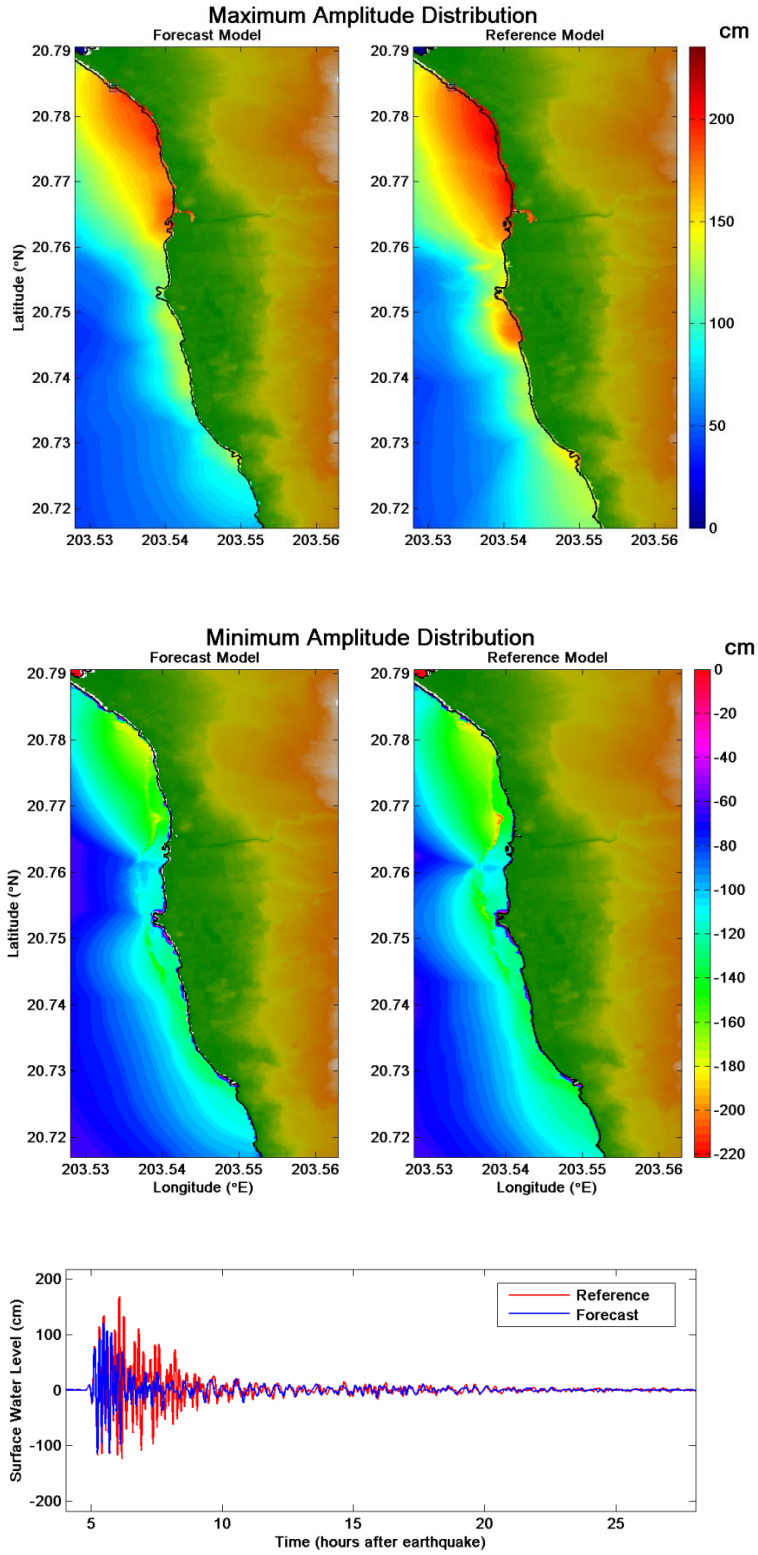

Figure 33. Comparative plot of maximum/minimum tsunami wave amplitude distribution and tsunami time series at the warning point for the 1946 Unimak tsunami between forecast and reference models.

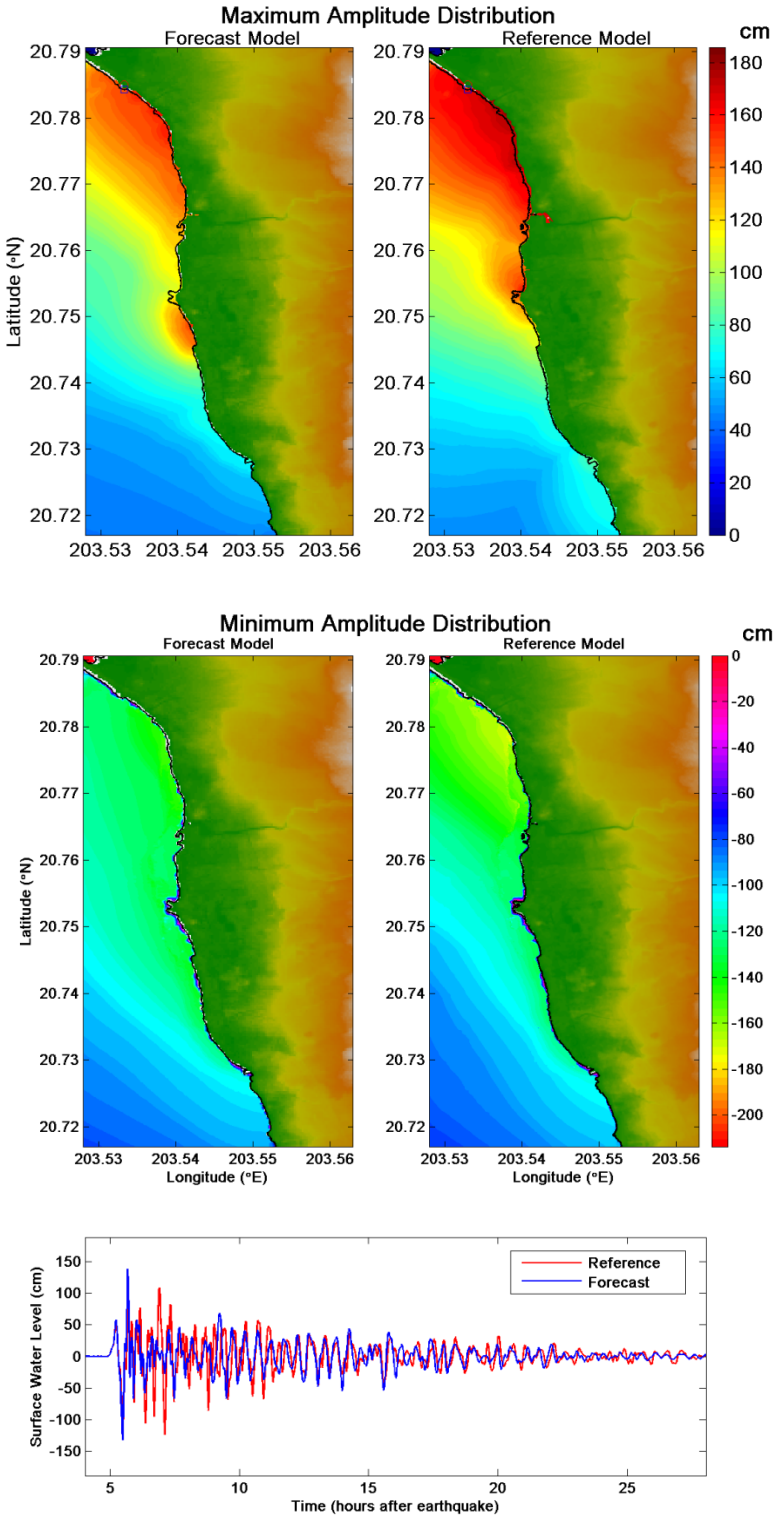

Figure 34. Comparative plot of maximum/minimum tsunami wave amplitude distribution and tsunami time series at the warning point for 1957 Andreanov tsunami between forecast and reference models.

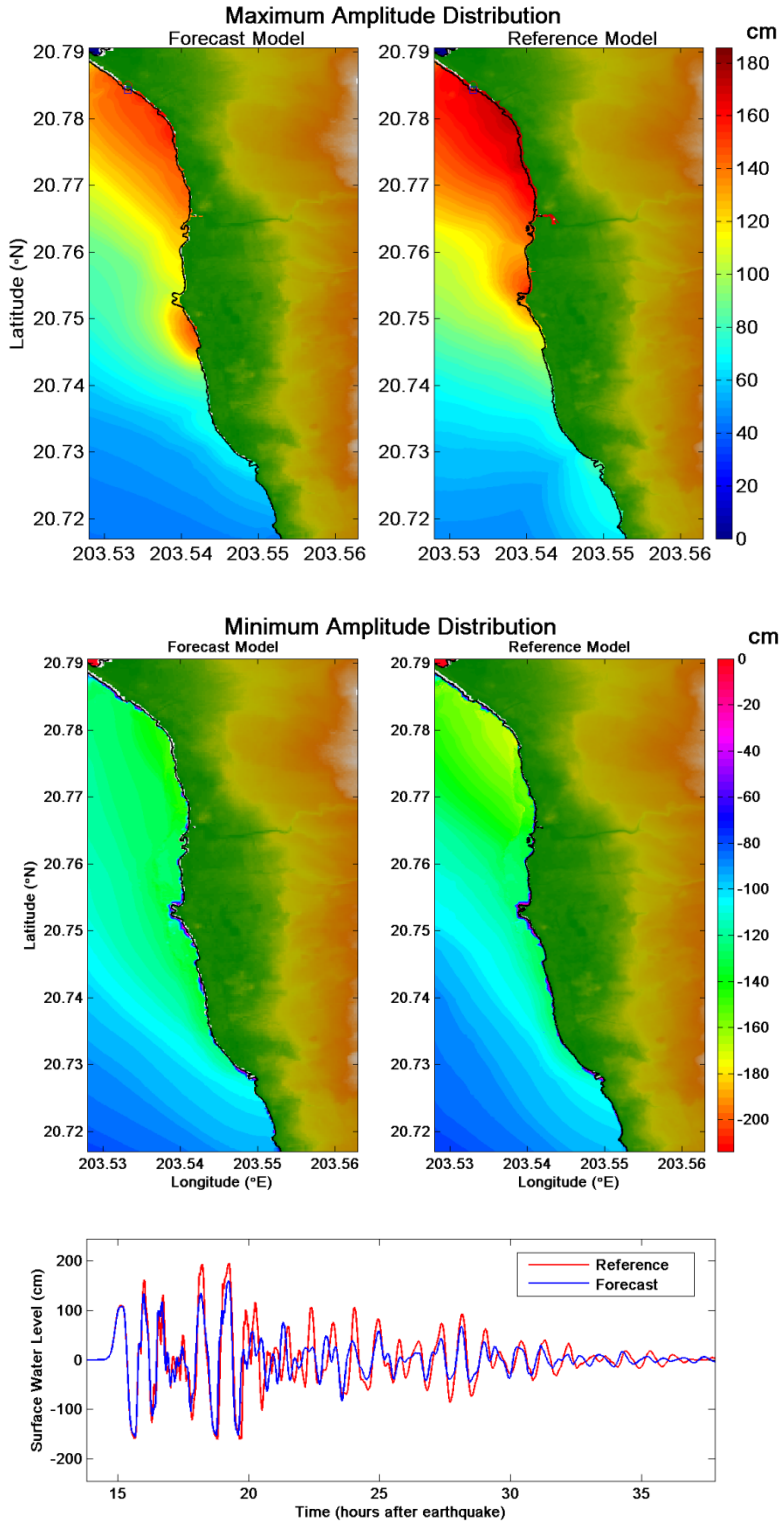

Figure 35. Comparative plot of maximum/minimum tsunami wave amplitude distribution and tsunami time series at the warning point for 1960 Chile tsunami between forecast and reference models.

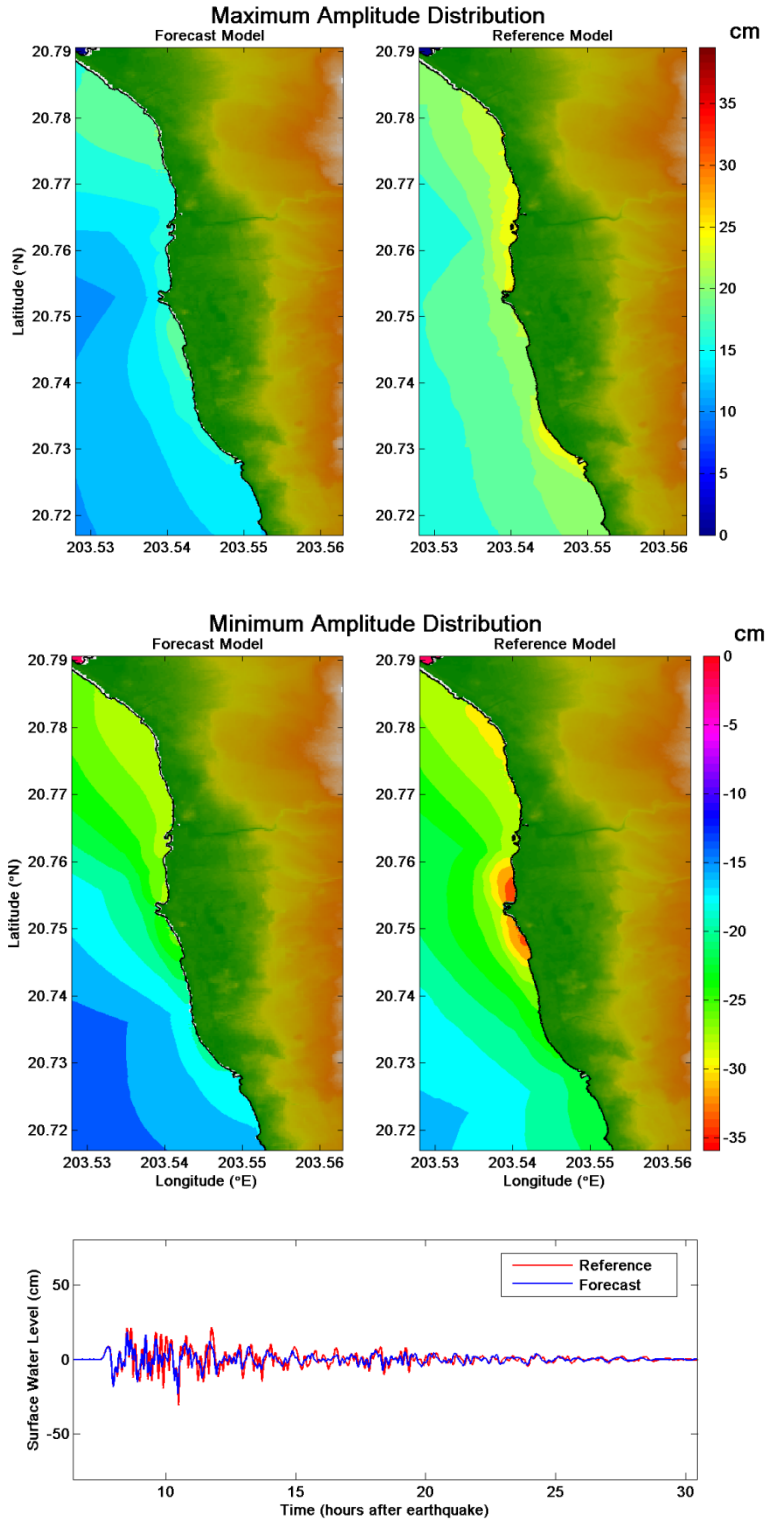

Figure 36. Comparative plot of maximum/minimum tsunami wave amplitude distribution and tsunami time series at the warning point for 1994 East Kuril tsunami between forecast and reference models.

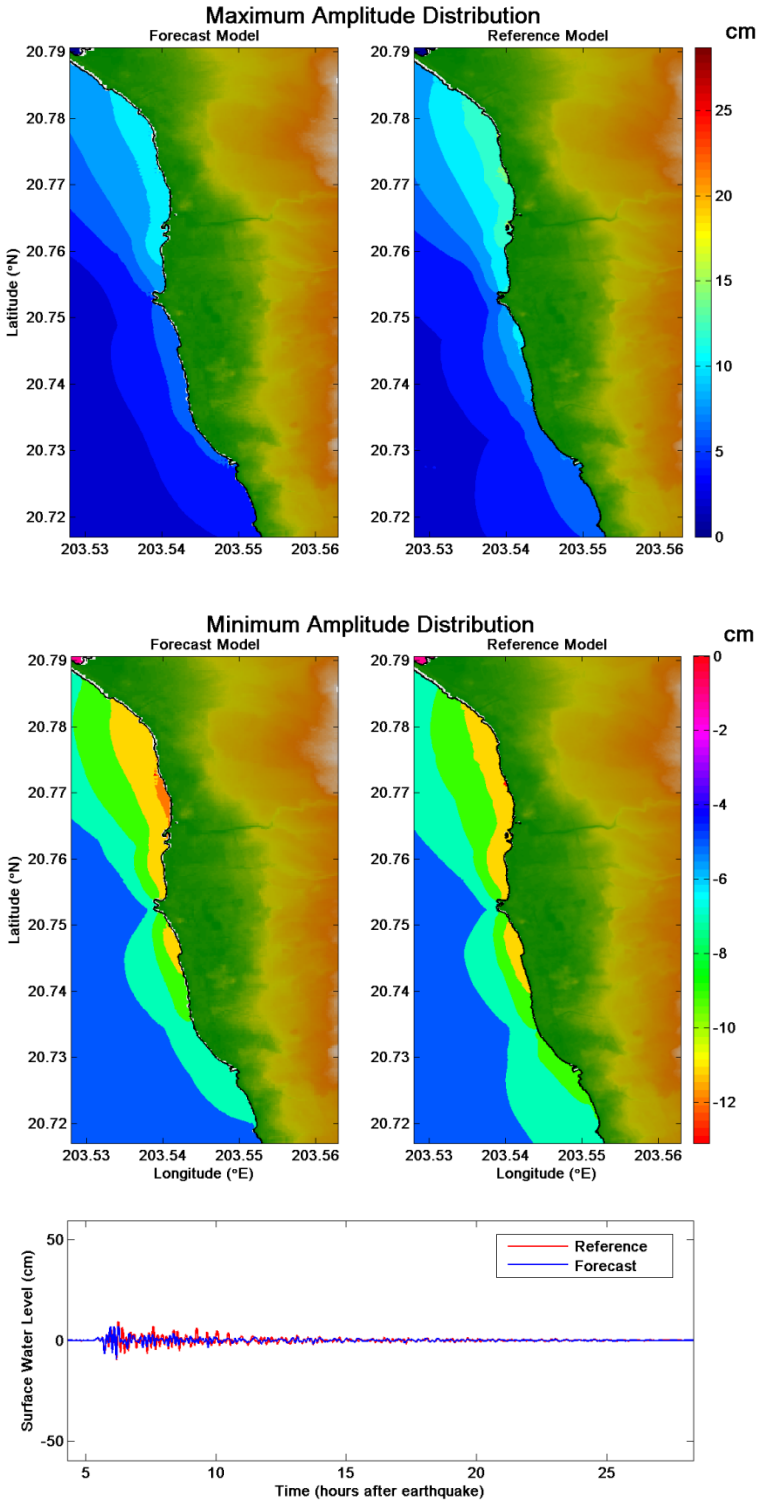

Figure 37. Comparative plot of maximum/minimum tsunami wave amplitude distribution and tsunami time series at the warning point for 2003 Rat Island tsunami between forecast and reference models.

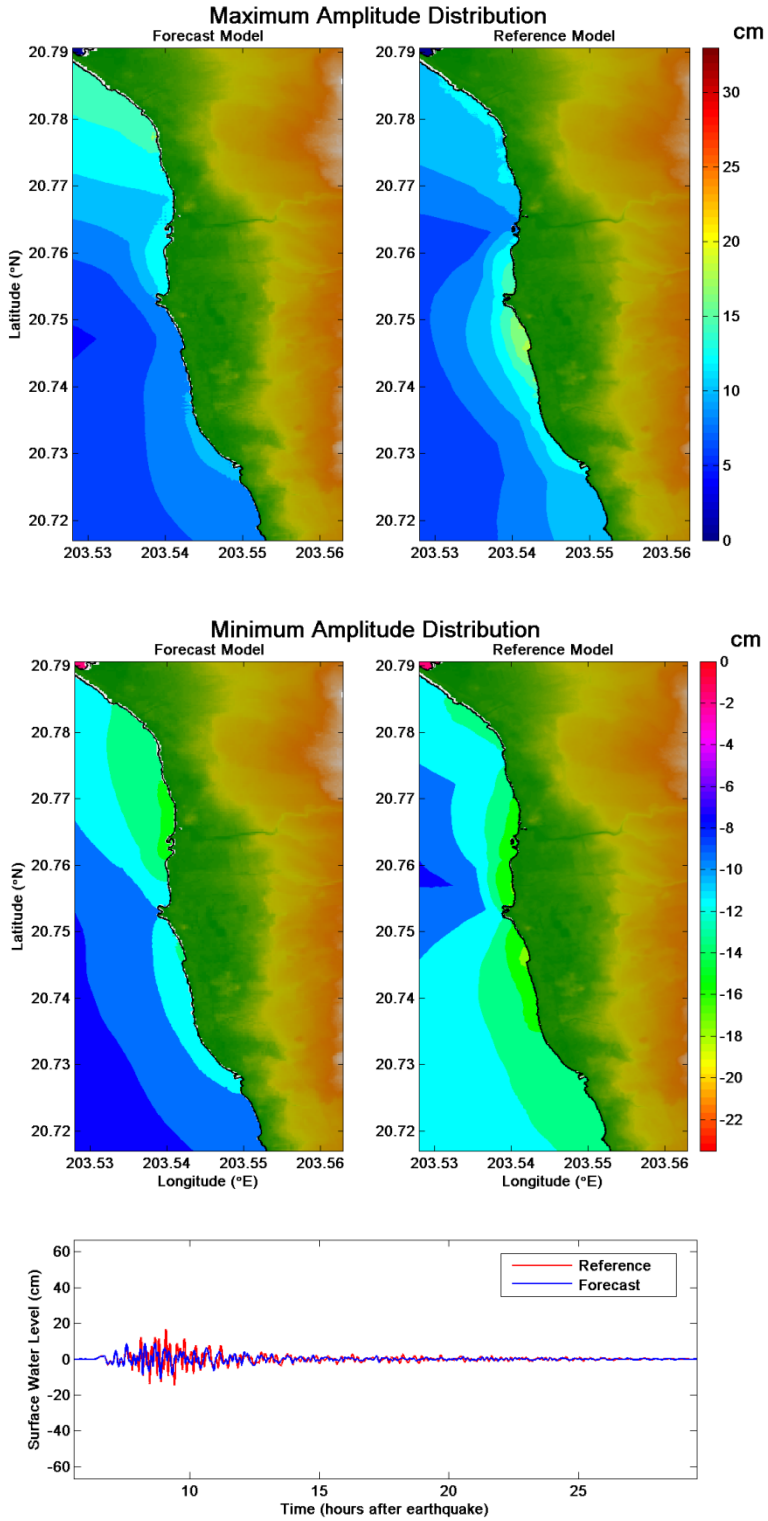

Figure 38. Comparative plot of maximum/minimum tsunami wave amplitude distribution and tsunami time series at the warning point for 2006 Tonga tsunami between forecast and reference models.

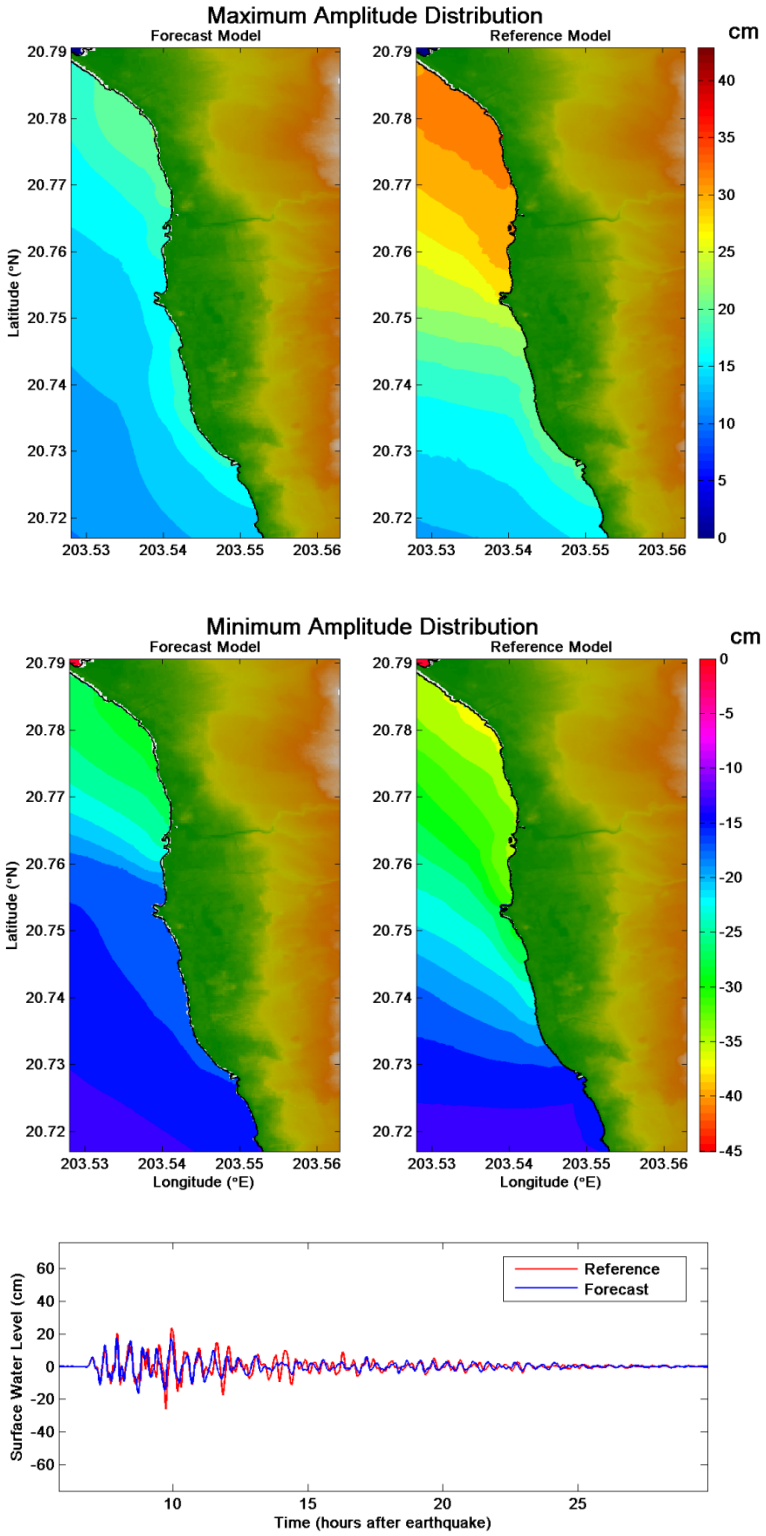

Figure 39. Comparative plot of maximum/minimum tsunami wave amplitude distribution and tsunami time series at the warning point for 2006 Kuril tsunami between forecast and reference models.

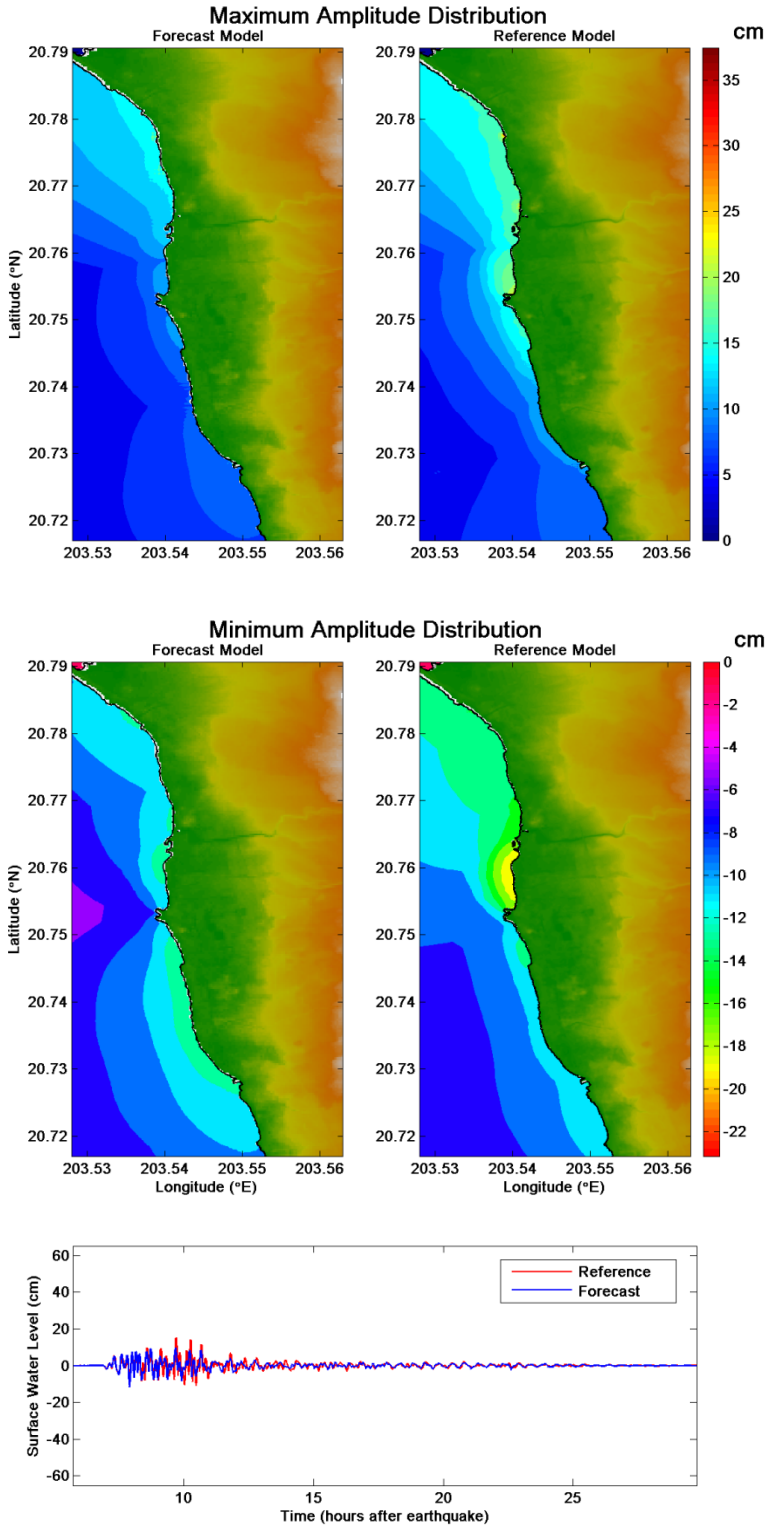

Figure 40. Comparative plot of maximum/minimum tsunami wave amplitude distribution and tsunami time series at the warning point for 2007 Kuril tsunami between forecast and reference models.

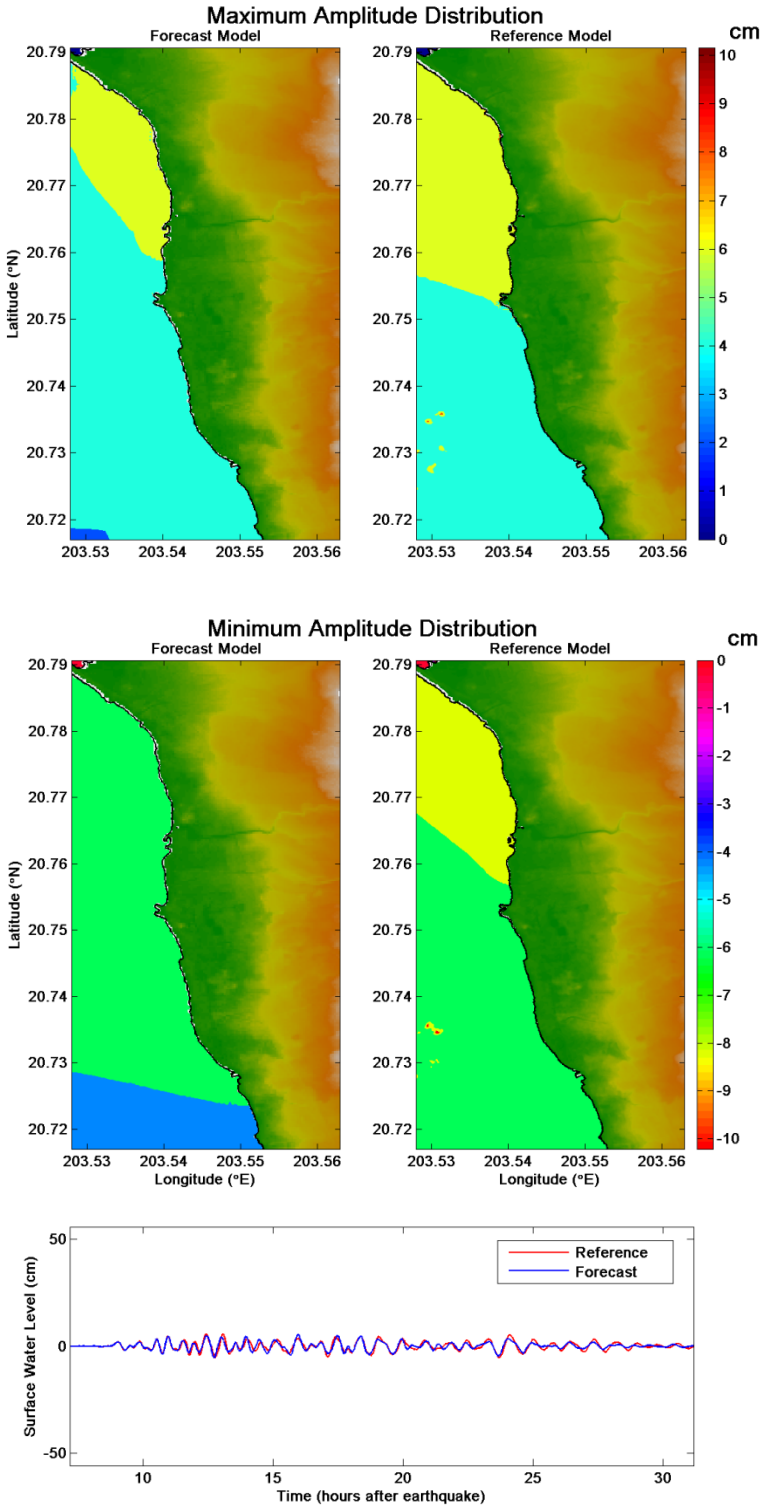

Figure 41. Comparative plot of maximum/minimum tsunami wave amplitude distribution and tsunami time series at the warning point for 2007 Solomon tsunami between forecast and reference models.

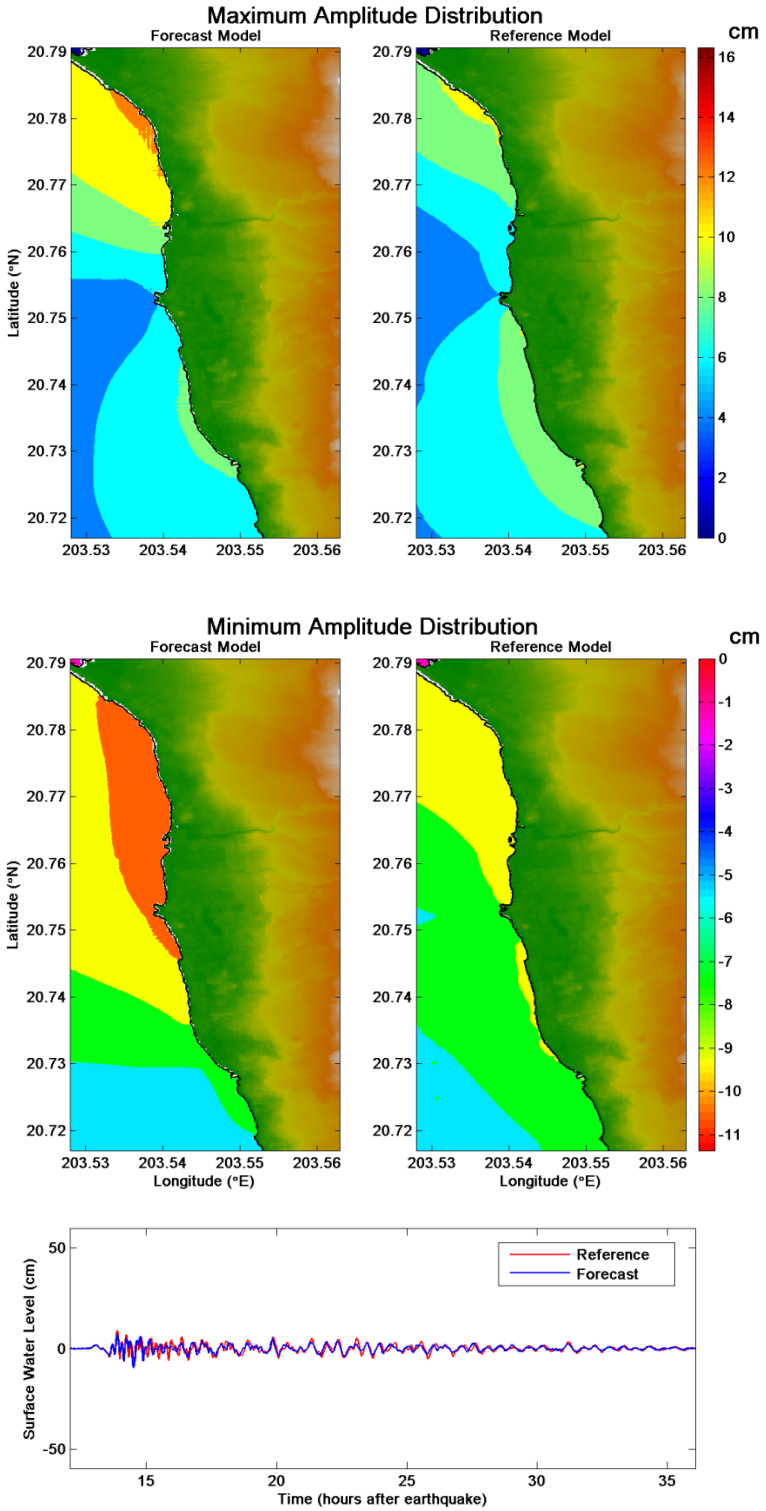

Figure 42. Comparative plot of maximum/minimum tsunami wave amplitude distribution and tsunami time series at the warning point for 2007 Peru tsunami between forecast and reference models.

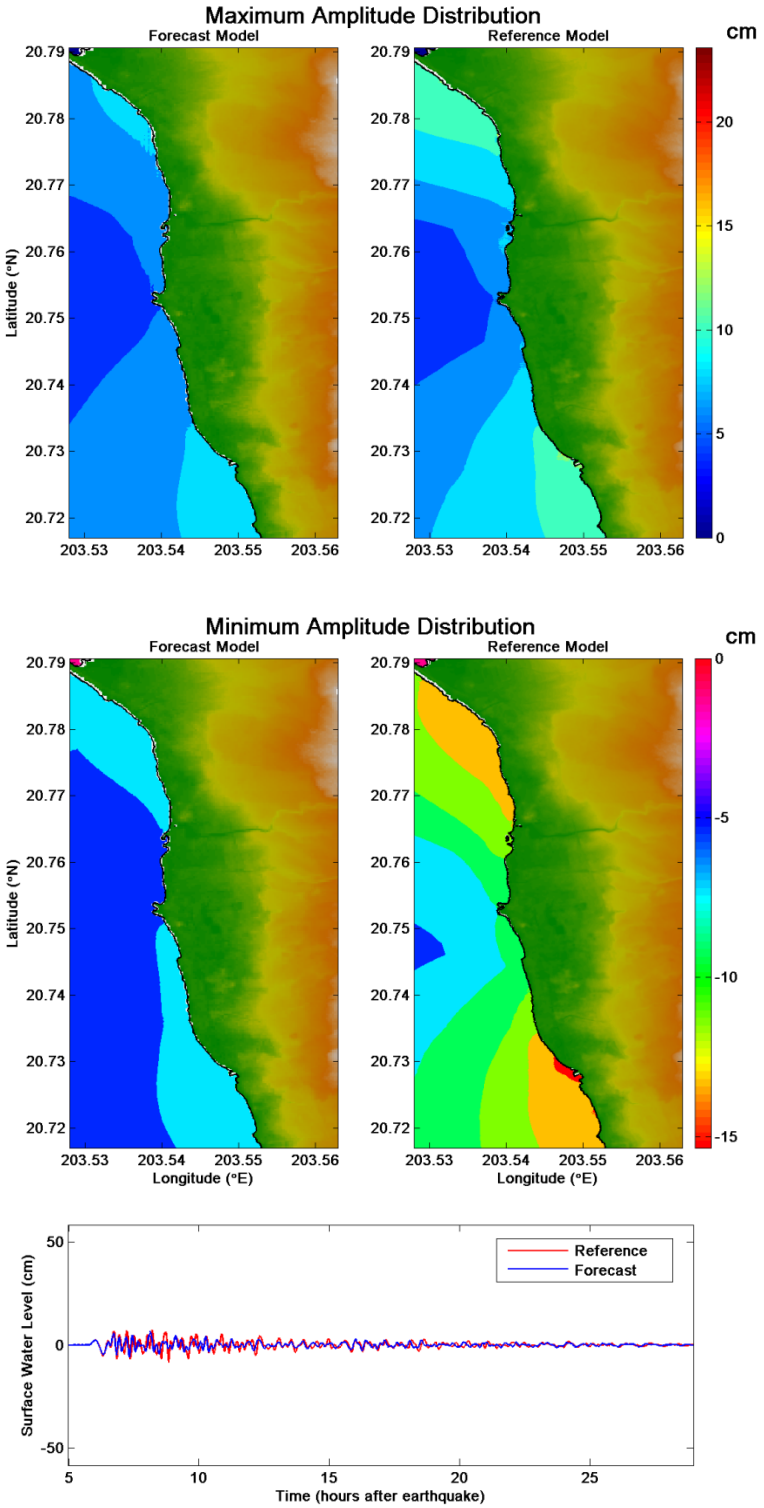

Figure 43. Comparative plot of maximum/minimum tsunami wave amplitude distribution and tsunami time series at at the warning point for 2009 Samoa tsunami between forecast and reference models.

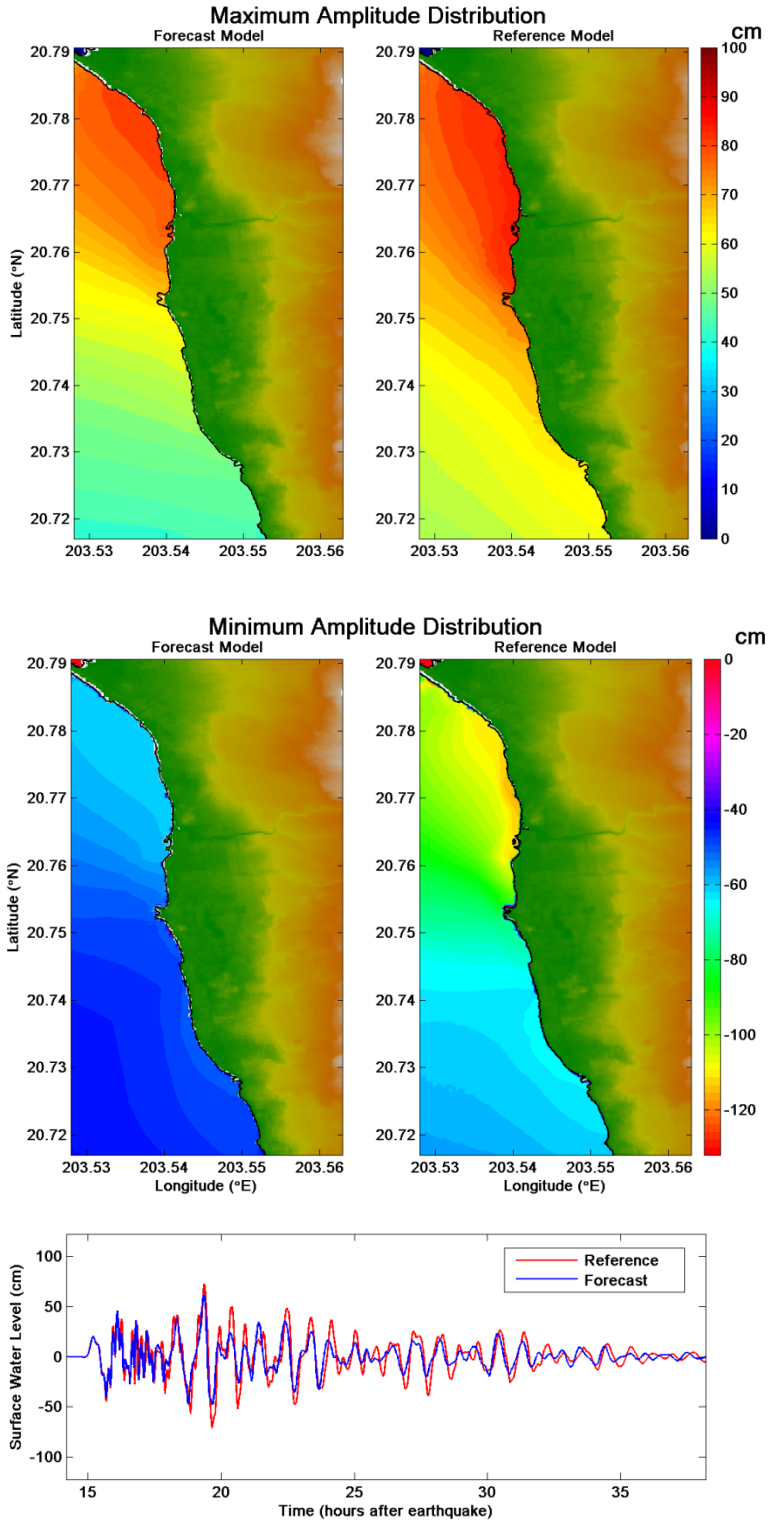

Figure 44. Comparative plot of maximum/minimum tsunami wave amplitude distribution and tsunami time series at the warning point for 2010 Chile tsunami between forecast and reference models.

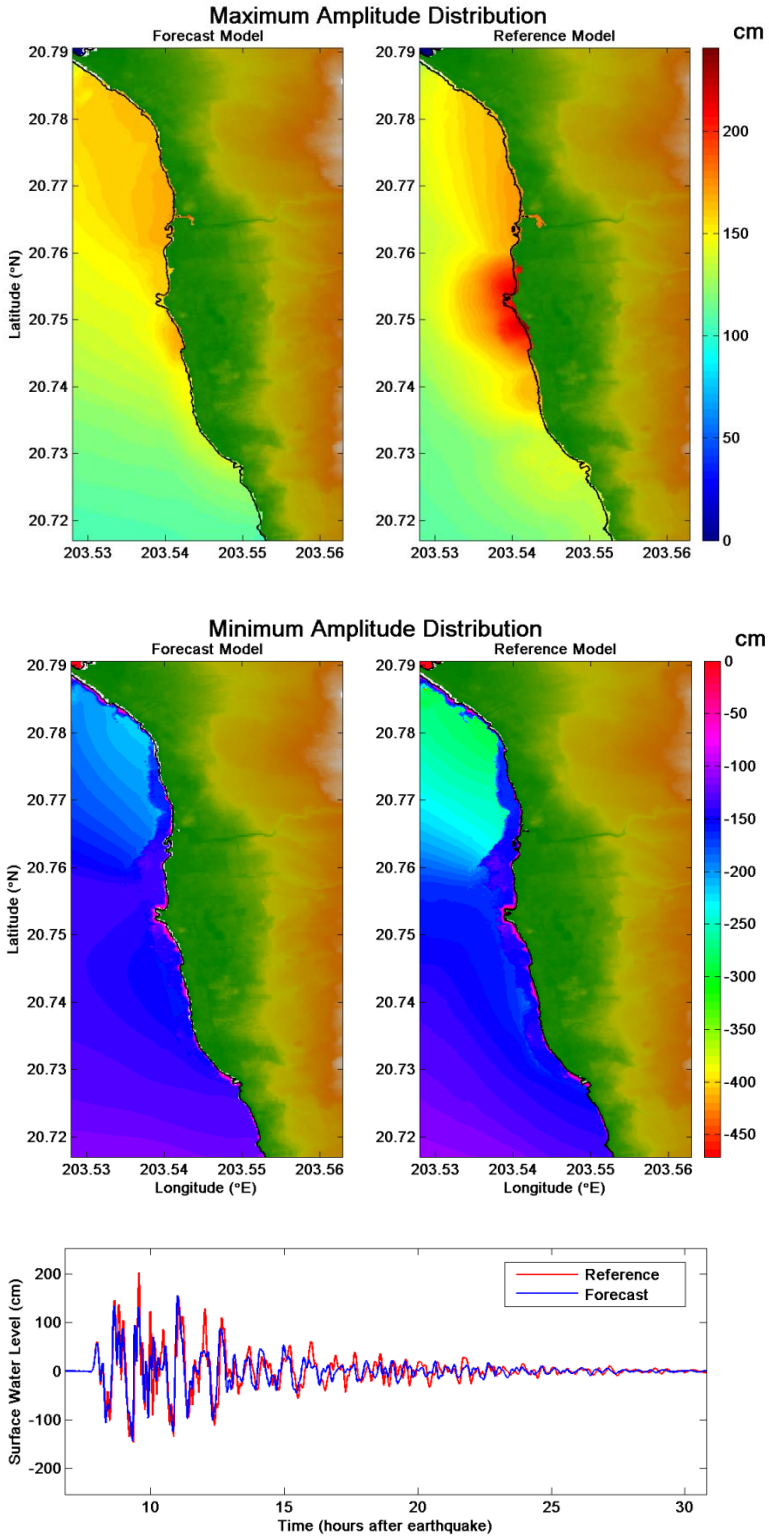

Figure 45. Comparative plot of maximum/minimum tsunami wave amplitude distribution and tsunami time series at the warning point for 2011 Honshu tsunami between forecast and reference models.

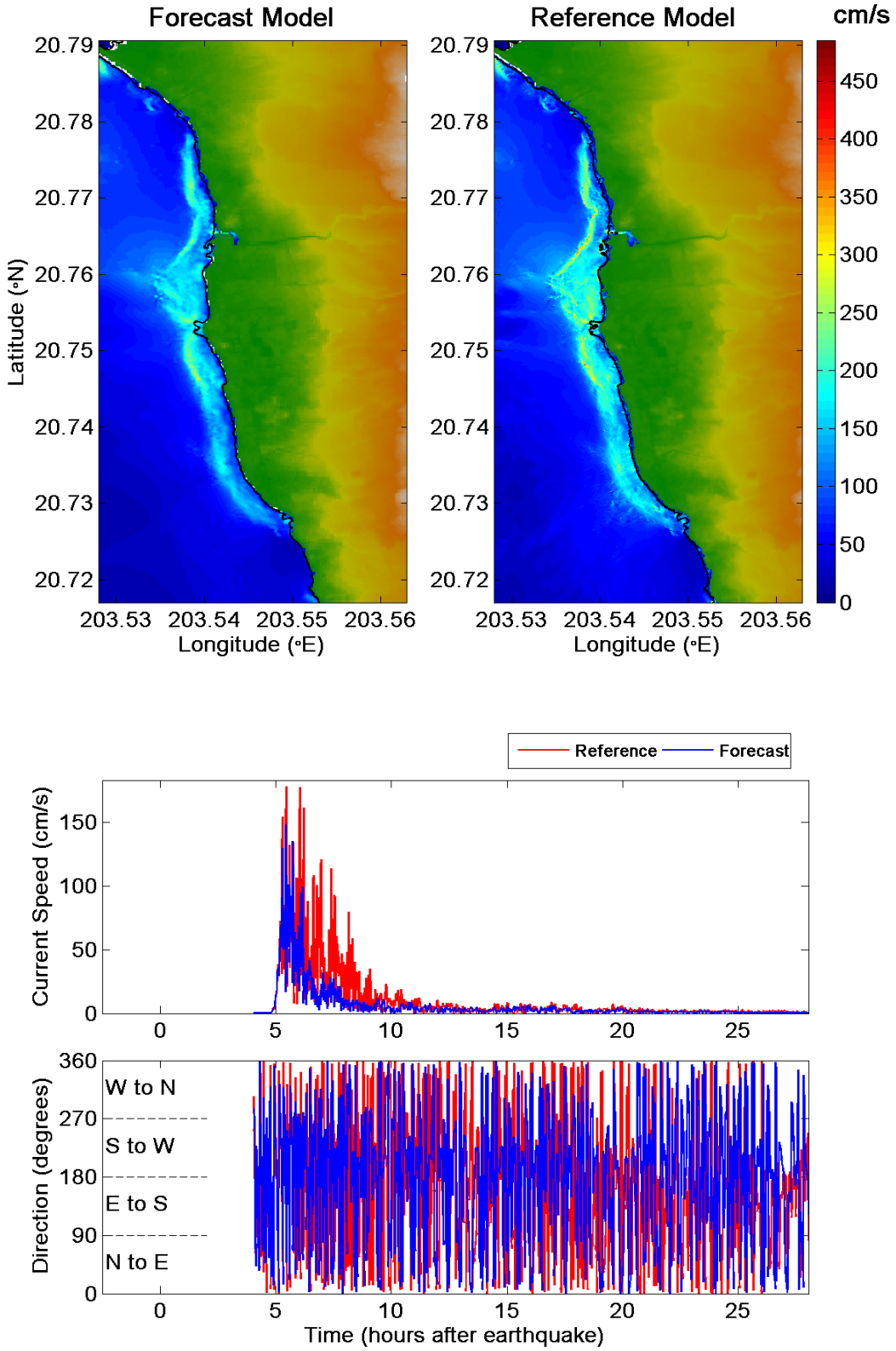

Figure 46. Comparative plot of maximum current speed distribution, current speed and directionality at the warning point for 1946 Unimak tsunami between forecast and reference models.

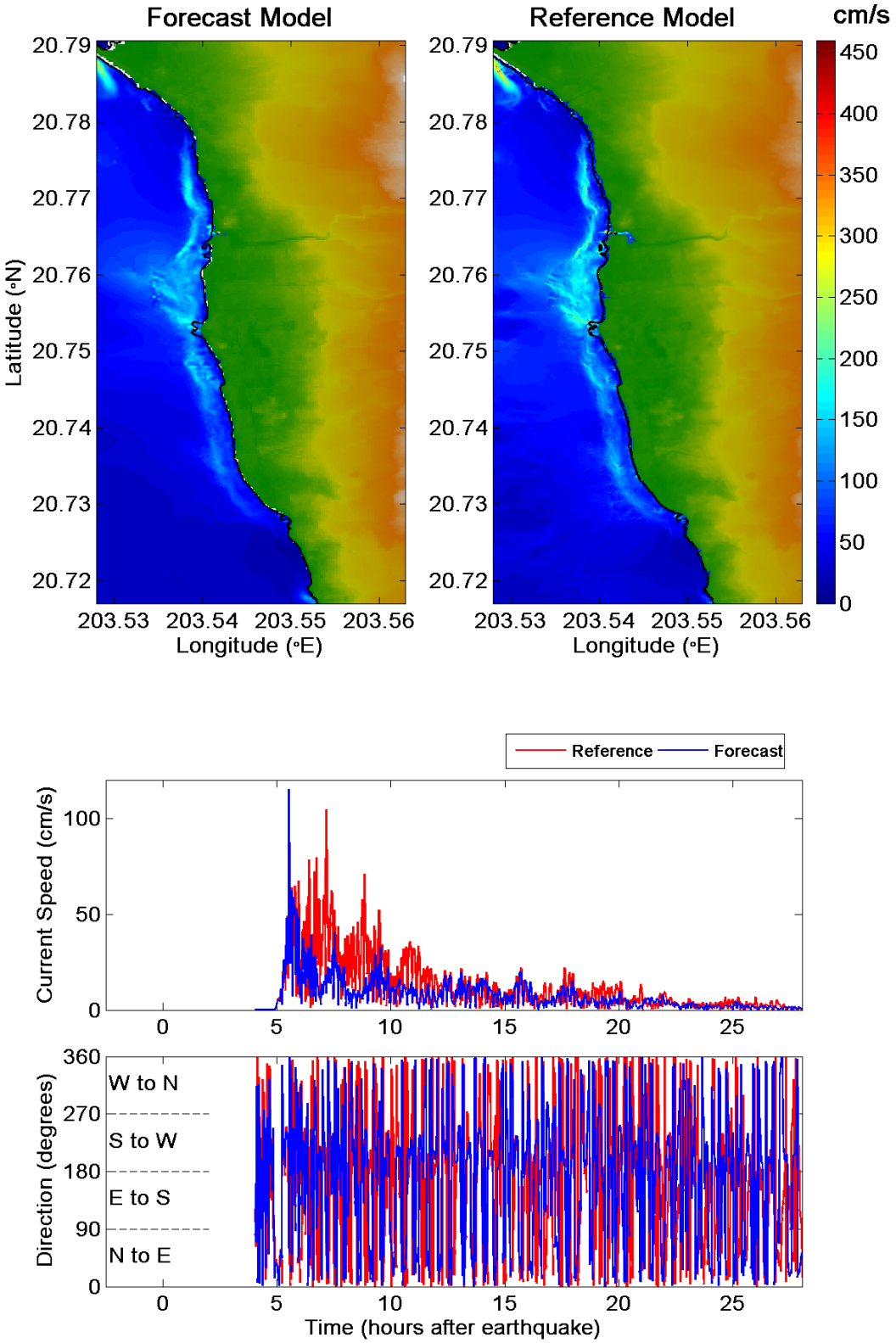

Figure 47. Comparative plot of maximum current speed distribution, current speed and directionality at the warning point for 1957 Andreanov tsunami between forecast and reference models.

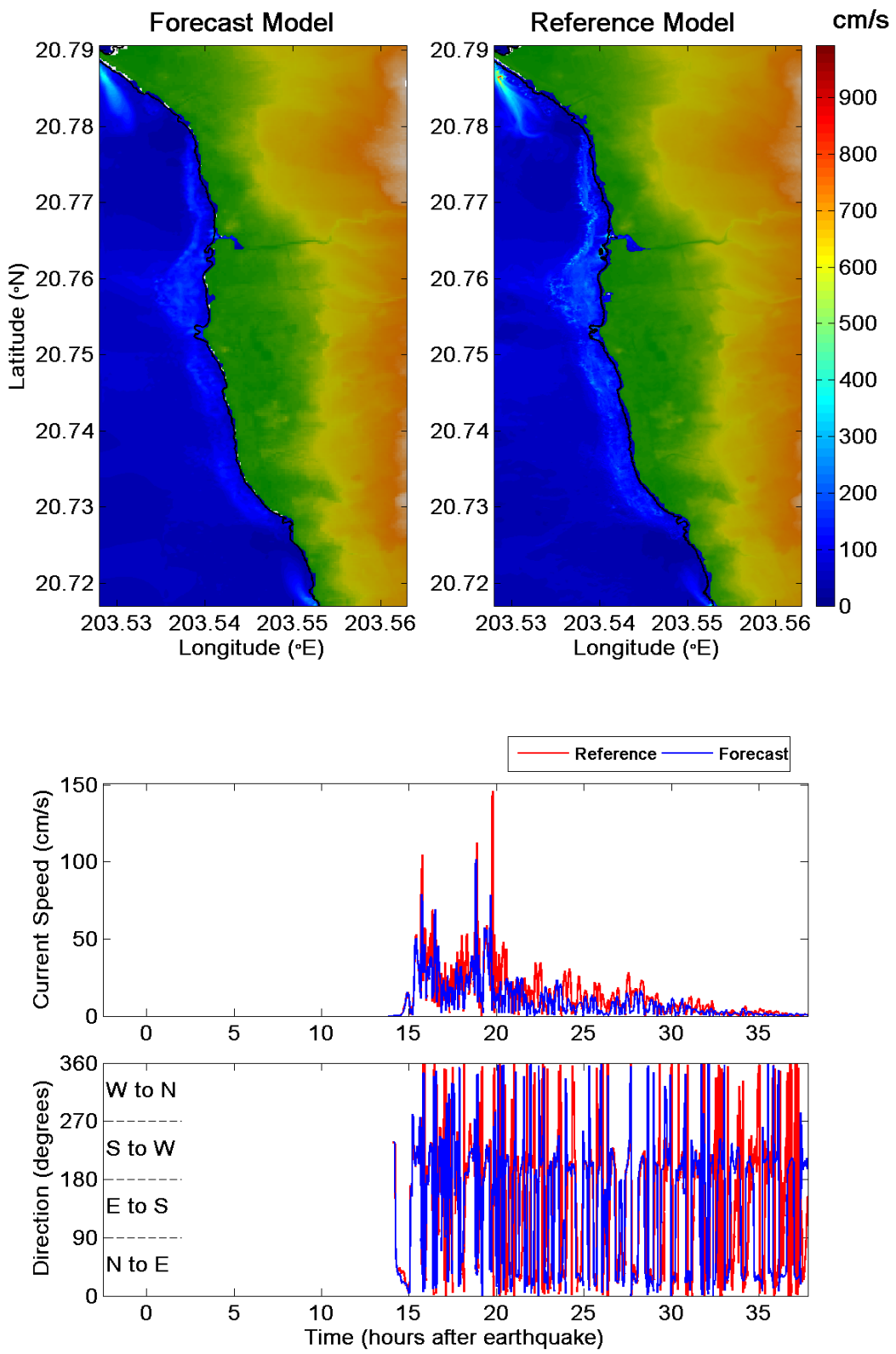

Figure 48. Comparative plot of maximum current speed distribution, current speed and directionality at the warning point at C-grid level for 1960 Chile tsunami between forecast reference models.

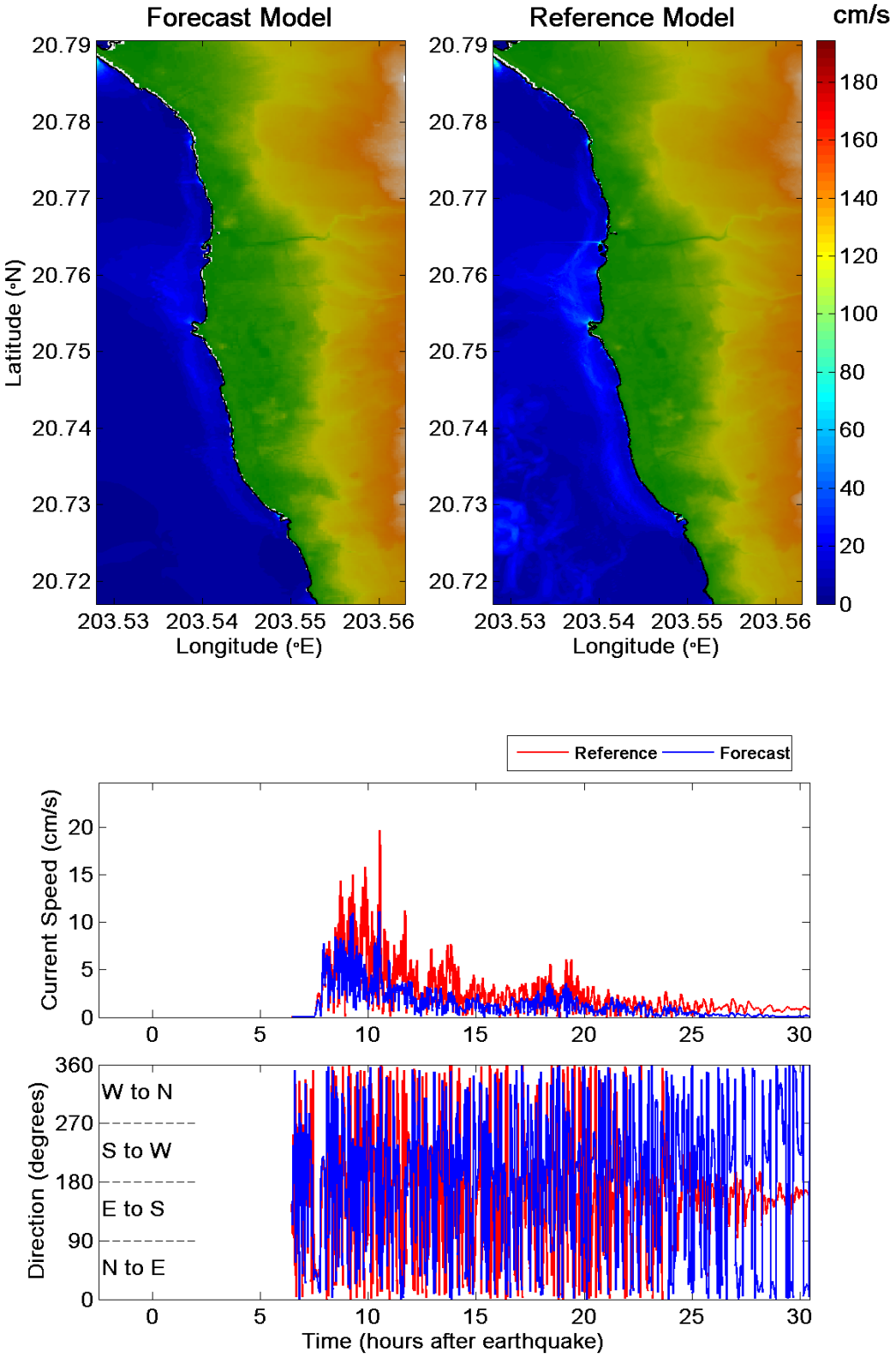

Figure 49. Comparative plot of maximum current speed distribution, current speed and directionality at the warning point at C-grid level for 1994 East Kuril tsunami between forecast reference models.

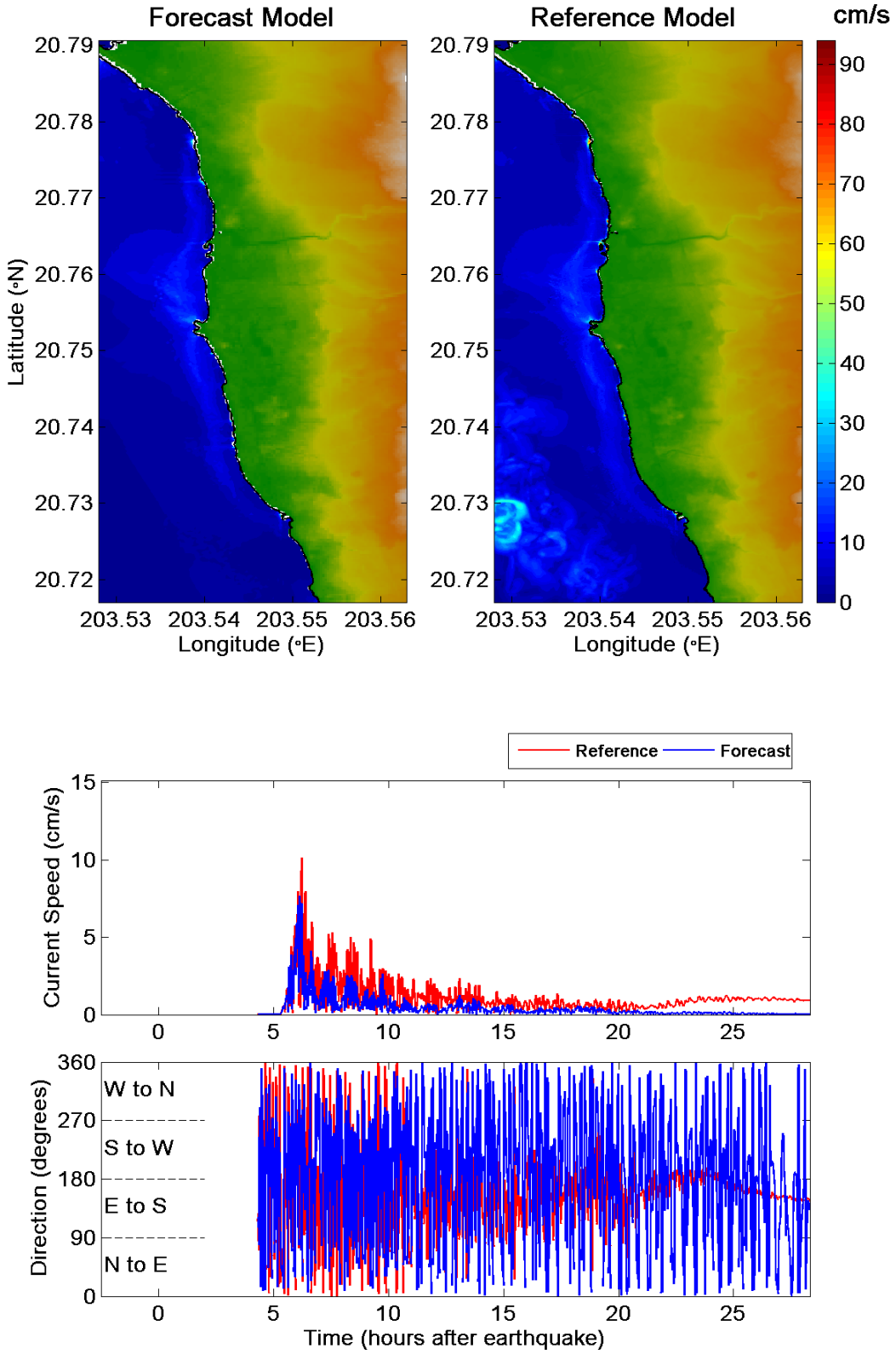

Figure 50. Comparative plot of maximum current speed distribution, current speed and directionality at the warning point at C-grid level for 2003 Rat Island tsunami between forecast reference models.

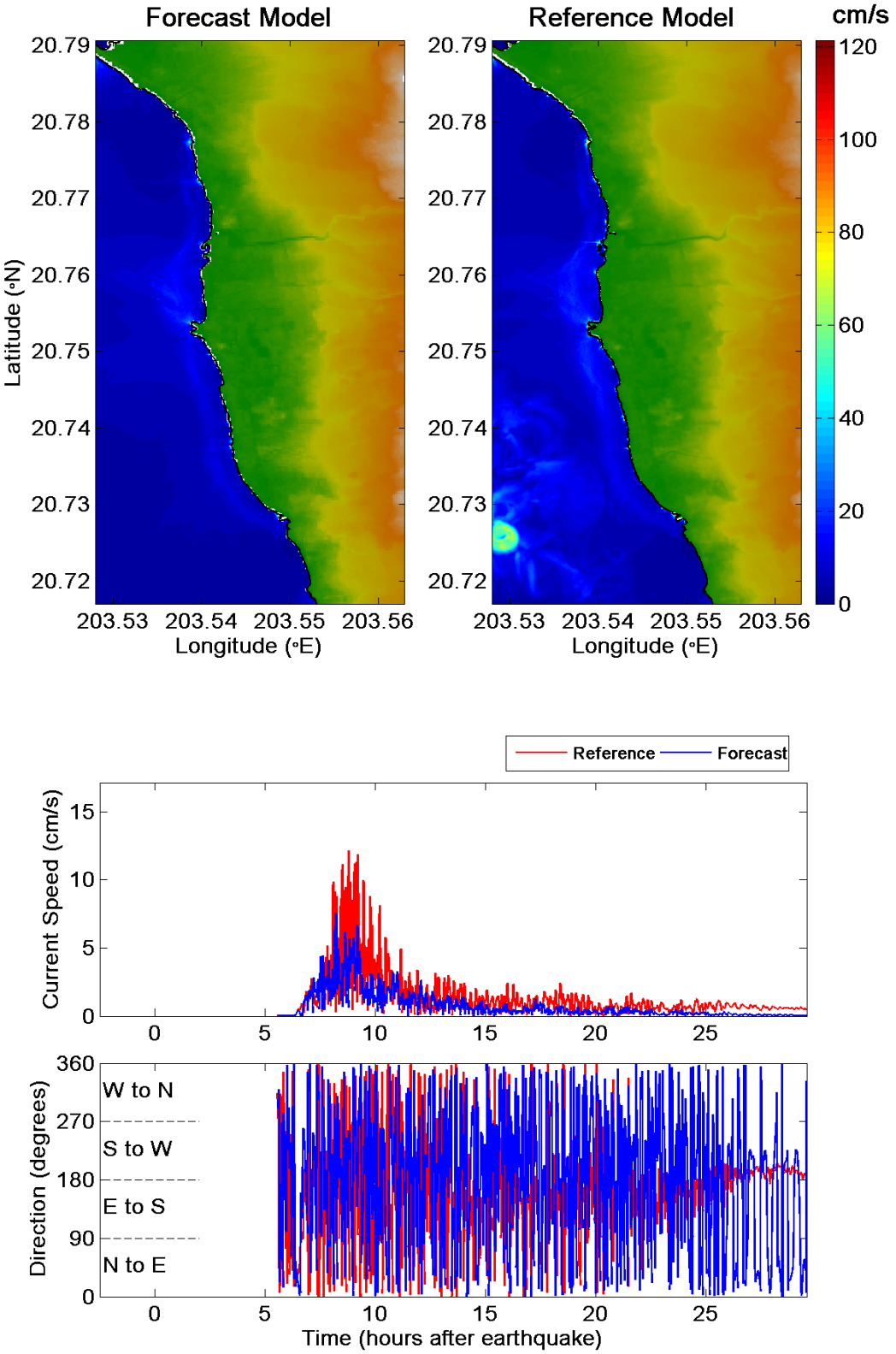

Figure 51. Comparative plot of maximum current speed distribution, current speed and directionality at the warning point at C-grid level for 2006 Tonga tsunami between forecast reference models.

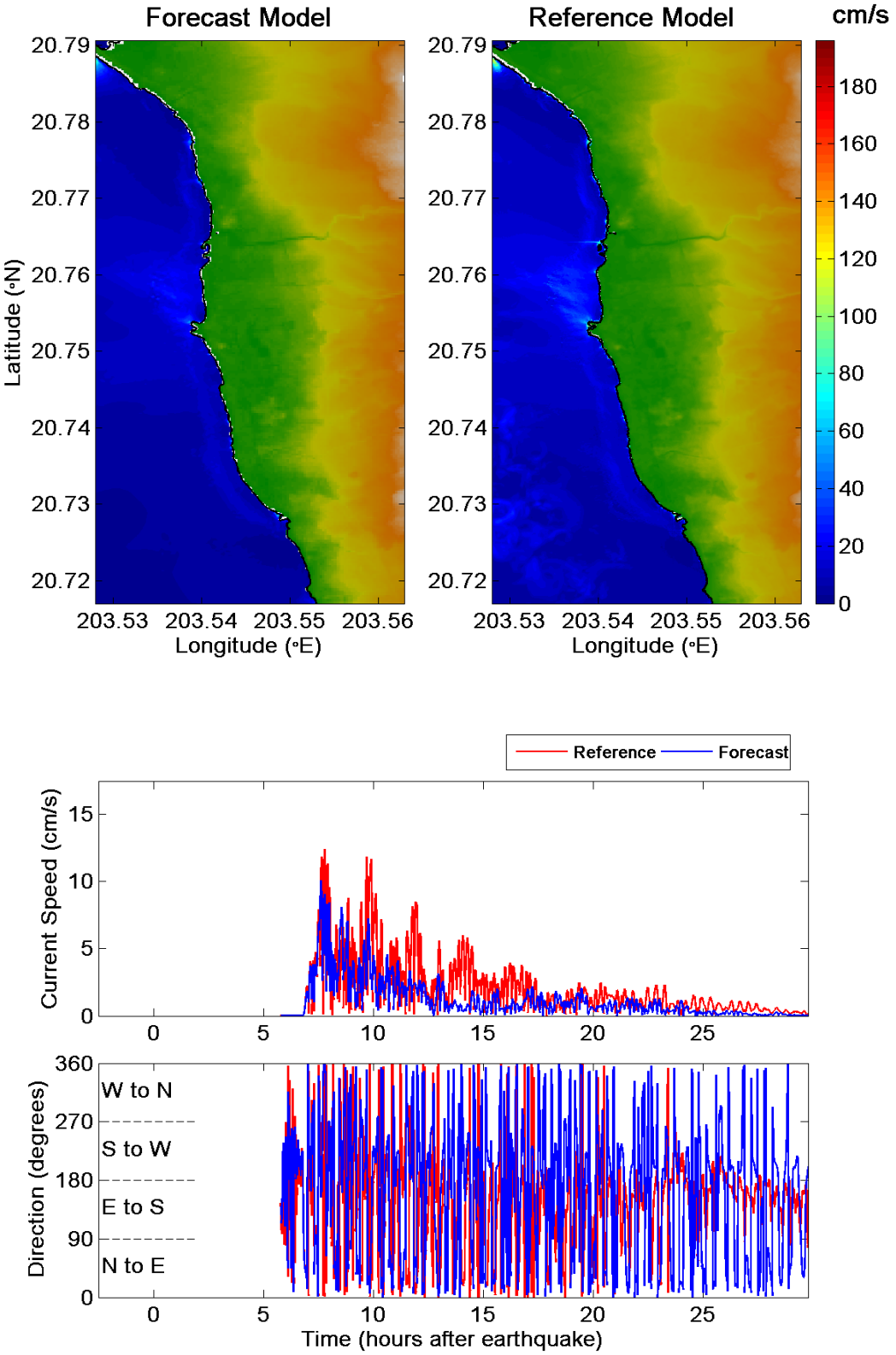

Figure 52. Comparative plot of maximum current speed distribution, current speed and directionality at the warning point at C-grid level for 2006 Kuril tsunami between forecast reference models.

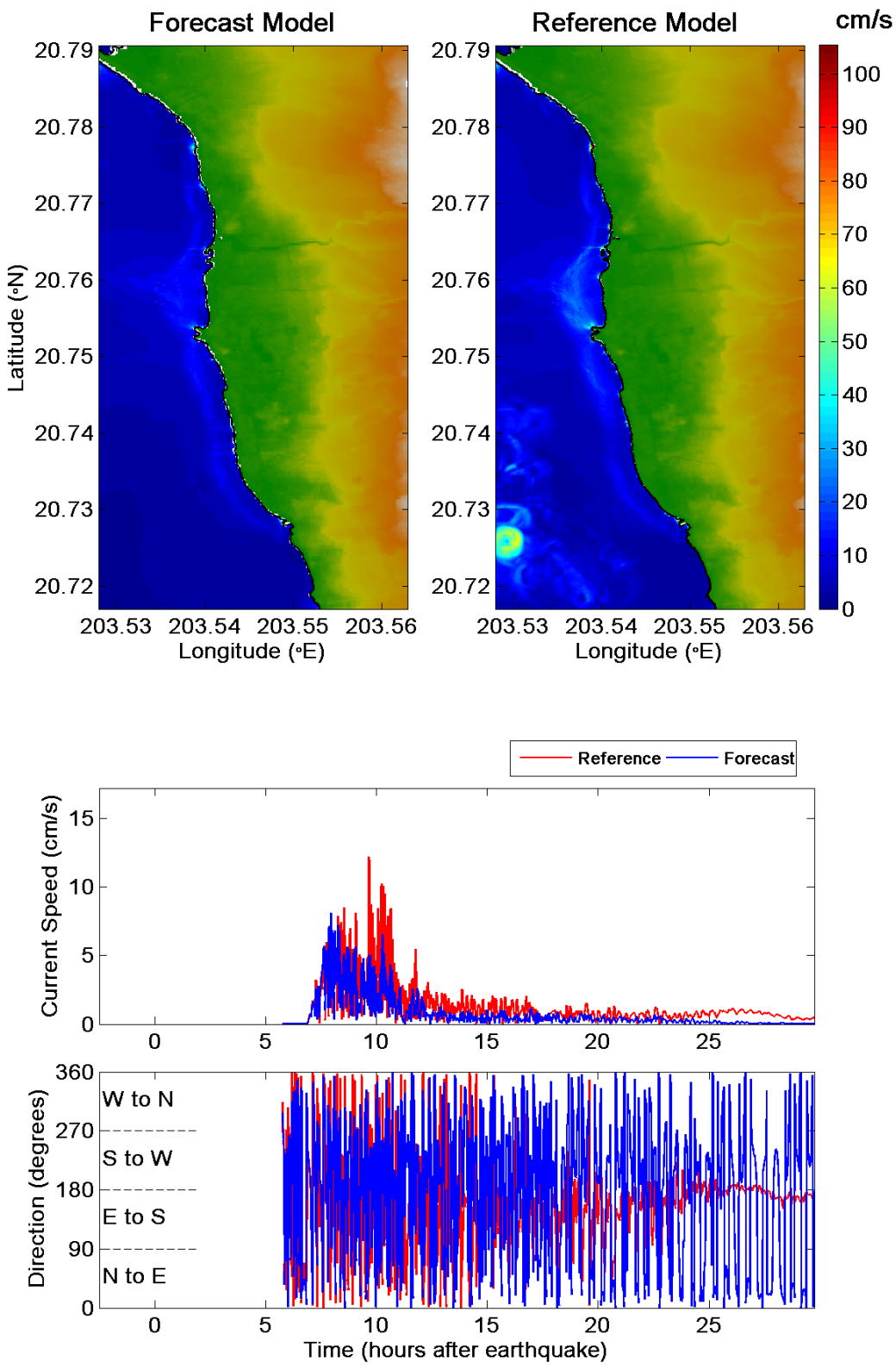

Figure 53. Comparative plot of maximum current speed distribution, current speed and directionality at the warning point at C-grid level for 2007 Kuril tsunami between forecast reference models.

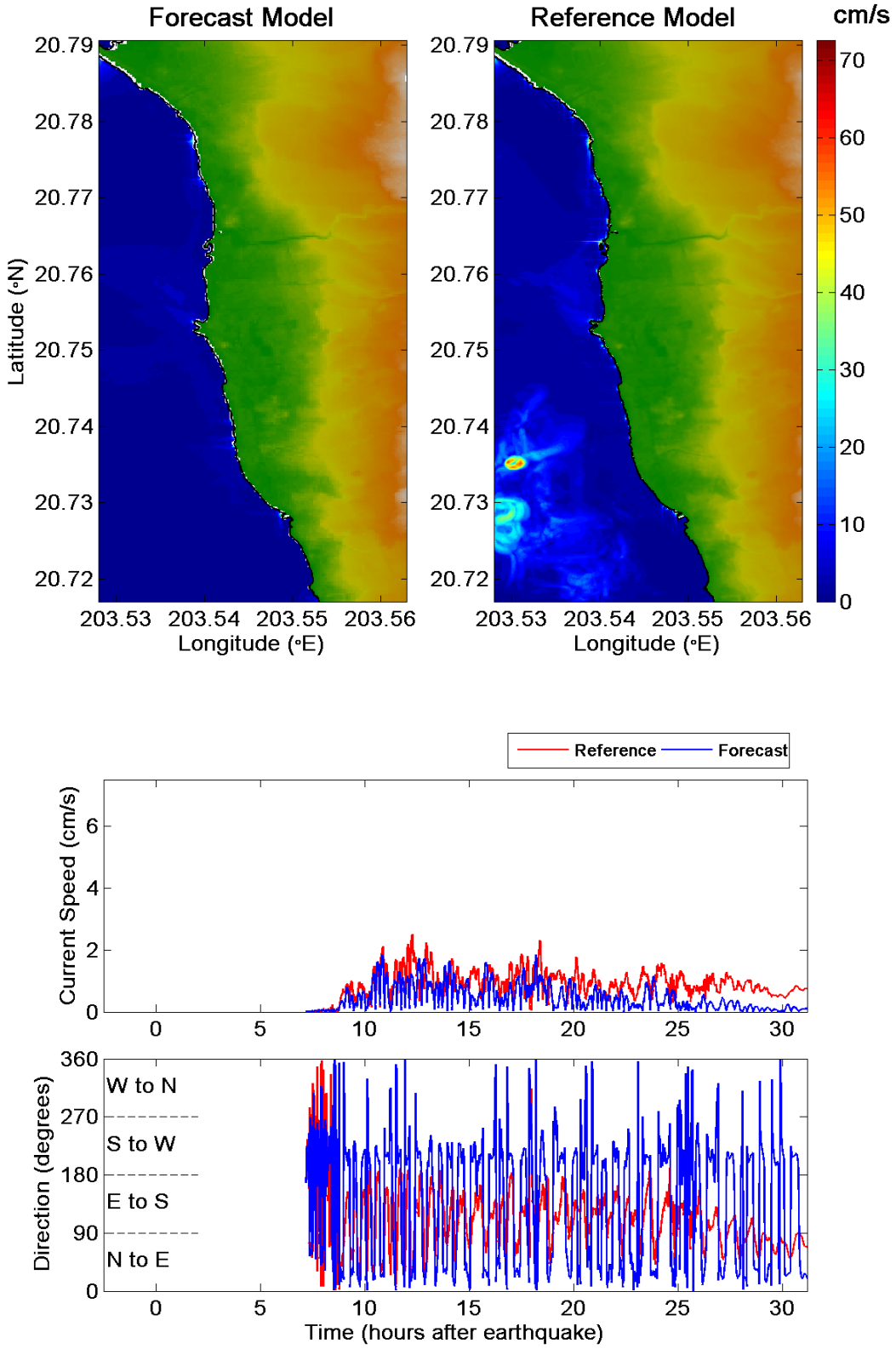

Figure 54. Comparative plot of maximum current speed distribution, current speed and directionality at the warning point at C-grid level for 2007 Solomon tsunami between forecast reference models.

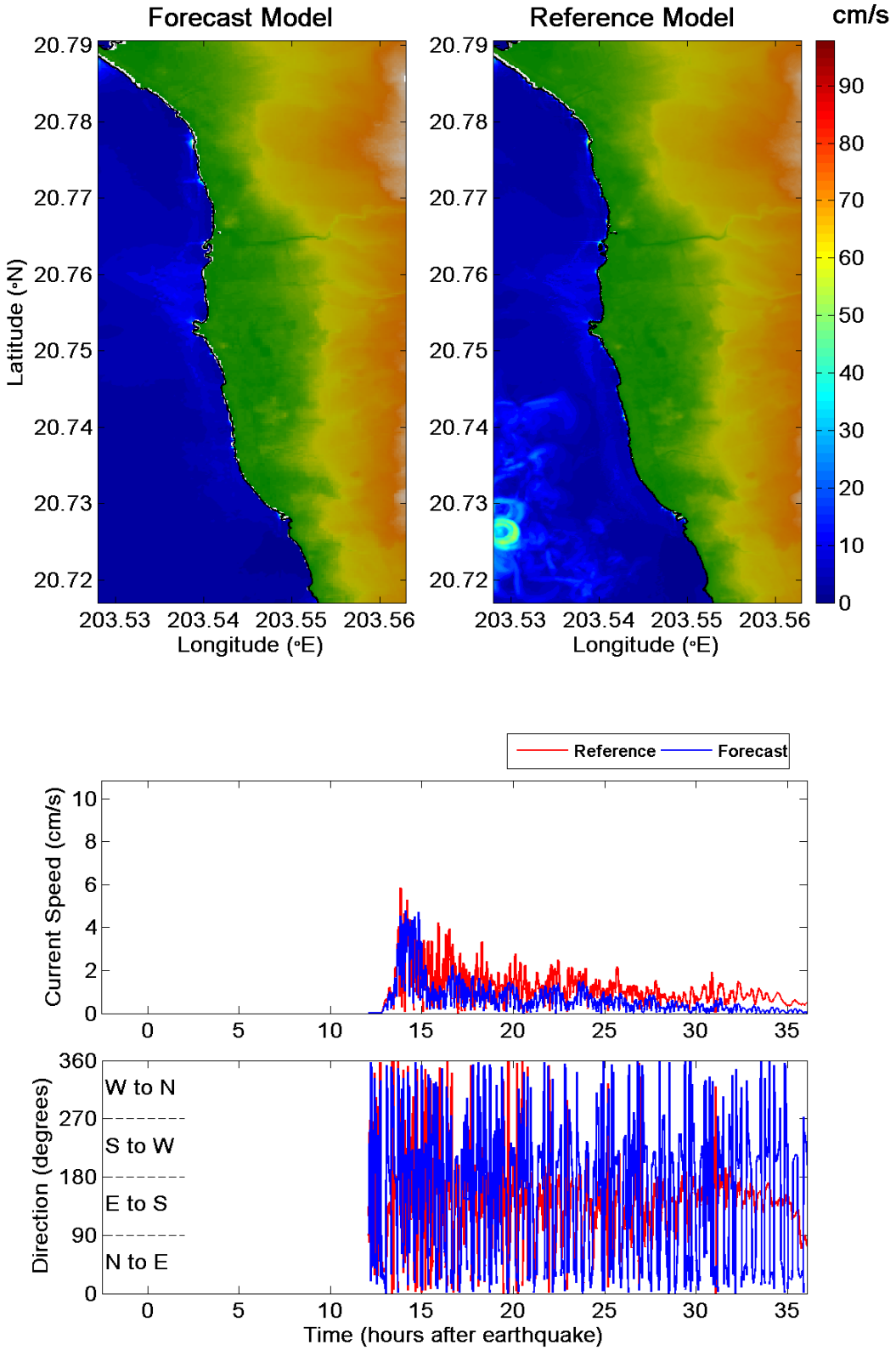

Figure 55. Comparative plot of maximum current speed distribution, current speed and directionality at the warning point at C-grid level for 2007 Peru tsunami between forecast reference models.

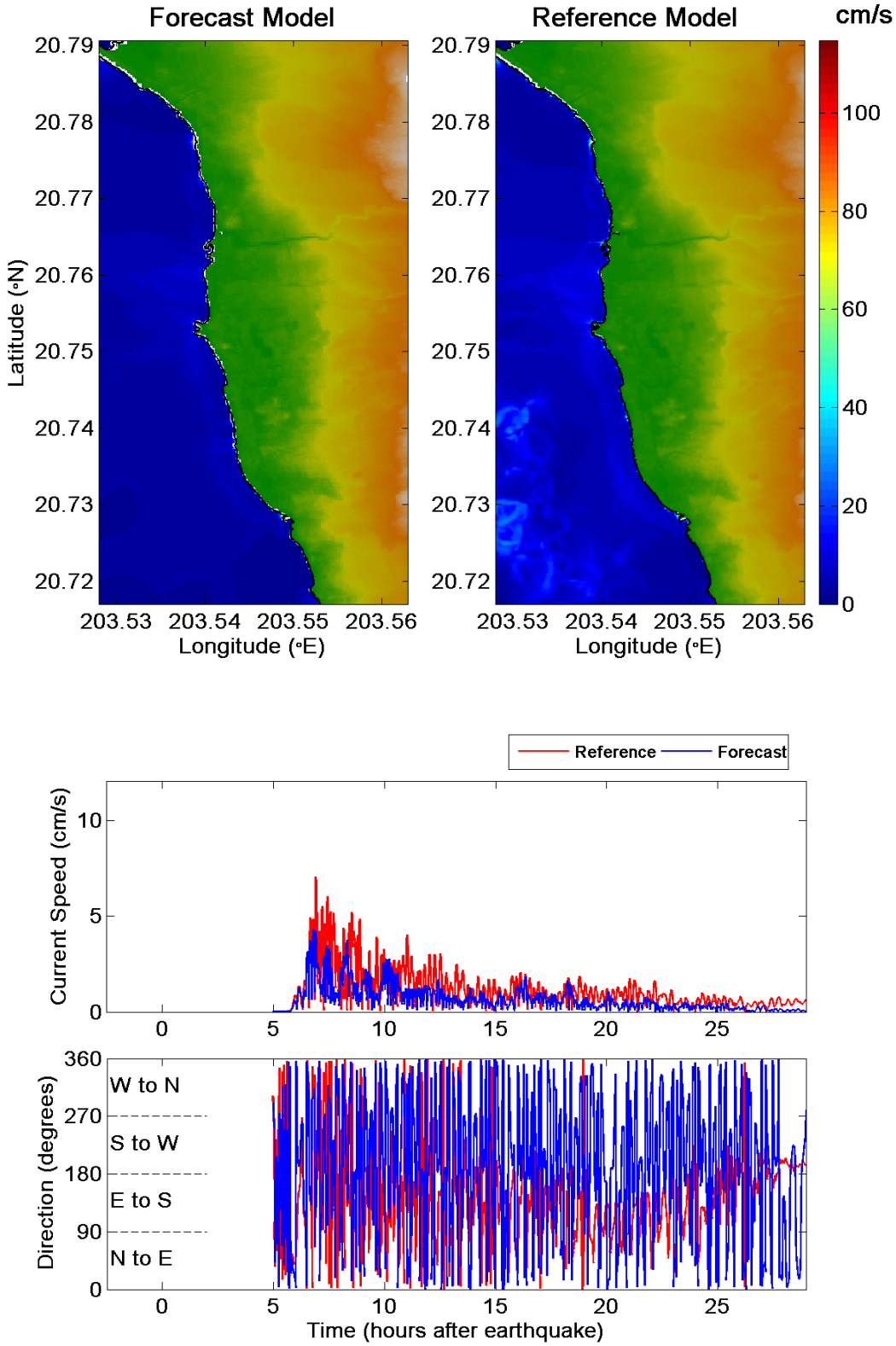

Figure 56. Comparative plot of maximum current speed distribution, current speed and directionality at the warning point at C-grid level for 2009 Samoa tsunami between forecast reference models.

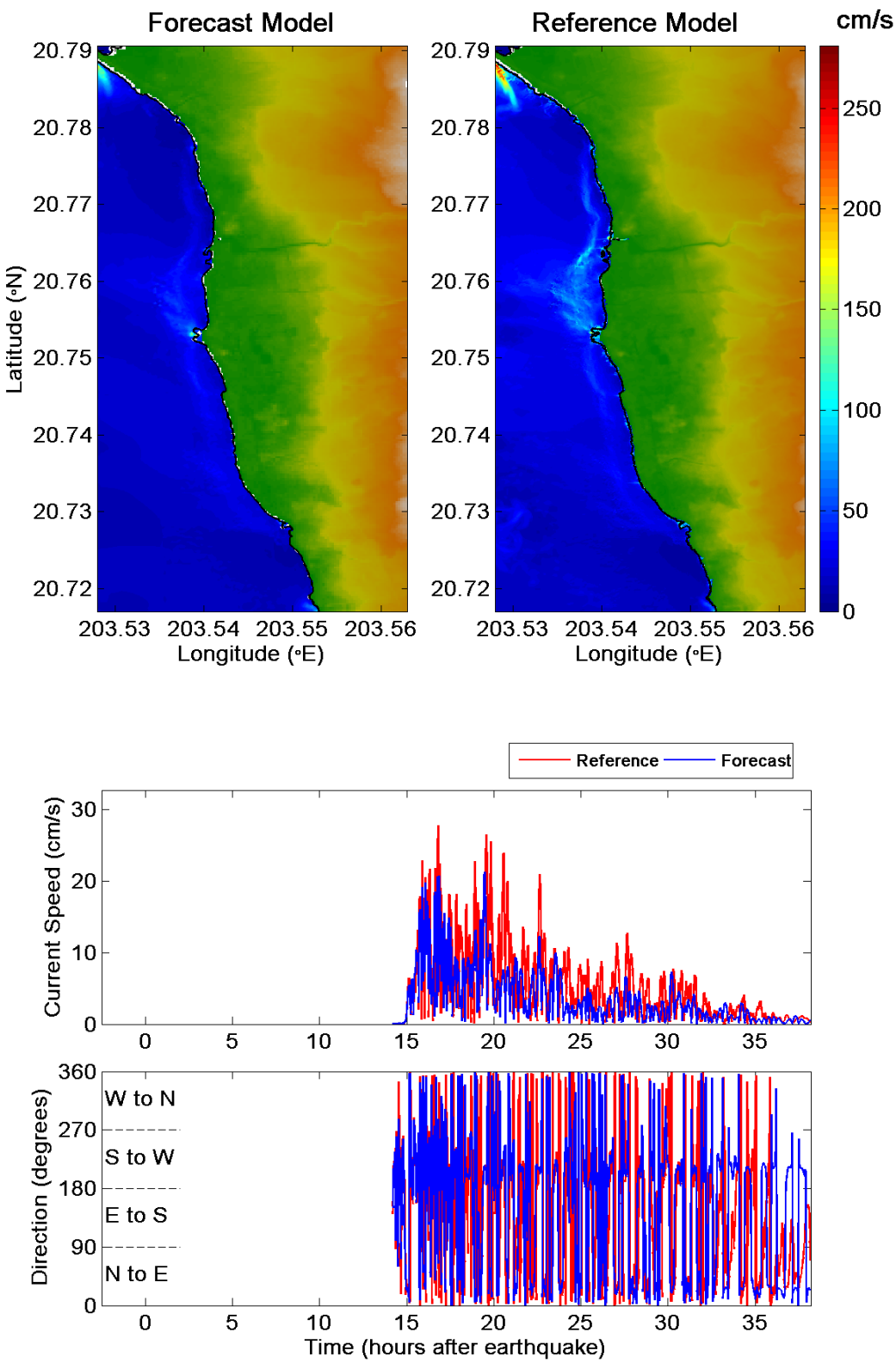

Figure 57. Comparative plot of maximum current speed distribution, current speed and directionality at the warning point at C-grid level for 2010 Chile tsunami between forecast reference models.

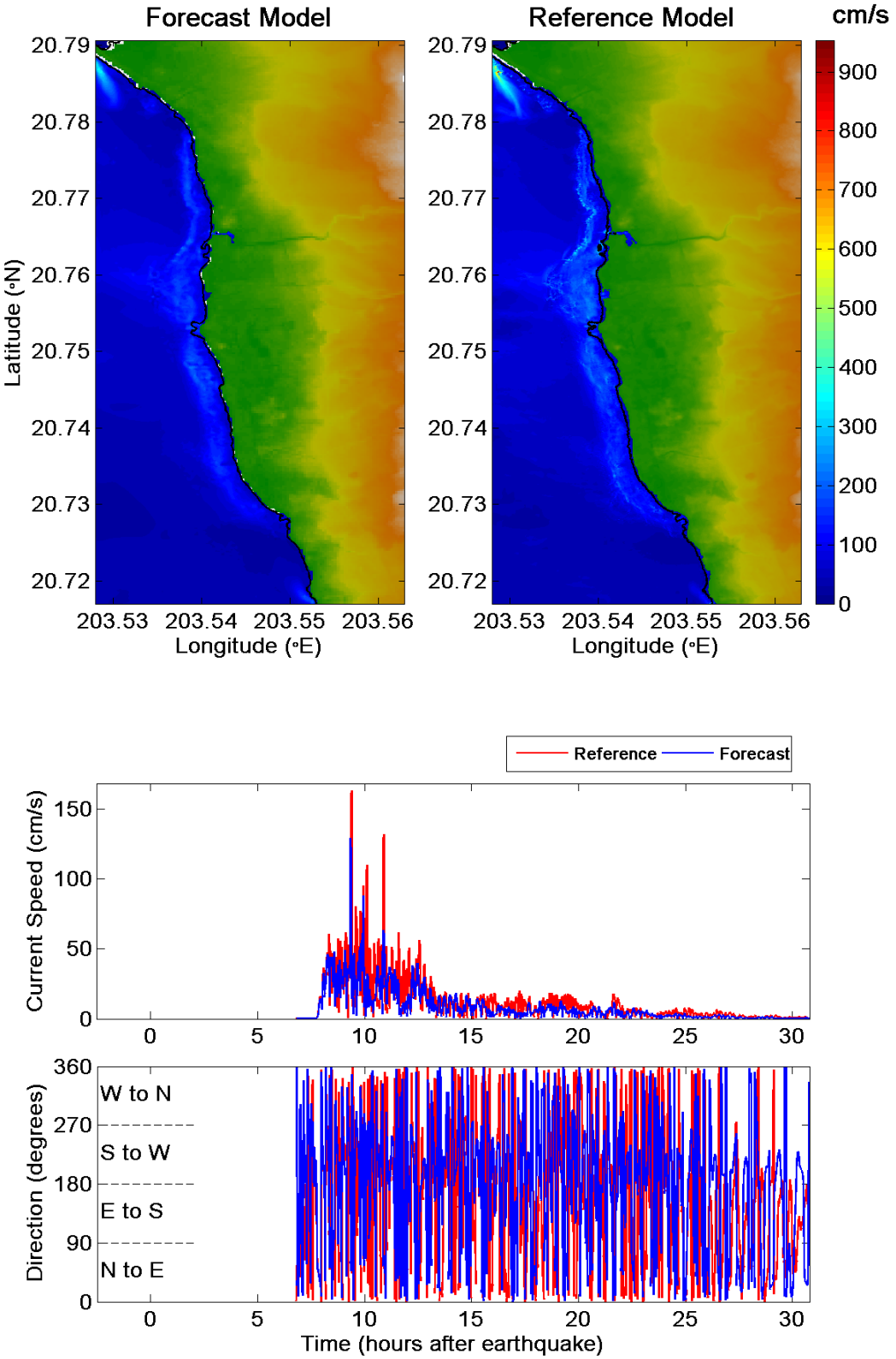

Figure 58. Comparative plot of maximum current speed distribution, current speed and directionality at the warning point at C-grid level for 2011 Honshu tsunami between forecast reference models.

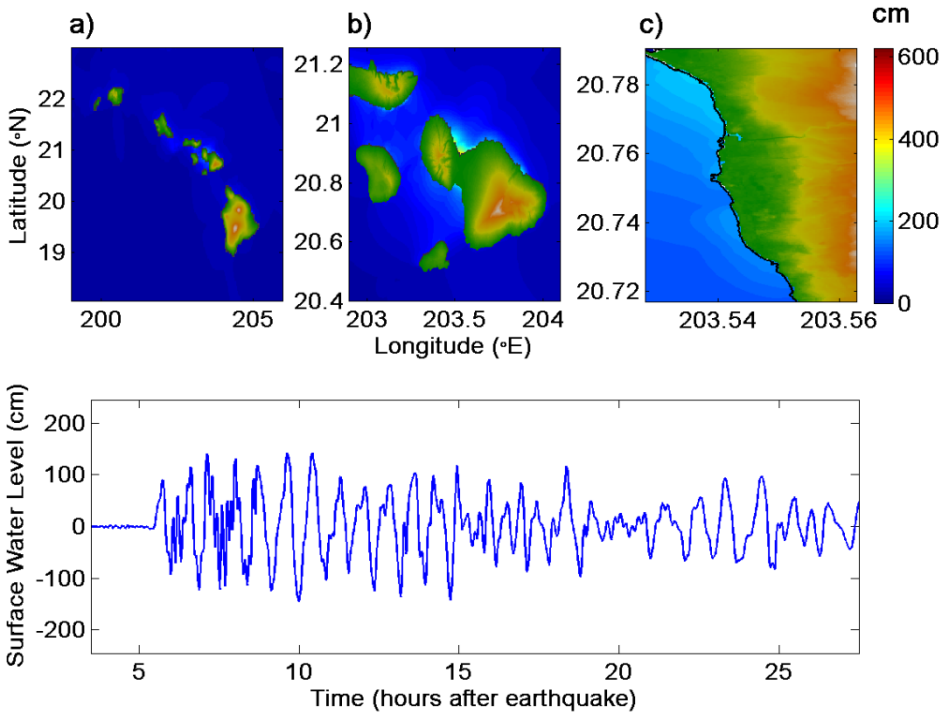

Figure 59. Plot of maximum tsunami wave amplitude distribution for Grids A, B and C and tsunami time series at the warning point for synthetic case AC01-10 with forecast model.

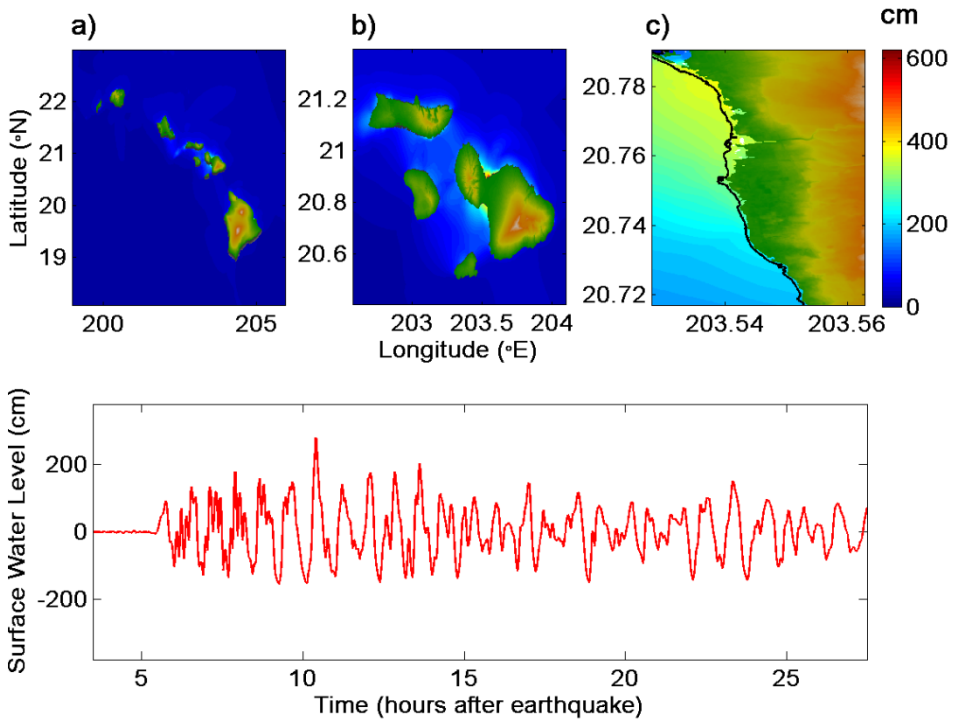

Figure 60. Plot of maximum tsunami wave amplitude distribution for Grids A, B and C and tsunami time series at the warning point for synthetic case AC01-10 with reference model.

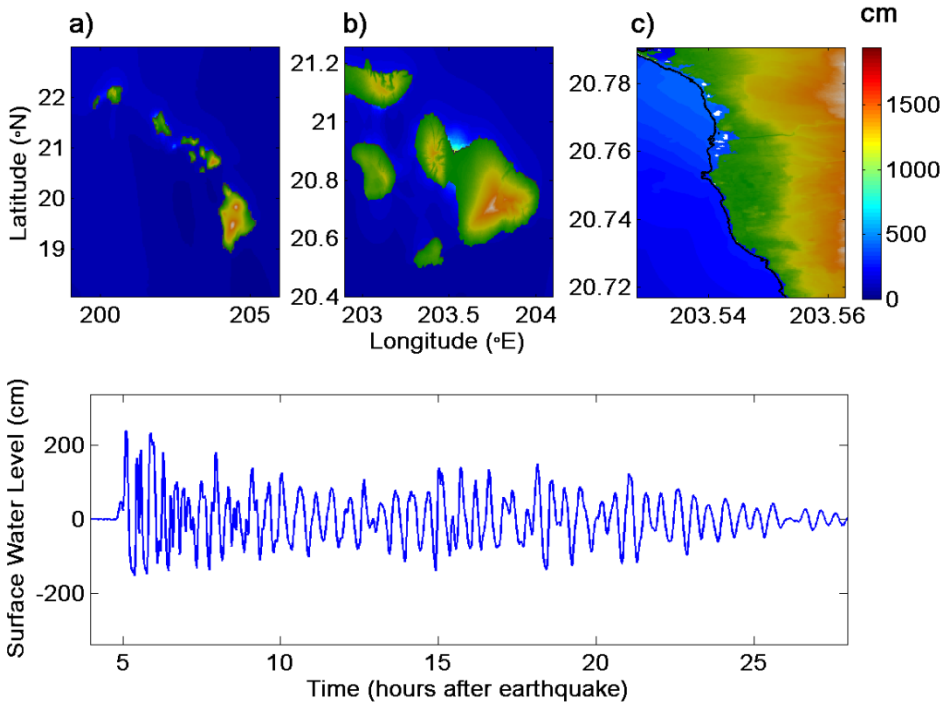

Figure 61. Plot of maximum tsunami wave amplitude distribution for Grids A, B and C and tsunami time series at the warning point for synthetic case AC11-20 with forecast model. White areas on land indicate non-inundated sections.

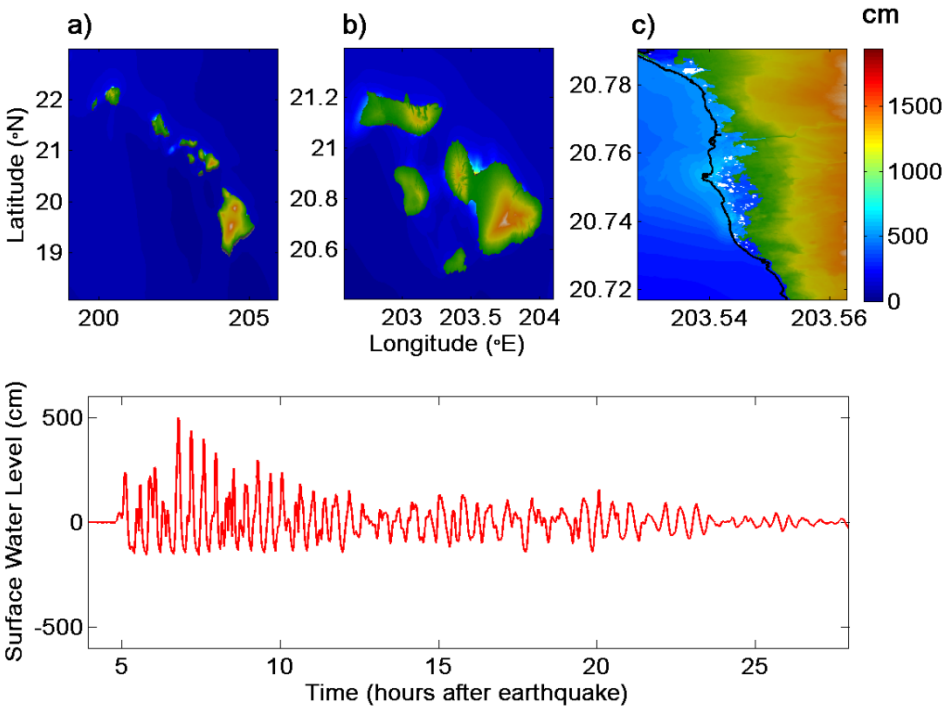

Figure 62. Plot of maximum tsunami wave amplitude distribution for Grids A, B and C and tsunami time series at the warning point for synthetic case AC11-20 with reference model. White areas on land indicate non-inundated sections.

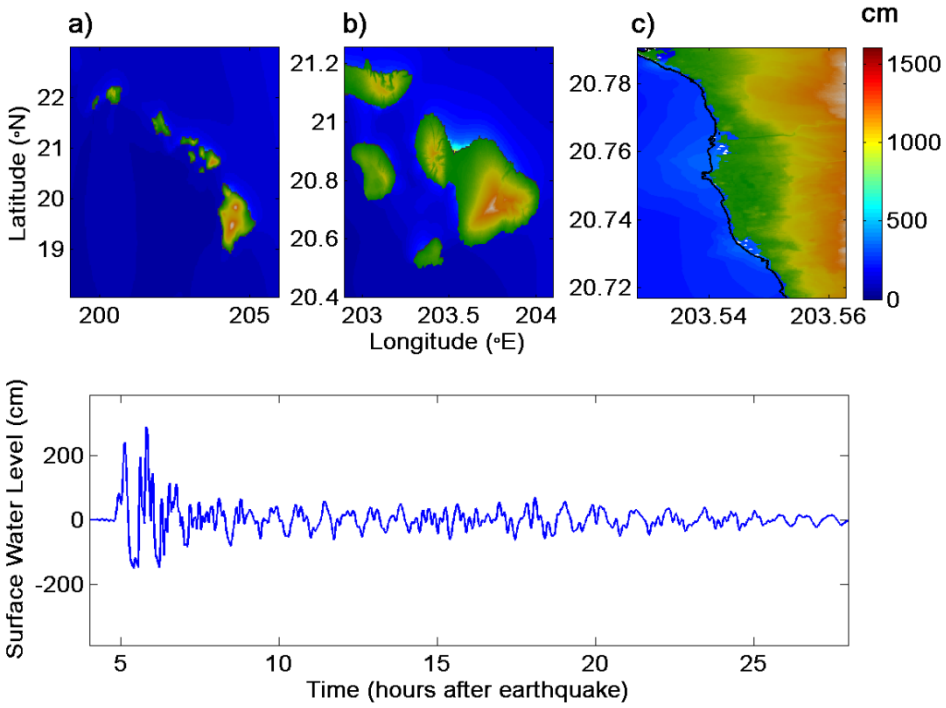

Figure 63. Plot of maximum tsunami wave amplitude distribution for Grids A, B and C and tsunami time series at the warning point for synthetic case AC21-30 with forecast model. White areas on land indicate non-inundated sections.

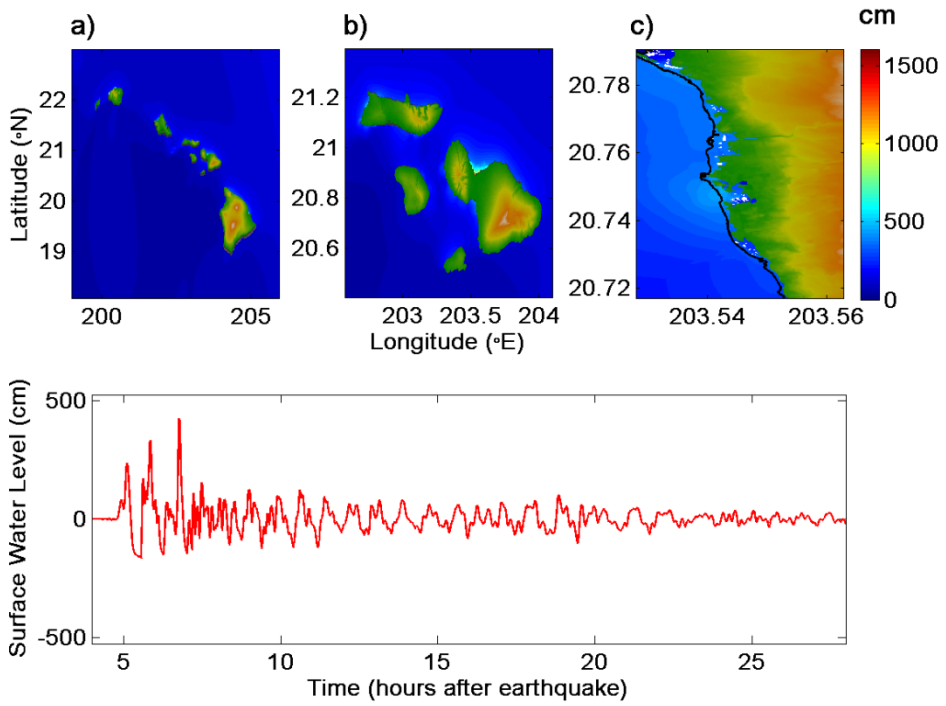

Figure 64. Plot of maximum tsunami wave amplitude distribution for Grids A, B and C and tsunami time series at the warning point for synthetic case AC21-30 with reference model. White areas on land indicate non-inundated sections.

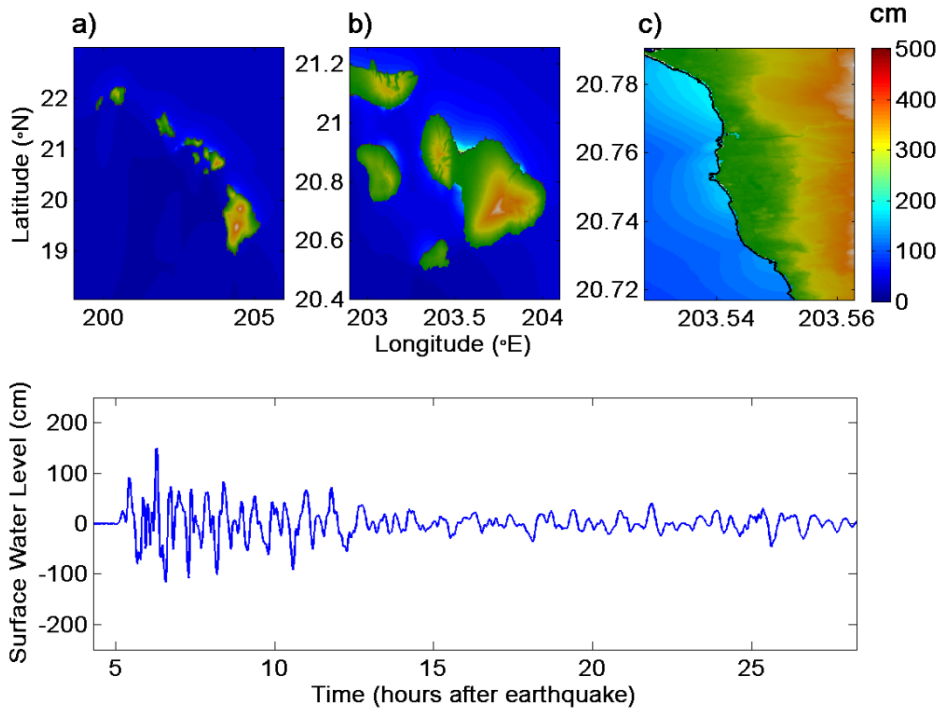

Figure 65. Plot of maximum tsunami wave amplitude distribution for Grids A, B and C and tsunami time series at the warning point for synthetic case AC31-40 with forecast model.

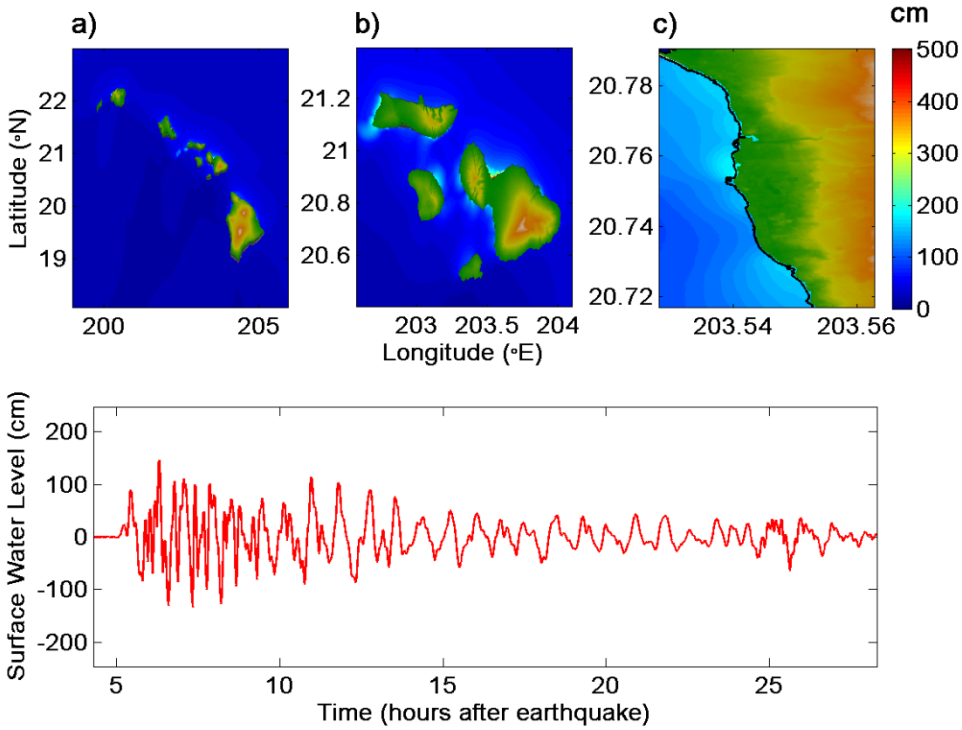

Figure 66. Plot of maximum tsunami wave amplitude distribution for Grids A, B and C and tsunami time series at the warning point for synthetic case AC31-40 with reference model.

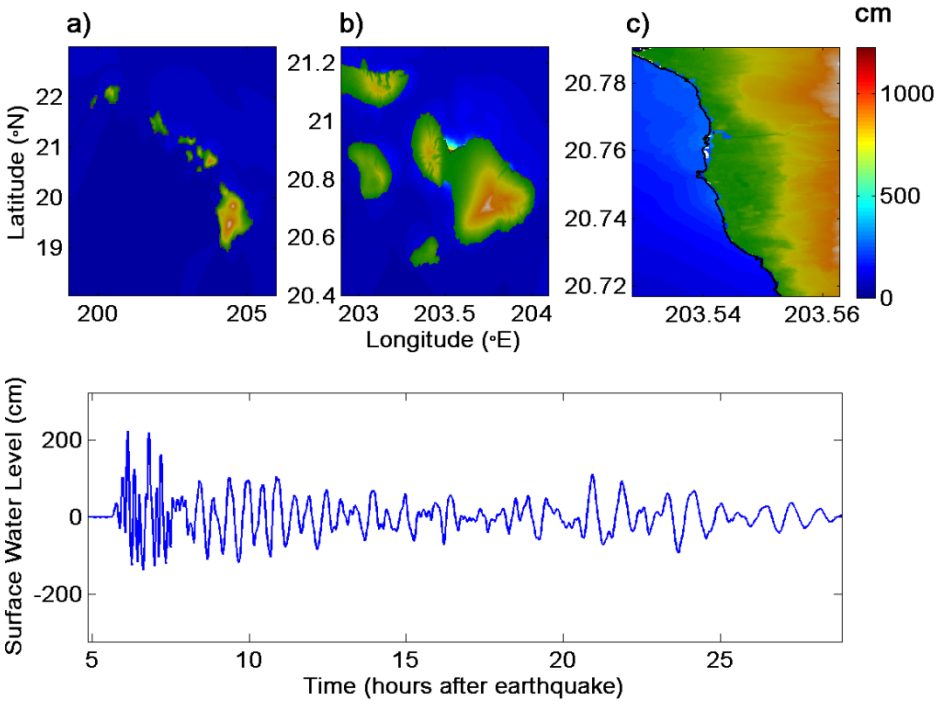

Figure 67. Plot of maximum tsunami wave amplitude distribution for Grids A, B and C and tsunami time series at the warning point for synthetic case AC41-50 with forecast model. White areas on land indicate non-inundated sections.

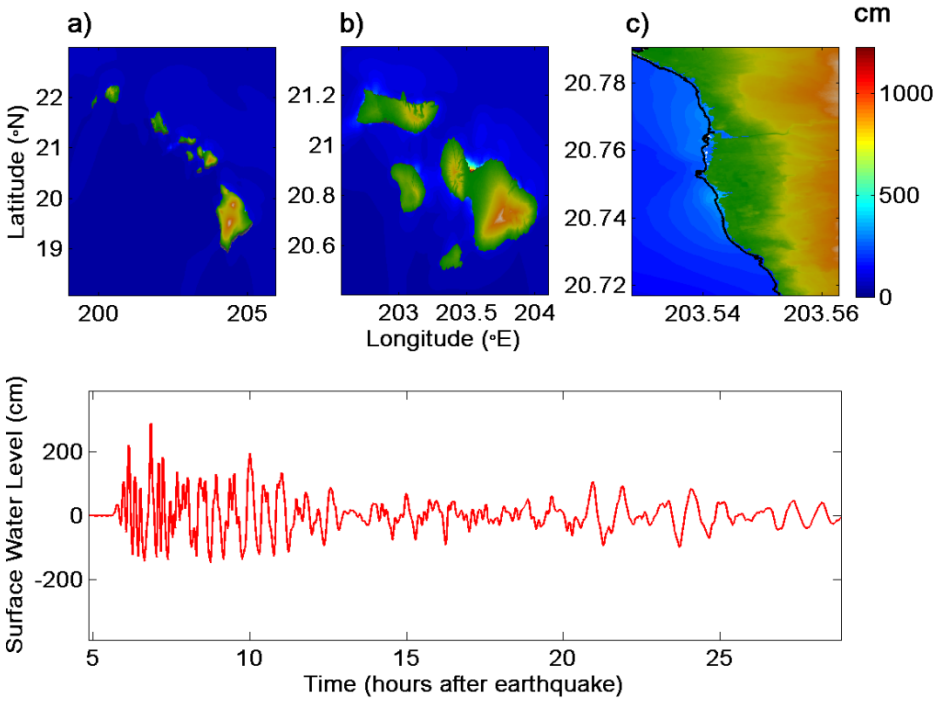

Figure 68. Plot of maximum tsunami wave amplitude distribution for Grids A, B and C and tsunami time series at the warning point for synthetic case AC41-50 with reference model. White areas on land indicate non-inundated sections.

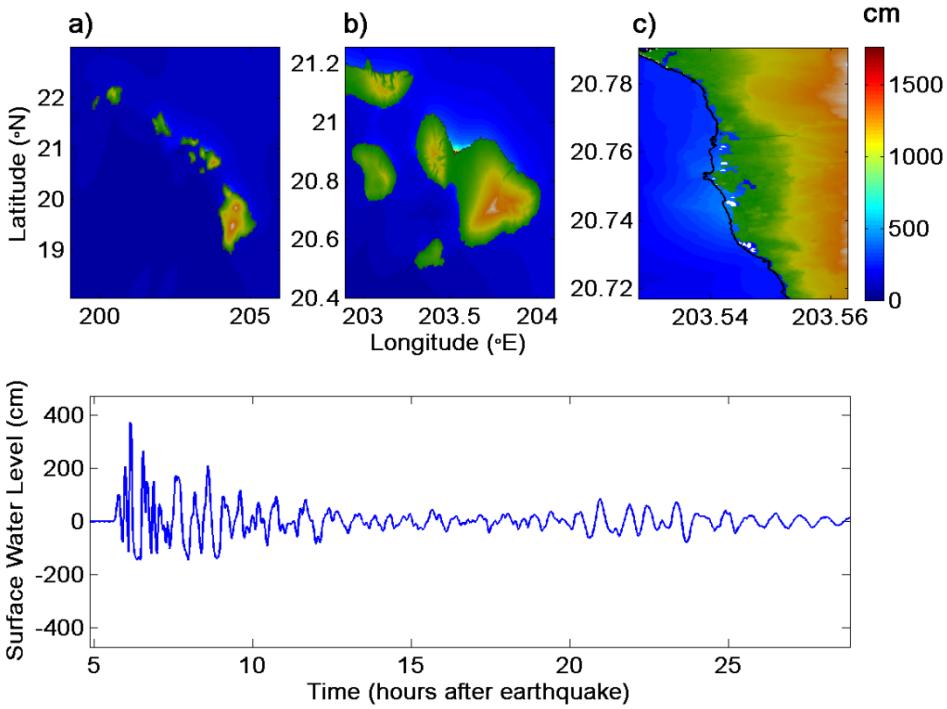

Figure 69. Plot of maximum tsunami wave amplitude distribution for Grids A, B and C and tsunami time series at the warning point for synthetic case AC46-55 with forecast model. White areas on land indicate non-inundated sections.

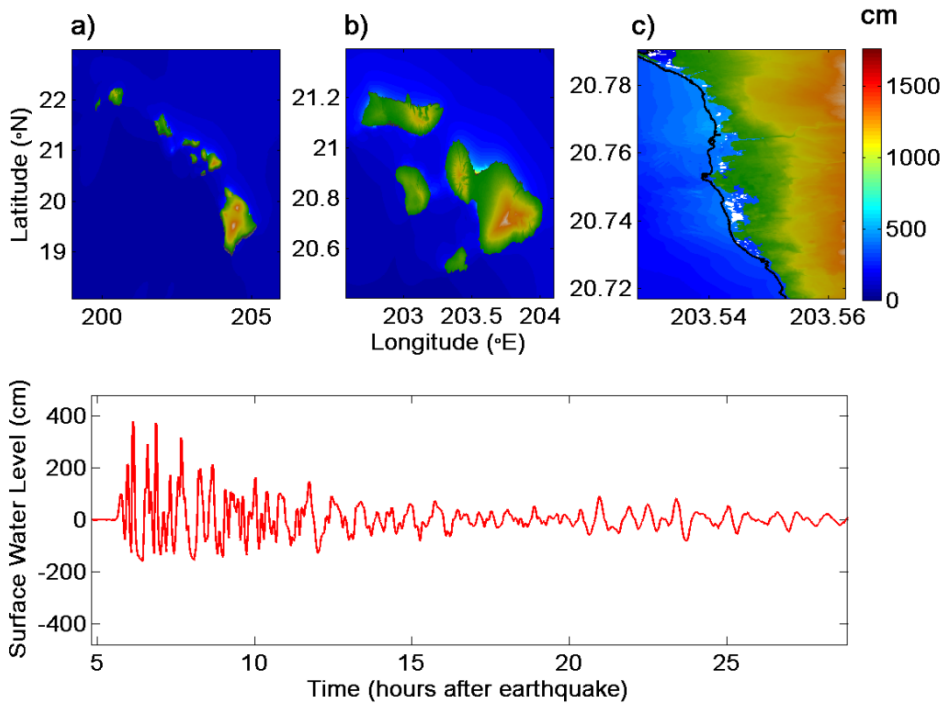

Figure 70. Plot of maximum tsunami wave amplitude distribution for Grids A, B and C and tsunami time series at the warning point for synthetic case AC46-55 with reference model. White areas on land indicate non-inundated sections.

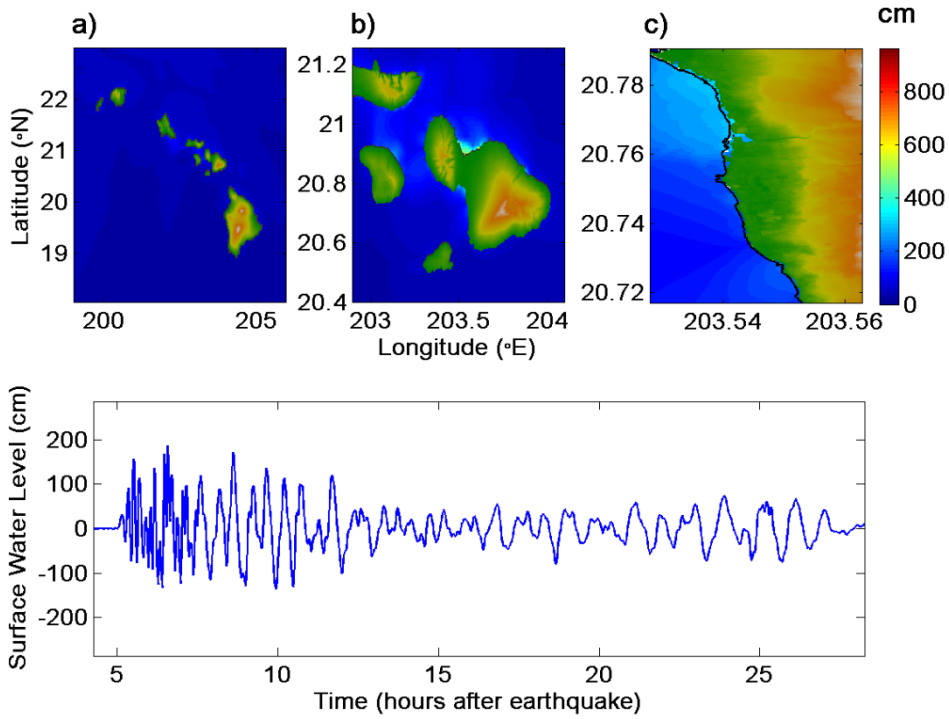

Figure 71. Plot of maximum tsunami wave amplitude distribution for Grids A, B and C and tsunami time series at the warning point for synthetic case AC56-65 with forecast model.

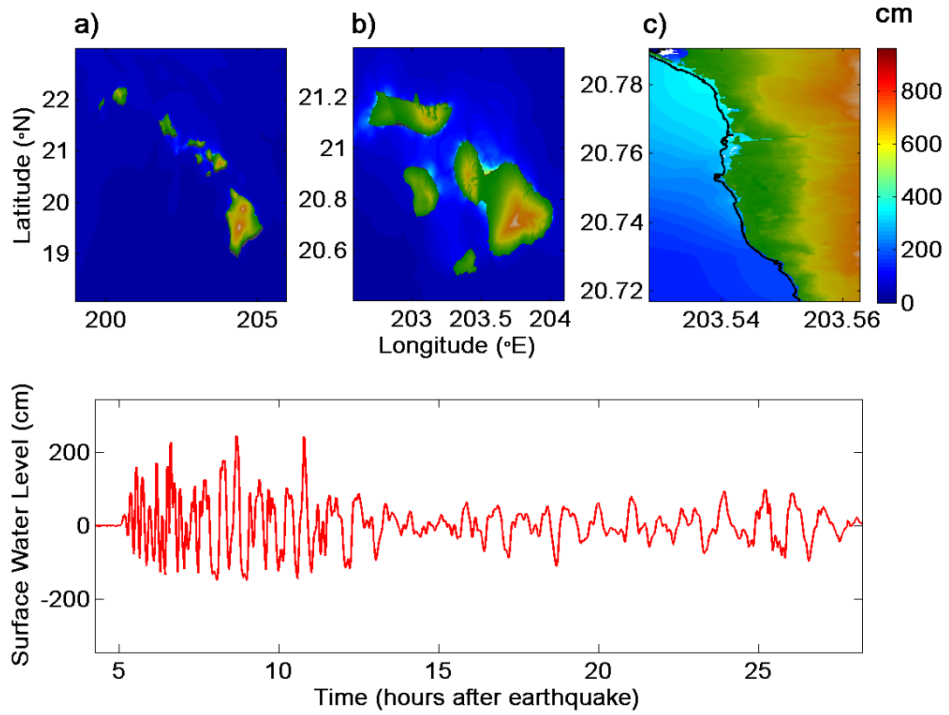

Figure 72. Plot of maximum tsunami wave amplitude distribution for Grids A, B and C and tsunami time series at the warning point for synthetic case AC56-65 with reference model.

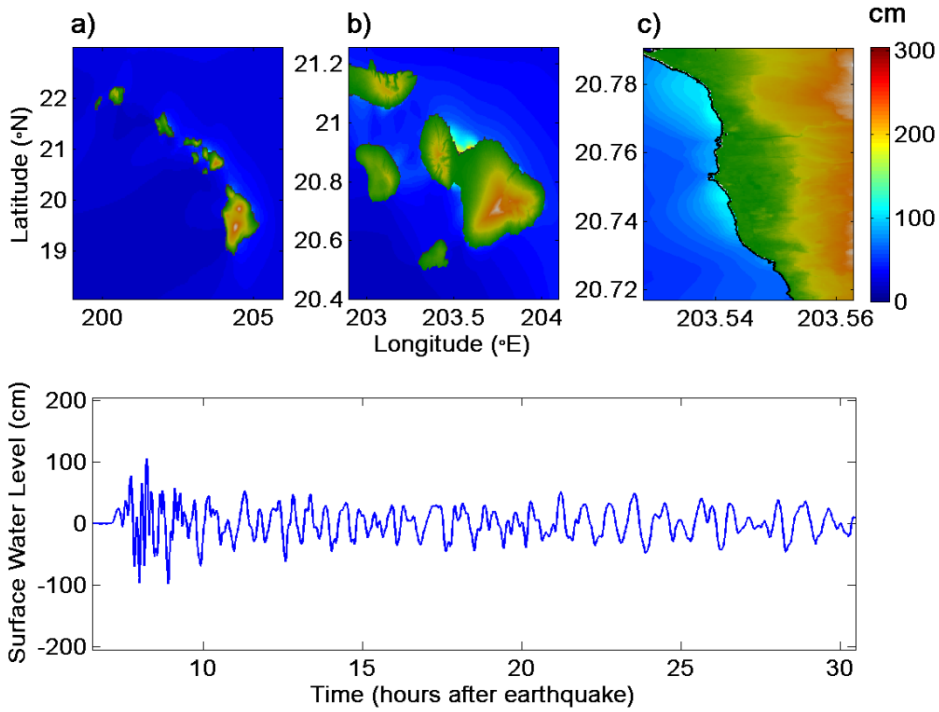

Figure 73. Plot of maximum tsunami wave amplitude distribution for Grids A, B and C and tsunami time series at the warning point for synthetic case CS01-10 with forecast model.

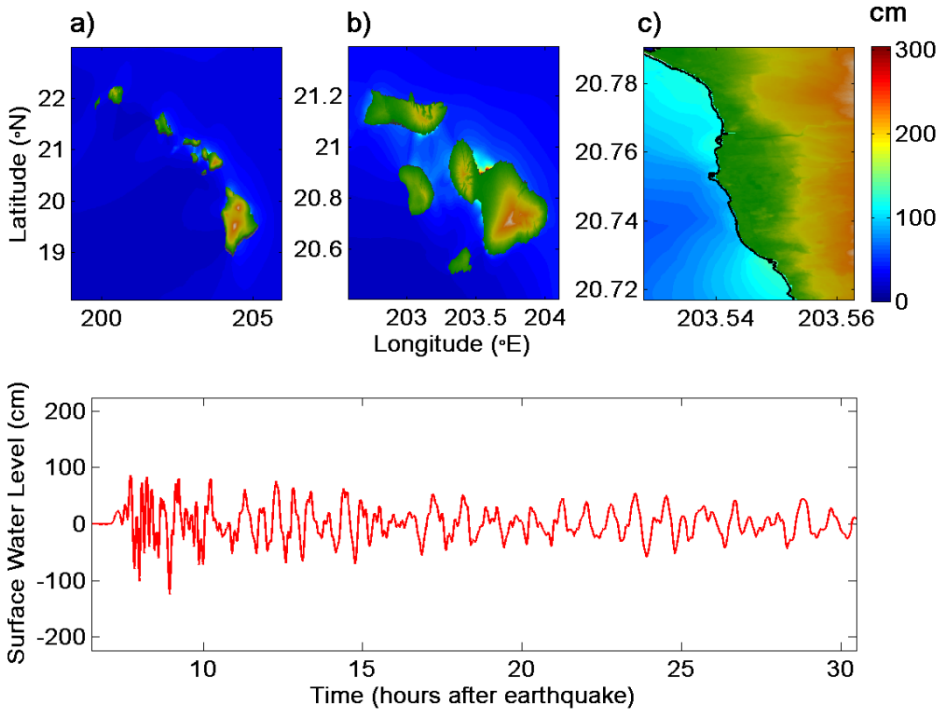

Figure 74. Plot of maximum tsunami wave amplitude distribution for Grids A, B and C and tsunami time series at the warning point for synthetic case CS01-10 with reference model.

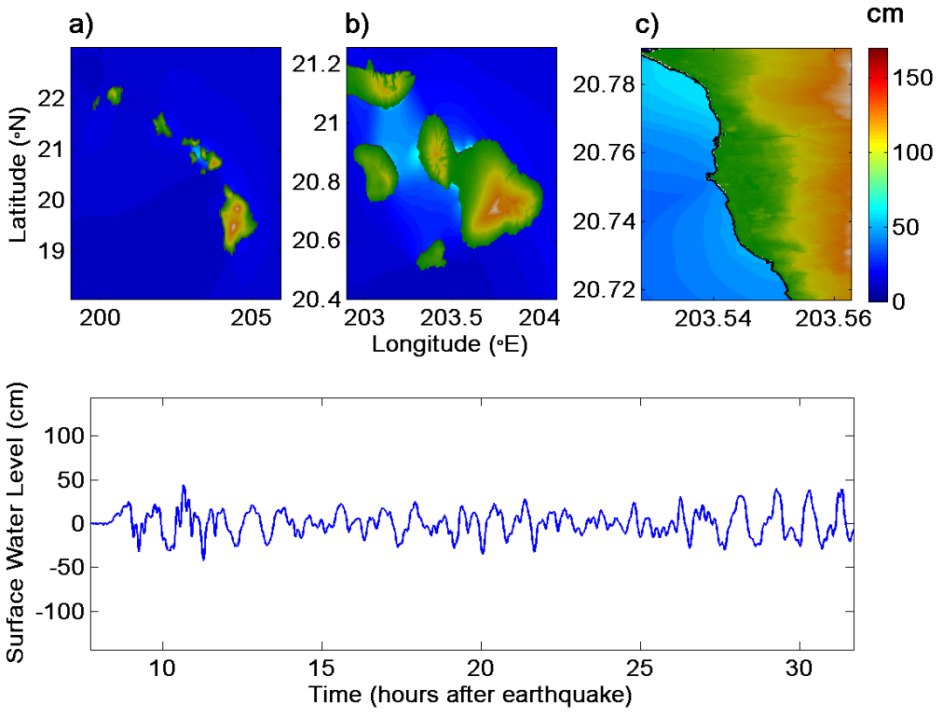

Figure 75. Plot of maximum tsunami wave amplitude distribution for Grids A, B and C and tsunami time series at the warning point for synthetic case CS11-20 with forecast model.

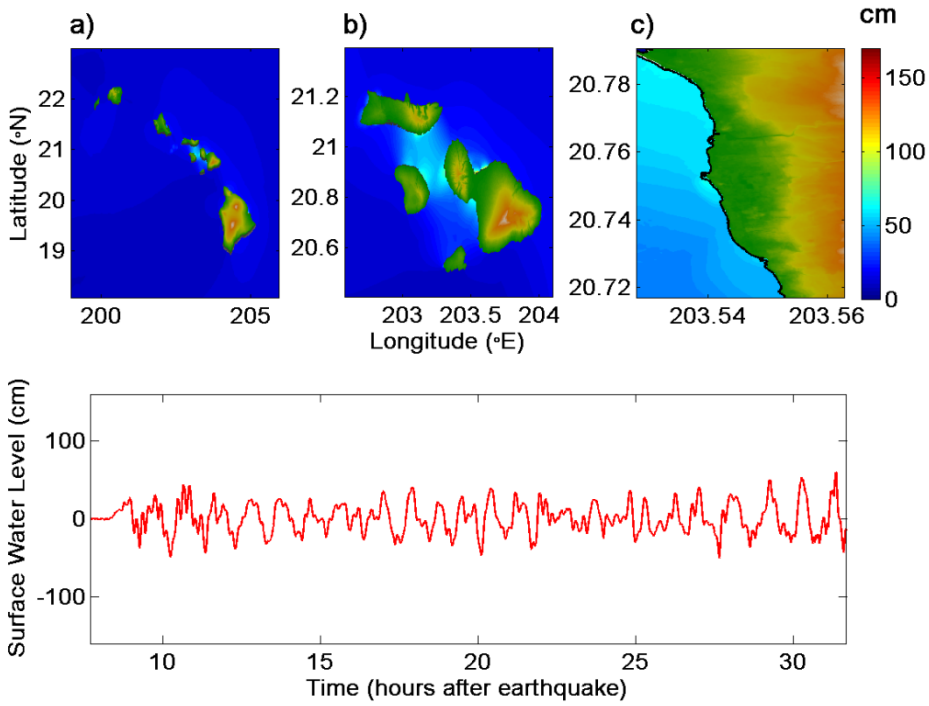

Figure 76. Plot of maximum tsunami wave amplitude distribution for Grids A, B and C and tsunami time series at the warning point for synthetic case CS11-20 with reference model.

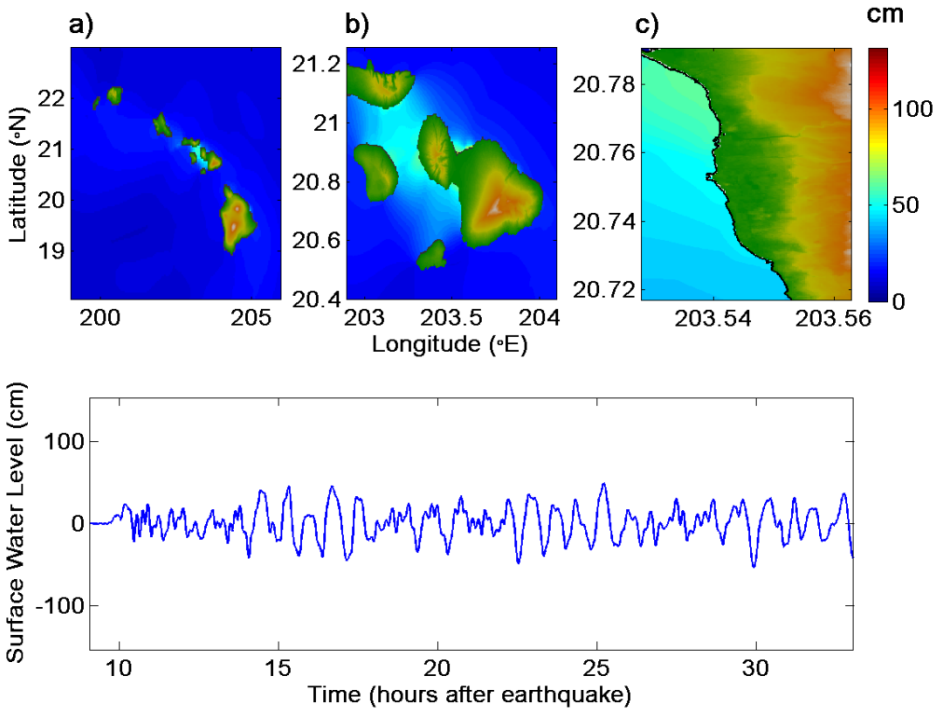

Figure 77. Plot of maximum tsunami wave amplitude distribution for Grids A, B and C and tsunami time series at the warning point for synthetic case CS21-30 with forecast model.

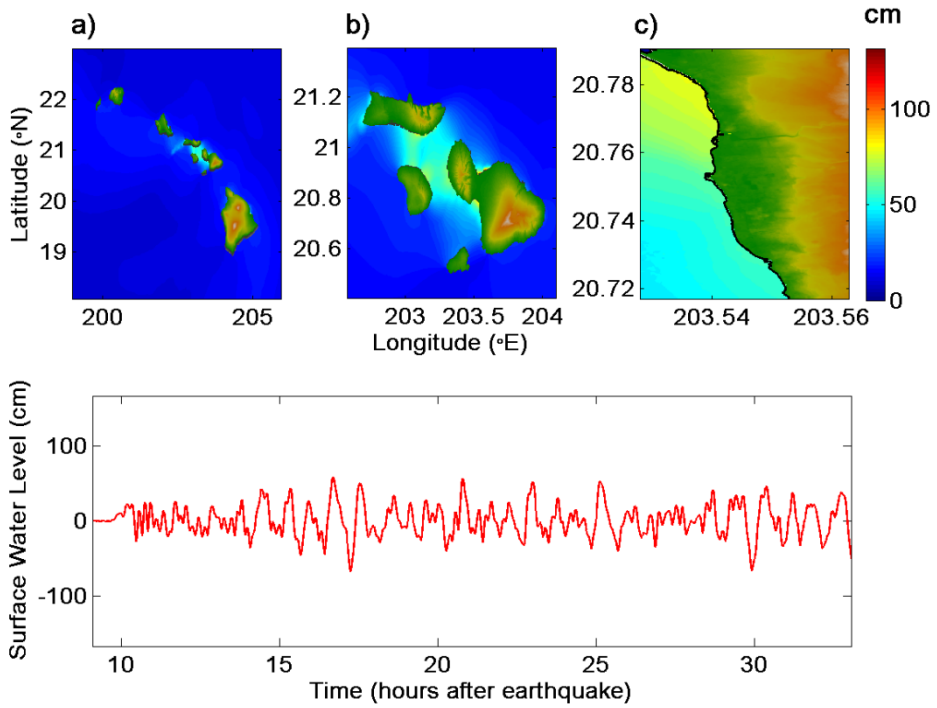

Figure 78. Plot of maximum tsunami wave amplitude distribution for Grids A, B and C and tsunami time series at the warning point for synthetic case CS21-30 with reference model.

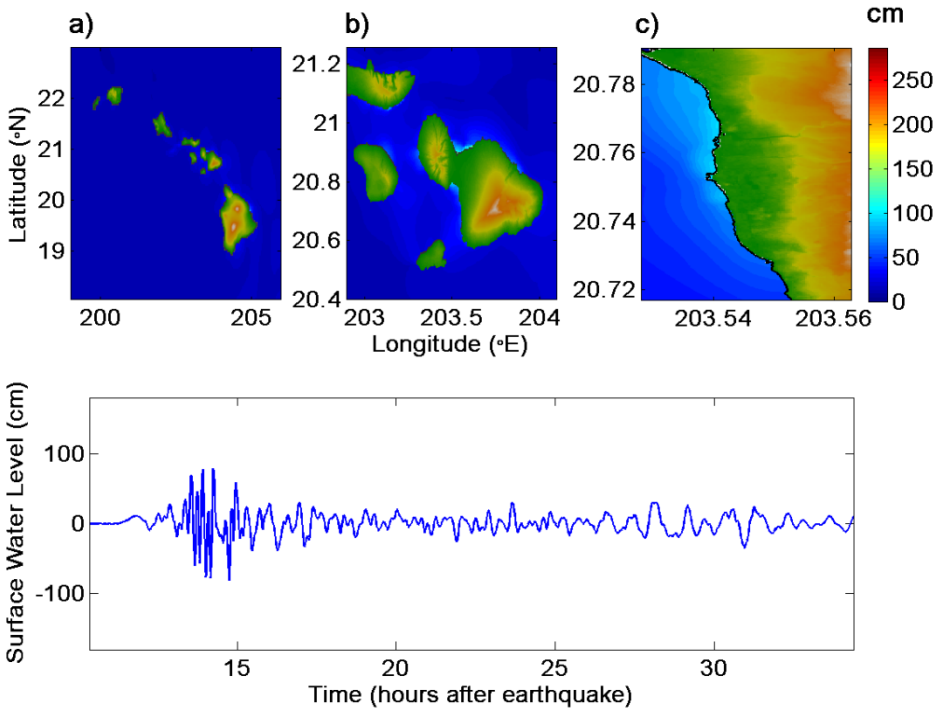

Figure 79. Plot of maximum tsunami wave amplitude distribution for Grids A, B and C and tsunami time series at the warning point for synthetic case CS31-40 with forecast model.

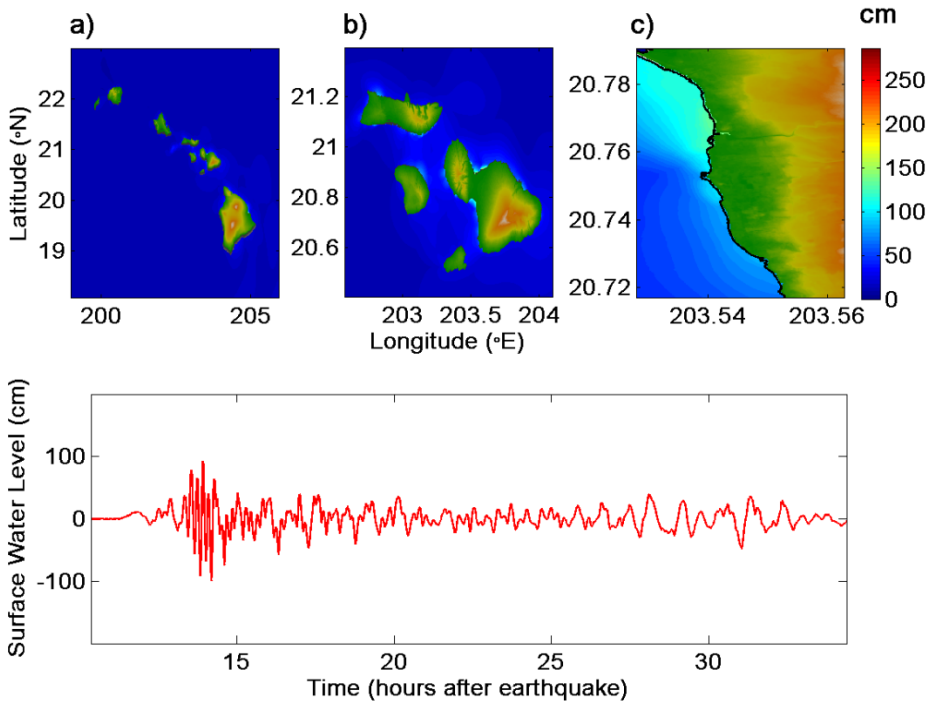

Figure 80. Plot of maximum tsunami wave amplitude distribution for Grids A, B and C and tsunami time series at the warning point for synthetic case CS31-40 with reference model.

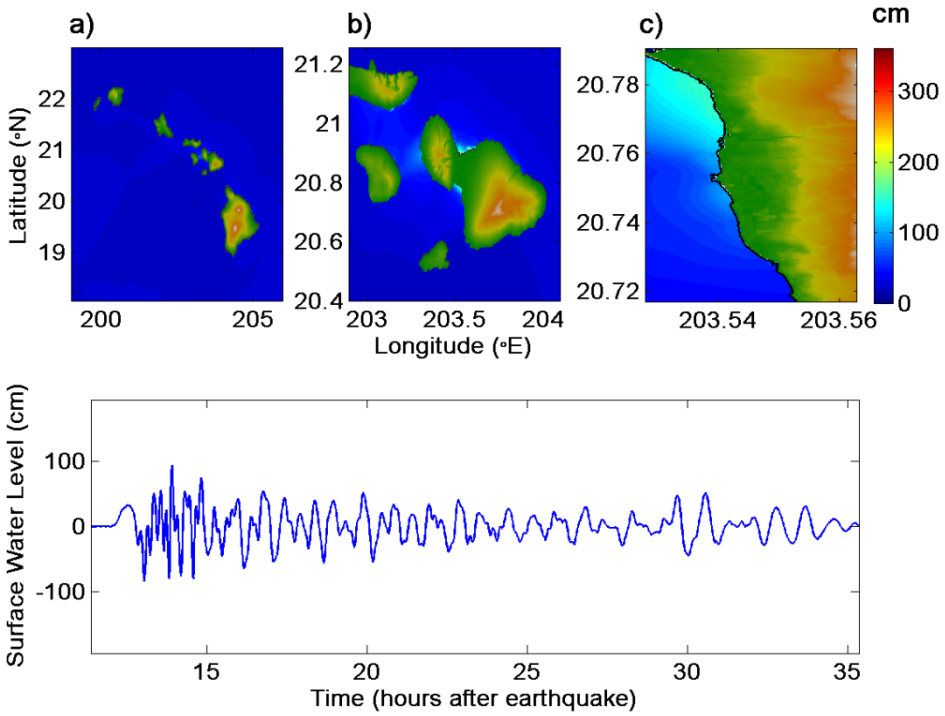

Figure 81. Plot of maximum tsunami wave amplitude distribution for Grids A, B and C and tsunami time series at the warning point for synthetic case CS41-50 with forecast model.

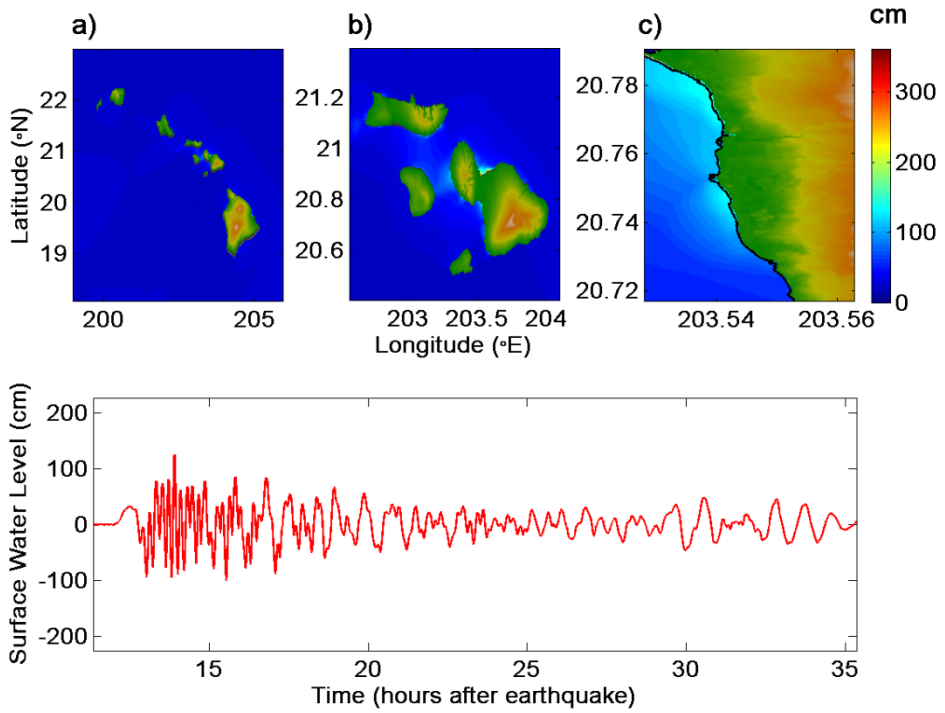

Figure 82. Plot of maximum tsunami wave amplitude distribution for Grids A, B and C and tsunami time series at the warning point for synthetic case CS41-50 with reference model.

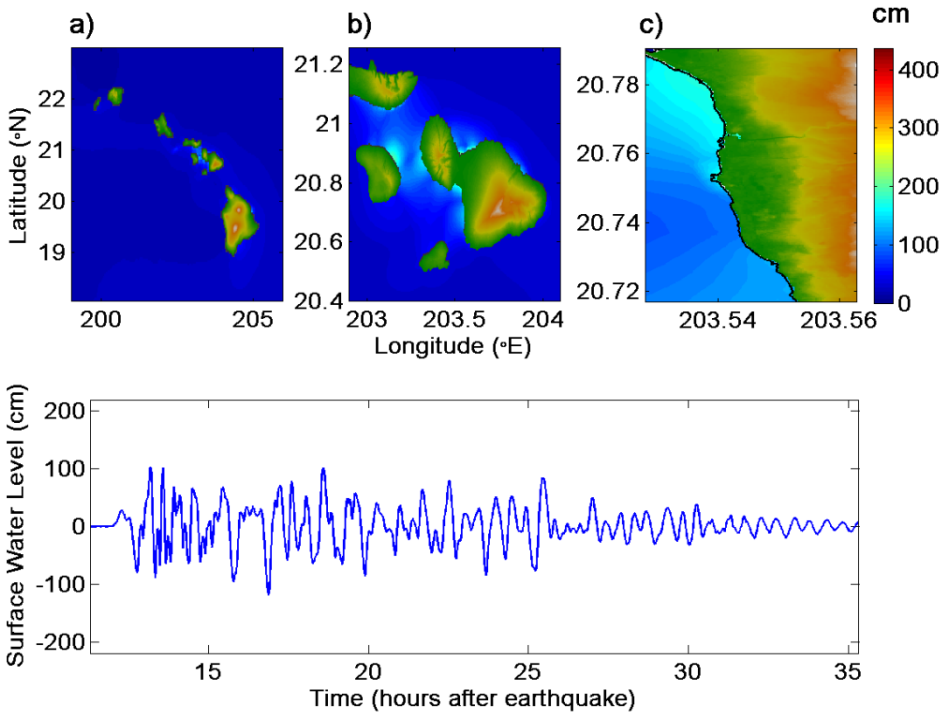

Figure 83. Plot of maximum tsunami wave amplitude distribution for Grids A, B and C and tsunami time series at the warning point for synthetic case CS51-60 with forecast model.

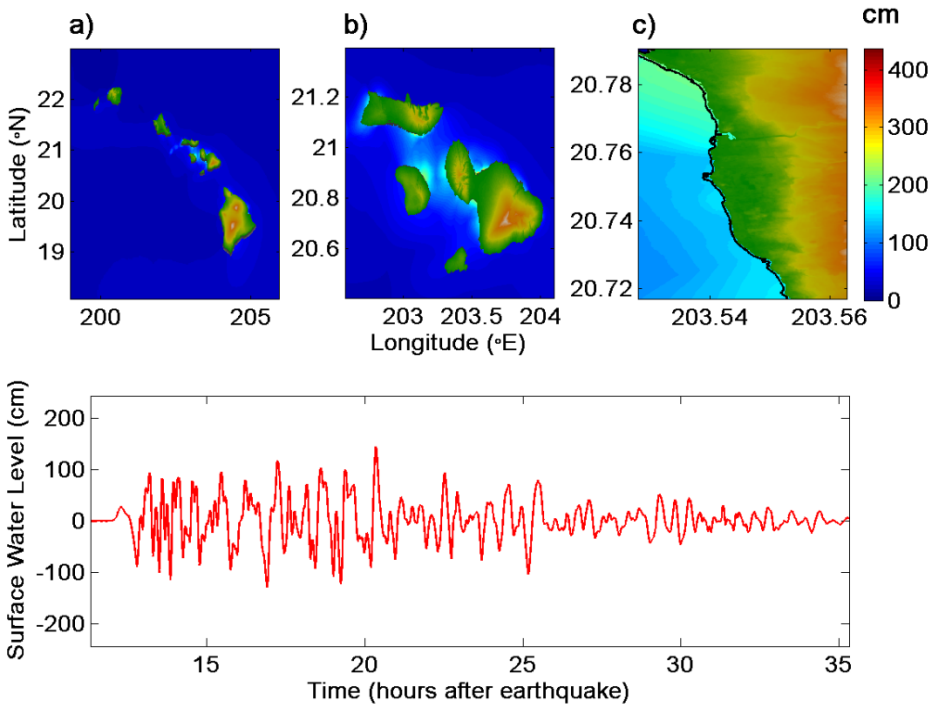

Figure 84. Plot of maximum tsunami wave amplitude distribution for Grids A, B and C and tsunami time series at the warning point for synthetic case CS51-60 with reference model.

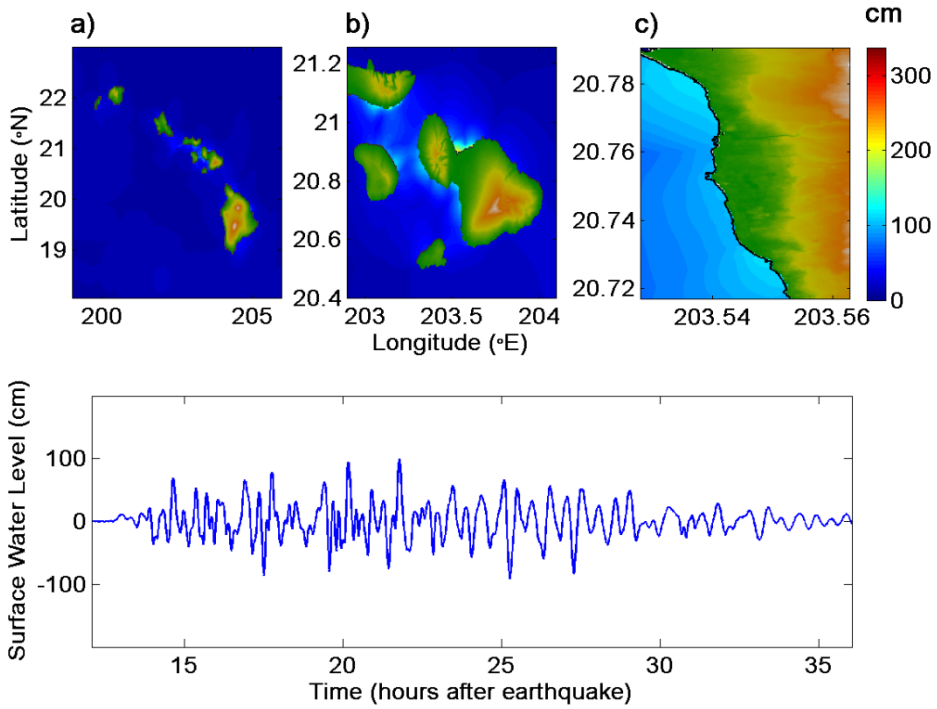

Figure 85. Plot of maximum tsunami wave amplitude distribution for Grids A, B and C and tsunami time series at the warning point for synthetic case CSSZ 61-70 with forecast model.

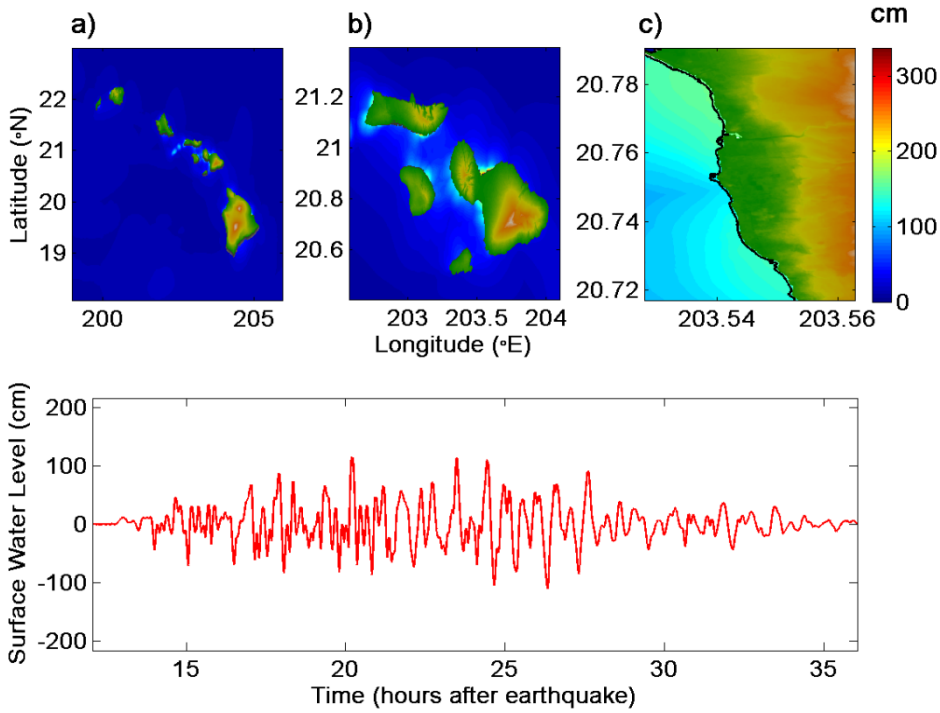

Figure 86. Plot of maximum tsunami wave amplitude distribution for Grids A, B and C and tsunami time series at the warning point for synthetic case CSSZ 61-70 with reference model.

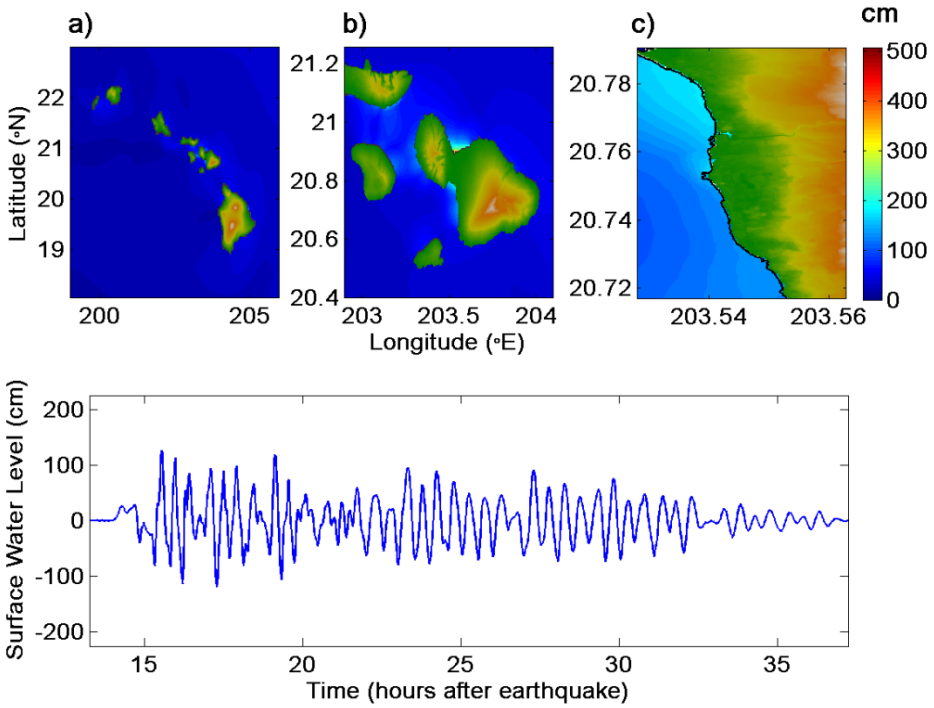

Figure 87. Plot of maximum tsunami wave amplitude distribution for Grids A, B and C and tsunami time series at the warning point for synthetic case CSSZ 71-80 with forecast model.

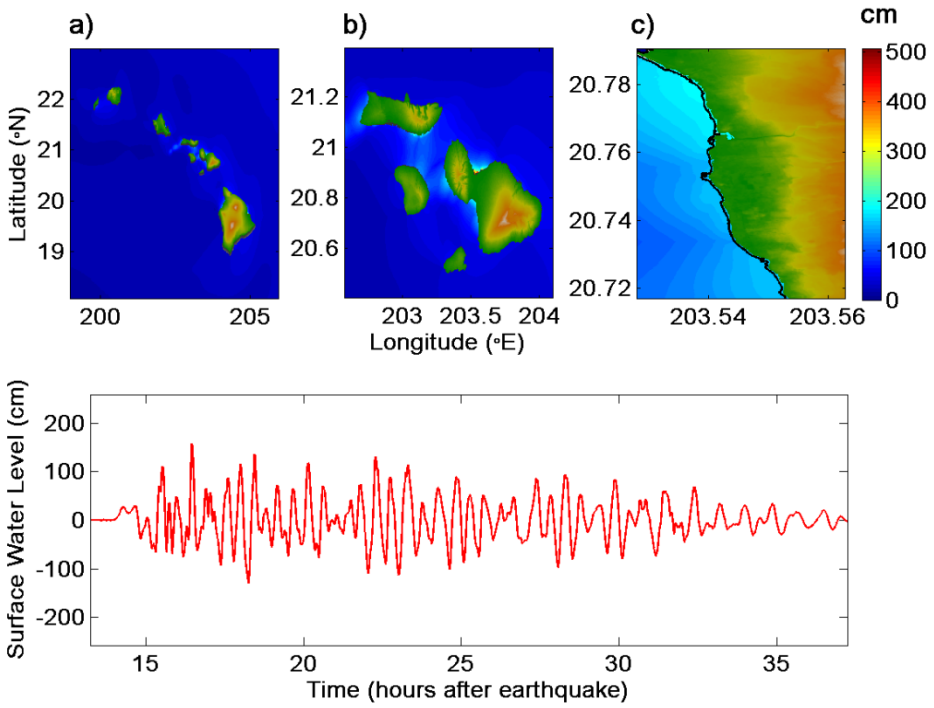

Figure 88. Plot of maximum tsunami wave amplitude distribution for Grids A, B and C and tsunami time series at the warning point for synthetic case CSSZ 71-80 with reference model.

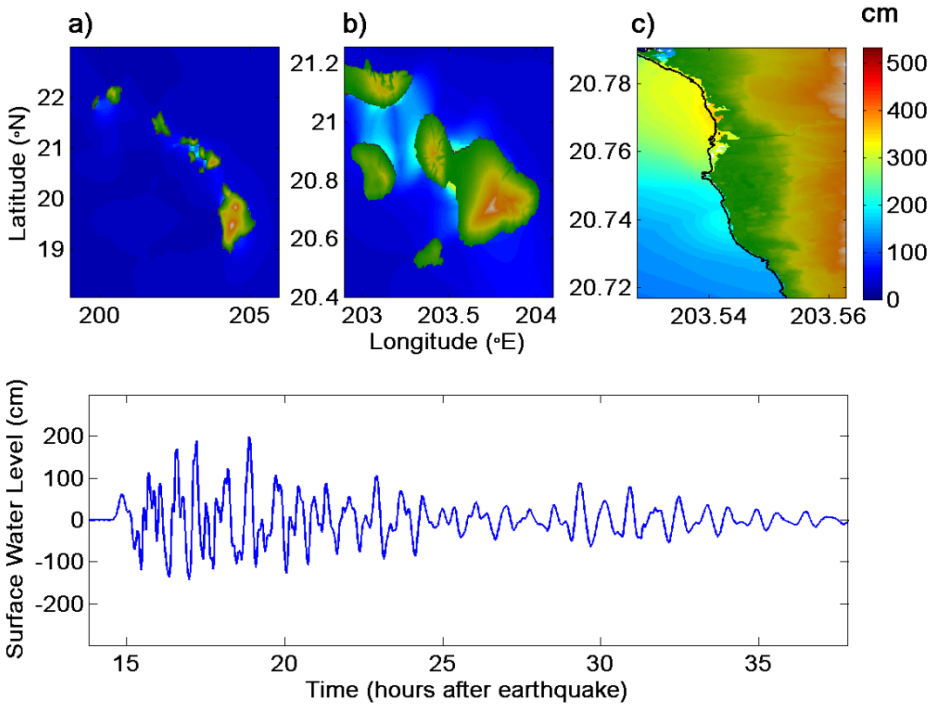

Figure 89. Plot of maximum tsunami wave amplitude distribution for Grids A, B and C and tsunami time series at the warning point for synthetic case CSSZ 81-90 with forecast model. White areas on land indicate non-inundated sections.

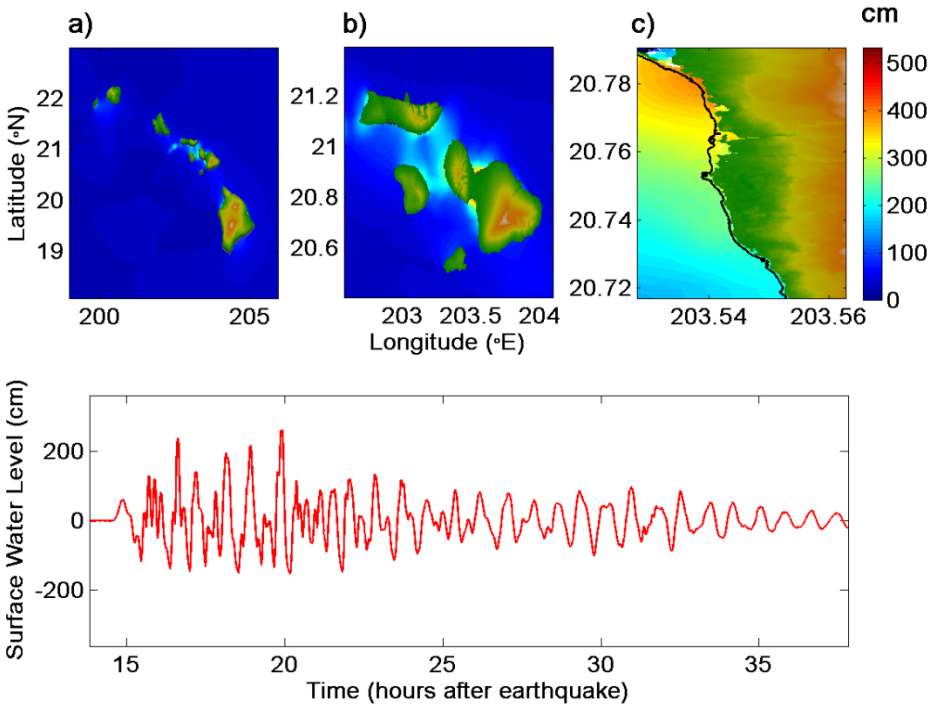

Figure 90. Plot of maximum tsunami wave amplitude distribution for Grids A, B and C and tsunami time series at the warning point for synthetic case CSSZ 81-90 with reference model. White areas on land indicate non-inundated sections.

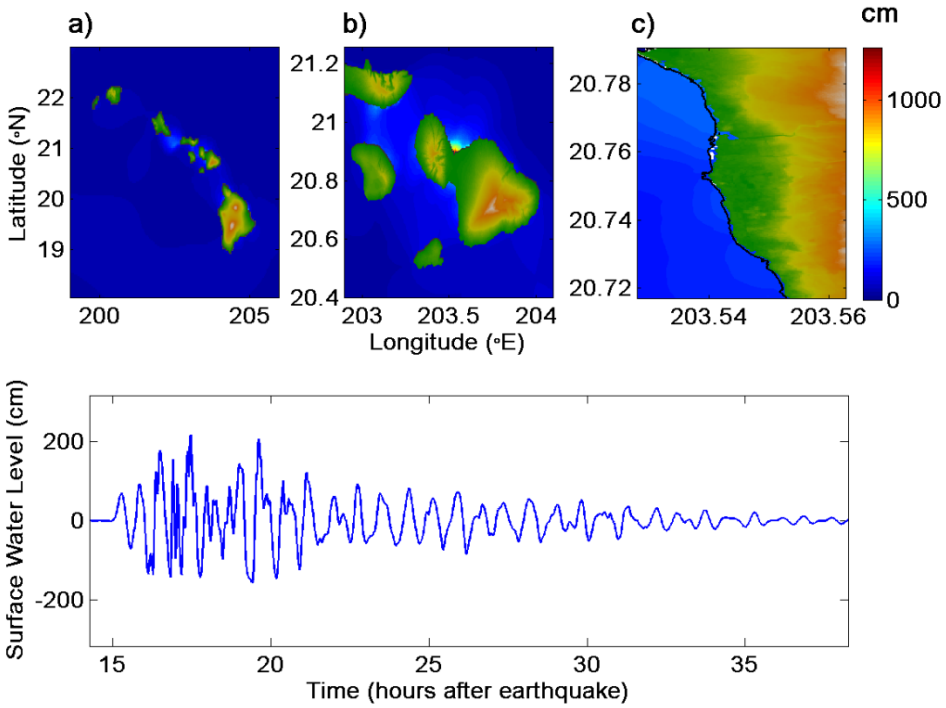

Figure 91. Plot of maximum tsunami wave amplitude distribution for Grids A, B and C and tsunami time series at the warning point for synthetic case CSSZ 91-100 with forecast model. White areas on land indicate non-inundated sections.

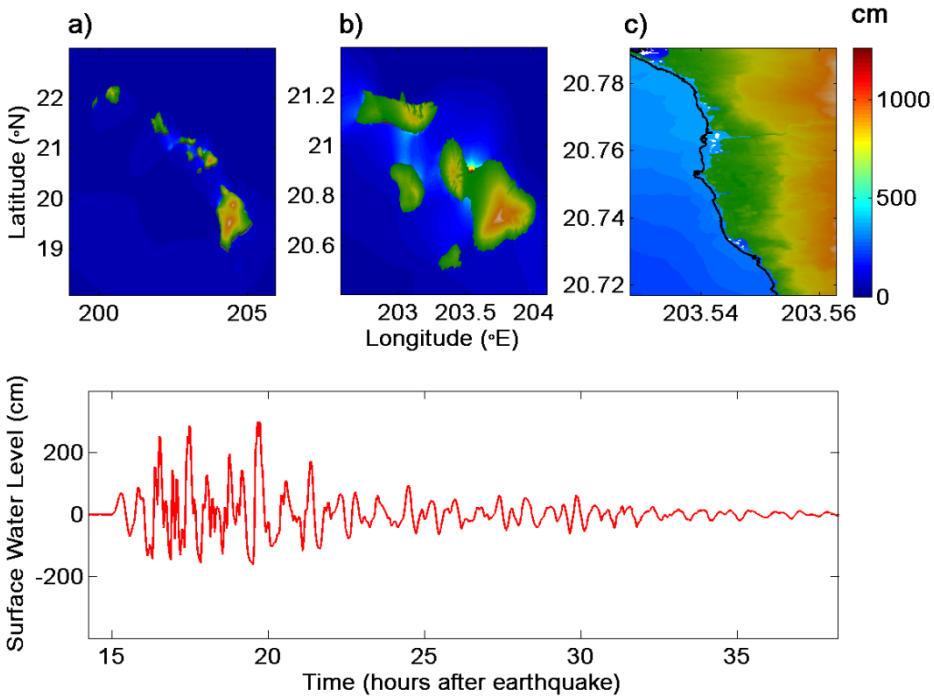

Figure 92. Plot of maximum tsunami wave amplitude distribution for Grids A, B and C and tsunami time series at the warning point for synthetic case CSSZ 91-100 with reference model. White areas on land indicate non-inundated sections.

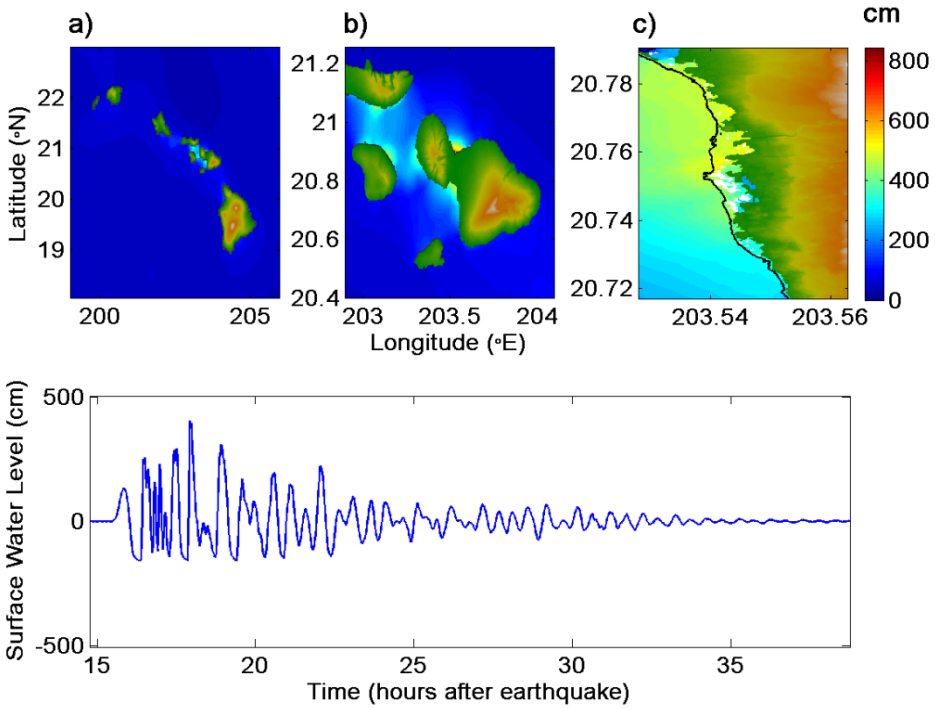

Figure 93. Plot of maximum tsunami wave amplitude distribution for Grids A, B and C and tsunami time series at the warning point for synthetic case CSSZ 101-110 with forecast model. White areas on land indicate non-inundated sections.

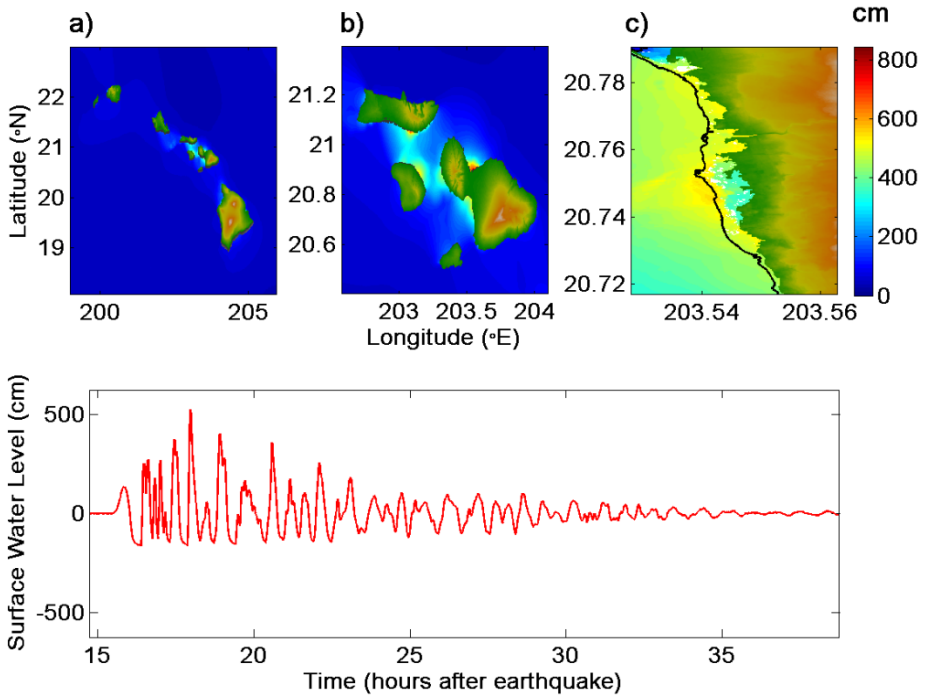

Figure 94. Plot of maximum tsunami wave amplitude distribution for Grids A, B and C and tsunami time series at the warning point for synthetic case CSSZ 101-110 with reference model. White areas on land indicate non-inundated sections.

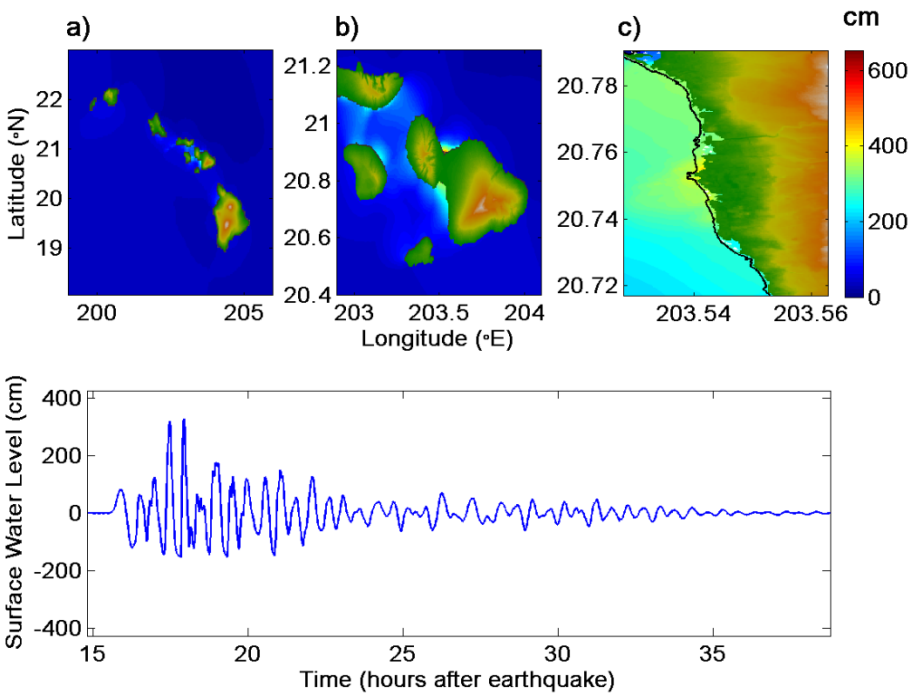

Figure 95. Plot of maximum tsunami wave amplitude distribution for Grids A, B and C and tsunami time series at the warning point for synthetic case CSSZ 106-115 with forecast model. White areas on land indicate non-inundated sections.

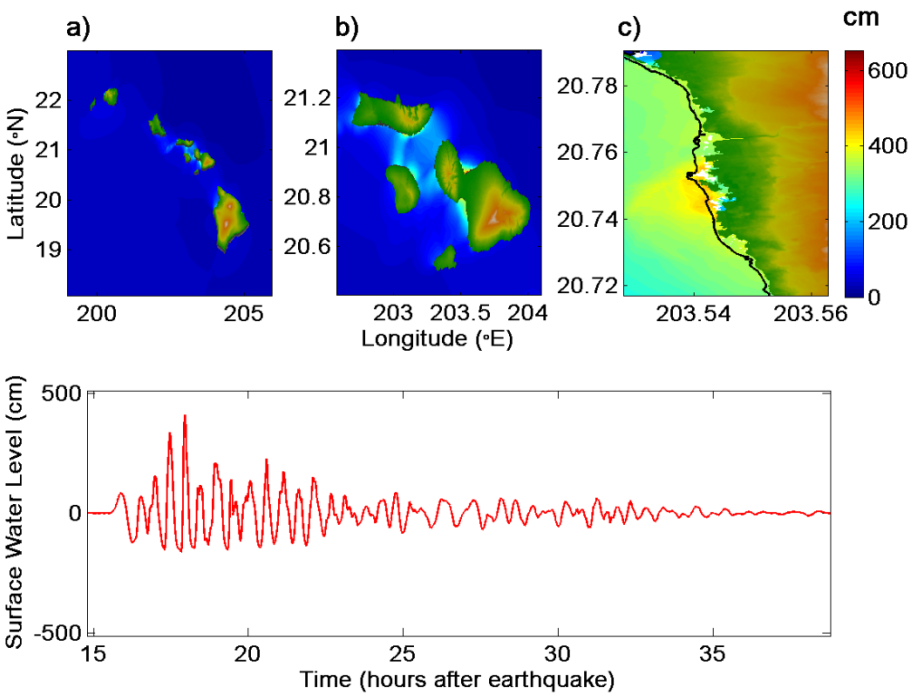

Figure 96. Plot of maximum tsunami wave amplitude distribution for Grids A, B and C and tsunami time series at the warning point for synthetic case CSSZ 106-115 with reference model. White areas on land indicate non-inundated sections.

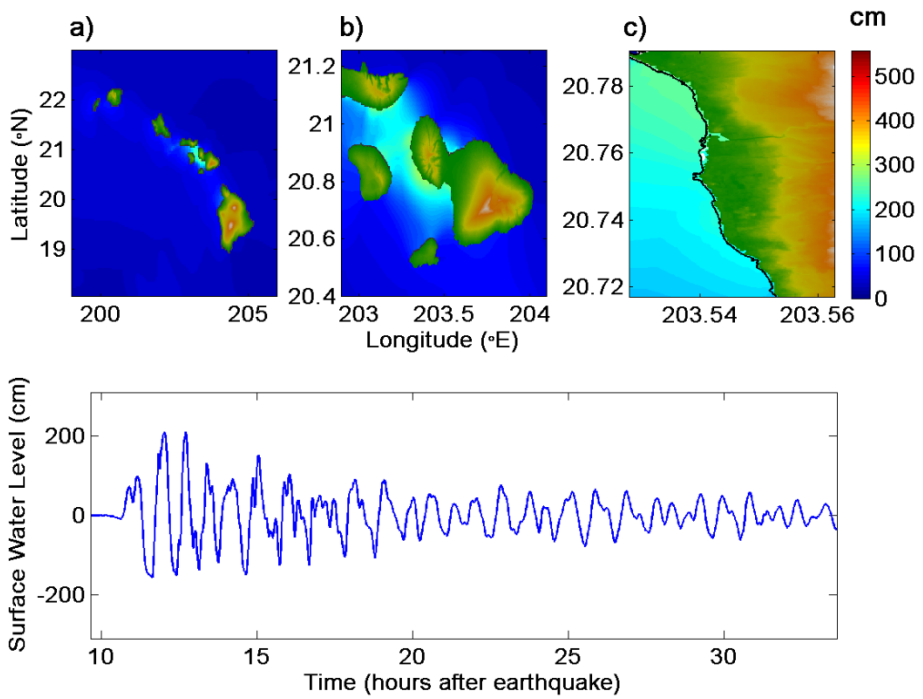

Figure 97. Plot of maximum tsunami wave amplitude distribution for Grids A, B and C and tsunami time series at the warning point for synthetic case EPSZ 01-10 with forecast model. White areas on land indicate non-inundated sections.

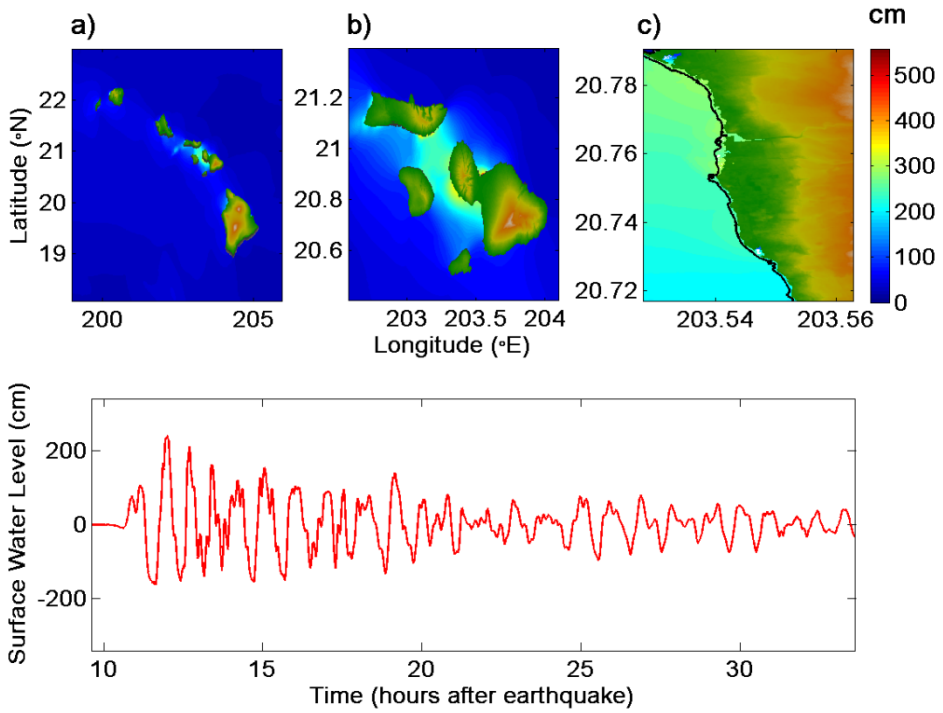

Figure 98. Plot of maximum tsunami wave amplitude distribution for Grids A, B and C and tsunami time series at the warning point for synthetic case EPSZ 01-10 with reference model. White areas on land indicate non-inundated sections.

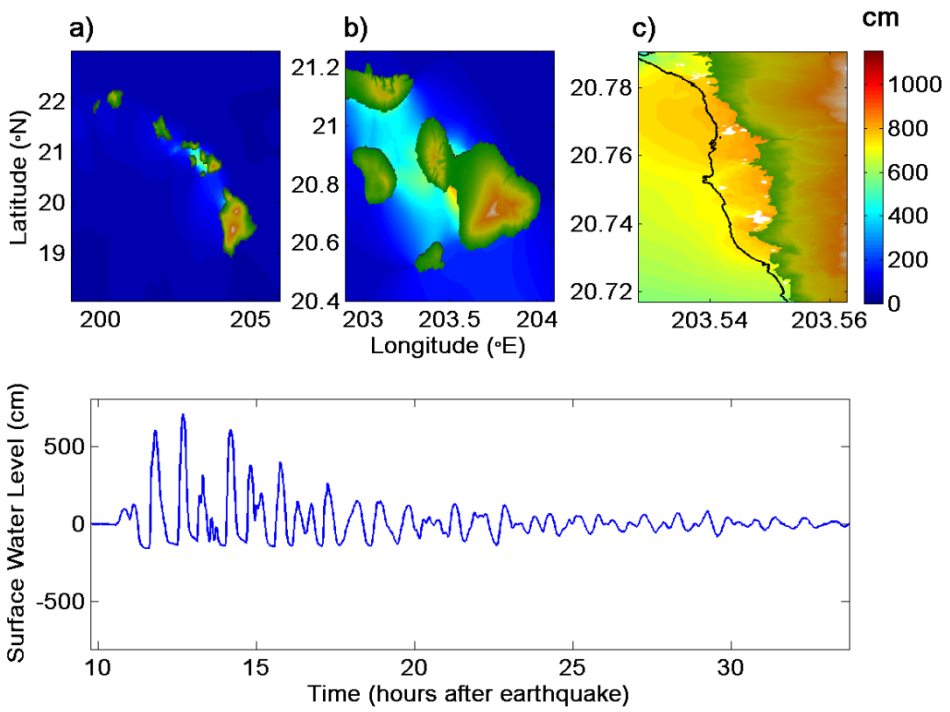

Figure 99. Plot of maximum tsunami wave amplitude distribution for Grids A, B and C and tsunami time series at the warning point for synthetic case EPSZ 09-18 with forecast model. White areas on land indicate non-inundated sections.

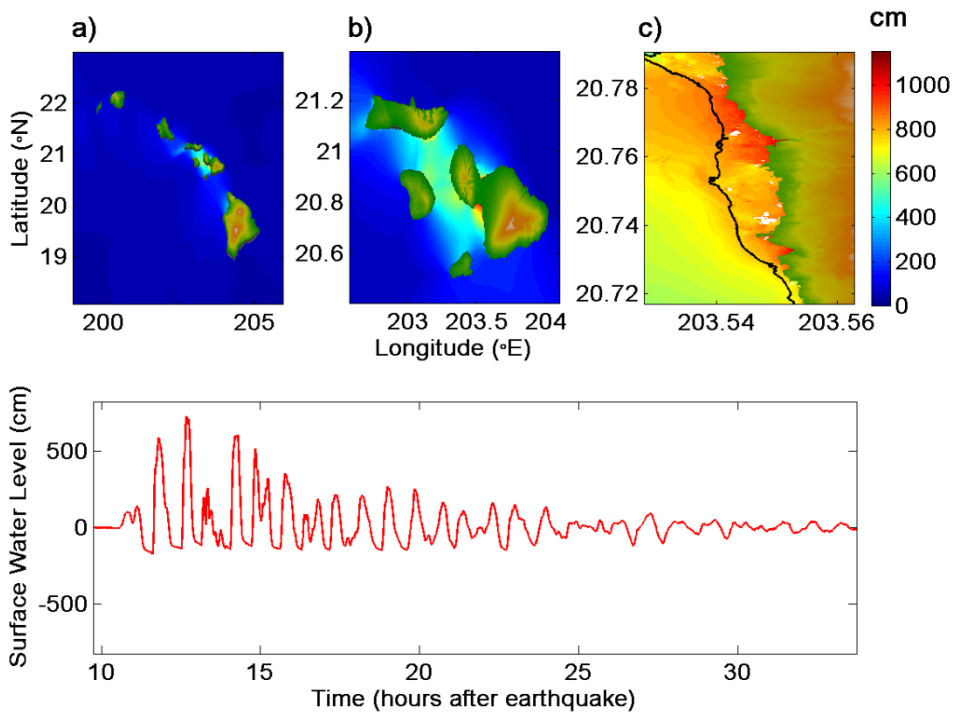

Figure 100. Plot of maximum tsunami wave amplitude distribution for Grids A, B and C and tsunami time series at the warning point for synthetic case EPSZ 09-18 with reference model. White areas on land indicate non-inundated sections.

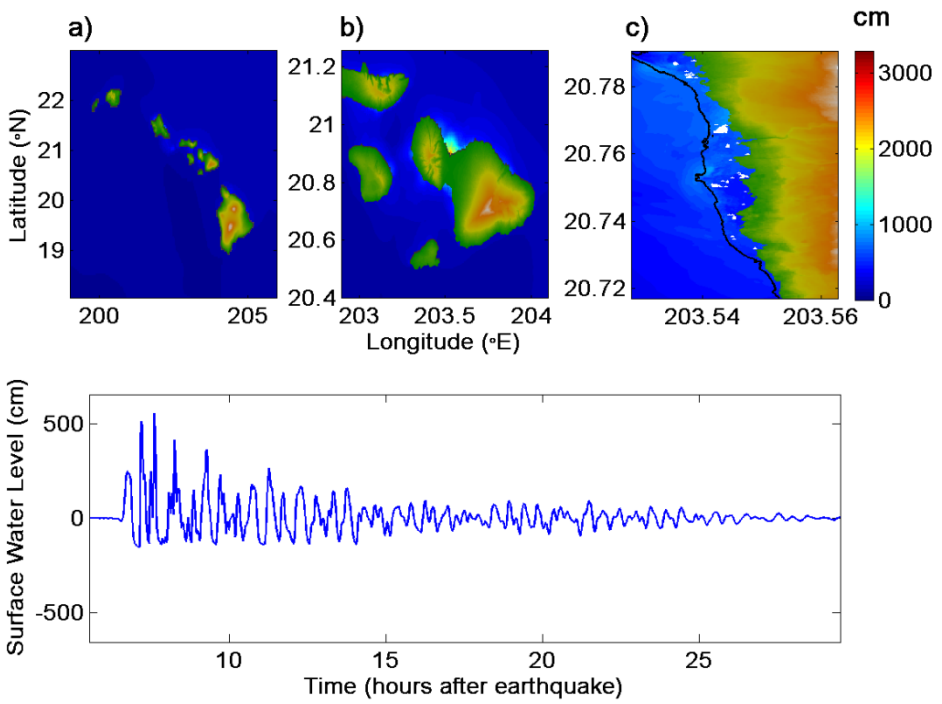

Figure 101. Plot of maximum tsunami wave amplitude distribution for Grids A, B and C and tsunami time series at the warning point for synthetic case KISZ 01-10 with forecast model. White areas on land indicate non-inundated sections.

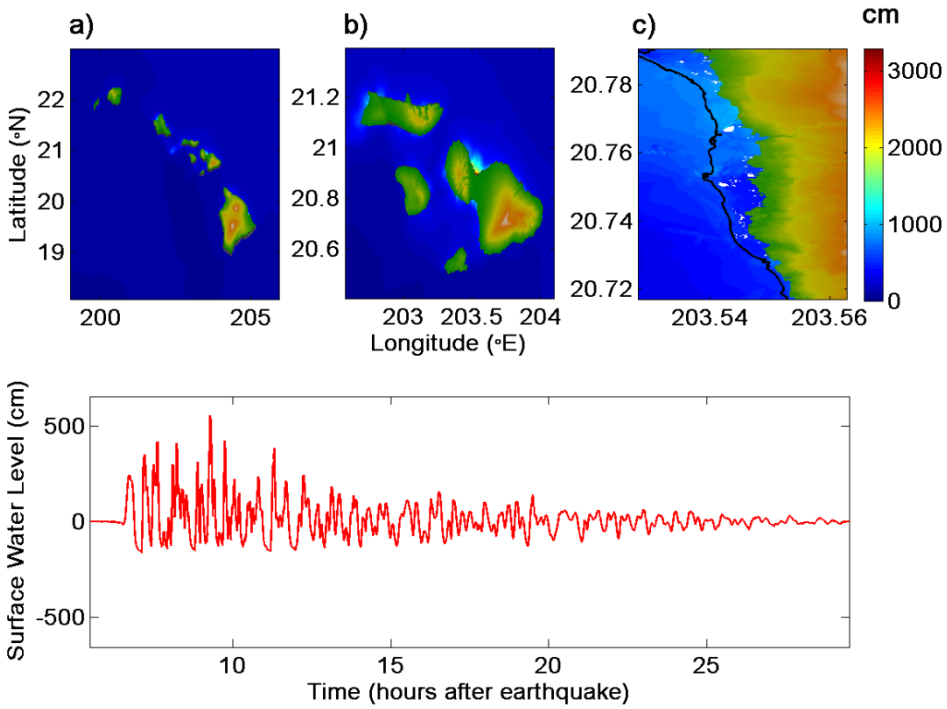

Figure 102. Plot of maximum tsunami wave amplitude distribution for Grids A, B and C and tsunami time series at the warning point for synthetic case KISZ 01-10 with reference model. White areas on land indicate non-inundated sections.

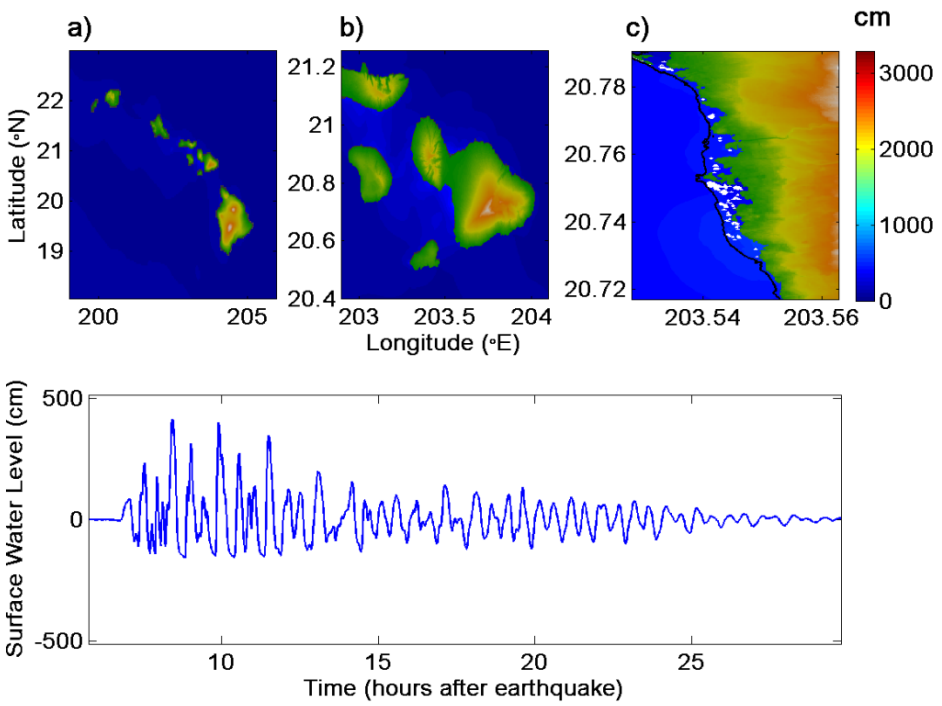

Figure 103. Plot of maximum tsunami wave amplitude distribution for Grids A, B and C and tsunami time series at the warning point for synthetic case KISZ 11-20 with forecast model. White areas on land indicate non-inundated sections.

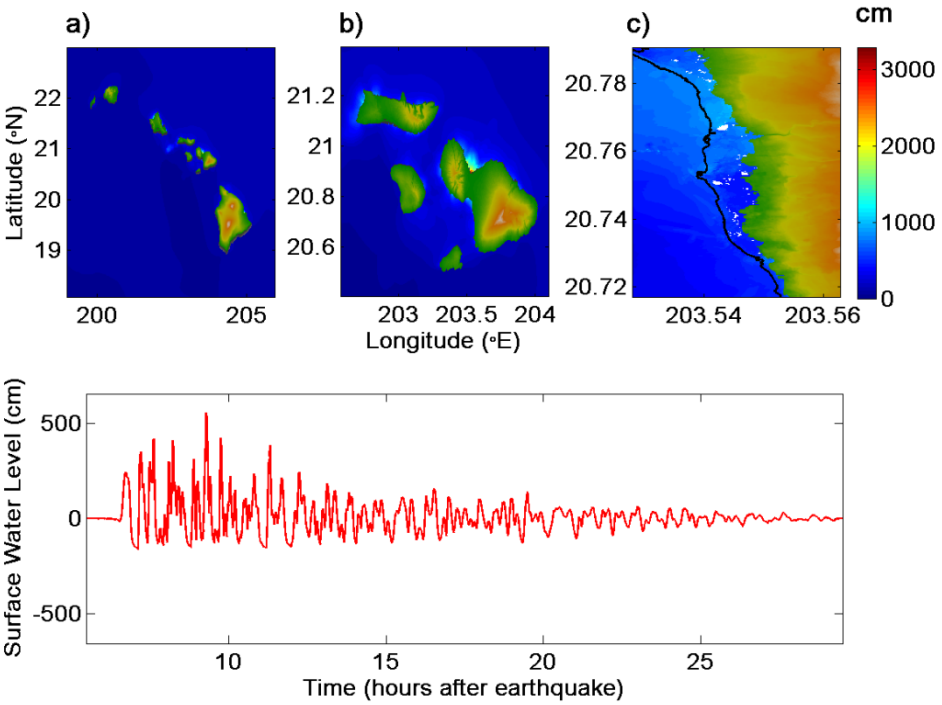

Figure 104. Plot of maximum tsunami wave amplitude distribution for Grids A, B and C and tsunami time series at the warning point for synthetic case KISZ 11-20 with reference model. White areas on land indicate non-inundated sections.

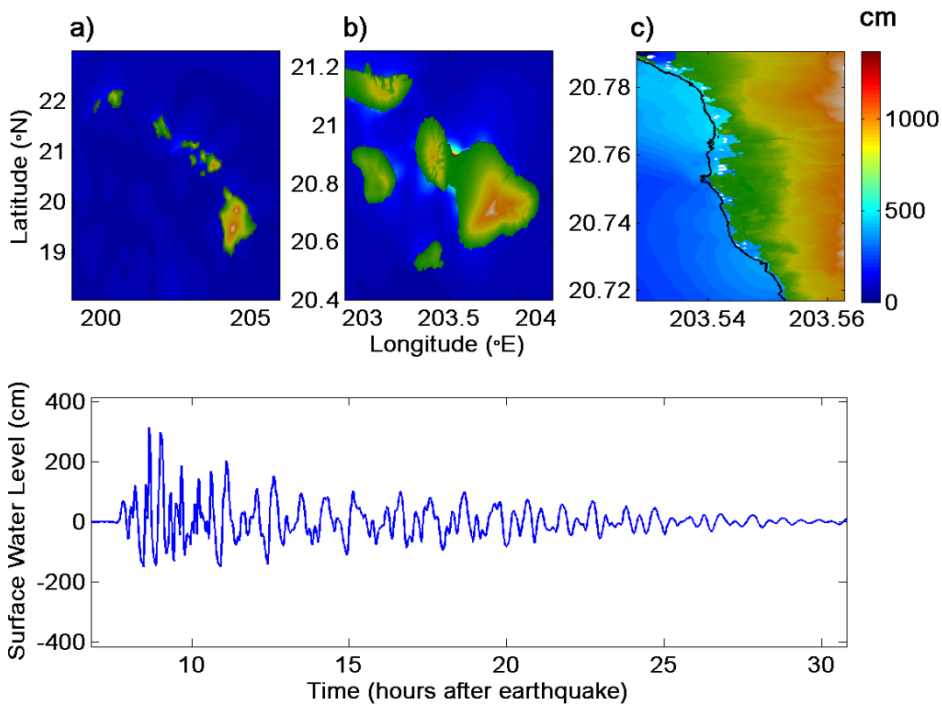

Figure 105. Plot of maximum tsunami wave amplitude distribution for Grids A, B and C and tsunami time series at the warning point for synthetic case KISZ 32-41 with forecast model. White areas on land indicate non-inundated sections.

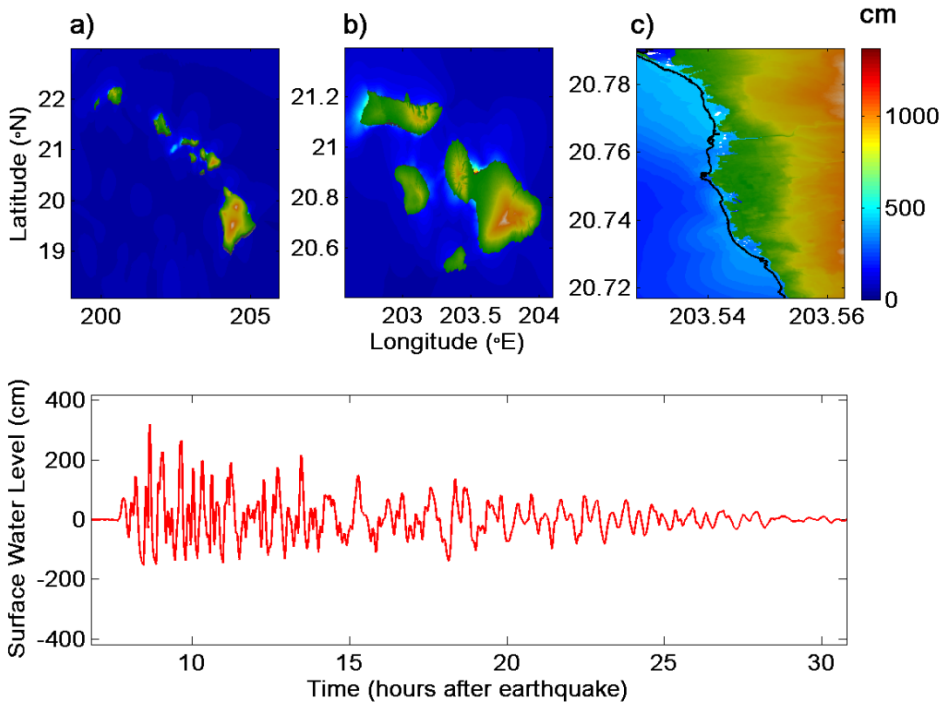

Figure 106. Plot of maximum tsunami wave amplitude distribution for Grids A, B and C and tsunami time series at the warning point for synthetic case KISZ 32-41 with reference model. White areas on land indicate non-inundated sections.

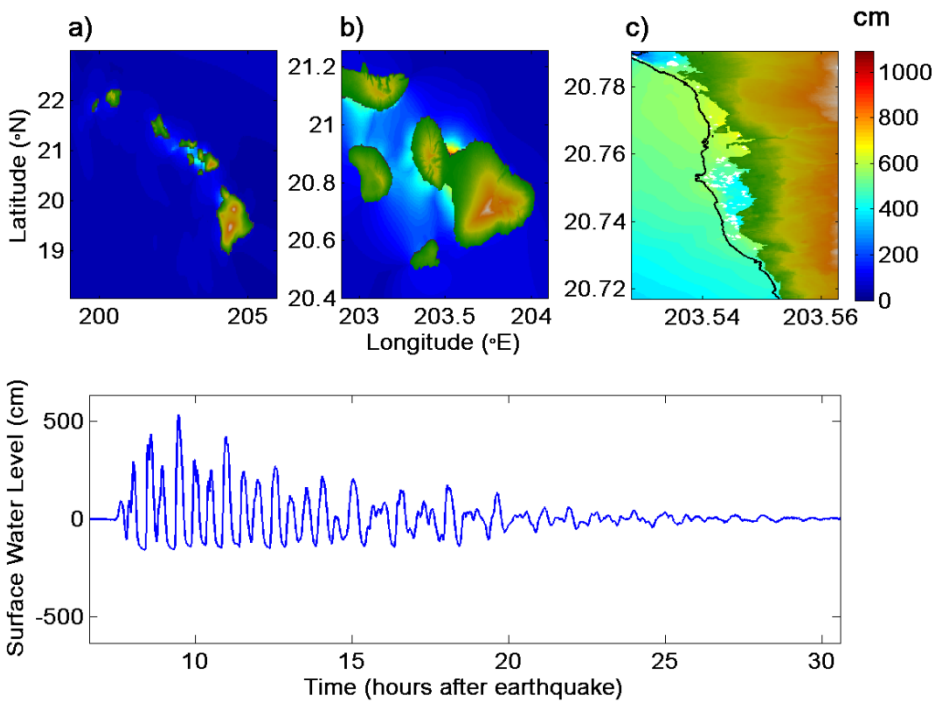

Figure 107. Plot of maximum tsunami wave amplitude distribution for Grids A, B and C and tsunami time series at the warning point for synthetic case KISZ421-51 with forecast model. White areas on land indicate non-inundated sections.

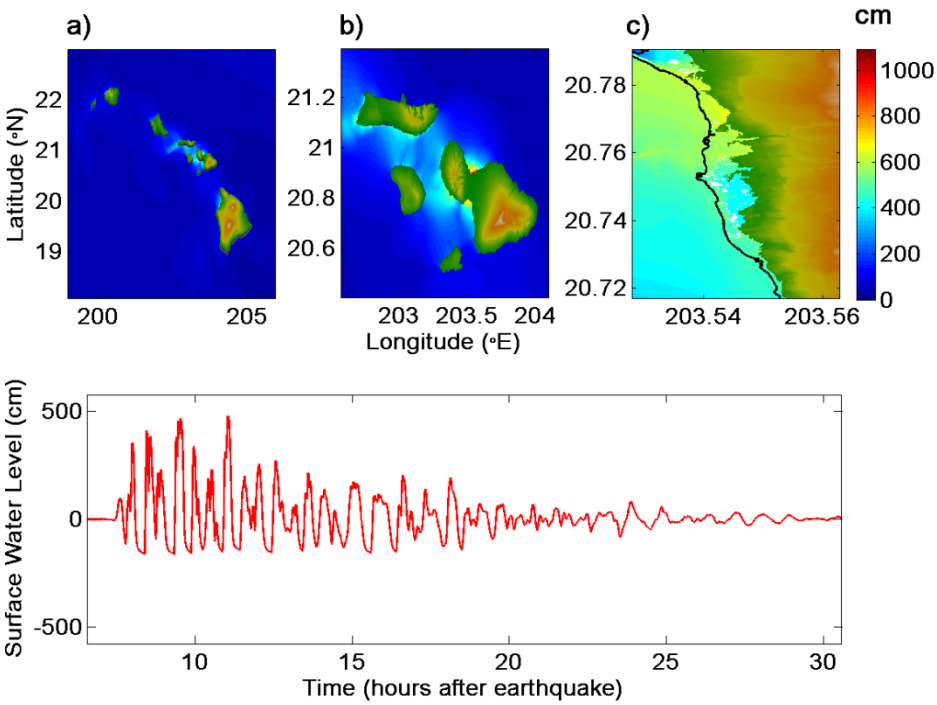

Figure 108. Plot of maximum tsunami wave amplitude distribution for Grids A, B and C and tsunami time series at the warning point for synthetic case KISZ 42-51 with reference model. White areas on land indicate non-inundated sections.

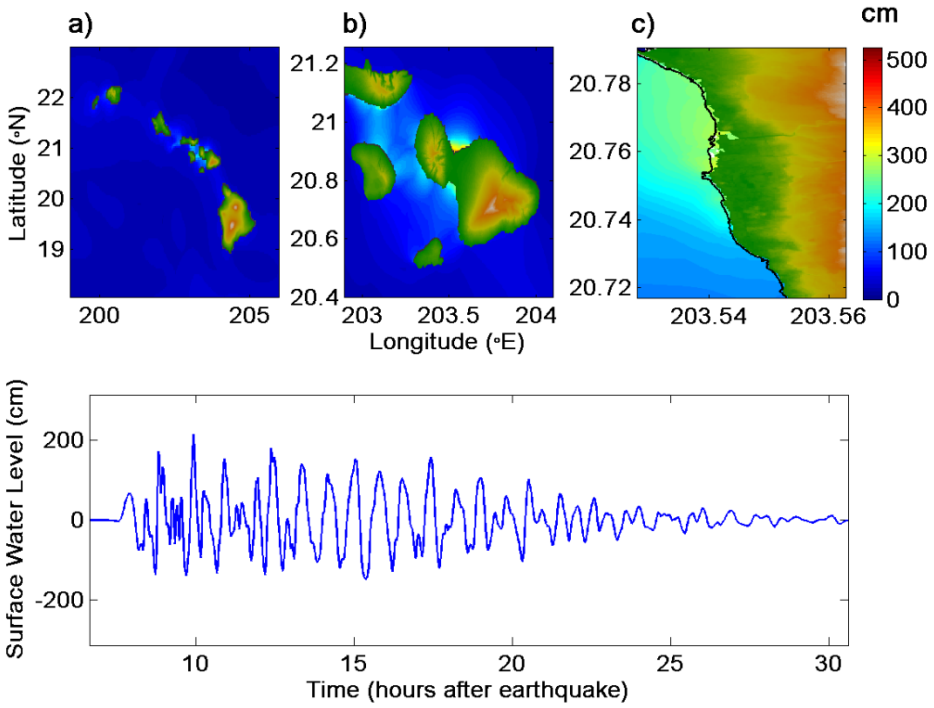

Figure 109. Plot of maximum tsunami wave amplitude distribution for Grids A, B and C and tsunami time series at the warning point for synthetic case KISZ52-61 with forecast model. White areas on land indicate non-inundated sections.

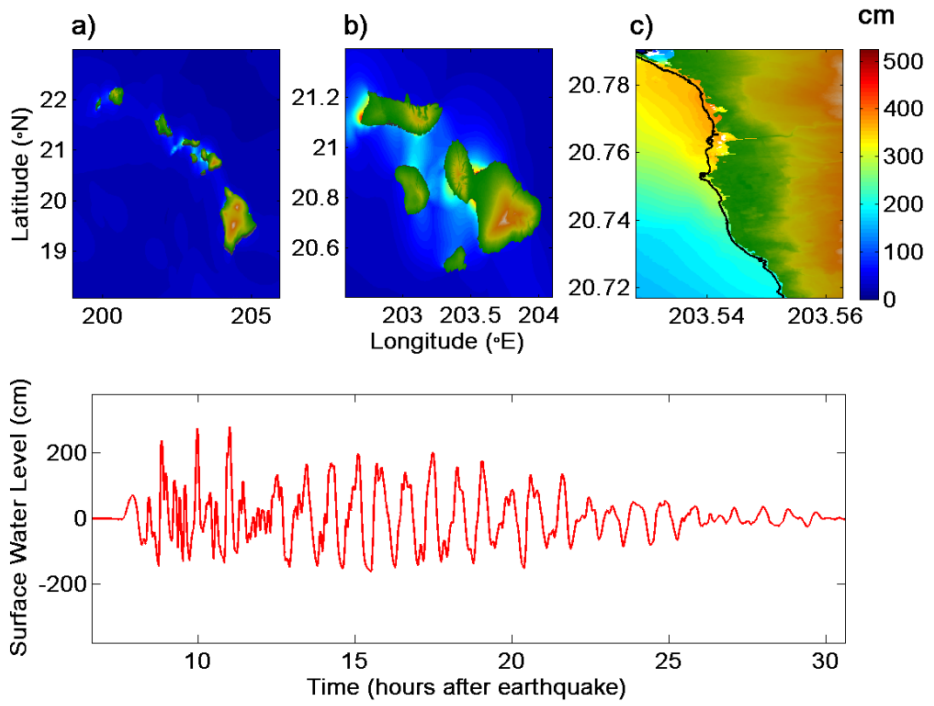

Figure 110. Plot of maximum tsunami wave amplitude distribution for Grids A, B and C and tsunami time series at the warning point for synthetic case KISZ 52-61 with reference model. White areas on land indicate non-inundated sections.

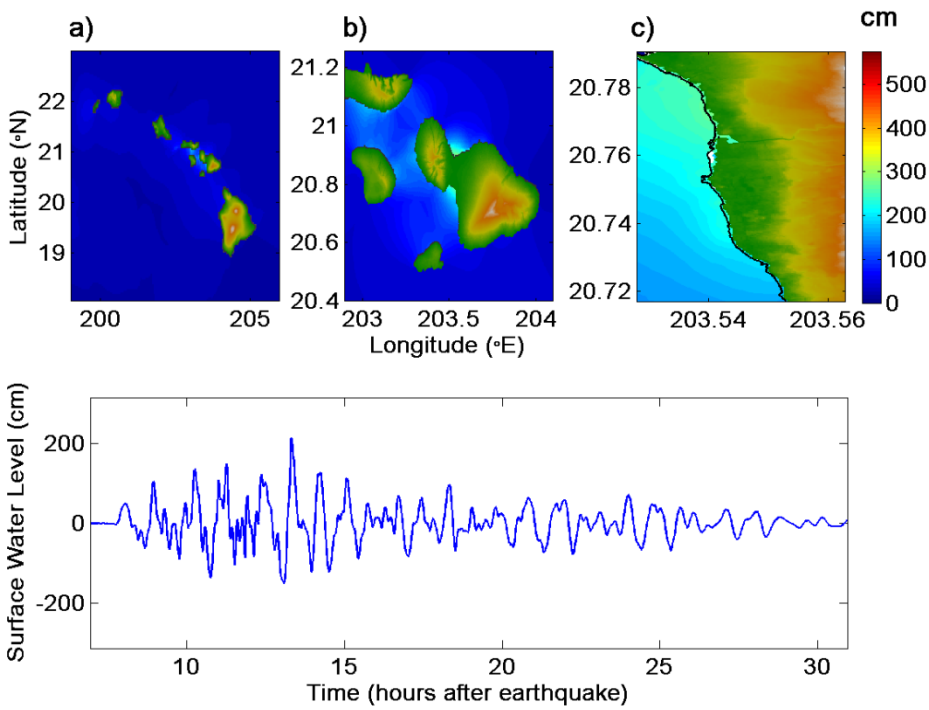

Figure 111. Plot of maximum tsunami wave amplitude distribution for Grids A, B and C and tsunami time series at the warning point for synthetic case KISZ56-65 with forecast model. White areas on land indicate non-inundated sections.

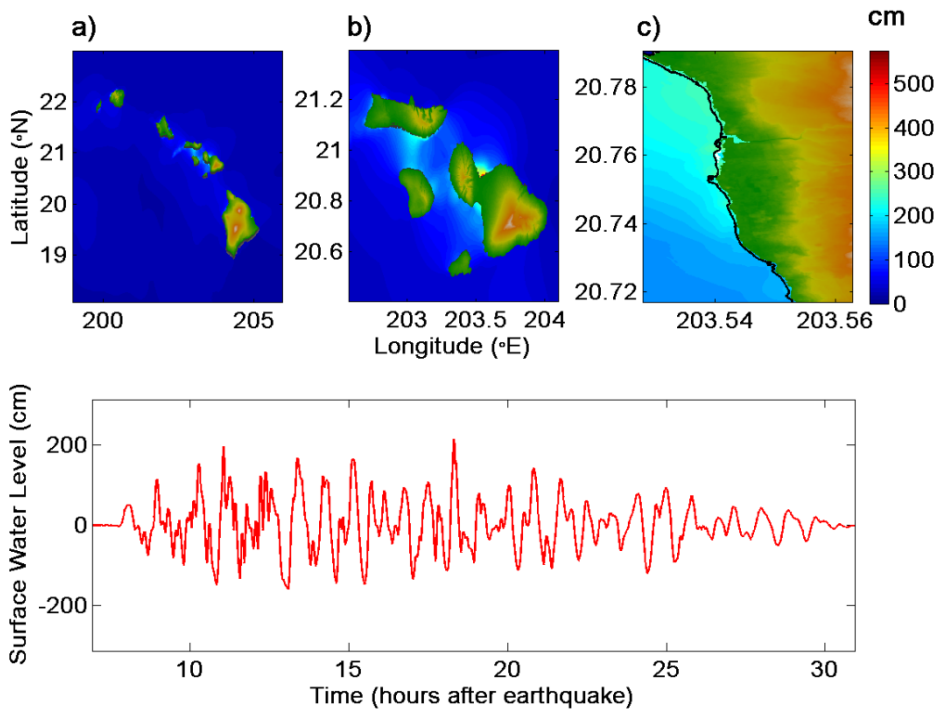

Figure 112. Plot of maximum tsunami wave amplitude distribution for Grids A, B and C and tsunami time series at the warning point for synthetic case KISZ 56-65 with reference model. White areas on land indicate non-inundated sections.

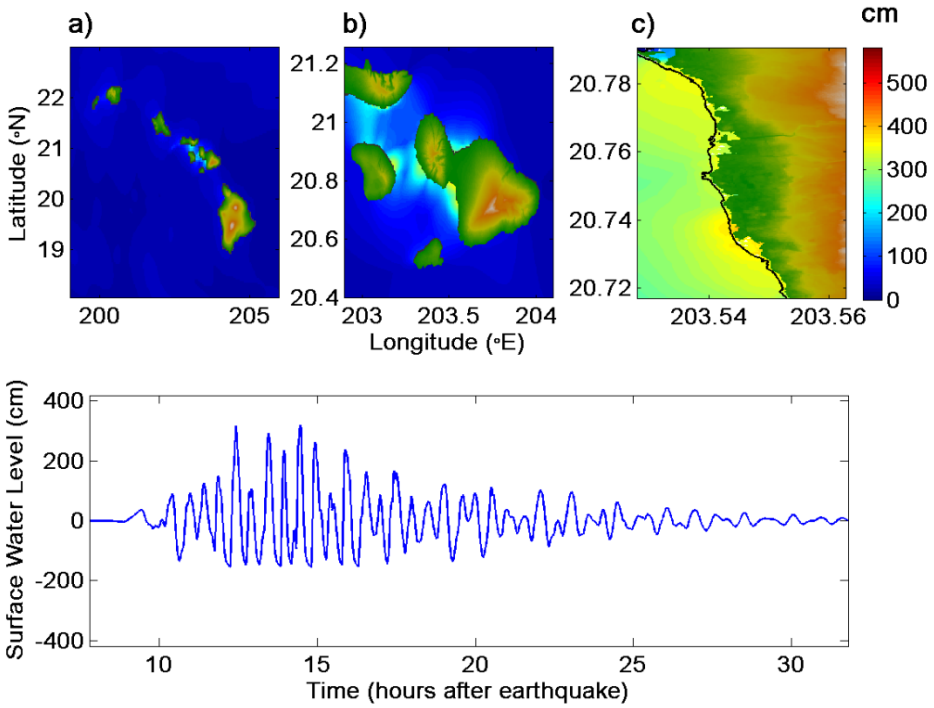

Figure 113. Plot of maximum tsunami wave amplitude distribution for Grids A, B and C and tsunami time series at the warning point for synthetic case KISZ66-75 with forecast model. White areas on land indicate non-inundated sections.

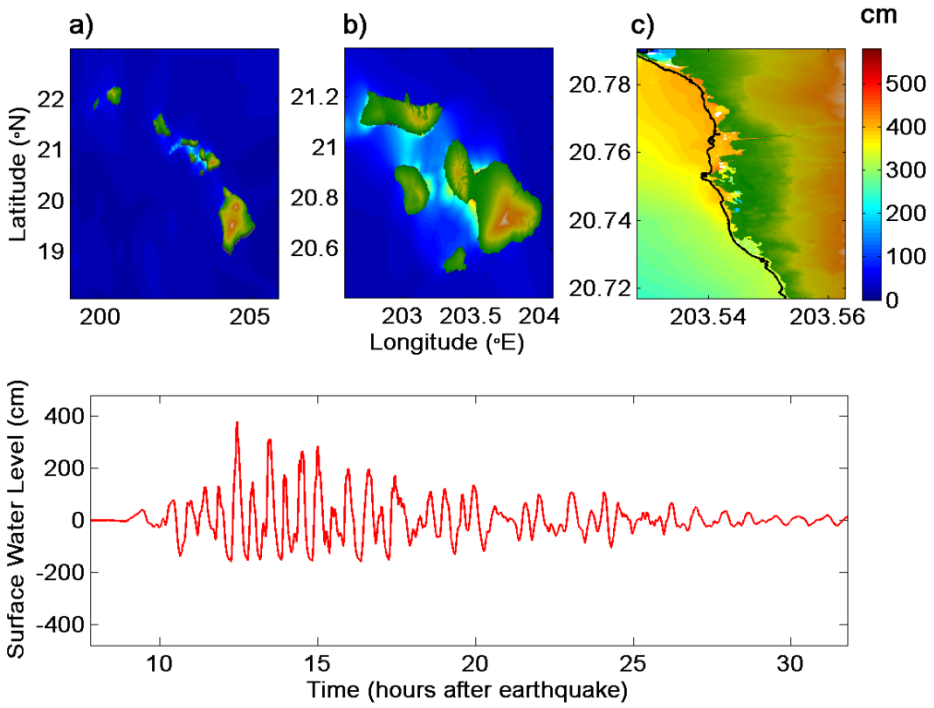

Figure 114. Plot of maximum tsunami wave amplitude distribution for Grids A, B and C and tsunami time series at the warning point for synthetic case KISZ66-75 with reference model. White areas on land indicate non-inundated sections.

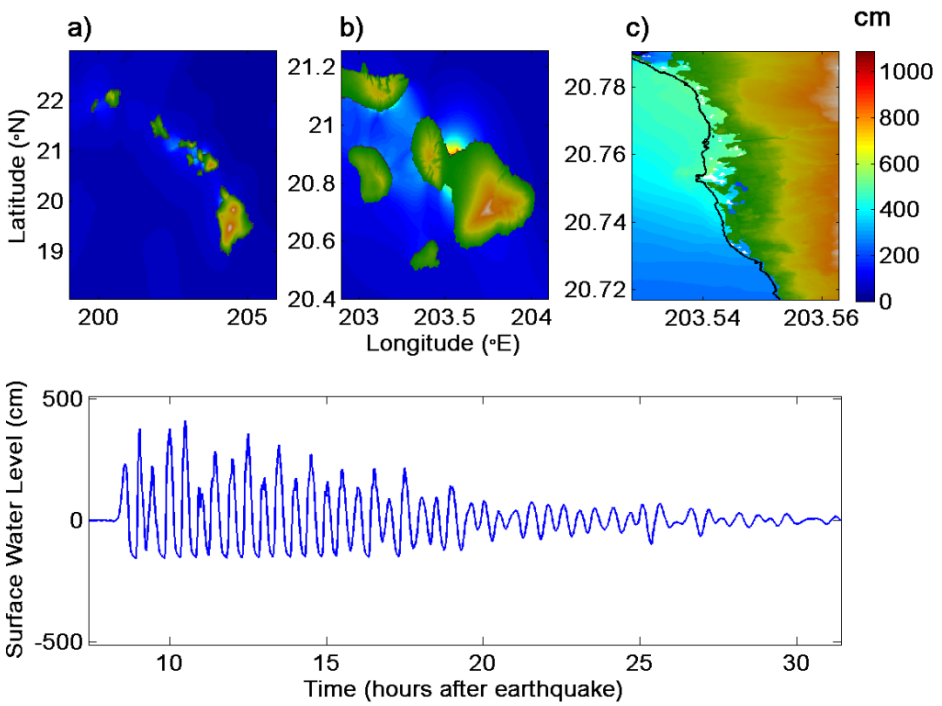

Figure 115. Plot of maximum tsunami wave amplitude distribution for Grids A, B and C and tsunami time series at the warning point for synthetic case MOSZ01-10 with forecast model. White areas on land indicate non-inundated sections.

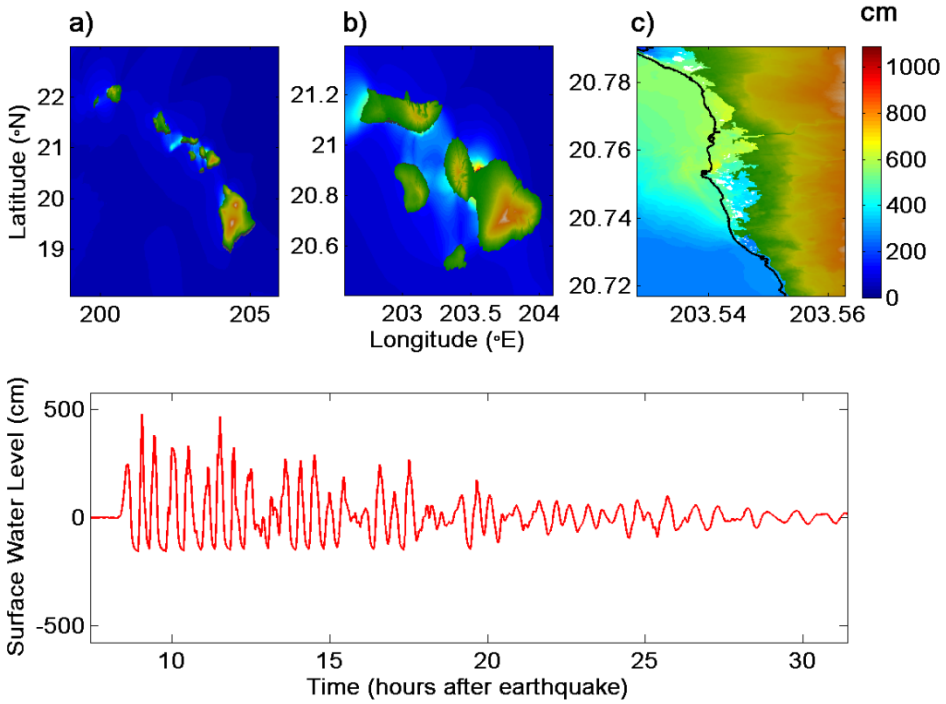

Figure 116. Plot of maximum tsunami wave amplitude distribution for Grids A, B and C and tsunami time series at the warning point for synthetic case MOSZ01-10 with reference model. White areas on land indicate non-inundated sections.

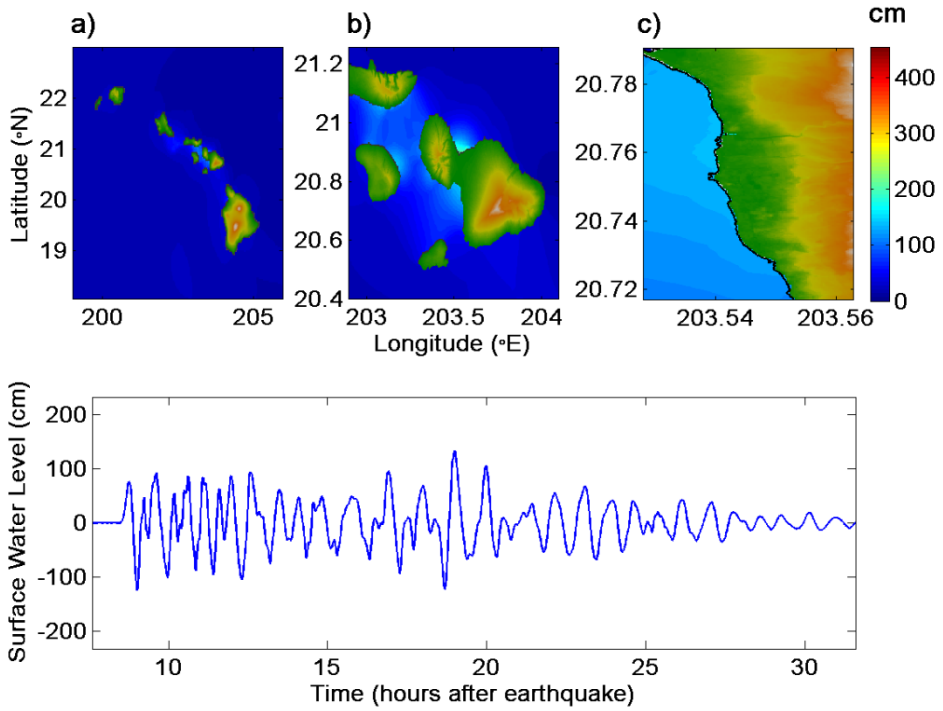

Figure 117. Plot of maximum tsunami wave amplitude distribution for Grids A, B and C and tsunami time series at the warning point for synthetic case MOSZ08-17 with forecast model.

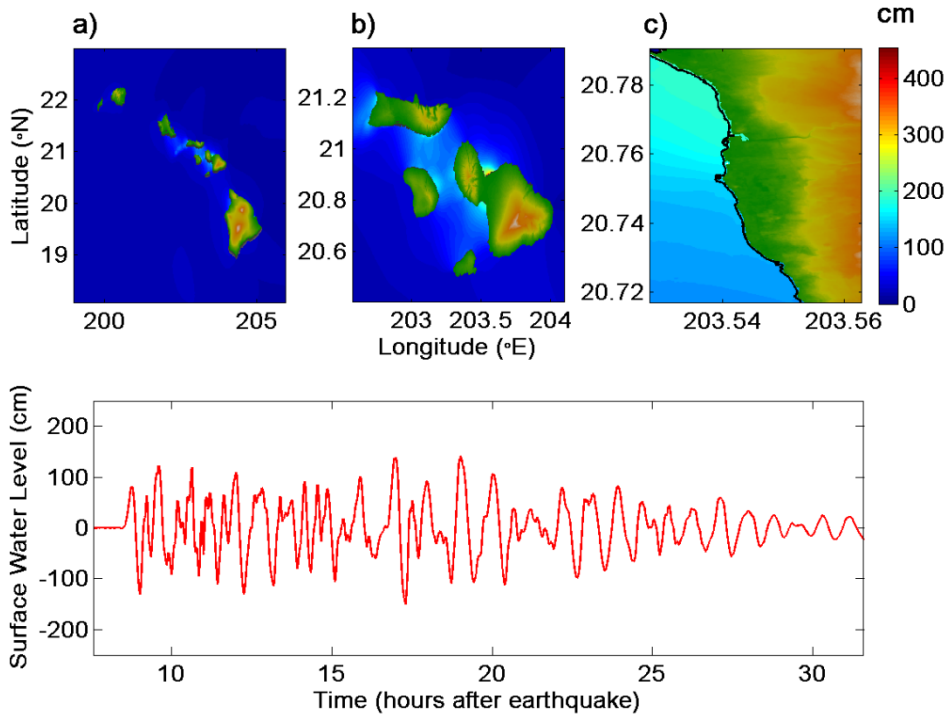

Figure 118. Plot of maximum tsunami wave amplitude distribution for Grids A, B and C and tsunami time series at the warning point for synthetic case MOSZ08-17 with reference model.

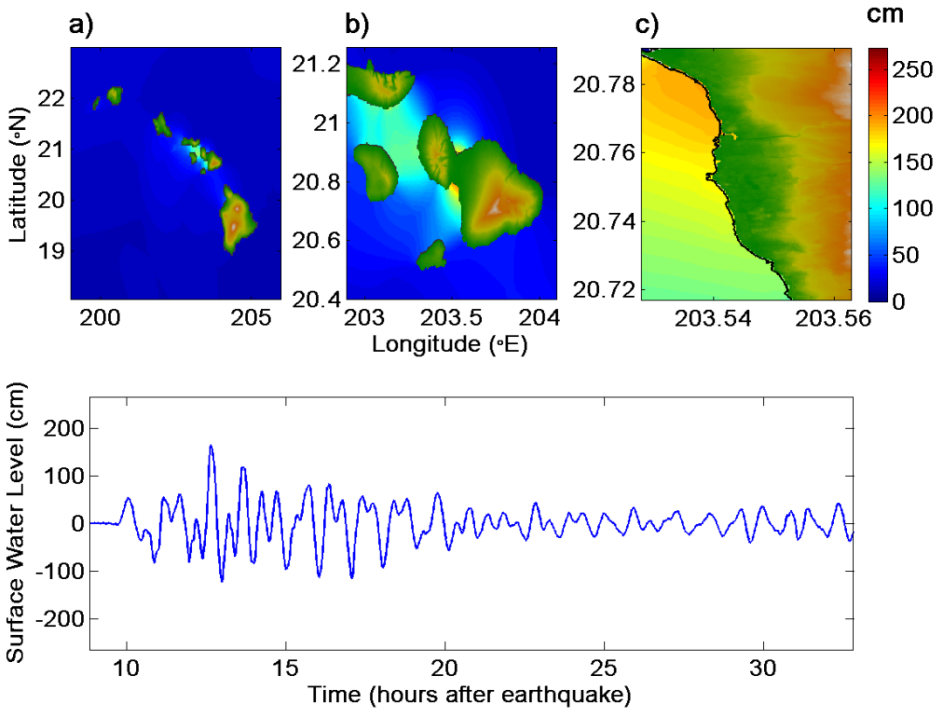

Figure 119. Plot of maximum tsunami wave amplitude distribution for Grids A, B and C and tsunami time series at the warning point for synthetic case NGSZ01-10 with forecast model.

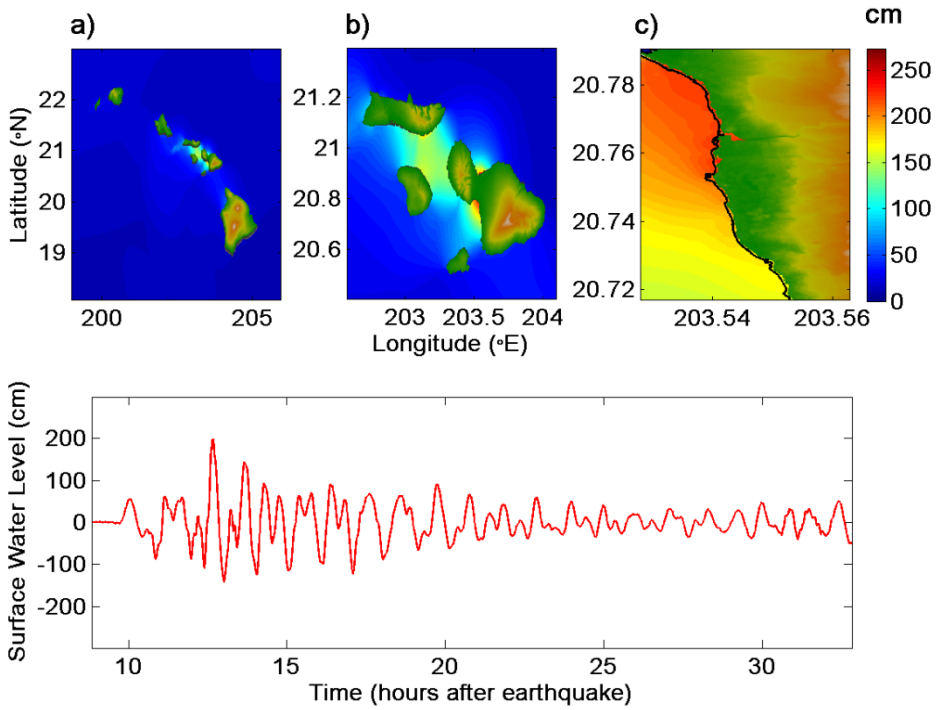

Figure 120. Plot of maximum tsunami wave amplitude distribution for Grids A, B and C and tsunami time series at the warning point for synthetic case NGSZ01-10 with reference model.

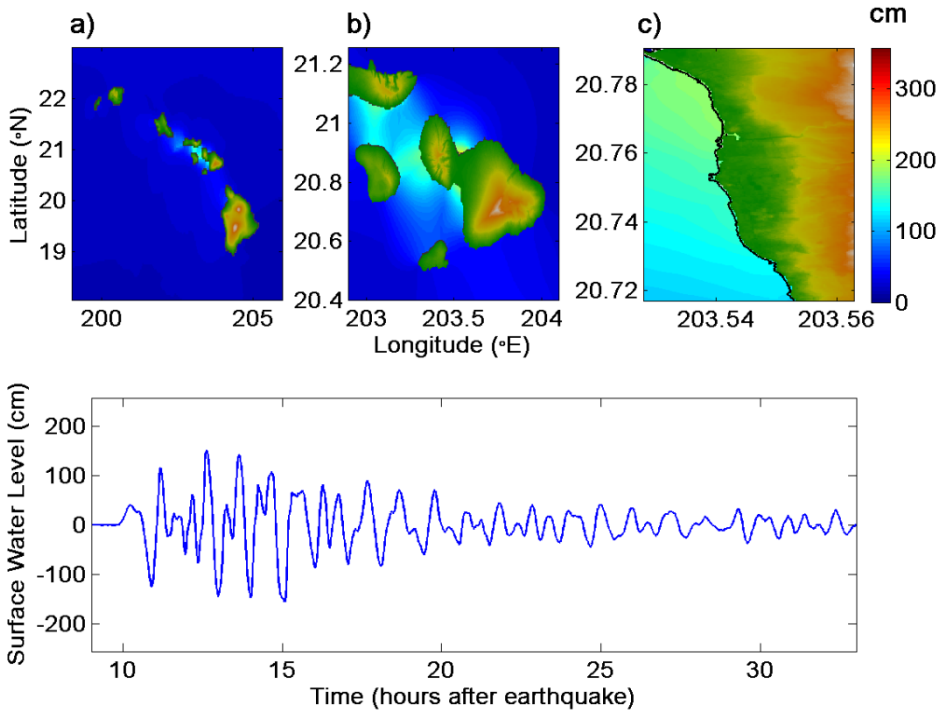

Figure 121. Plot of maximum tsunami wave amplitude distribution for Grids A, B and C and tsunami time series at the warning point for synthetic case NGSZ06-15 with forecast model.

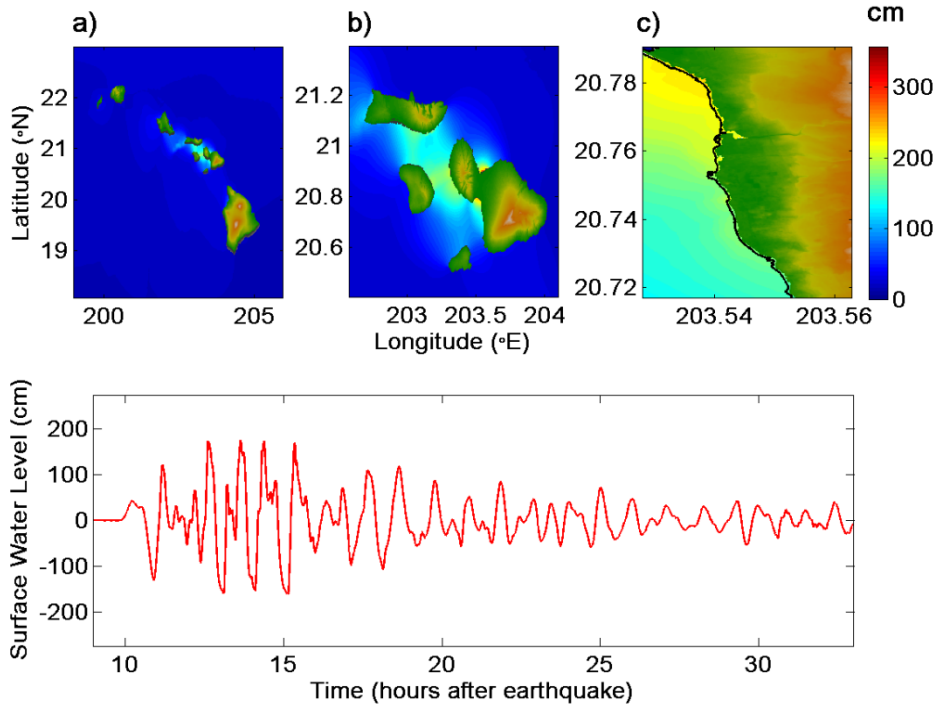

Figure 122. Plot of maximum tsunami wave amplitude distribution for Grids A, B and C and tsunami time series at the warning point for synthetic case NGSZ06-15 with reference model.

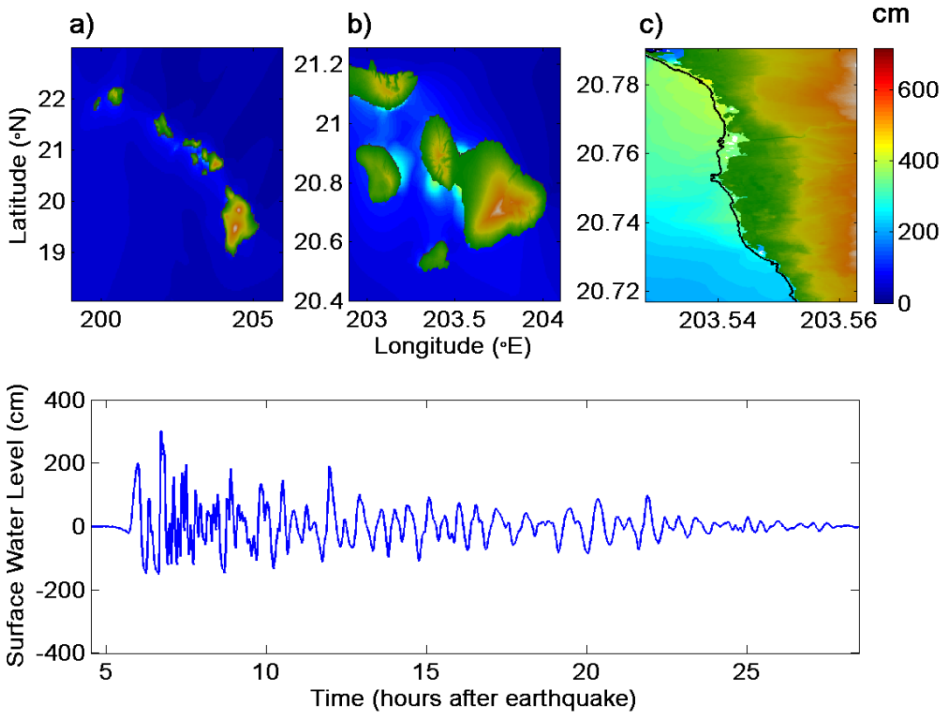

Figure 123. Plot of maximum tsunami wave amplitude distribution for Grids A, B and C and tsunami time series at the warning point for synthetic case NTSZ01-10 with forecast model.

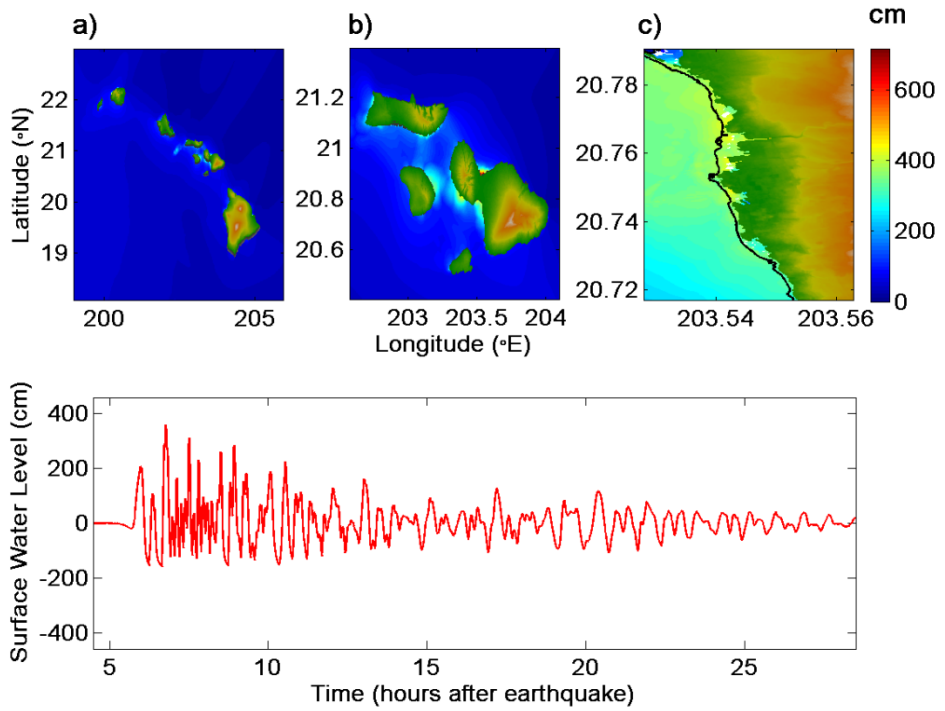

Figure 124. Plot of maximum tsunami wave amplitude distribution for Grids A, B and C and tsunami time series at the warning point for synthetic case NTSZ01-10 with reference model.

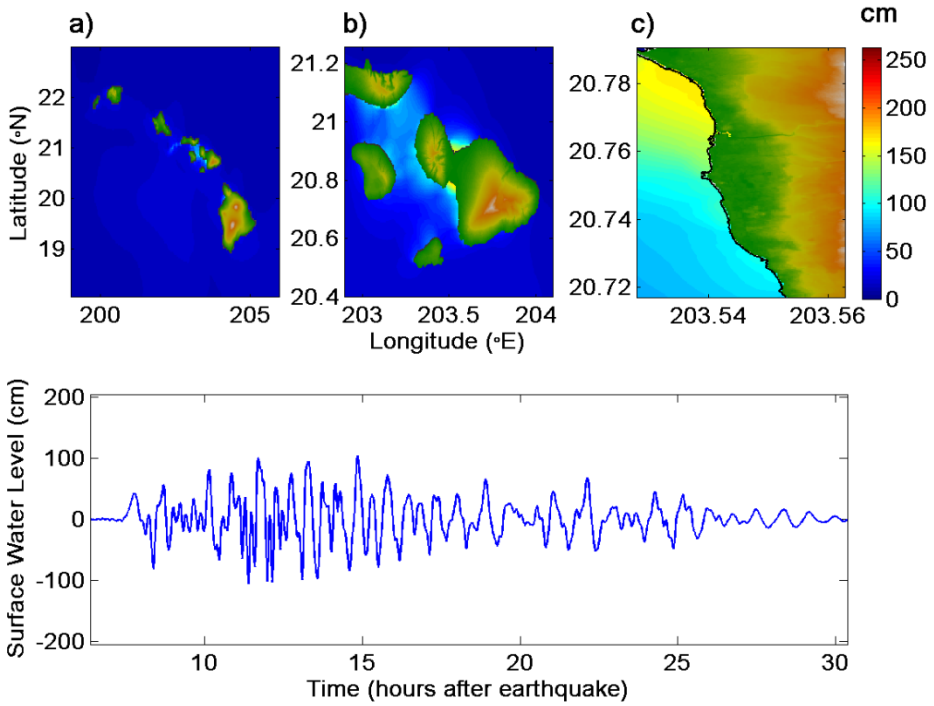

Figure 125. Plot of maximum tsunami wave amplitude distribution for Grids A, B and C and tsunami time series at the warning point for synthetic case NTSZ11-20 with forecast model.

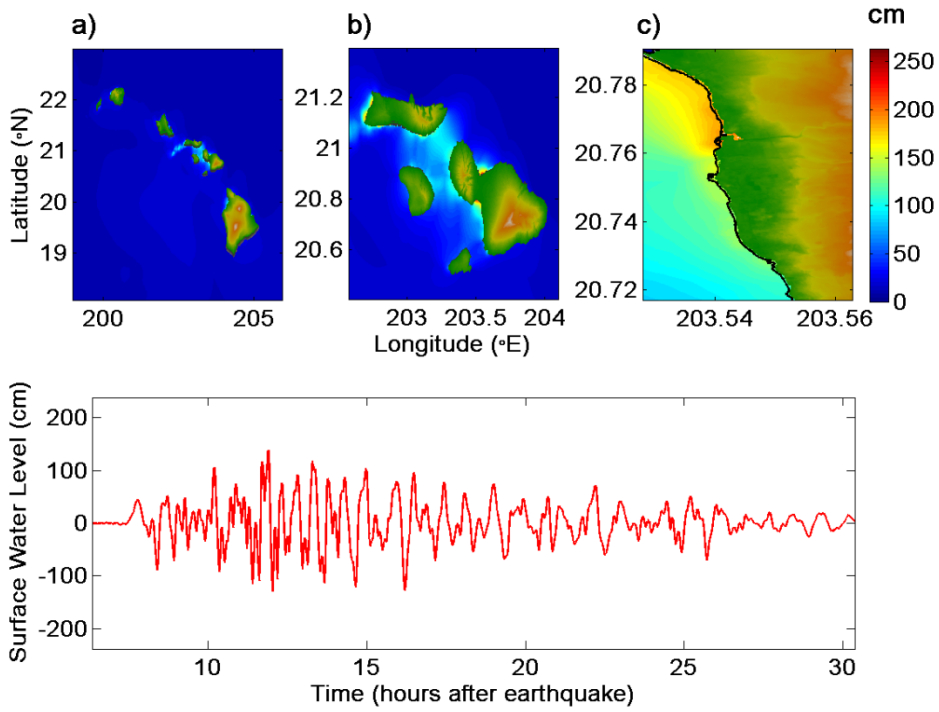

Figure 126. Plot of maximum tsunami wave amplitude distribution for Grids A, B and C and tsunami time series at the warning point for synthetic case NTSZ11-20 with reference model.

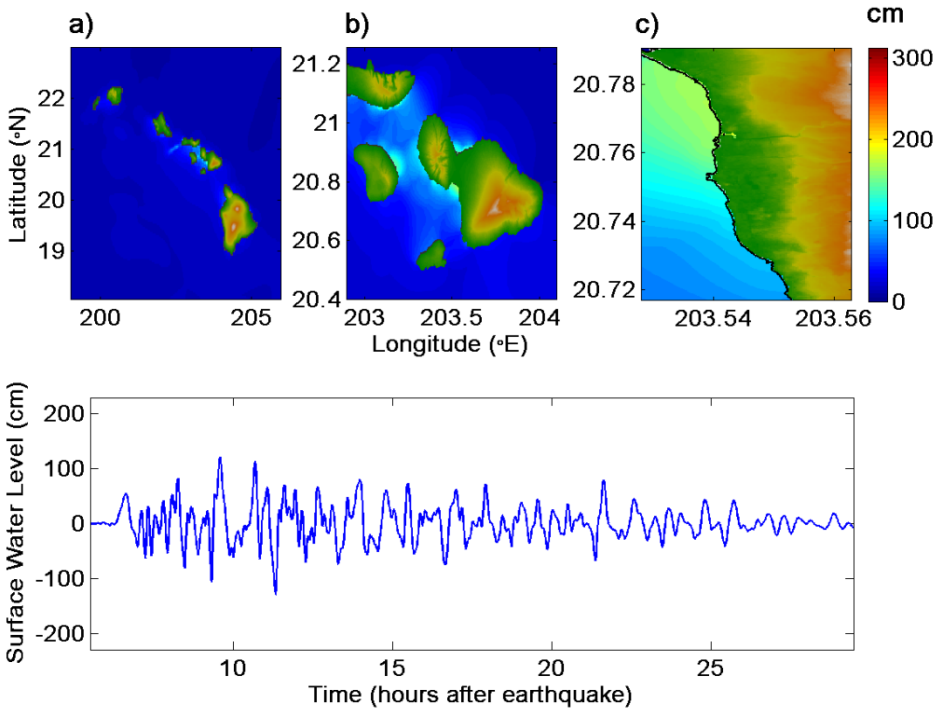

Figure 127. Plot of maximum tsunami wave amplitude distribution for Grids A, B and C and tsunami time series at the warning point for synthetic case NTSZ21-30 with forecast model.

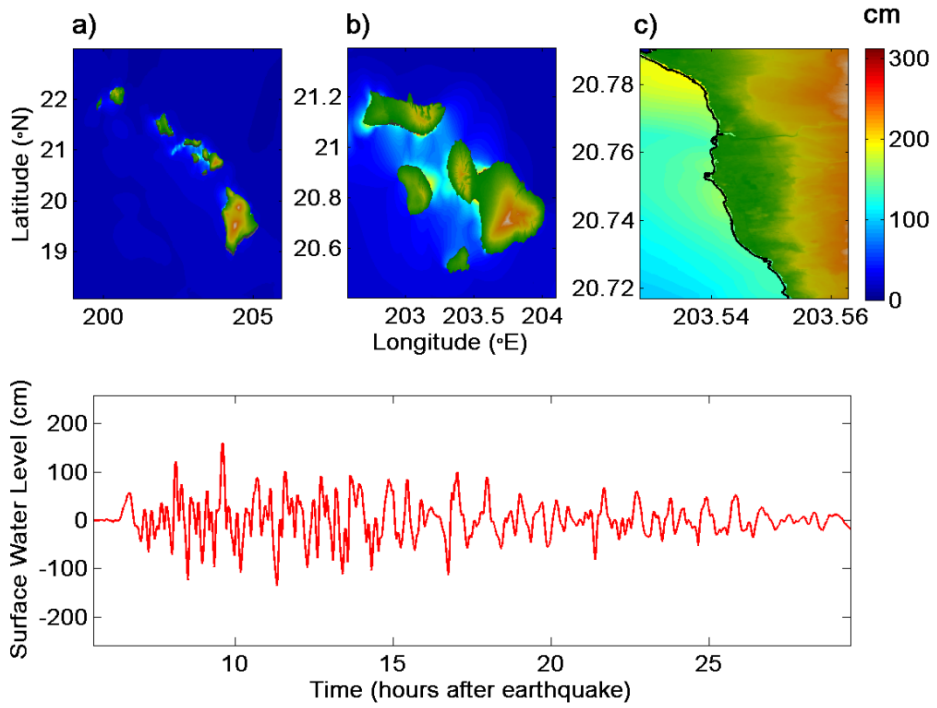

Figure 128. Plot of maximum tsunami wave amplitude distribution for Grids A, B and C and tsunami time series at the warning point for synthetic case NTSZ21-30 with reference model.

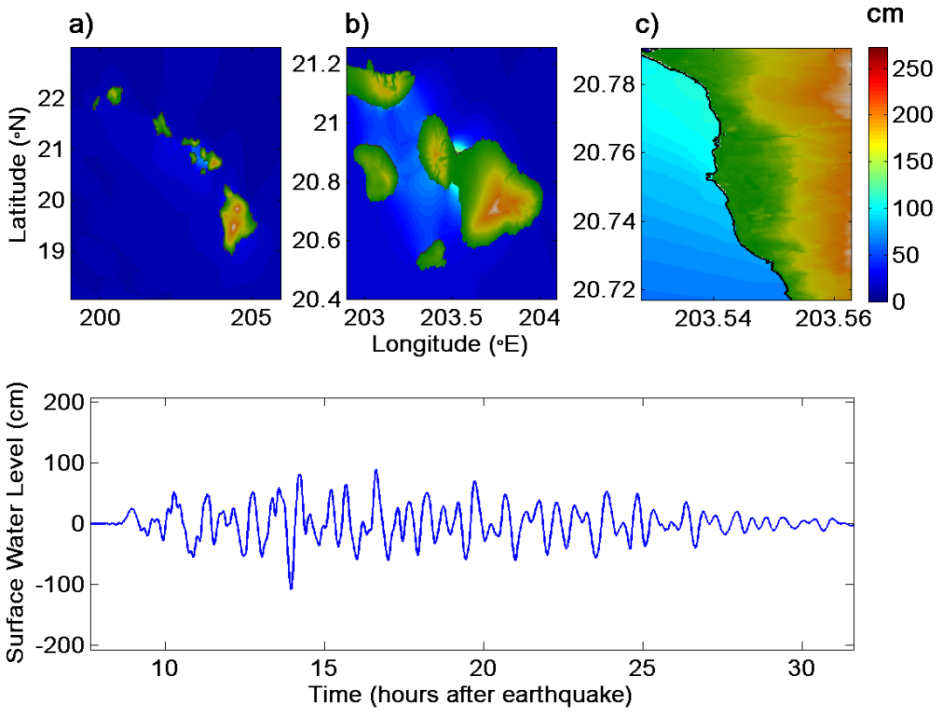

Figure 129. Plot of maximum tsunami wave amplitude distribution for Grids A, B and C and tsunami time series at the warning point for synthetic case NTSZ30-39 with forecast model.

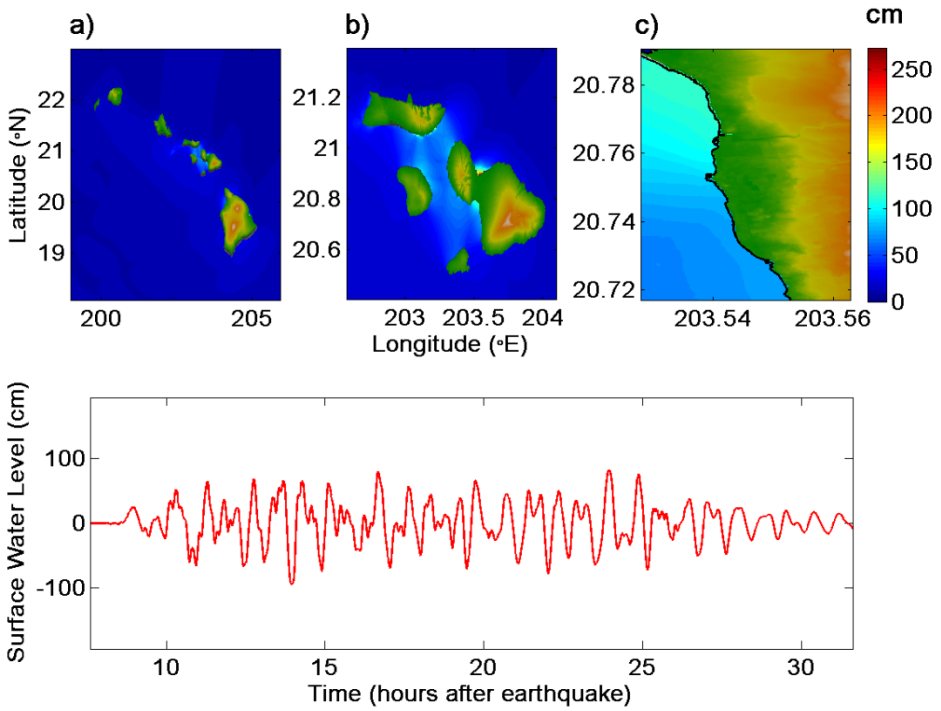

Figure 130. Plot of maximum tsunami wave amplitude distribution for Grids A, B and C and tsunami time series at the warning point for synthetic case NTSZ30-39 with reference model.

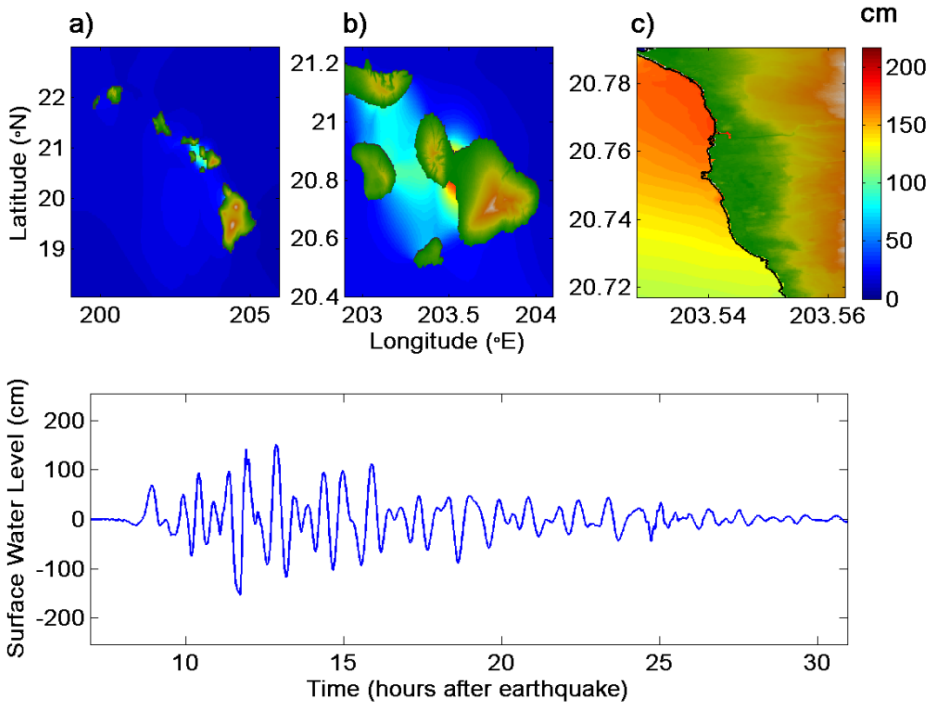

Figure 131. Plot of maximum tsunami wave amplitude distribution for Grids A, B and C and tsunami time series at the warning point for synthetic case NVSZ01-10 with forecast model.

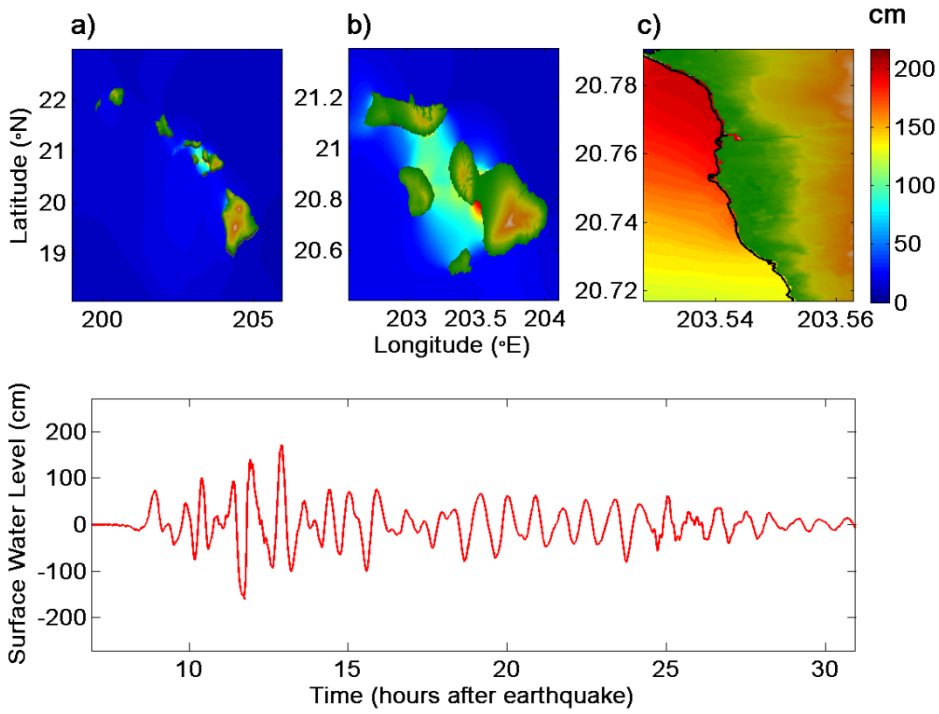

Figure 132. Plot of maximum tsunami wave amplitude distribution for Grids A, B and C and tsunami time series at the warning point for synthetic case NVSZ01-10 with reference model.

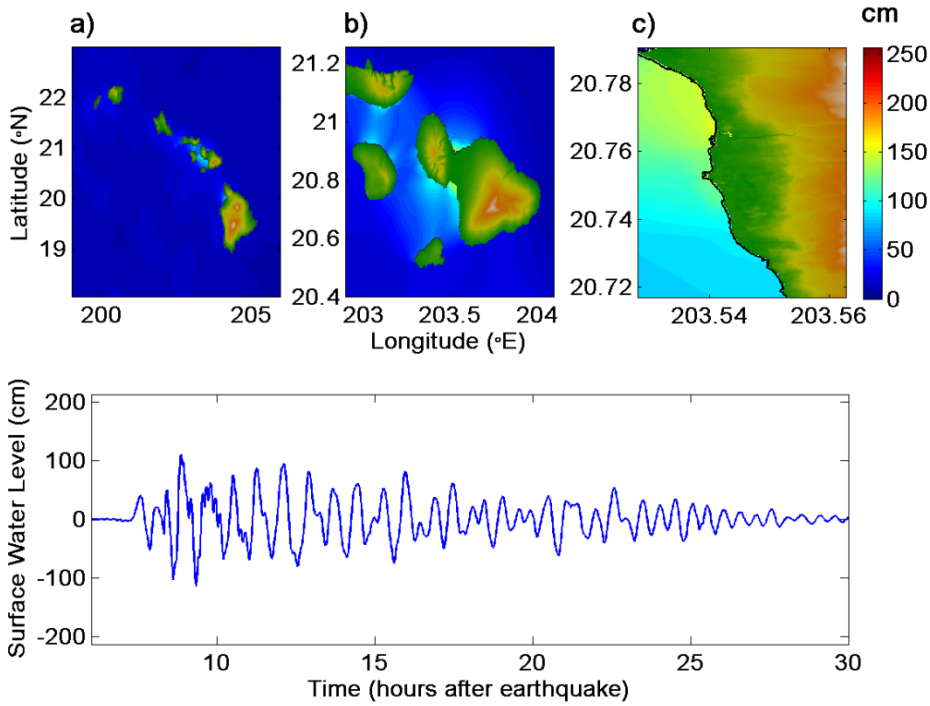

Figure 133. Plot of maximum tsunami wave amplitude distribution for Grids A, B and C and tsunami time series at the warning point for synthetic case NVSZ11-20 with forecast model.

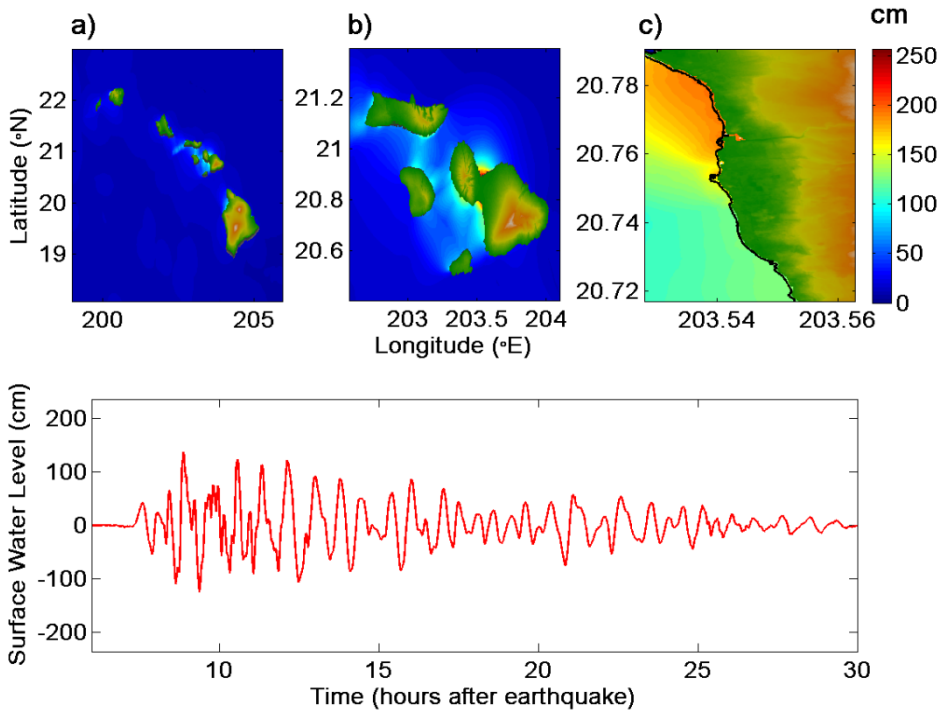

Figure 134. Plot of maximum tsunami wave amplitude distribution for Grids A, B and C and tsunami time series at the warning point for synthetic case NVSZ11-20 with reference model.

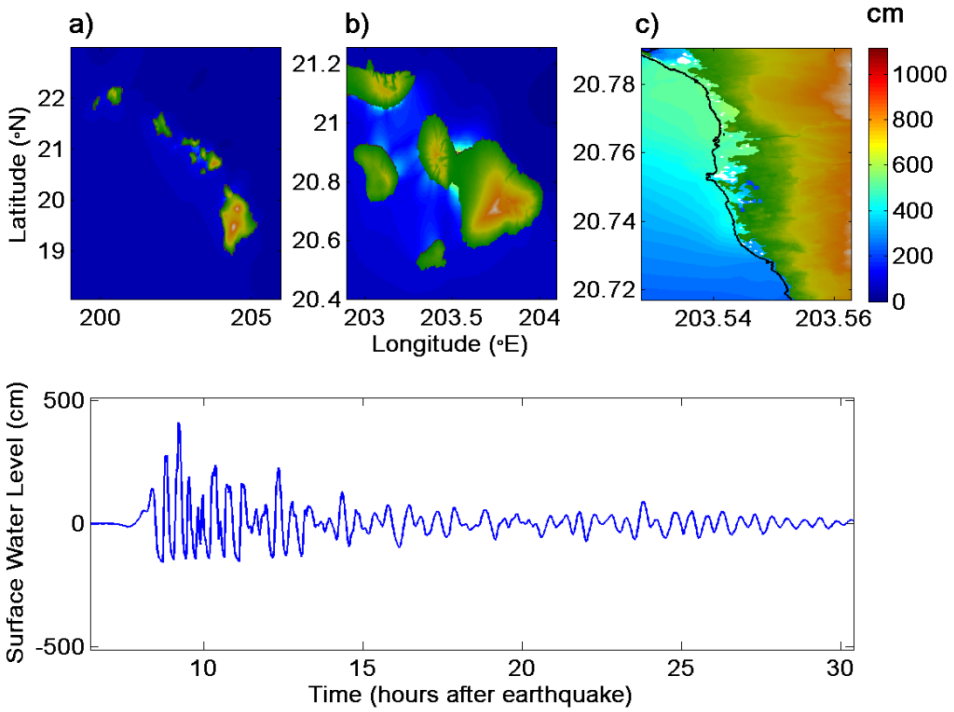

Figure 135. Plot of maximum tsunami wave amplitude distribution for Grids A, B and C and tsunami time series at the warning point for synthetic case NVSZ28-37 with forecast model. White areas on land indicate non-inundated sections.

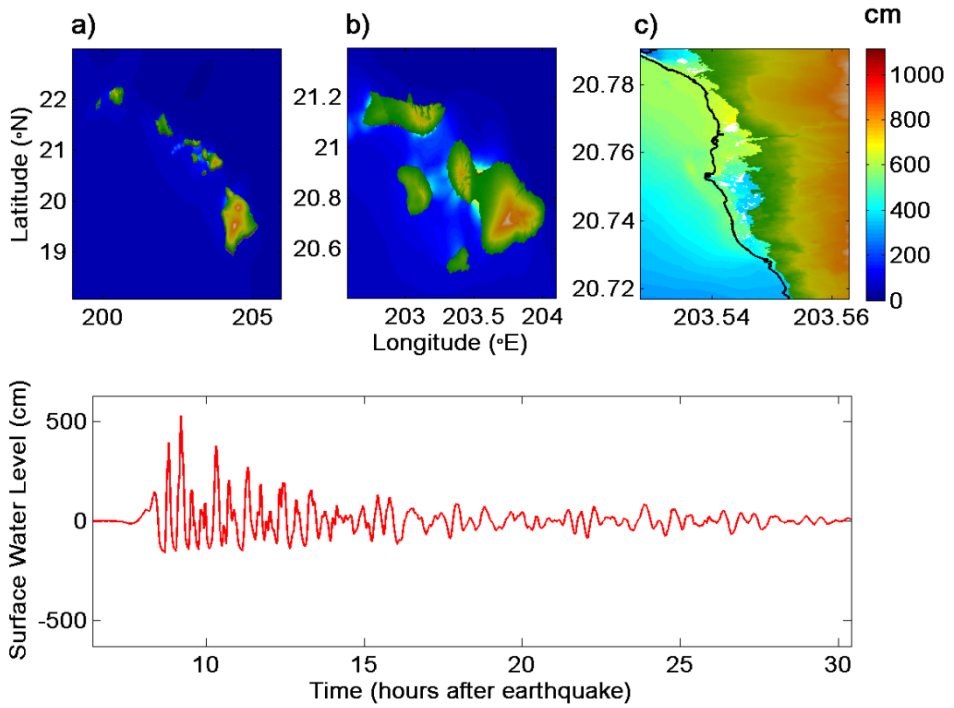

Figure 136. Plot of maximum tsunami wave amplitude distribution for Grids A, B and C and tsunami time series at the warning point for synthetic case NVSZ28-37 with reference model. White areas on land indicate non-inundated sections.

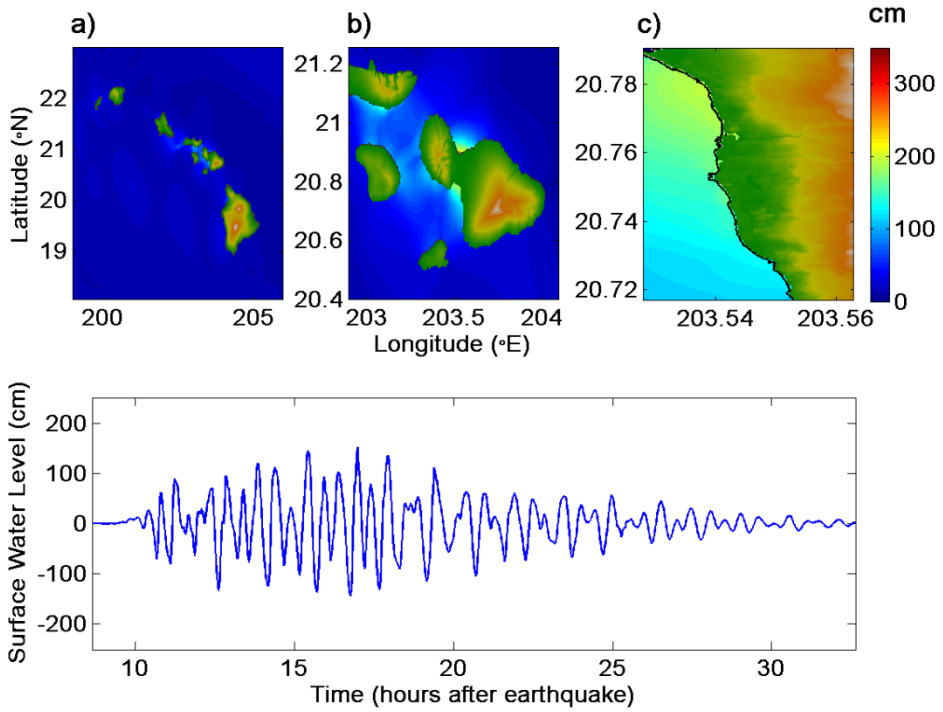

Figure 137. Plot of maximum tsunami wave amplitude distribution for Grids A, B and C and tsunami time series at the warning point for synthetic case RNSZ01-10 with forecast model.

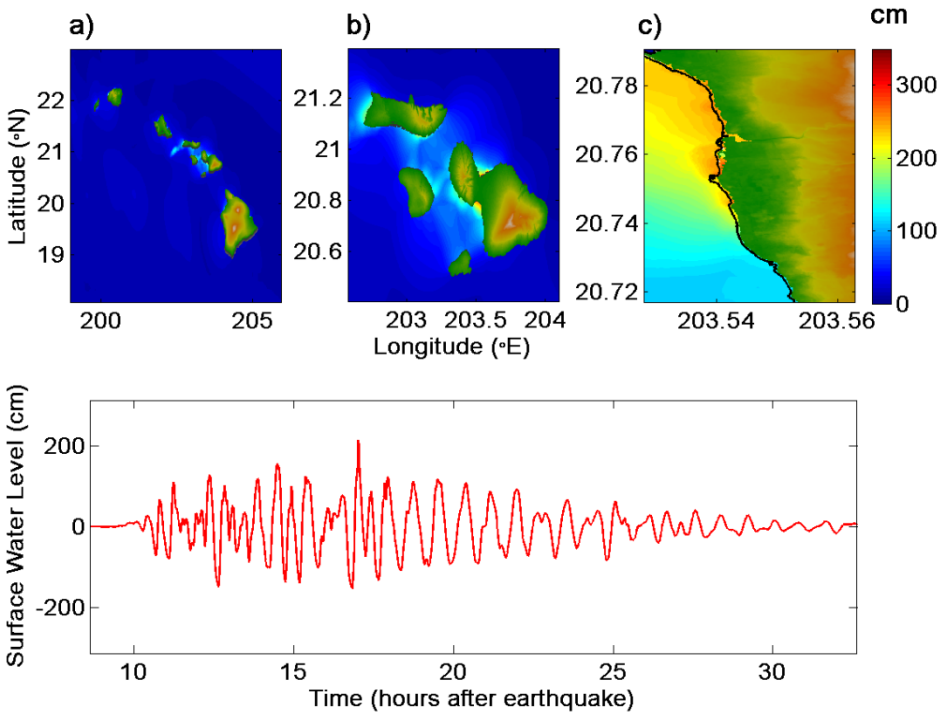

Figure 138. Plot of maximum tsunami wave amplitude distribution for Grids A, B and C and tsunami time series at the warning point for synthetic case RNSZ01-10 with reference model.

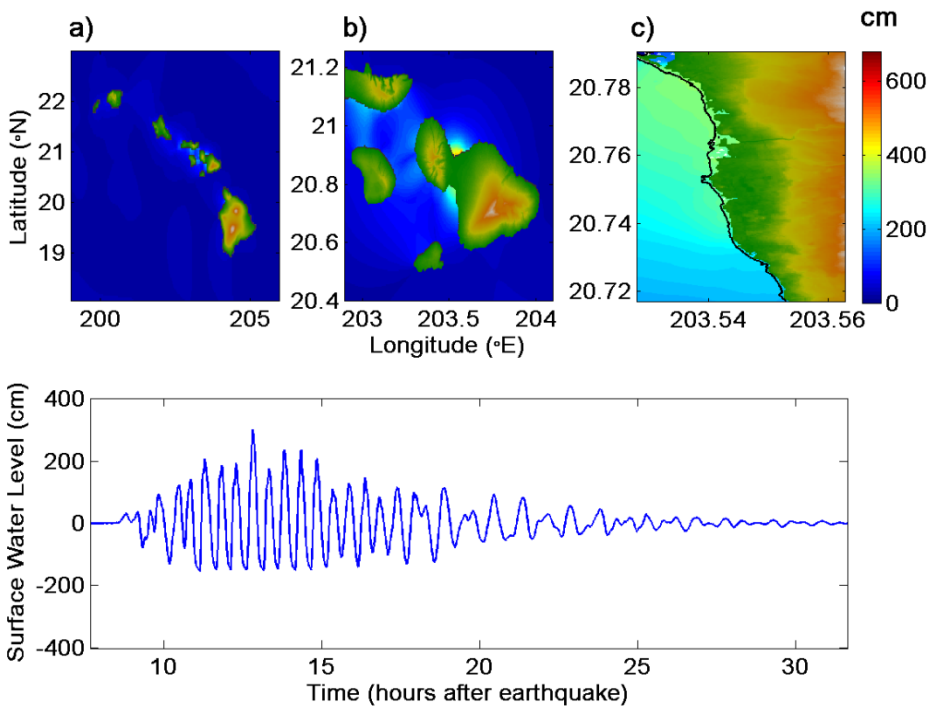

Figure 139. Plot of maximum tsunami wave amplitude distribution for Grids A, B and C and tsunami time series at the warning point for synthetic case RNSZ13-22 with forecast model. White areas on land indicate non-inundated sections.

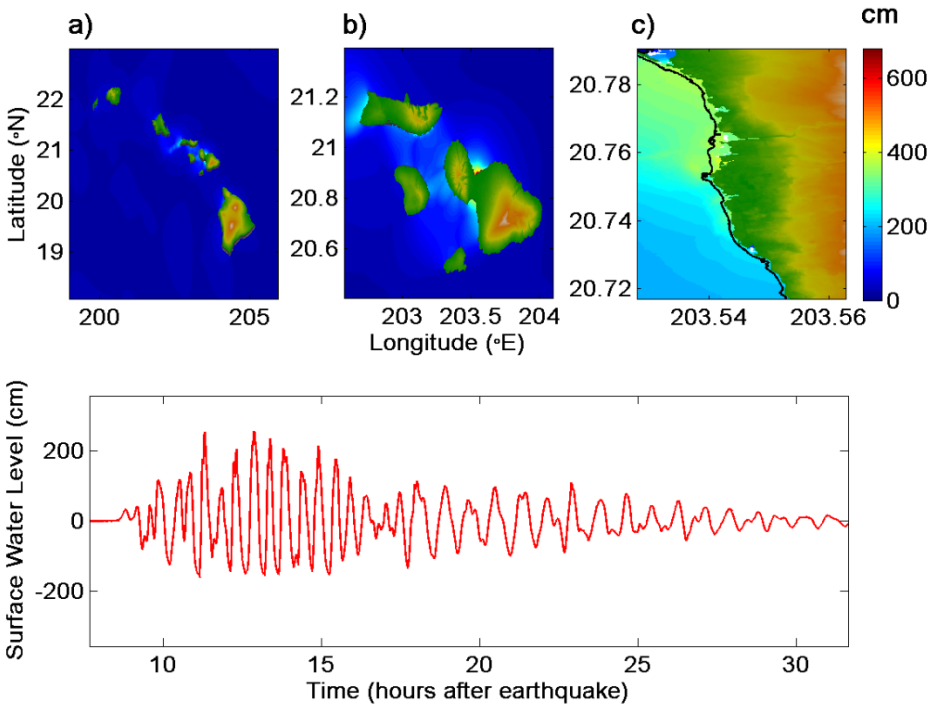

Figure 140. Plot of maximum tsunami wave amplitude distribution for Grids A, B and C and tsunami time series at the warning point for synthetic case RNSZ13-22 with reference model. White areas on land indicate non-inundated sections.

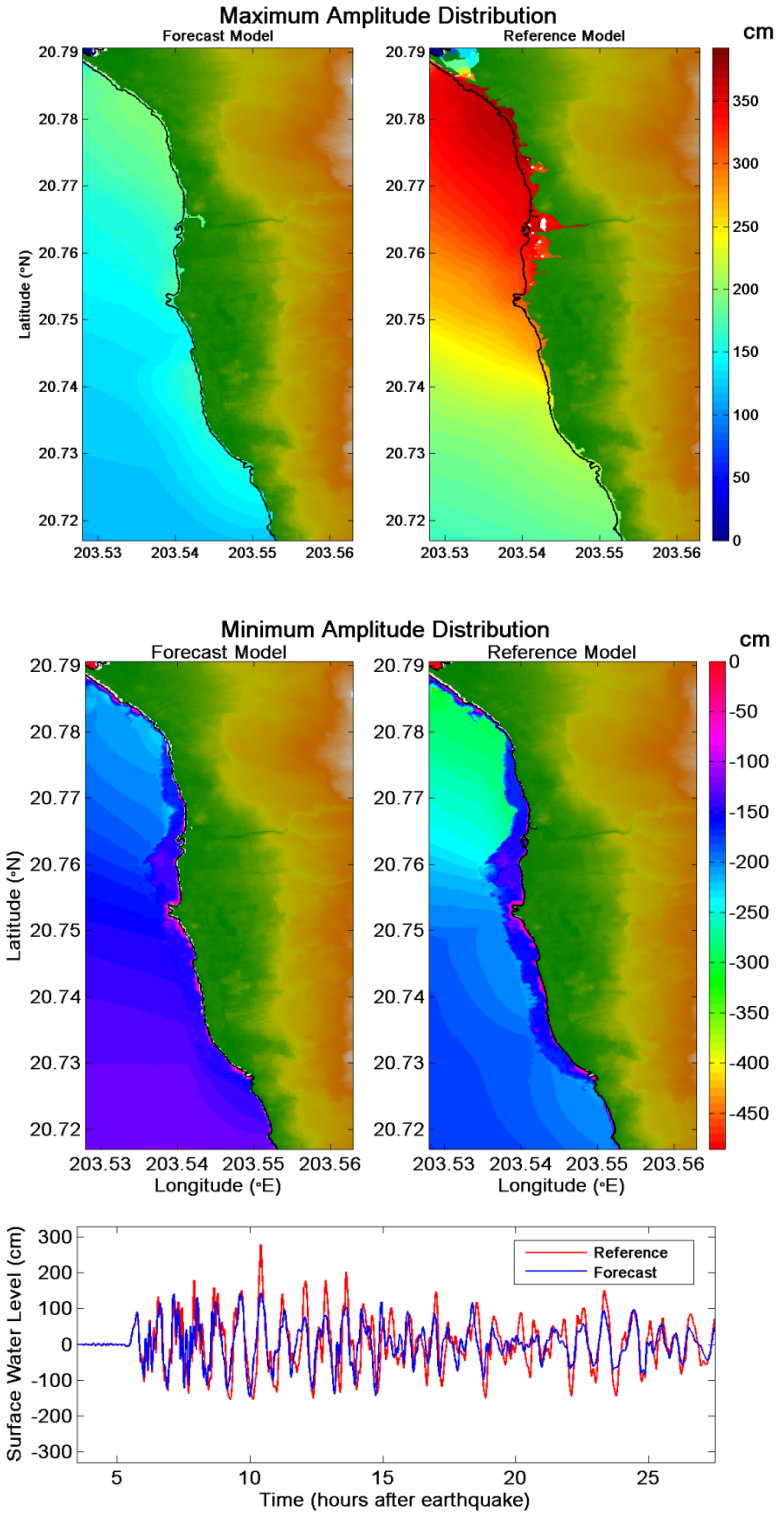

Figure 141. Comparative plot of maximum/minimum tsunami wave amplitude distribution and tsunami time series at C-grid level for synthetic case ACSZ01-10 between forecast and reference models. White areas on land for the top figure indicate non-inundated sections.

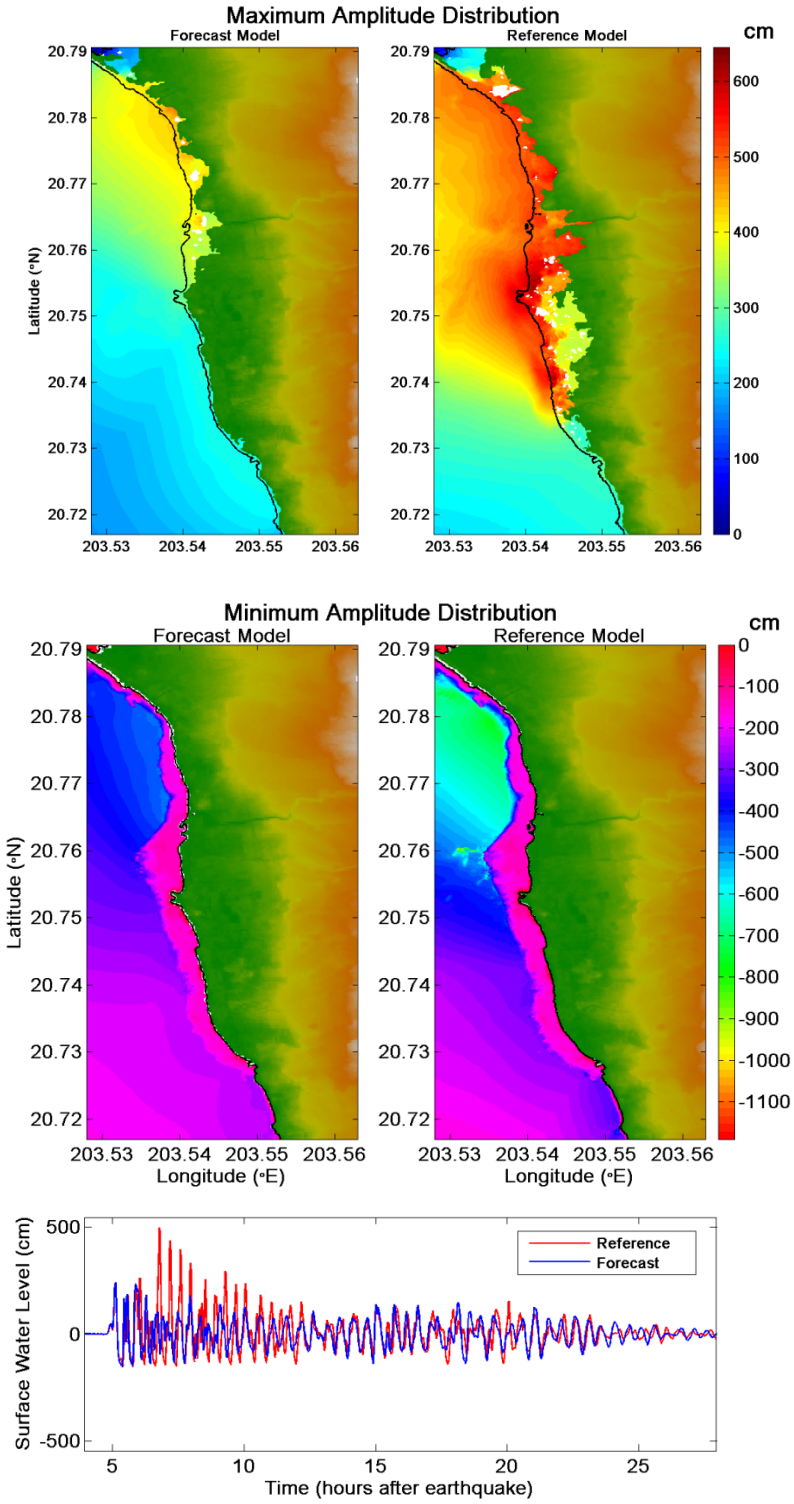

Figure 142. Comparative plot of maximum/minimum tsunami wave amplitude distribution and tsunami time series at C-grid level for synthetic case AC11-20 between forecast and reference models. White areas on land for the top figures indicate non-inundated sections.

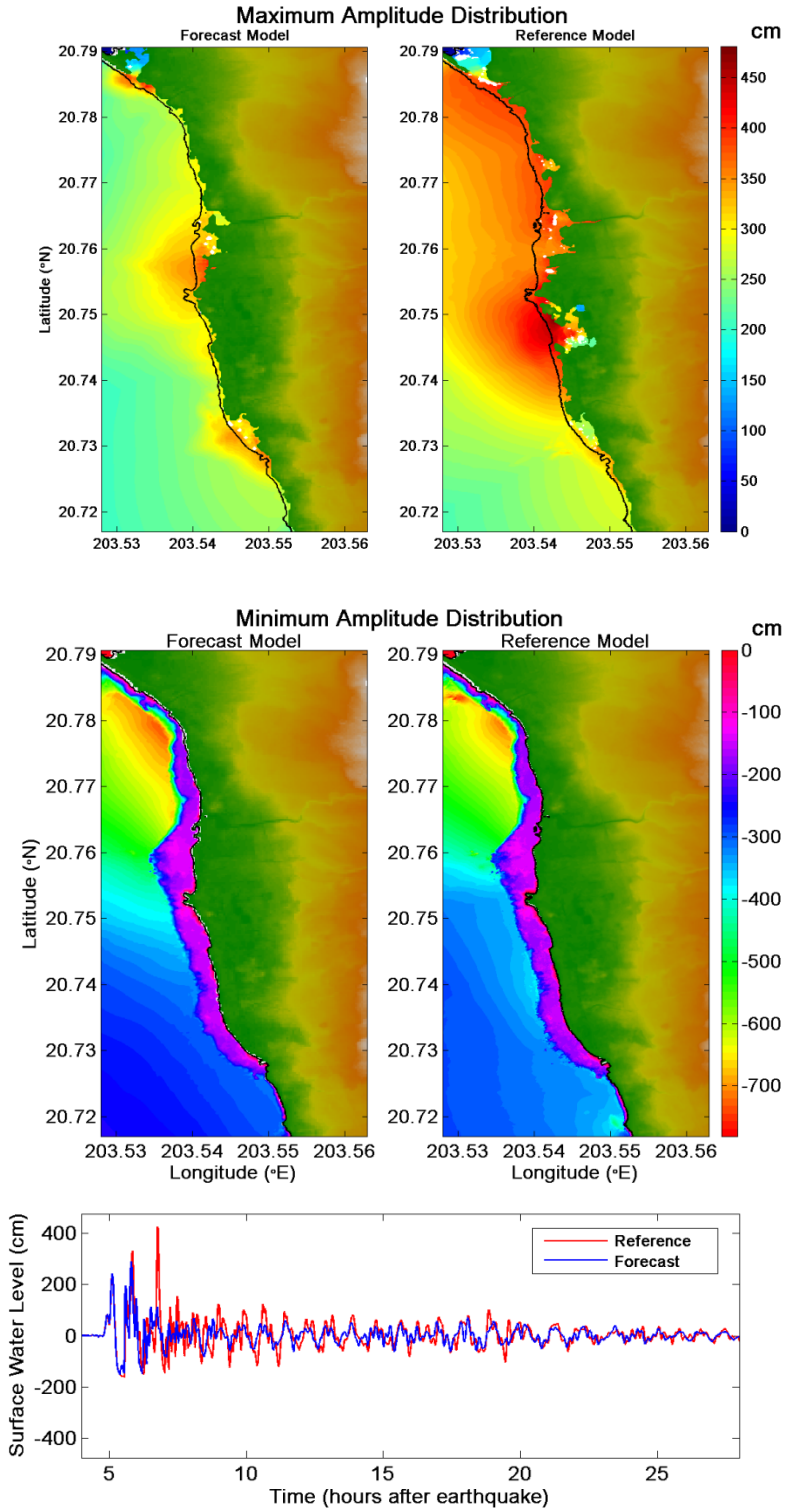

Figure 143. Comparative plot of maximum/minimum tsunami wave amplitude distribution and tsunami time series at C-grid level for synthetic case AC21-30 between forecast and reference models. White areas on land for the top figure indicate non-inundated sections.

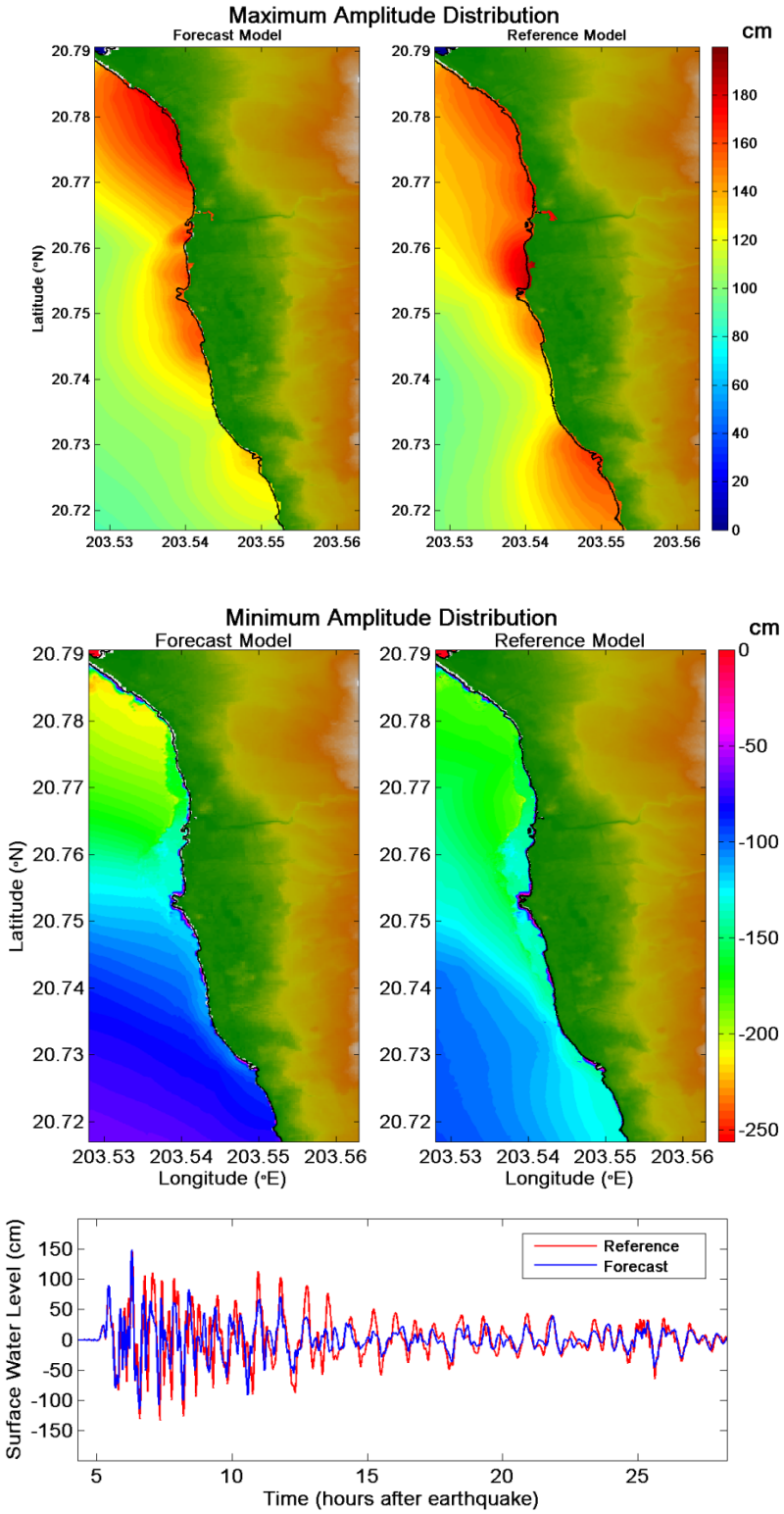

Figure 144. Comparative plot of maximum/minimum tsunami wave amplitude distribution and tsunami time series at C-grid level for synthetic case AC31-40 between forecast and reference models.

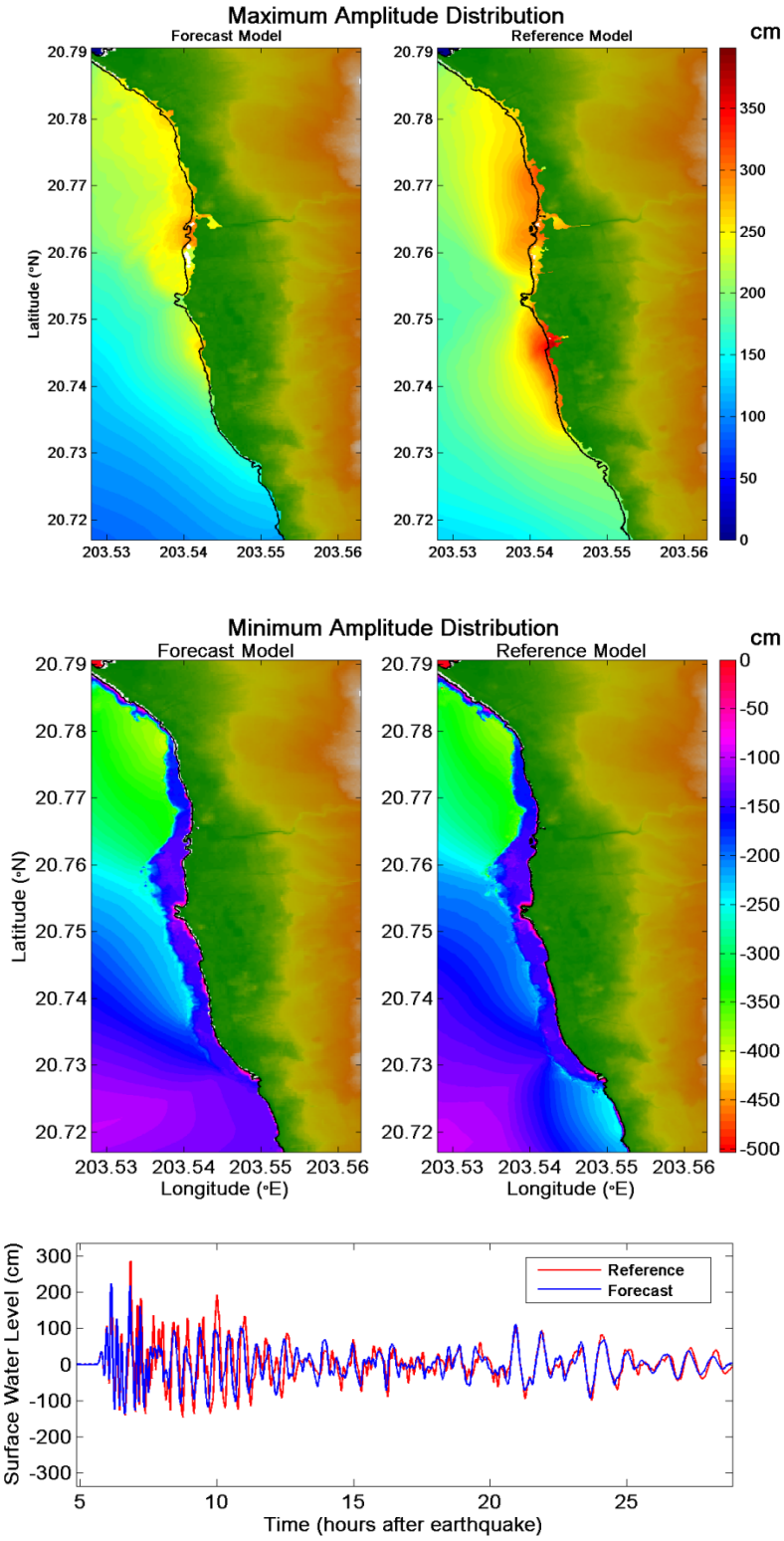

Figure 145. Comparative plot of maximum/minimum tsunami wave amplitude distribution and tsunami time series at C-grid level for synthetic case AC41-50 between forecast and reference models. White areas on land for the top figure indicate non-inundated sections.

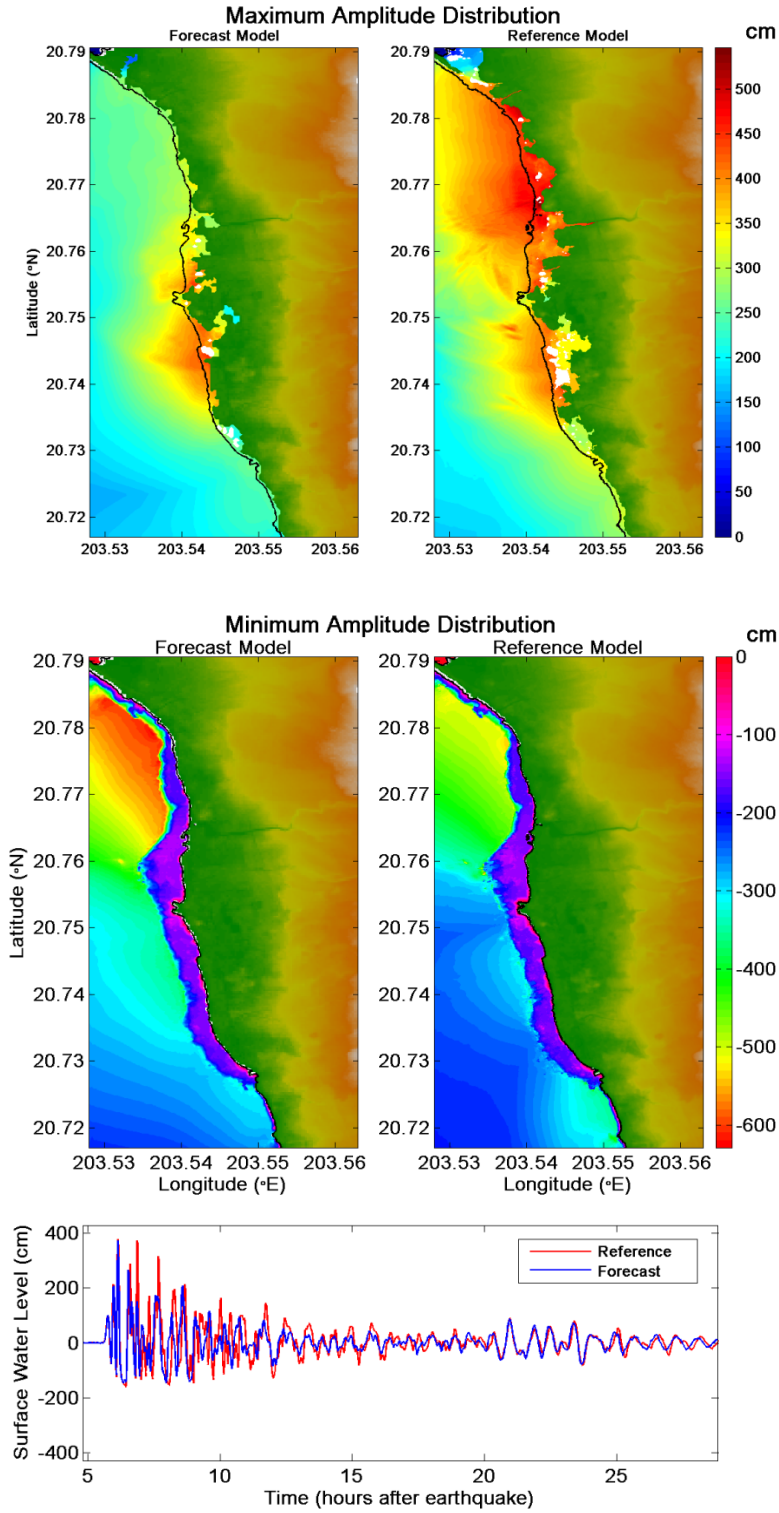

Figure 146. Comparative plot of maximum/minimum tsunami wave amplitude distribution and tsunami time series at C-grid level for synthetic case AC46-55 between forecast and reference models. White areas on land for the top figure indicate non-inundated sections.

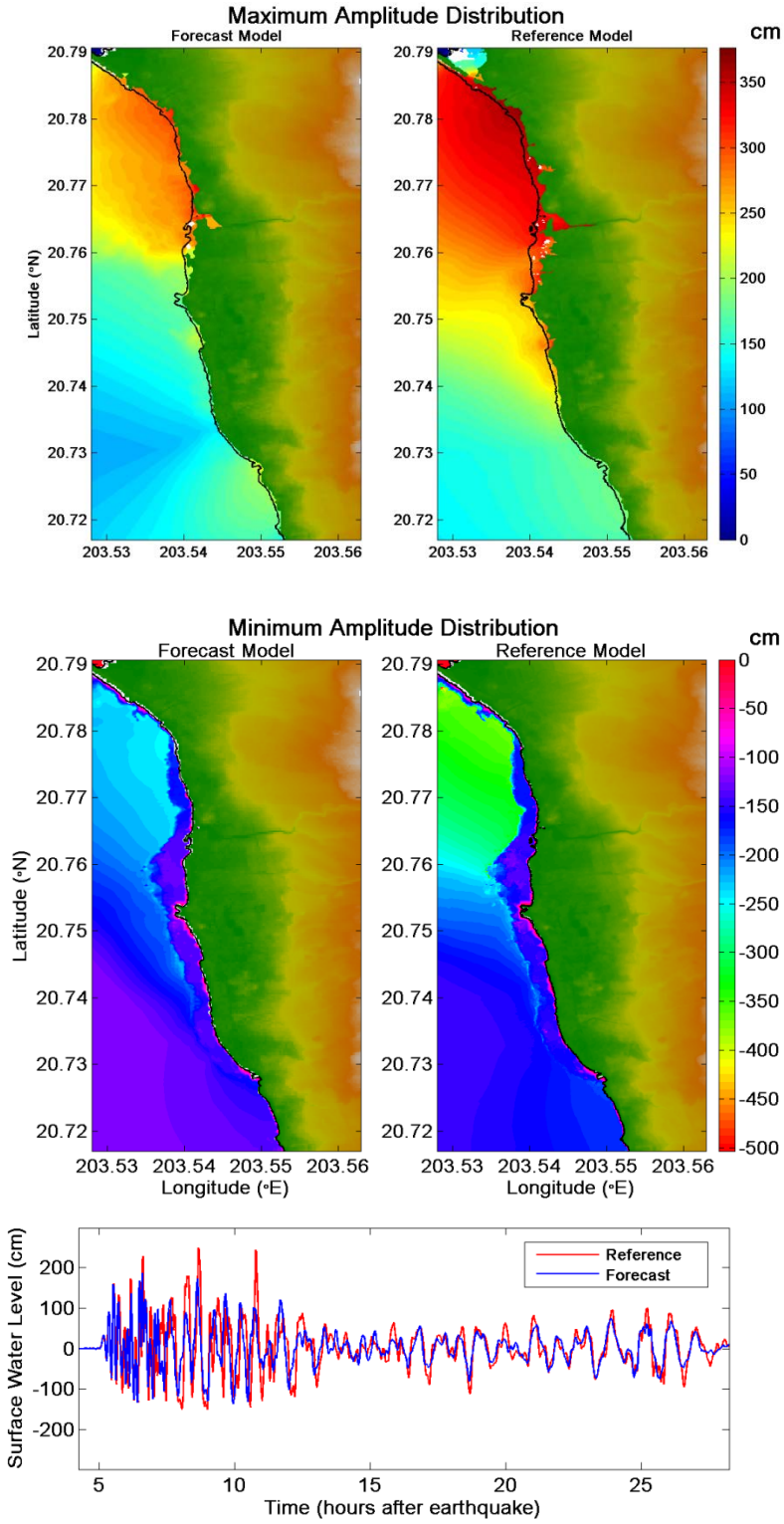

Figure 147. Comparative plot of maximum/minimum tsunami wave amplitude distribution and tsunami time series at C-grid level for synthetic case AC56-65 between forecast and reference models. White areas on land for the top figure indicate non-inundated sections.

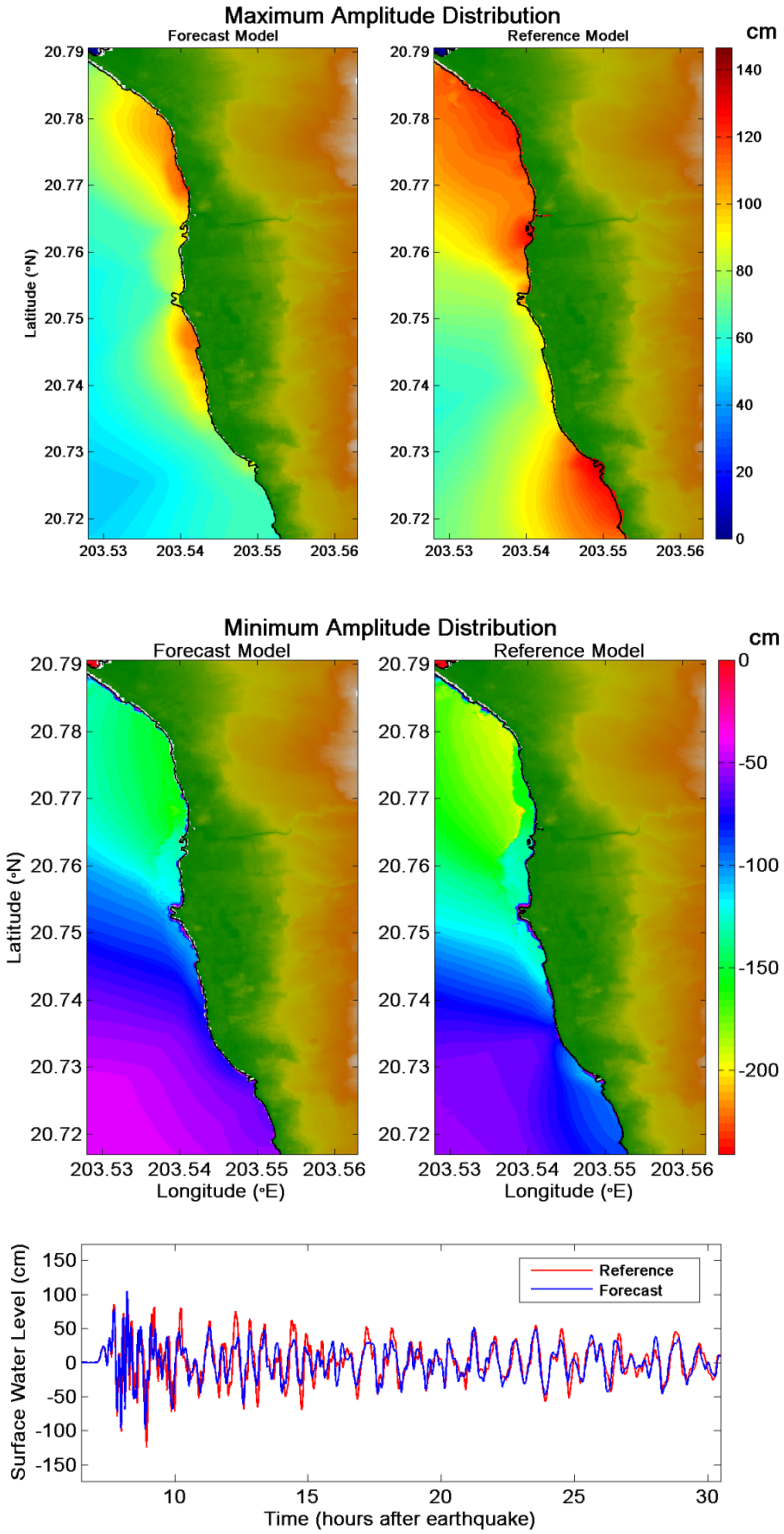

Figure 148. Comparative plot of maximum/minimum tsunami wave amplitude distribution and tsunami time series at C-grid level for synthetic case CS01-10 between forecast and reference models.

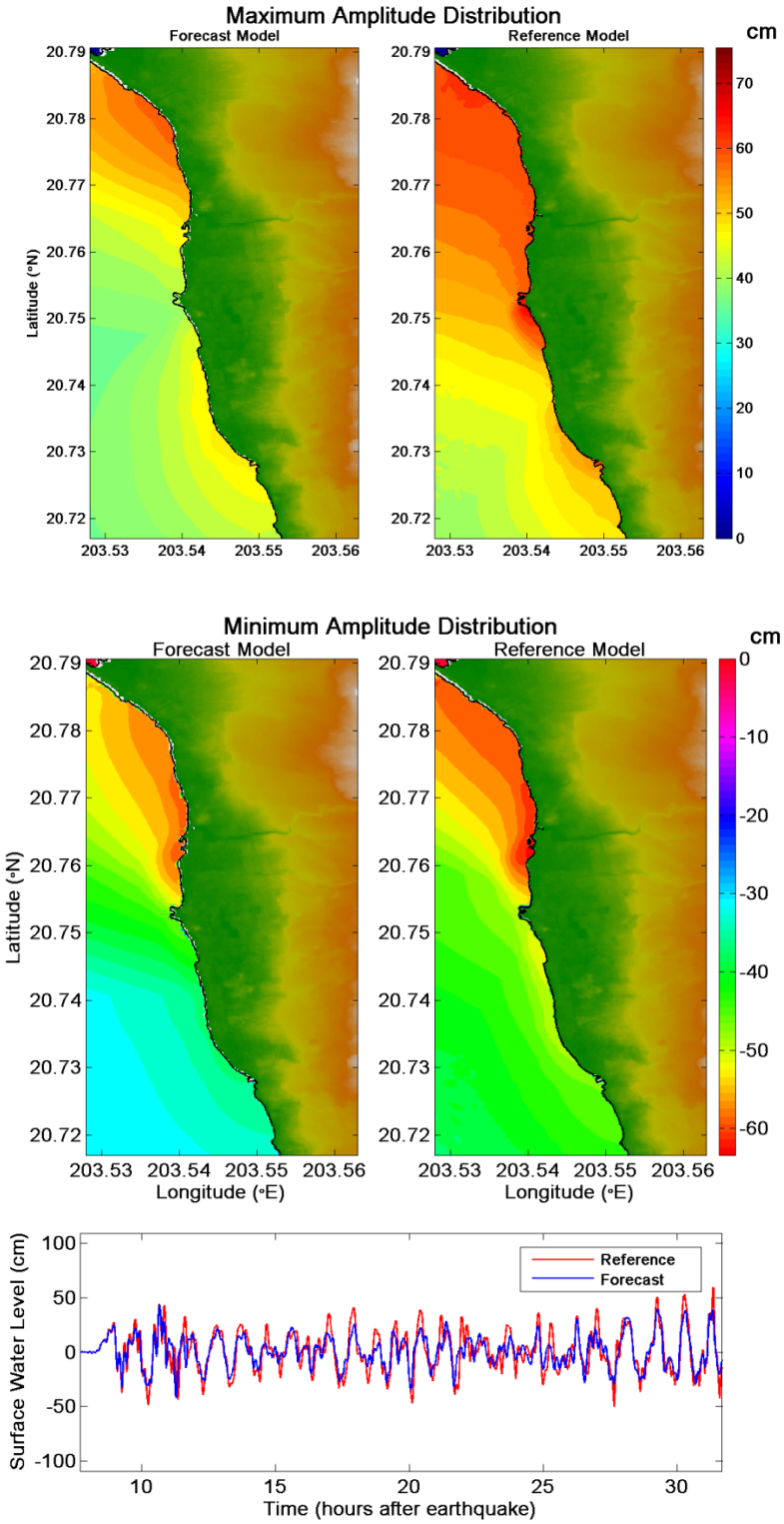

Figure 149. Comparative plot of maximum/minimum tsunami wave amplitude distribution and tsunami time series at C-grid level for synthetic case CS11-20 between forecast and reference models.

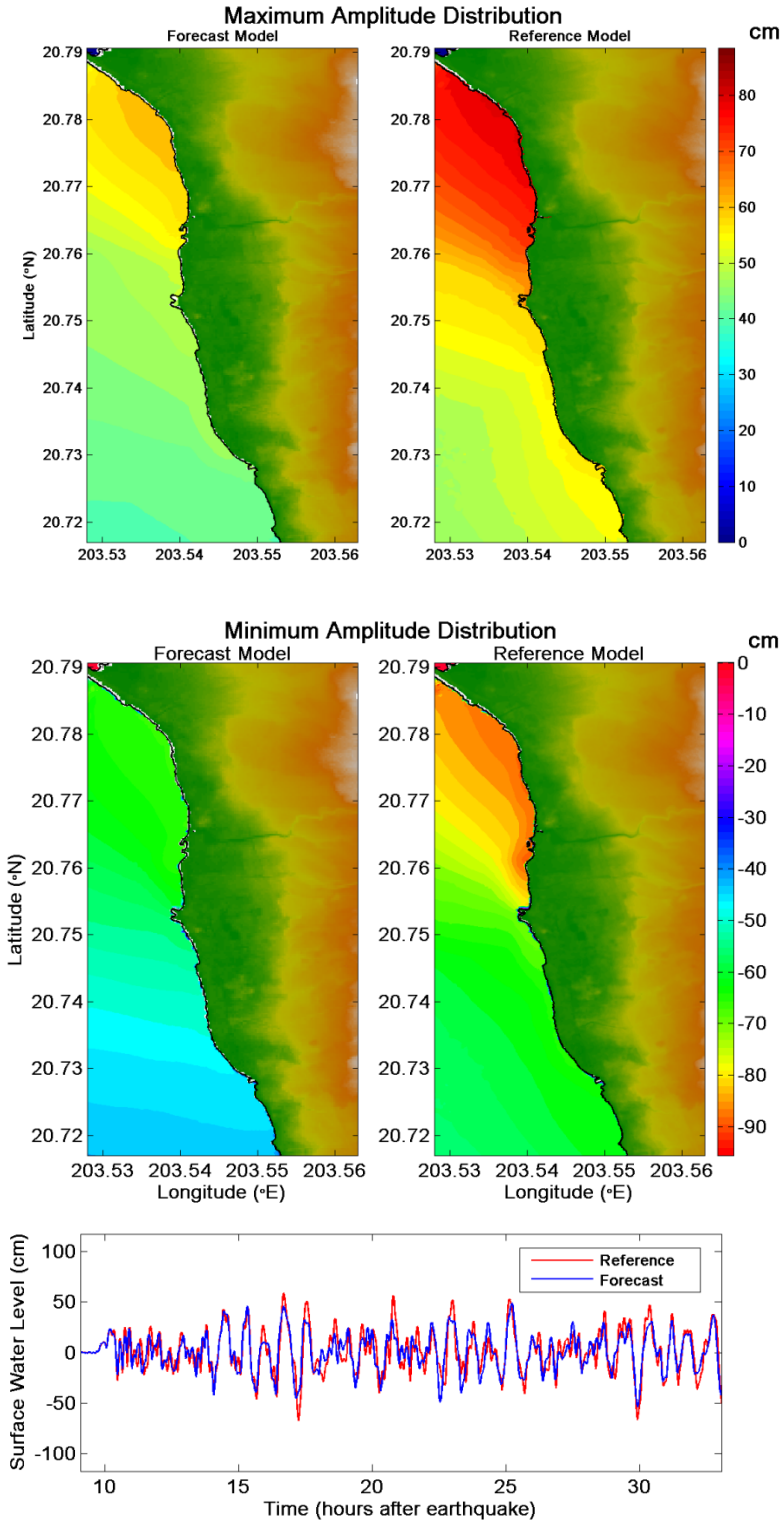

Figure 150. Comparative plot of maximum/minimum tsunami wave amplitude distribution and tsunami time series at C-grid level for synthetic case CS21-30 between forecast and reference models.

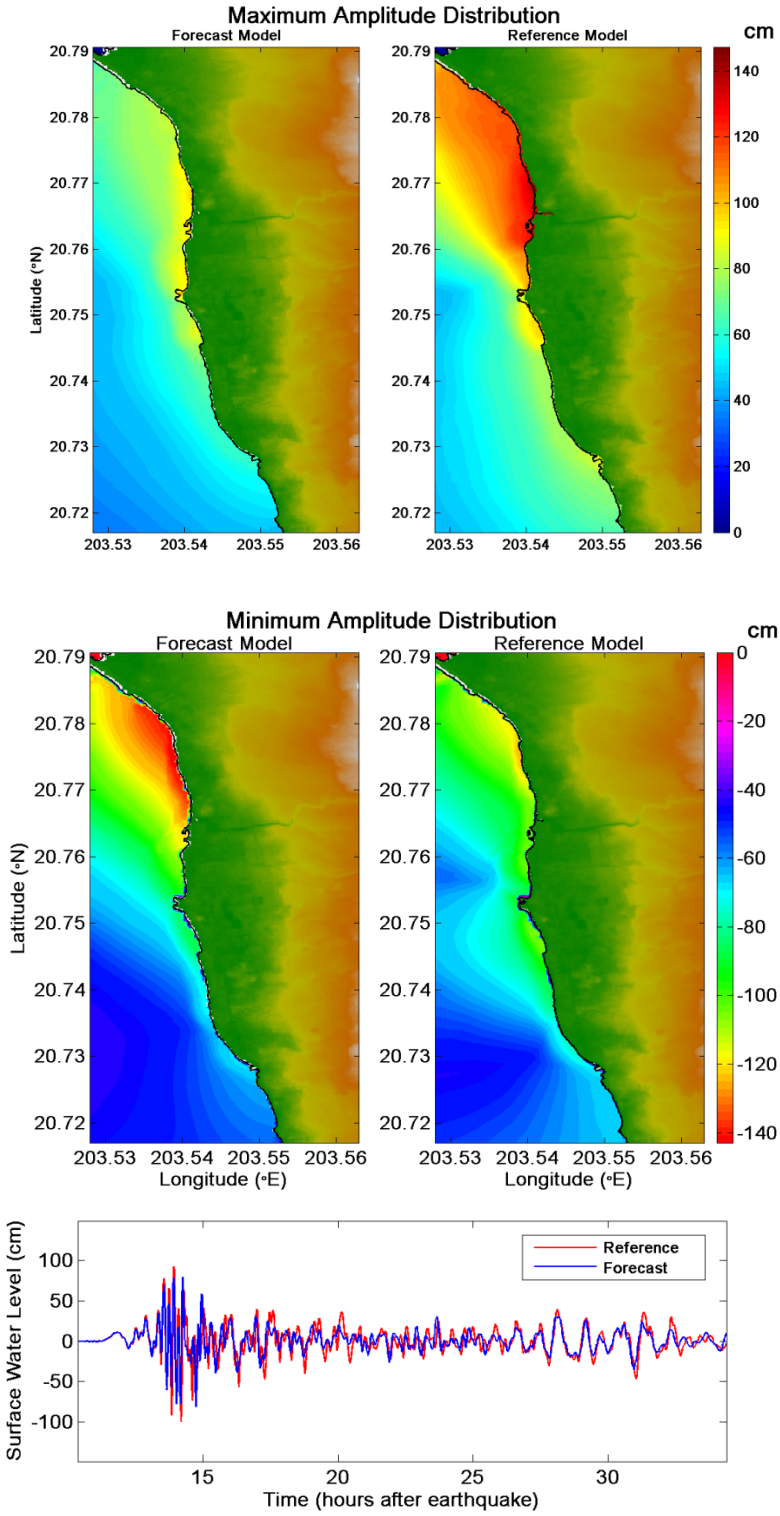

Figure 151. Comparative plot of maximum/minimum tsunami wave amplitude distribution and tsunami time series at C-grid level for synthetic case CS31-40 between forecast and reference models.

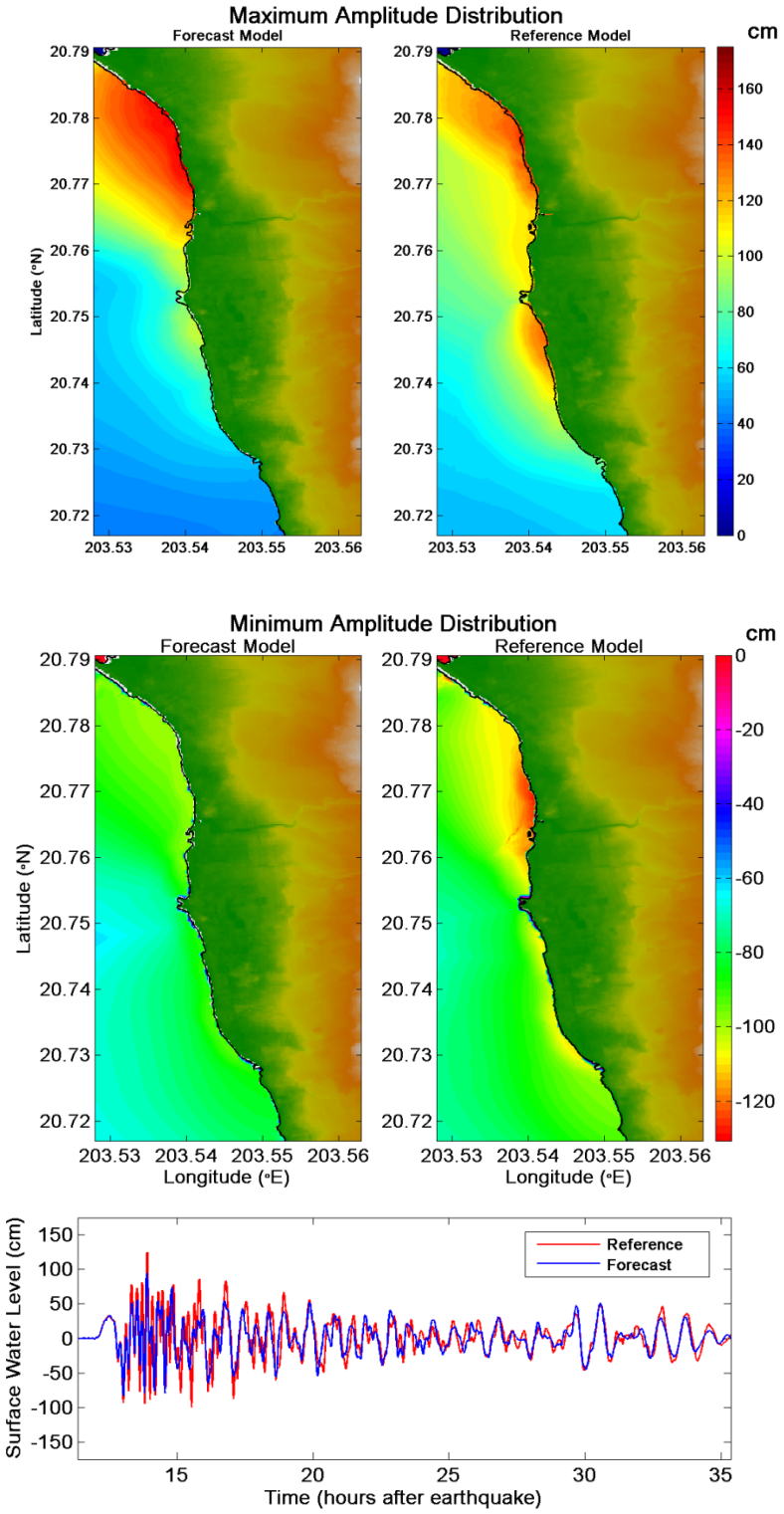

Figure 152. Comparative plot of maximum/minimum tsunami wave amplitude distribution and tsunami time series at C-grid level for synthetic case CS41-50 between forecast and reference models.

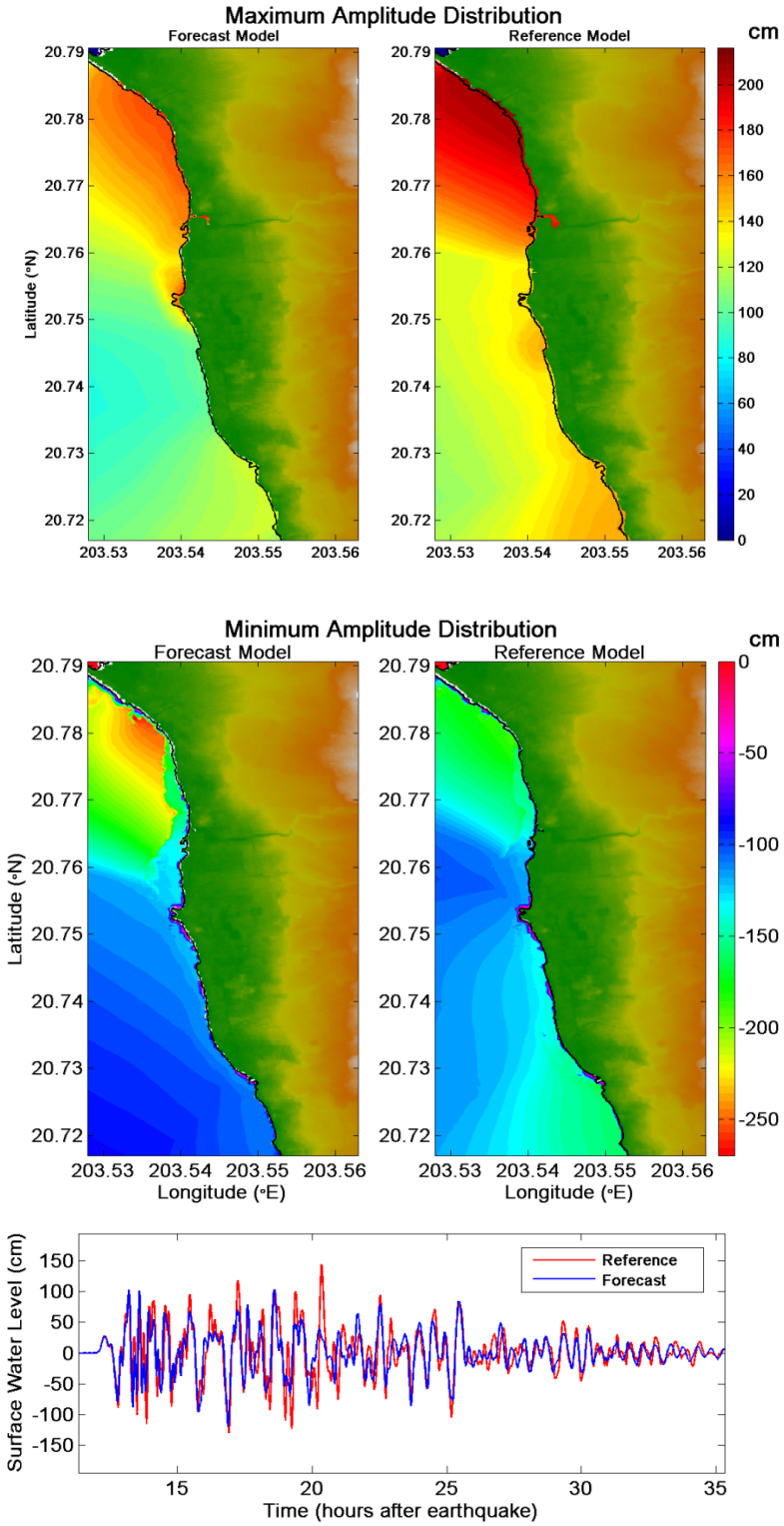

Figure 153. Comparative plot of maximum/minimum tsunami wave amplitude distribution and tsunami time series at C-grid level for synthetic case CS51-60 between forecast and reference models.

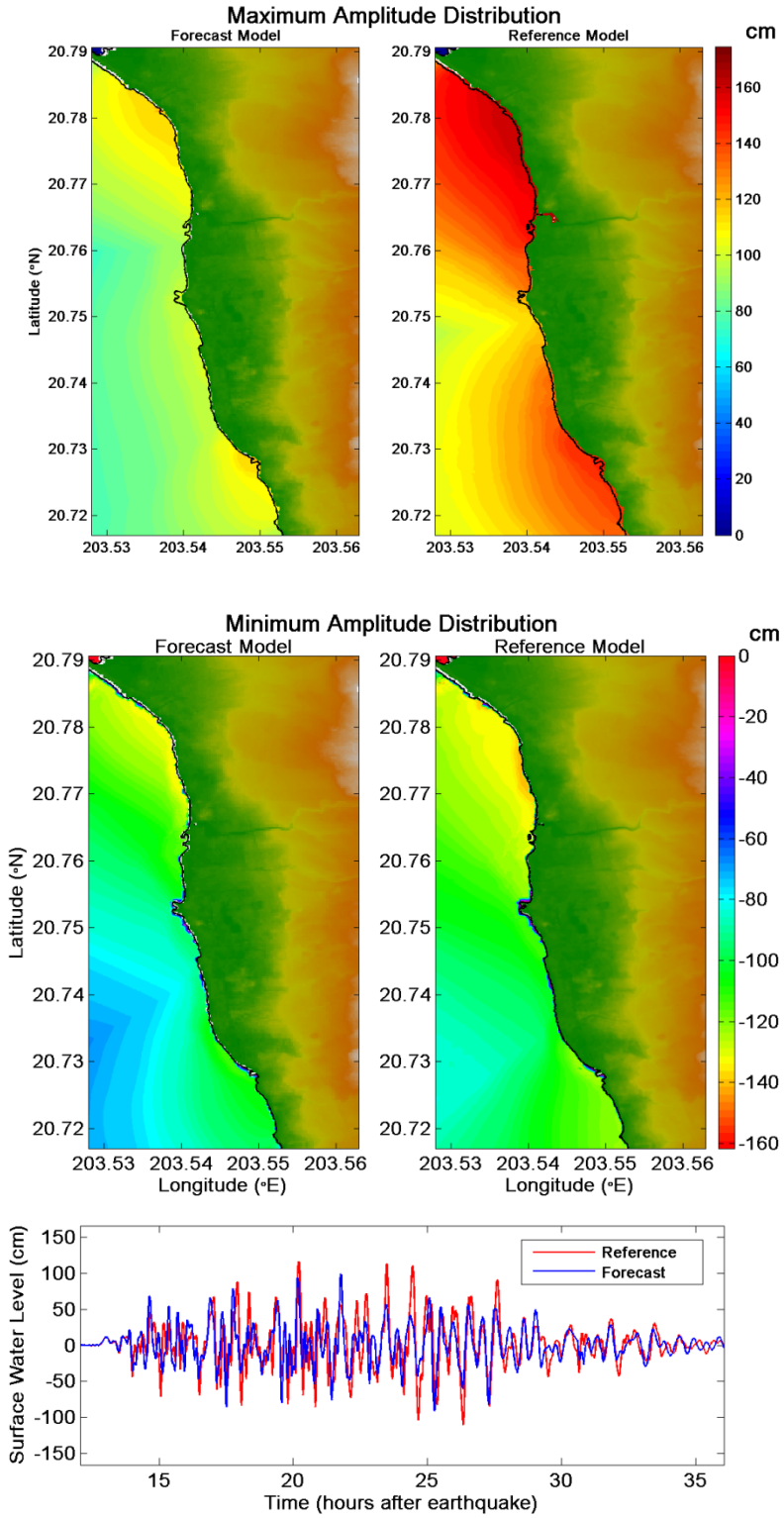

Figure 154. Comparative plot of maximum/minimum tsunami wave amplitude distribution and tsunami time series at C-grid level for synthetic case CSSZ 61-70 between forecast and reference models.

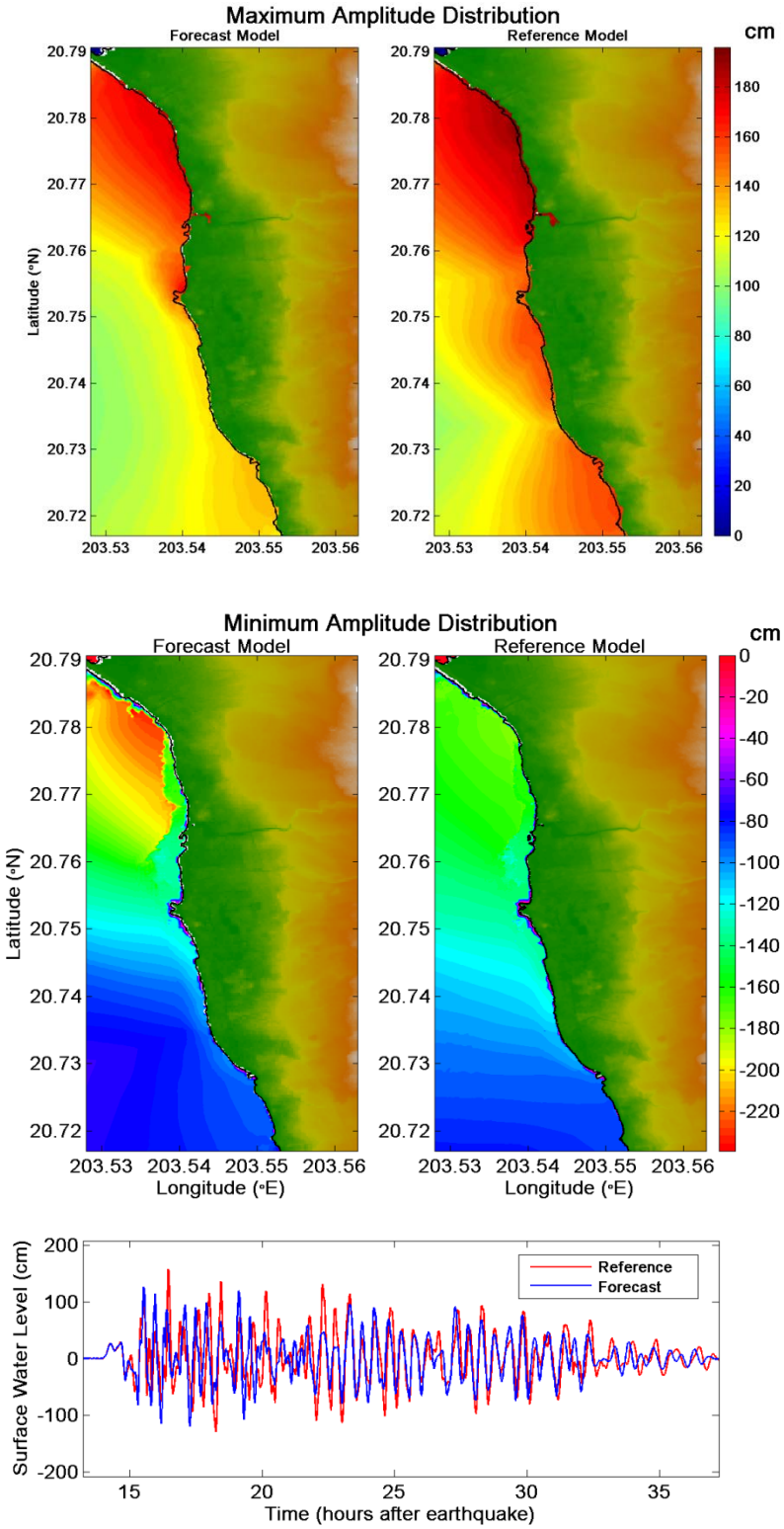

Figure 155. Comparative plot of maximum/minimum tsunami wave amplitude distribution and tsunami time series at C-grid level for synthetic case CSSZ 71-80 between forecast and reference models.

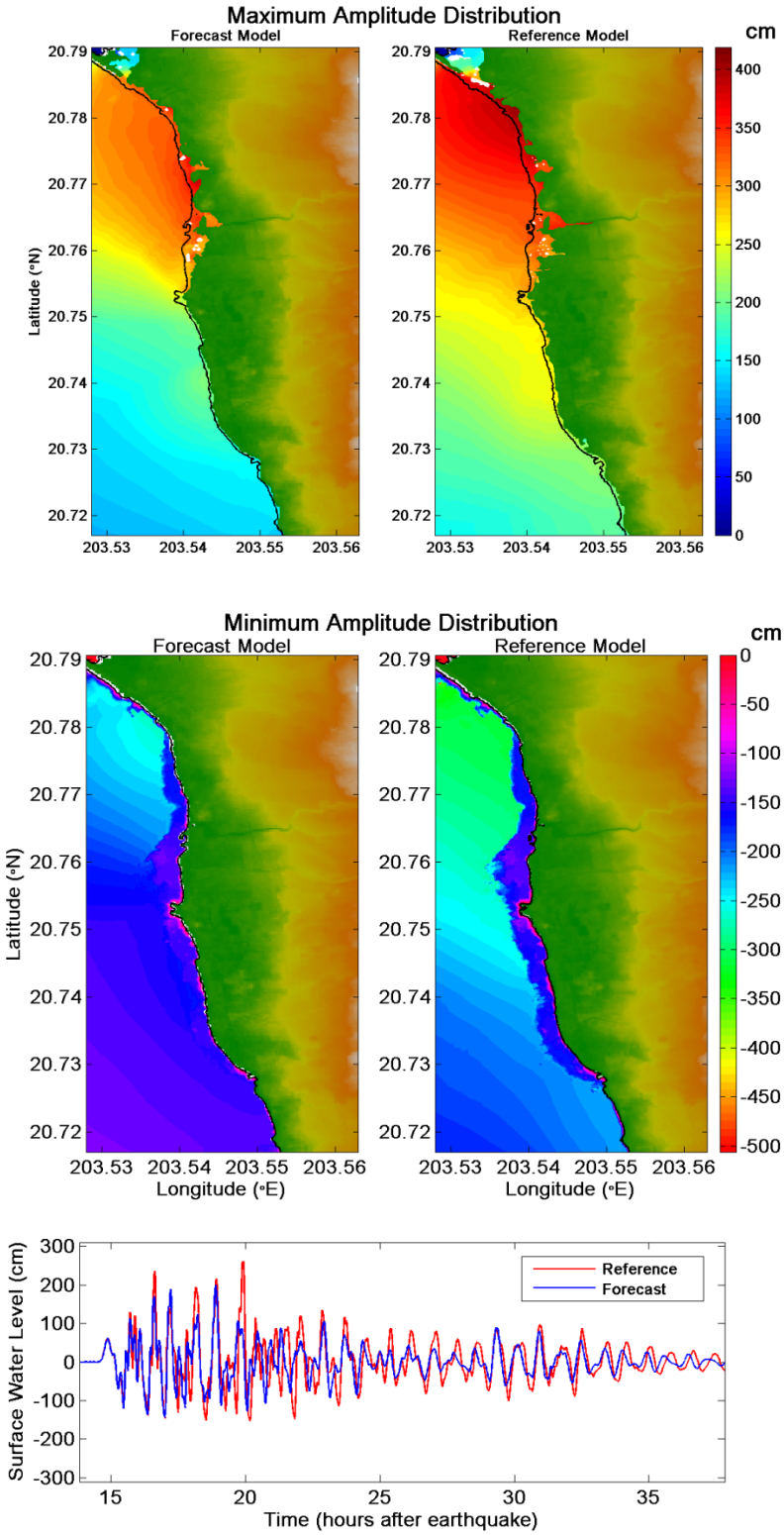

Figure 156. Comparative plot of maximum/minimum tsunami wave amplitude distribution and tsunami time series at C-grid level for synthetic case CSSZ 81-90 between forecast and reference models. White areas on land for the top figure indicate non-inundated sections.

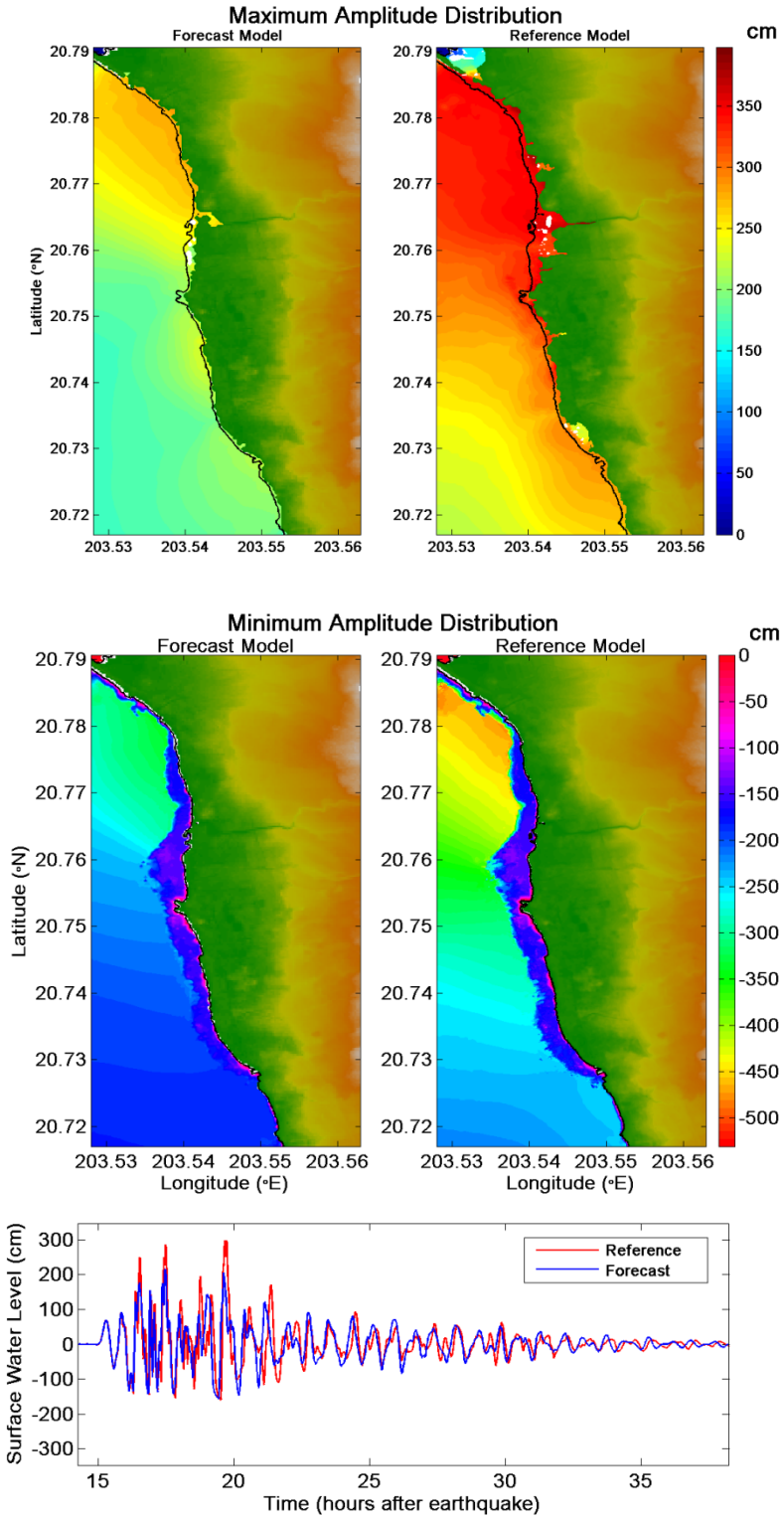

Figure 157. Comparative plot of maximum/minimum tsunami wave amplitude distribution and tsunami time series at C-grid level for synthetic case CSSZ 91-100 between forecast and reference models. White areas on land for the top figure indicate non-inundated sections.

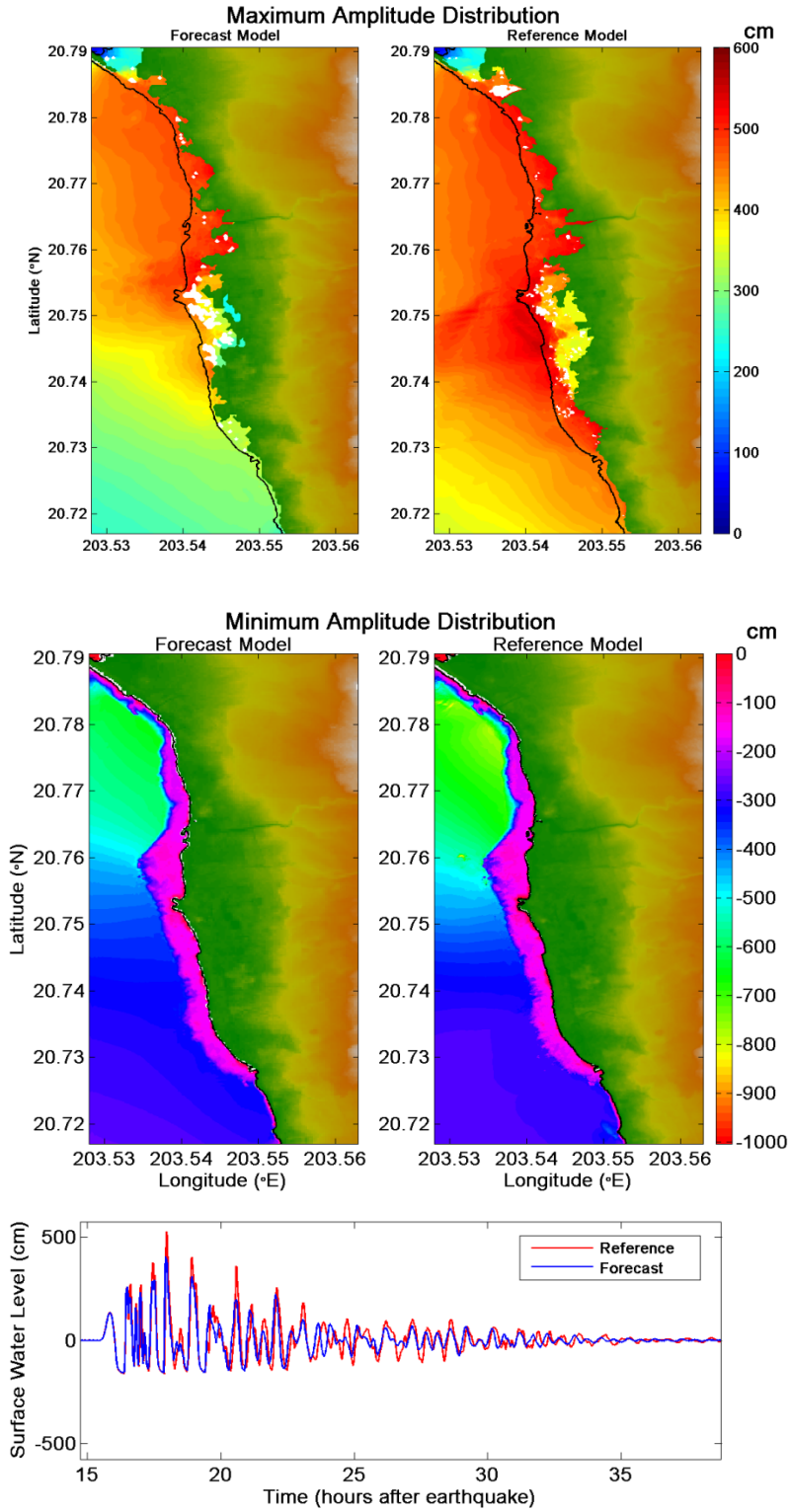

Figure 158. Comparative plot of maximum/minimum tsunami wave amplitude distribution and tsunami time series at C-grid level for synthetic case CSSZ 101-110 between forecast and reference models. White areas on land for the top figure indicate non-inundated sections.

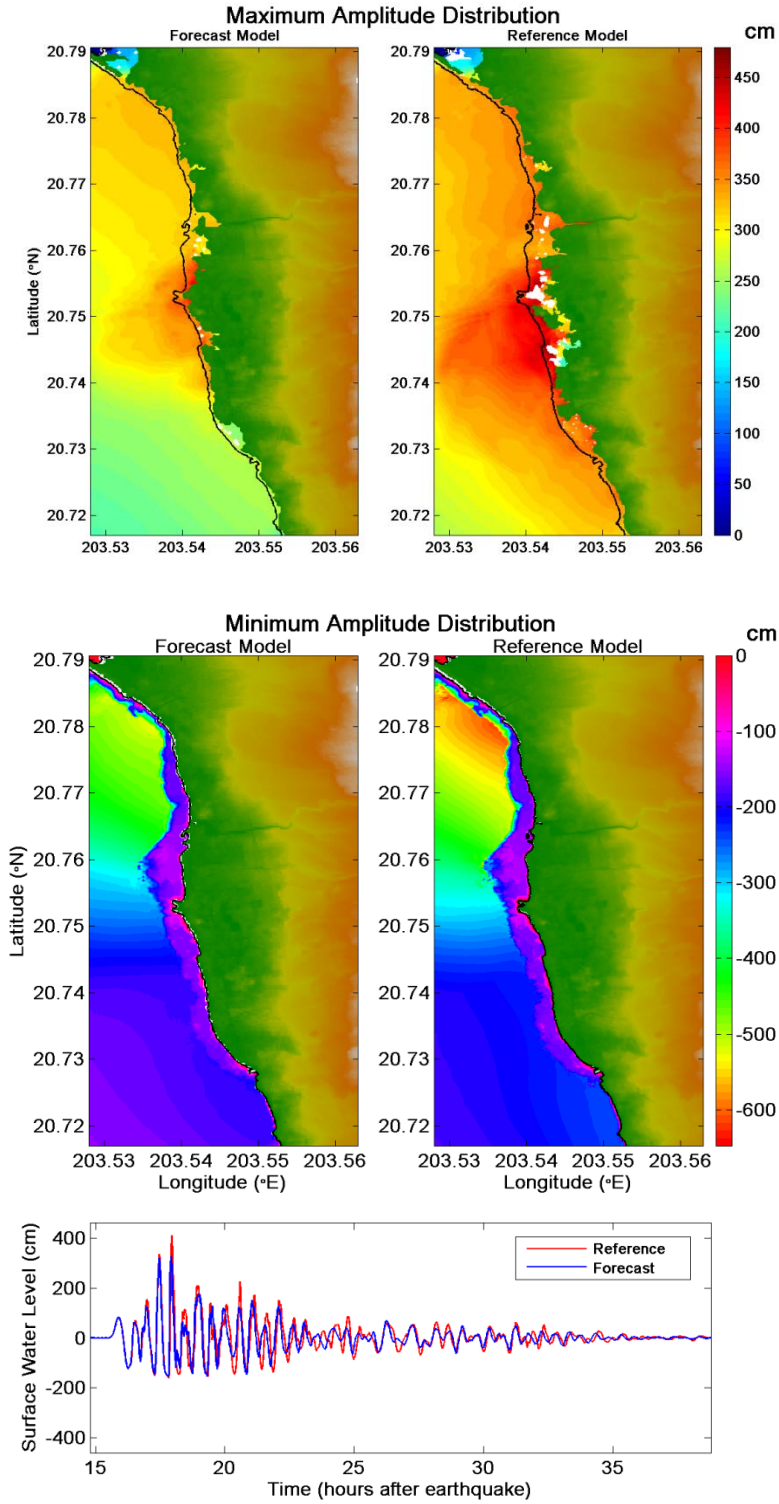

Figure 159. Comparative plot of maximum/minimum tsunami wave amplitude distribution and tsunami time series at C-grid level for synthetic case CSSZ 106-115 between forecast and reference models. White areas on land for the top figure indicate non-inundated sections.

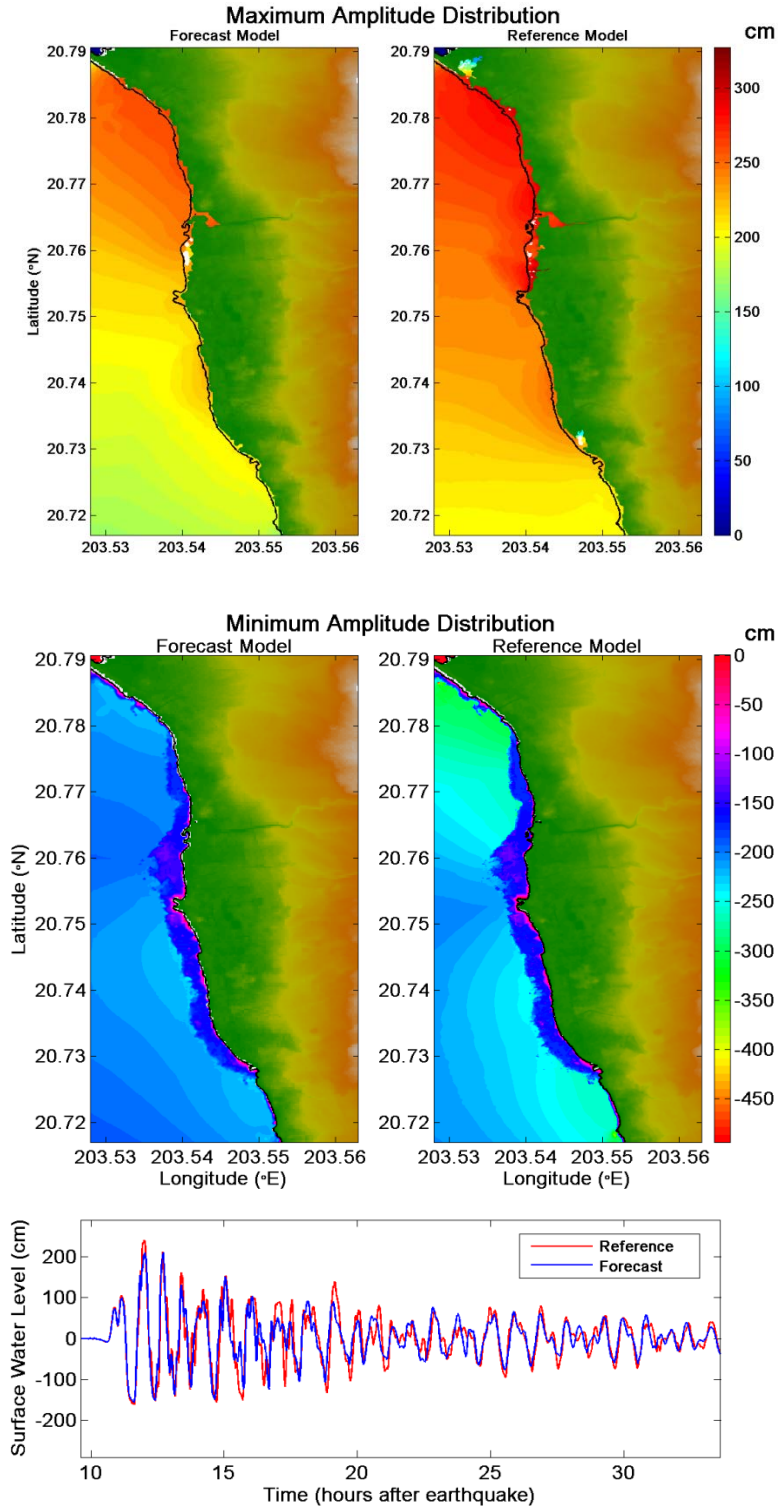

Figure 160. Comparative plot of maximum/minimum tsunami wave amplitude distribution and tsunami time series at C-grid level for synthetic case EPSZ 01-10 between forecast and reference models. White areas on land for the top figure indicate non-inundated sections.

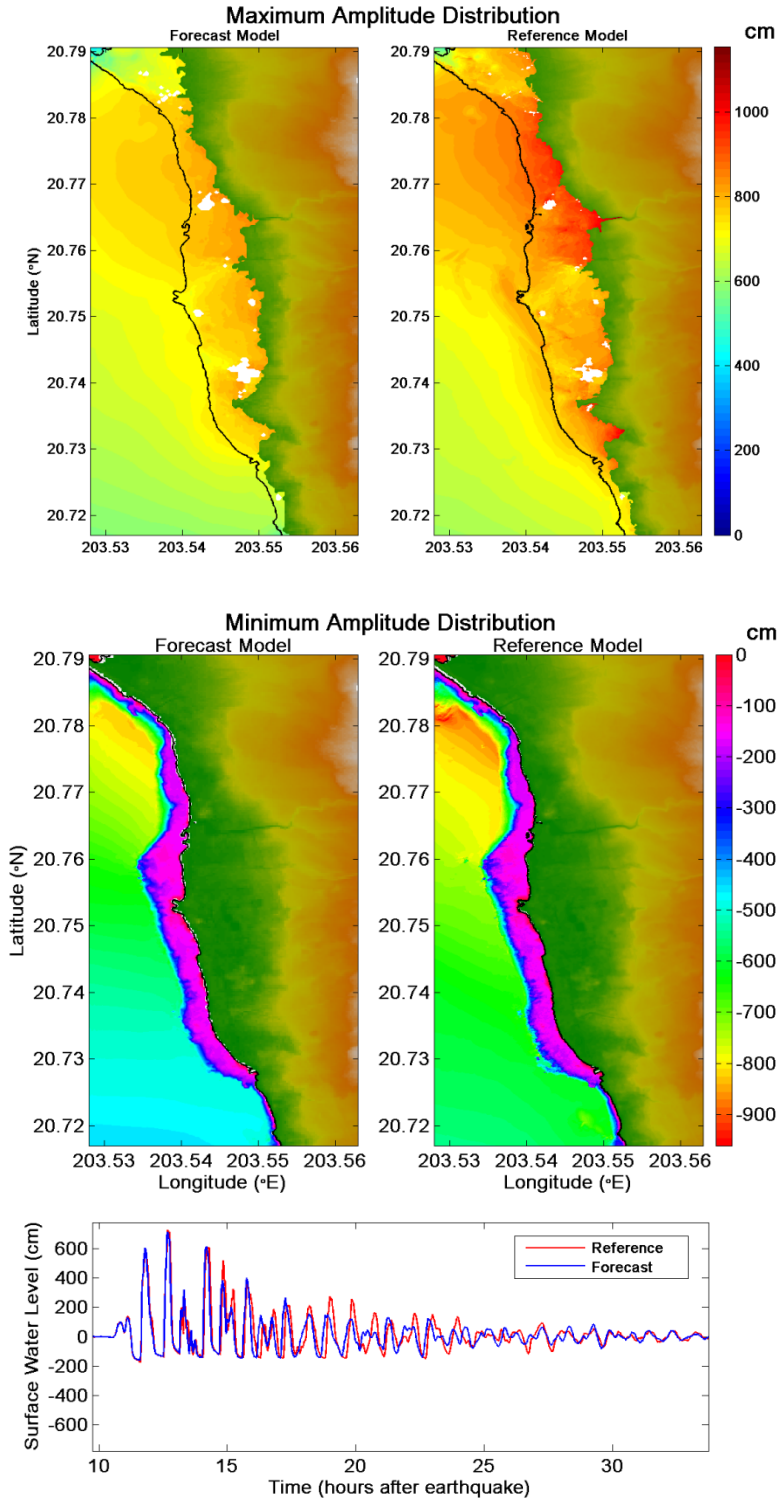

Figure 161. Comparative plot of maximum/minimum tsunami wave amplitude distribution and tsunami time series at C-grid level for synthetic case EPSZ 09-18 between forecast and reference models. White areas on land for the top figure indicate non-inundated sections.

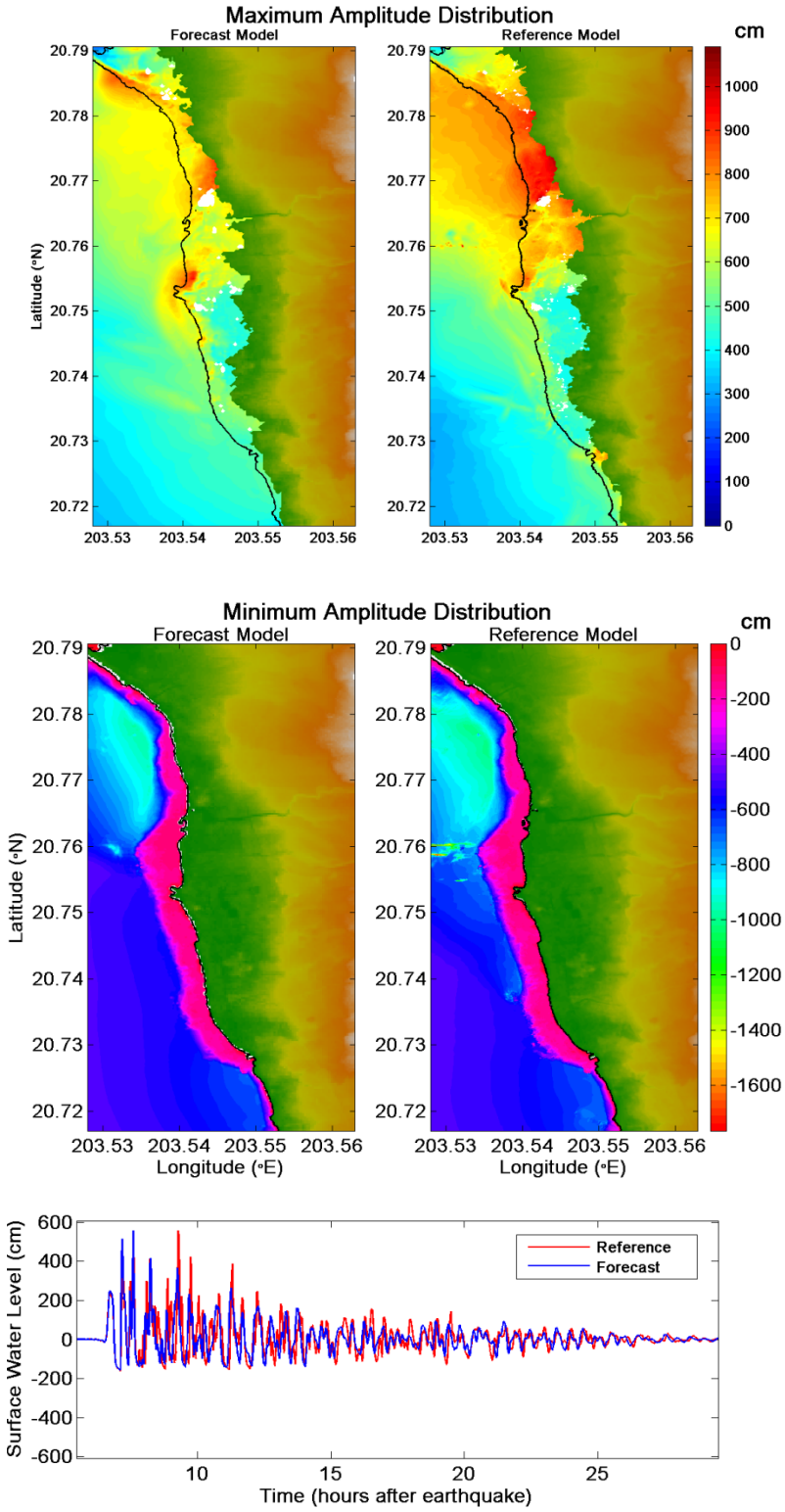

Figure 162. Comparative plot of maximum/minimum tsunami wave amplitude distribution and tsunami time series at C-grid level at the warning point for synthetic case KISZ 01-10 between forecast and reference models. White areas on land for the top figure indicate non-inundated sections.

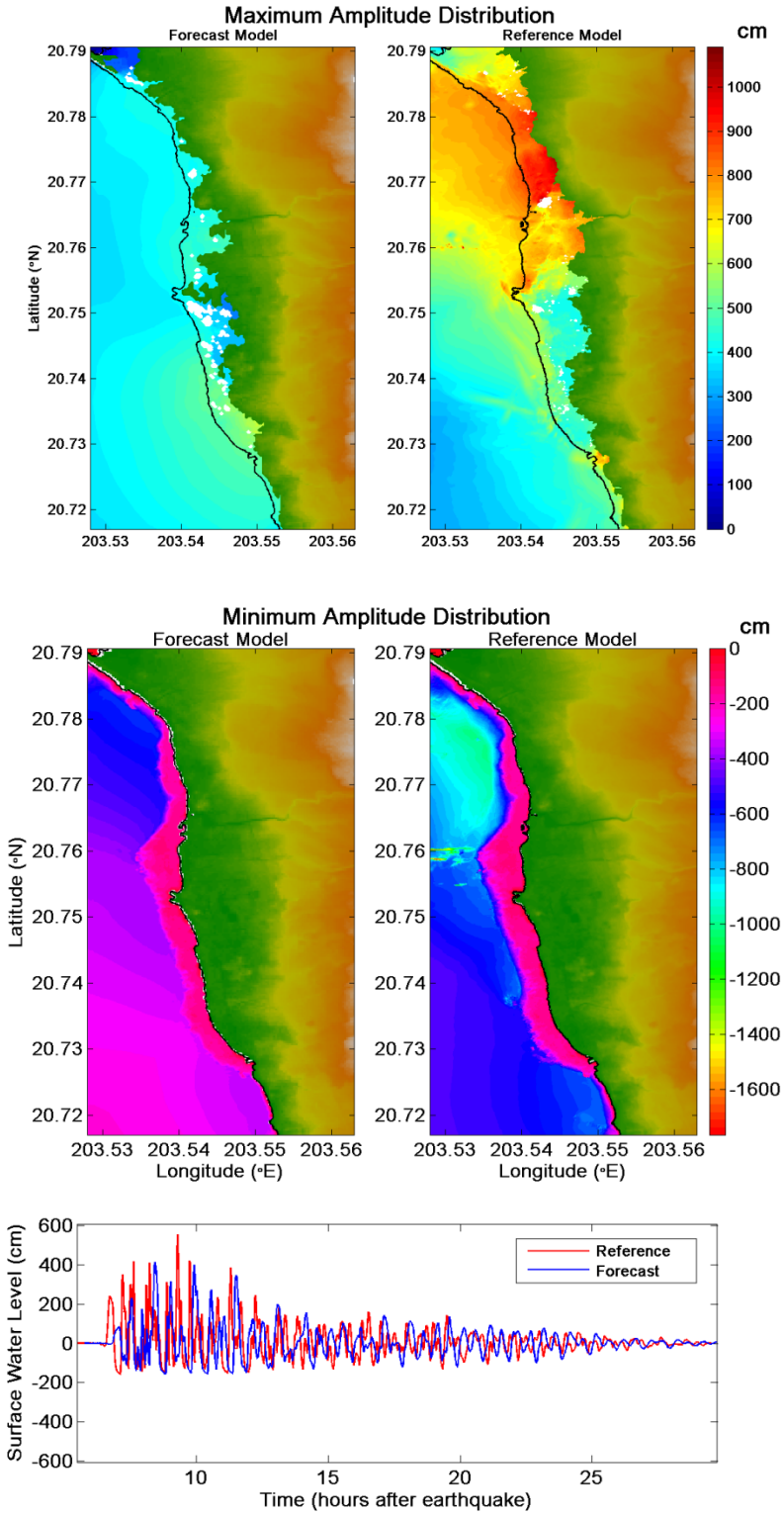

Figure 163. Comparative plot of maximum/minimum tsunami wave amplitude distribution and tsunami time series at C-grid level for synthetic case KISZ 11-20 between forecast and reference models. White areas on land for the top figure indicate non-inundated sections.

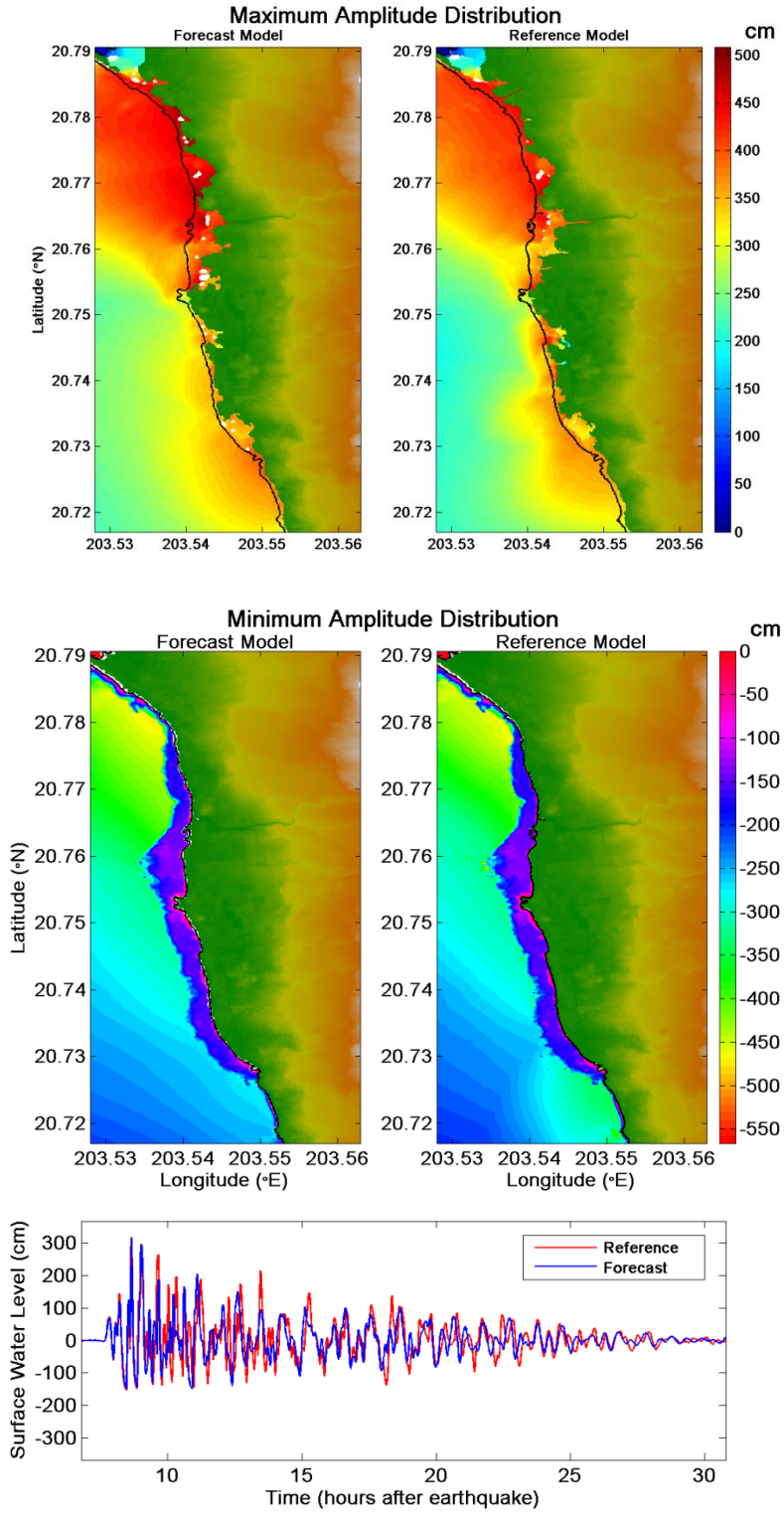

Figure 164. Comparative plot of maximum/minimum tsunami wave amplitude distribution and tsunami time series at C-grid level for synthetic case KISZ 32-41 between forecast and reference models. White areas on land for the top figure indicate non-inundated sections.

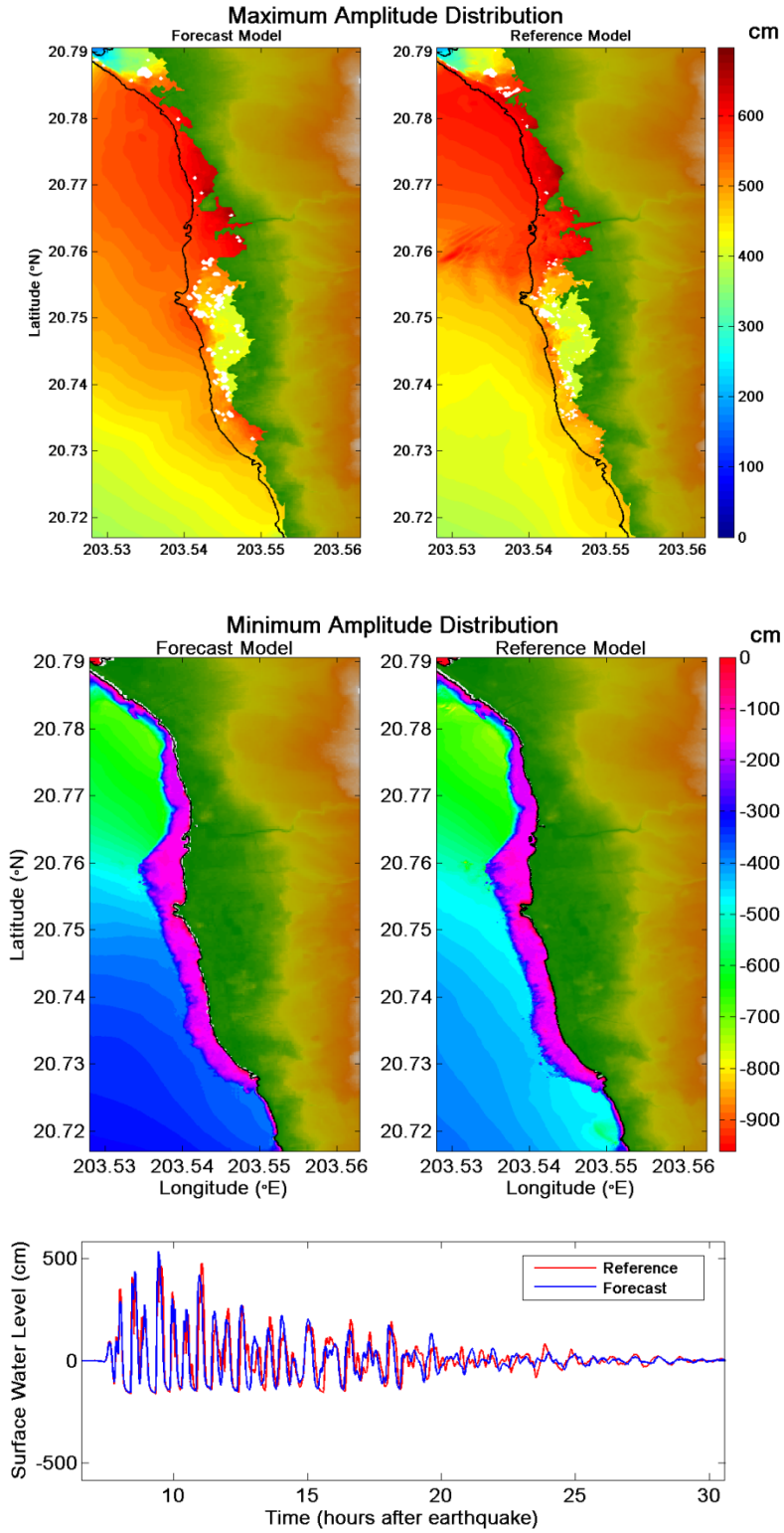

Figure 165. Comparative plot of maximum/minimum tsunami wave amplitude distribution and tsunami time series at C-grid level for synthetic case KISZ421-51 between forecast and reference models. White areas on land for the top figure indicate non-inundated sections.

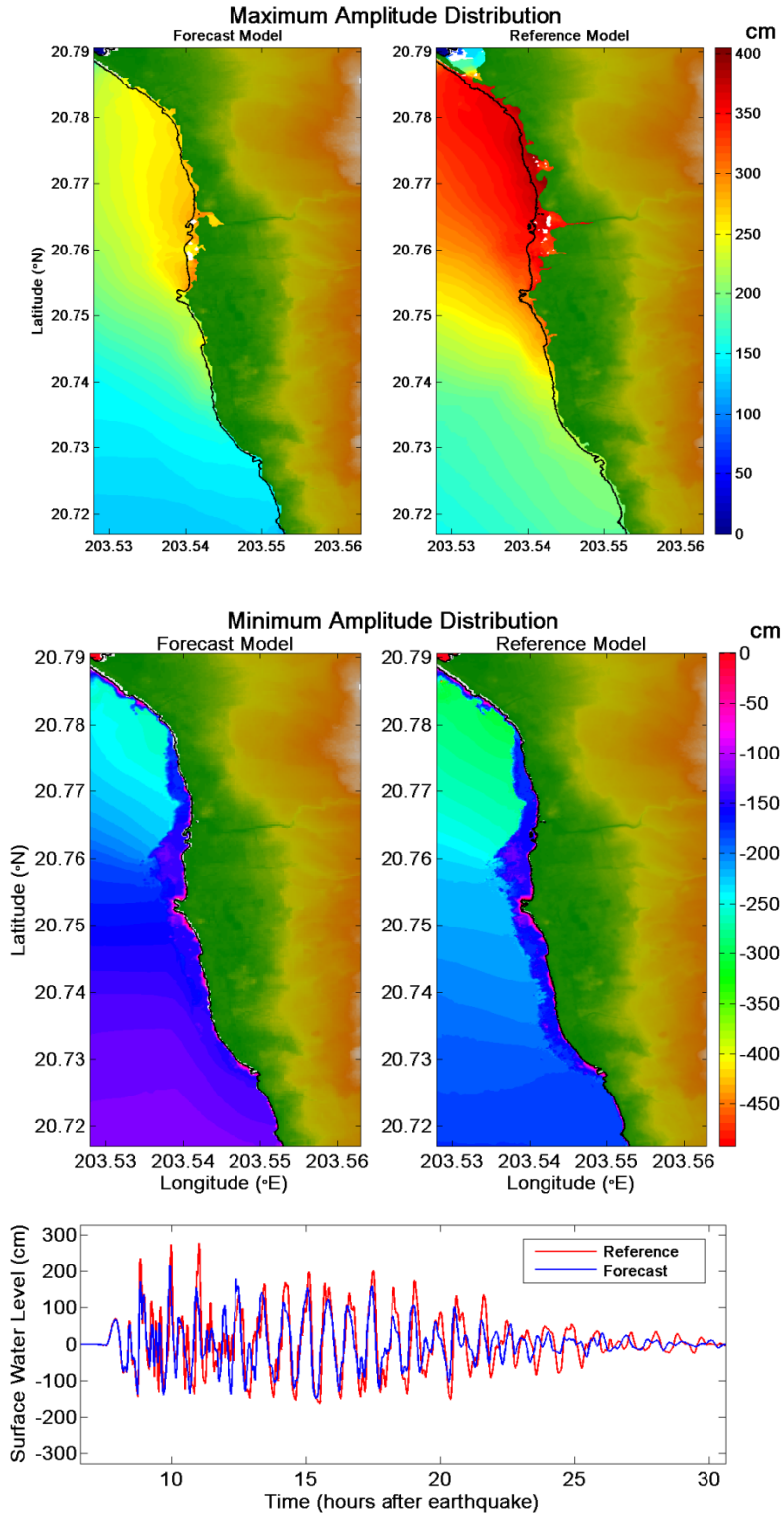

Figure 166. Comparative plot of maximum/minimum tsunami wave amplitude distribution and tsunami time series at C-grid level for synthetic case KISZ52-61 between forecast and reference models. White areas on land for the top figure indicate non-inundated sections.

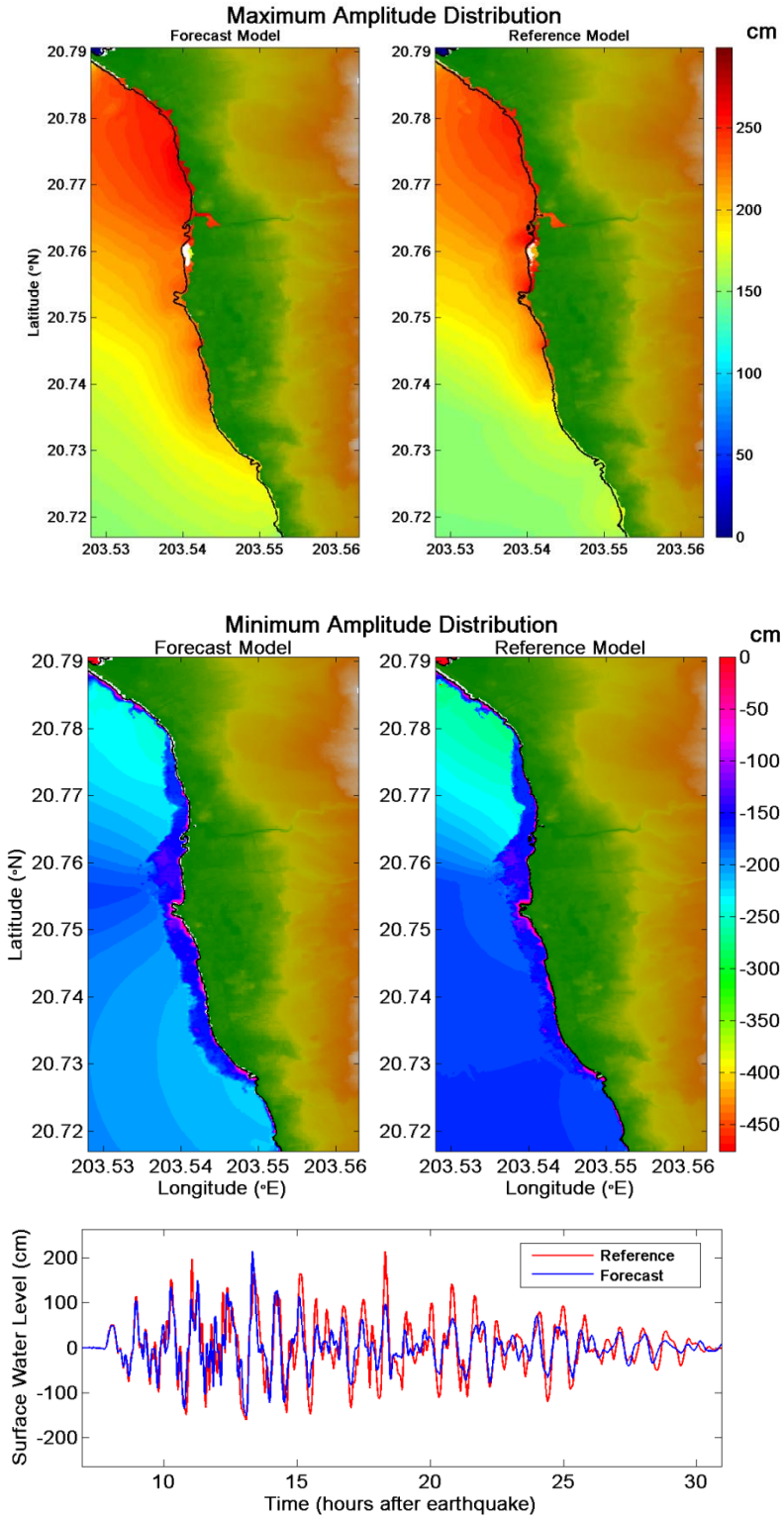

Figure 167. Comparative plot of maximum/minimum tsunami wave amplitude distribution and tsunami time series at C-grid level for synthetic case KISZ56-65 between forecast and reference models. White areas on land for the top figure indicate non-inundated sections.

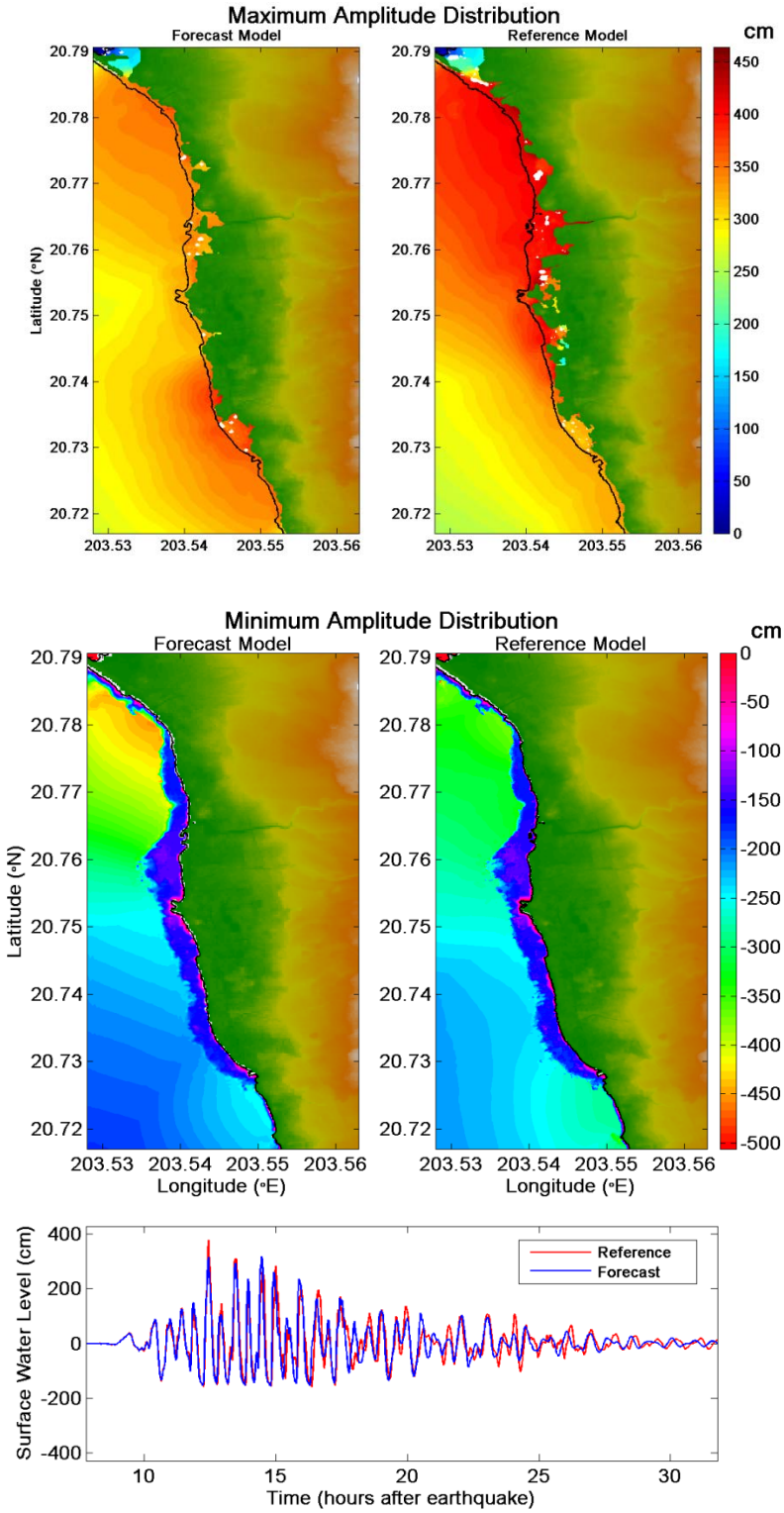

Figure 168. Comparative plot of maximum/minimum tsunami wave amplitude distribution and tsunami time series at C-grid level for synthetic case KISZ66-75 between forecast and reference models. White areas on land for the top figure indicate non-inundated sections.

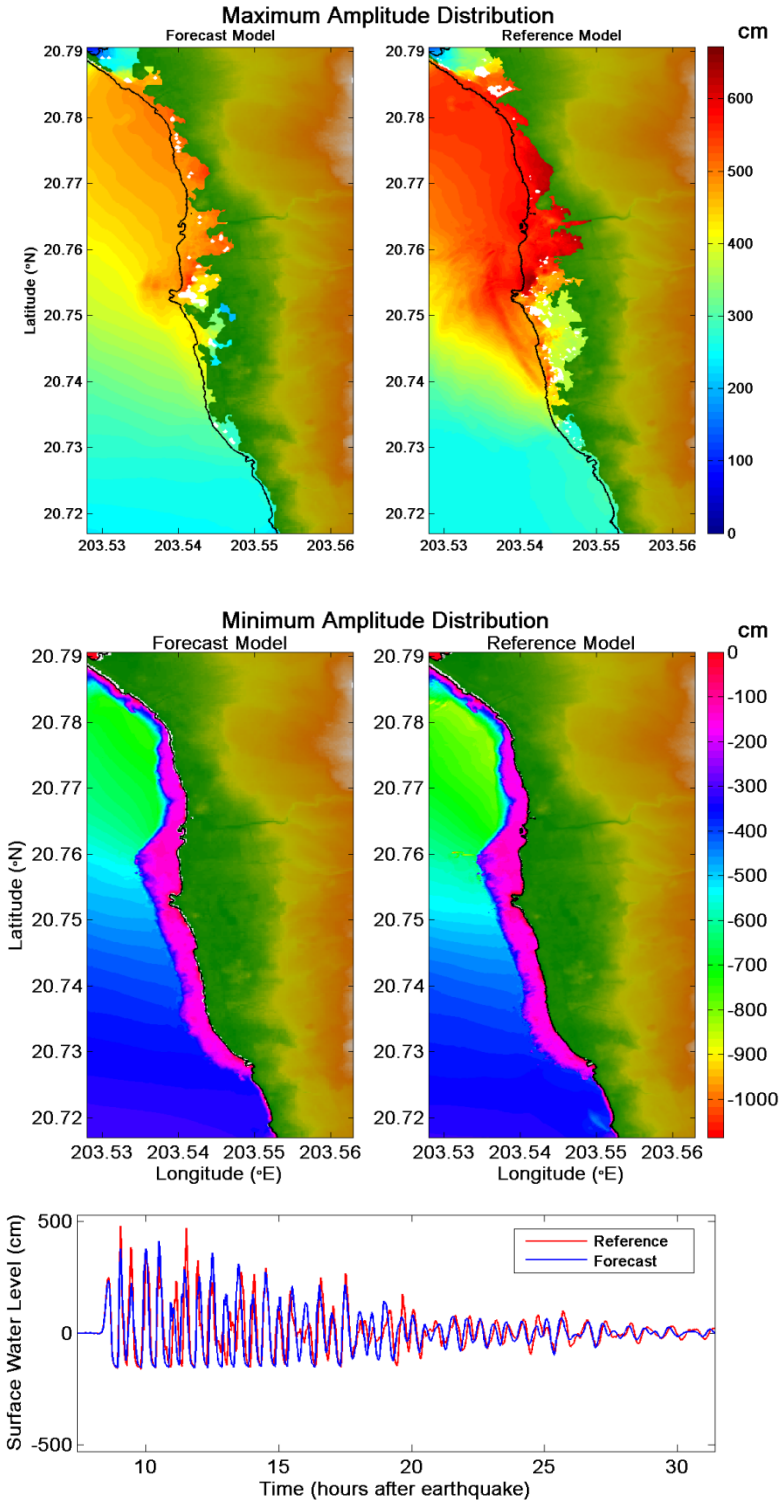

Figure 169. Comparative plot of maximum/minimum tsunami wave amplitude distribution and tsunami time series at C-grid level for synthetic case MOSZ01-10 between forecast and reference models. White areas on land for the top figure indicate non-inundated sections.

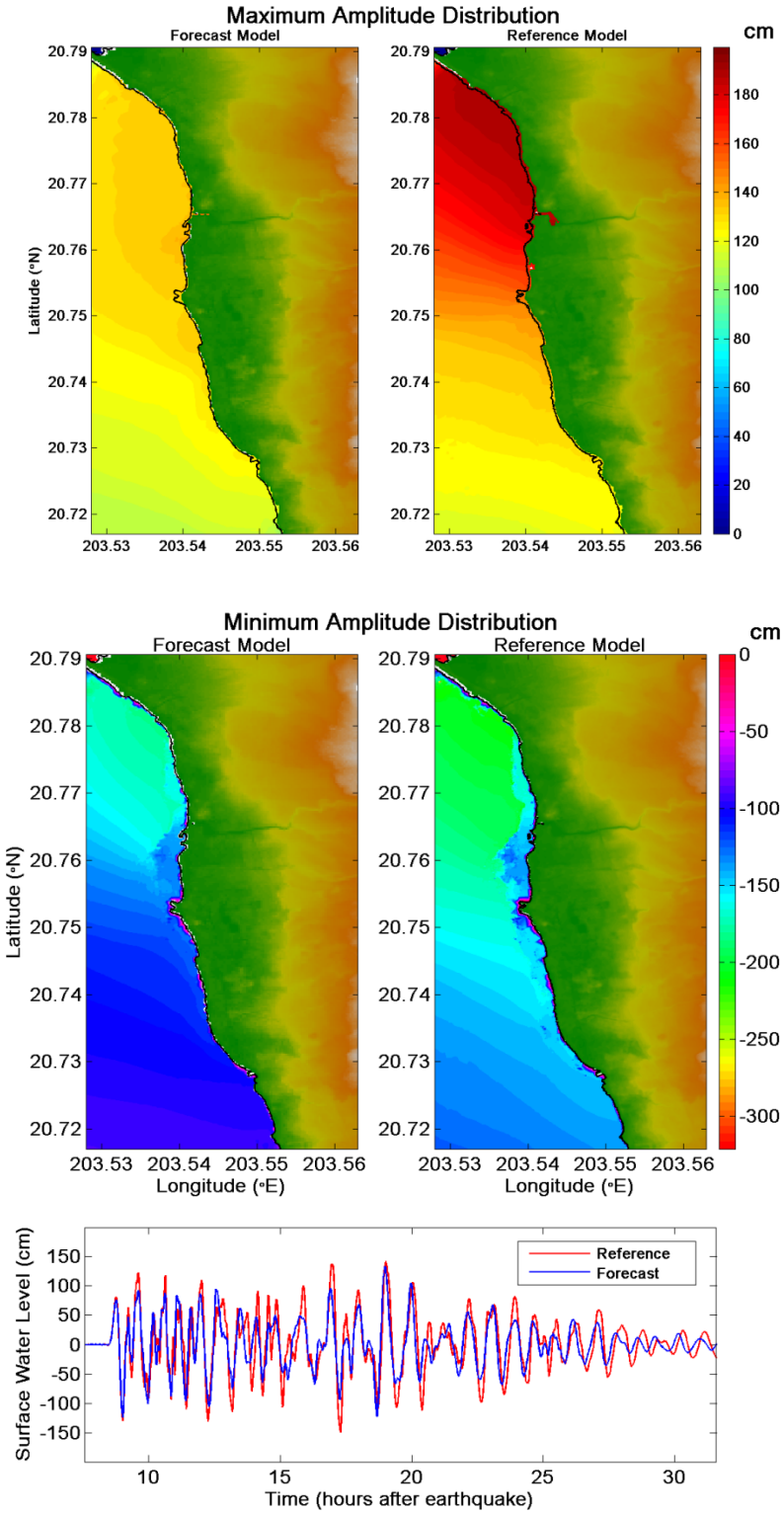

Figure 170. Comparative plot of maximum/minimum tsunami wave amplitude distribution and tsunami time series at C-grid level for synthetic case MOSZ08-17 between forecast and reference models.

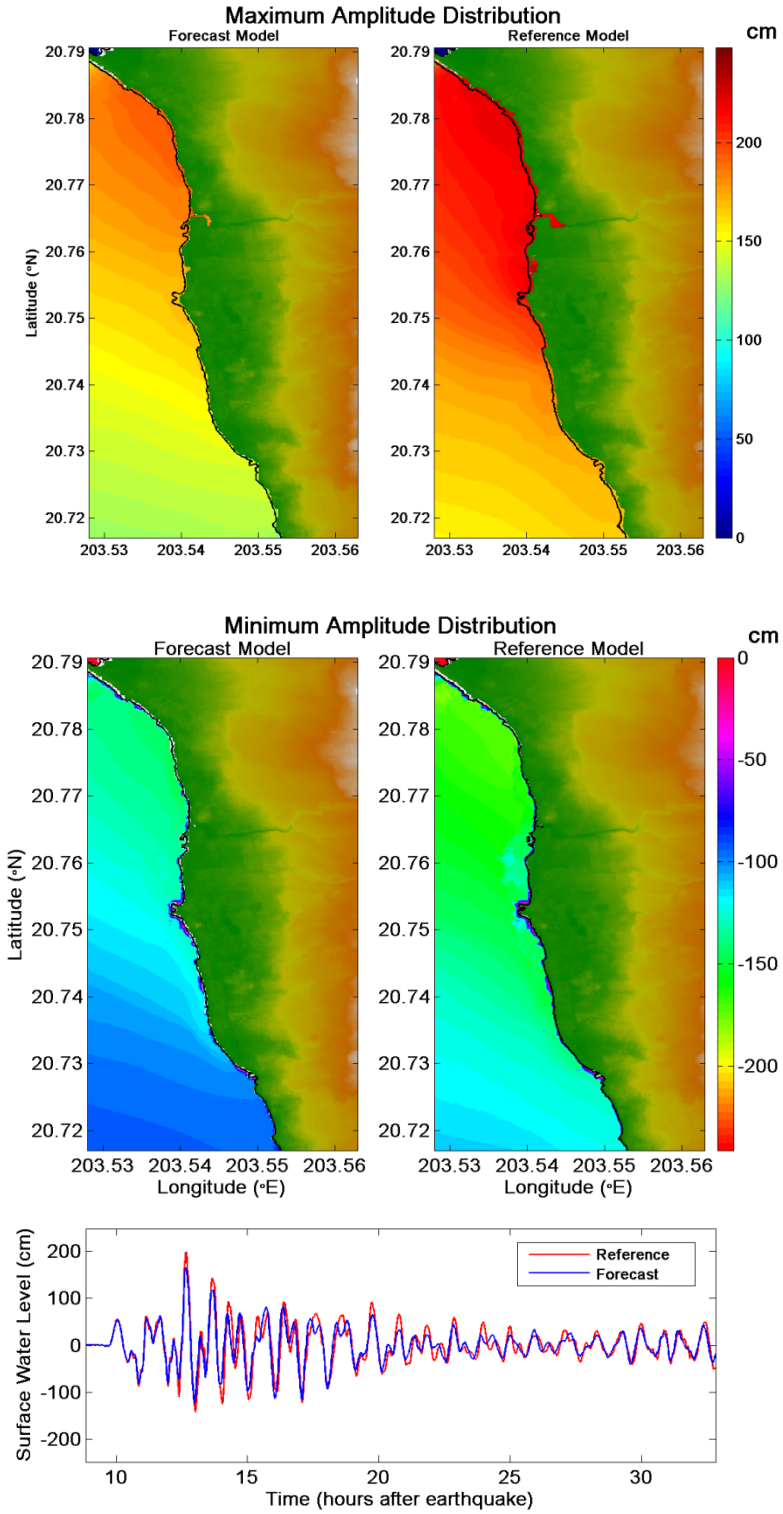

Figure 171. Comparative plot of maximum/minimum tsunami wave amplitude distribution and tsunami time series at C-grid level for synthetic case NGSZ01-10 between forecast and reference models.

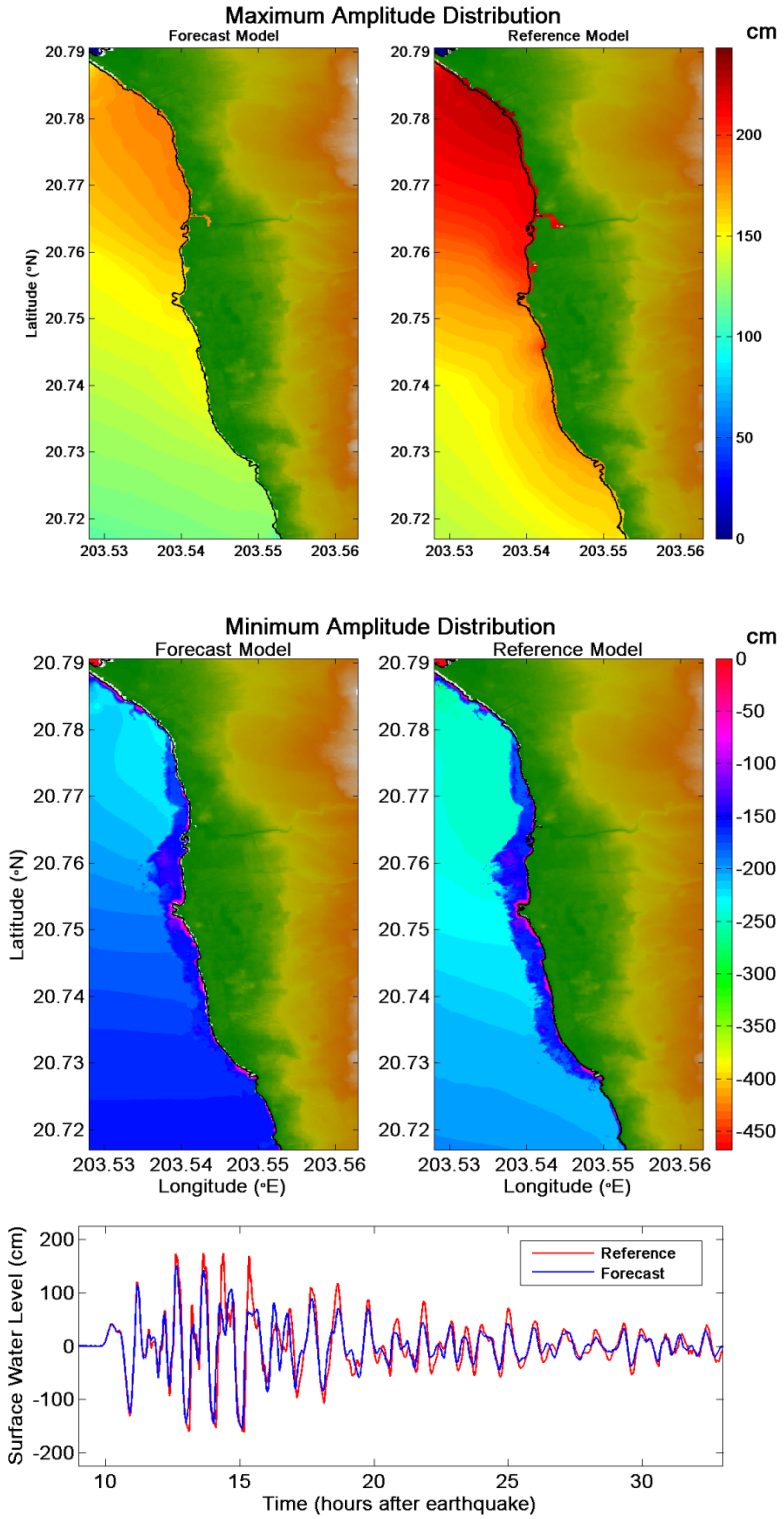

Figure 172. Comparative plot of maximum/minimum tsunami wave amplitude distribution and tsunami time series at C-grid level for synthetic case NGSZ06-15 between forecast and reference models.

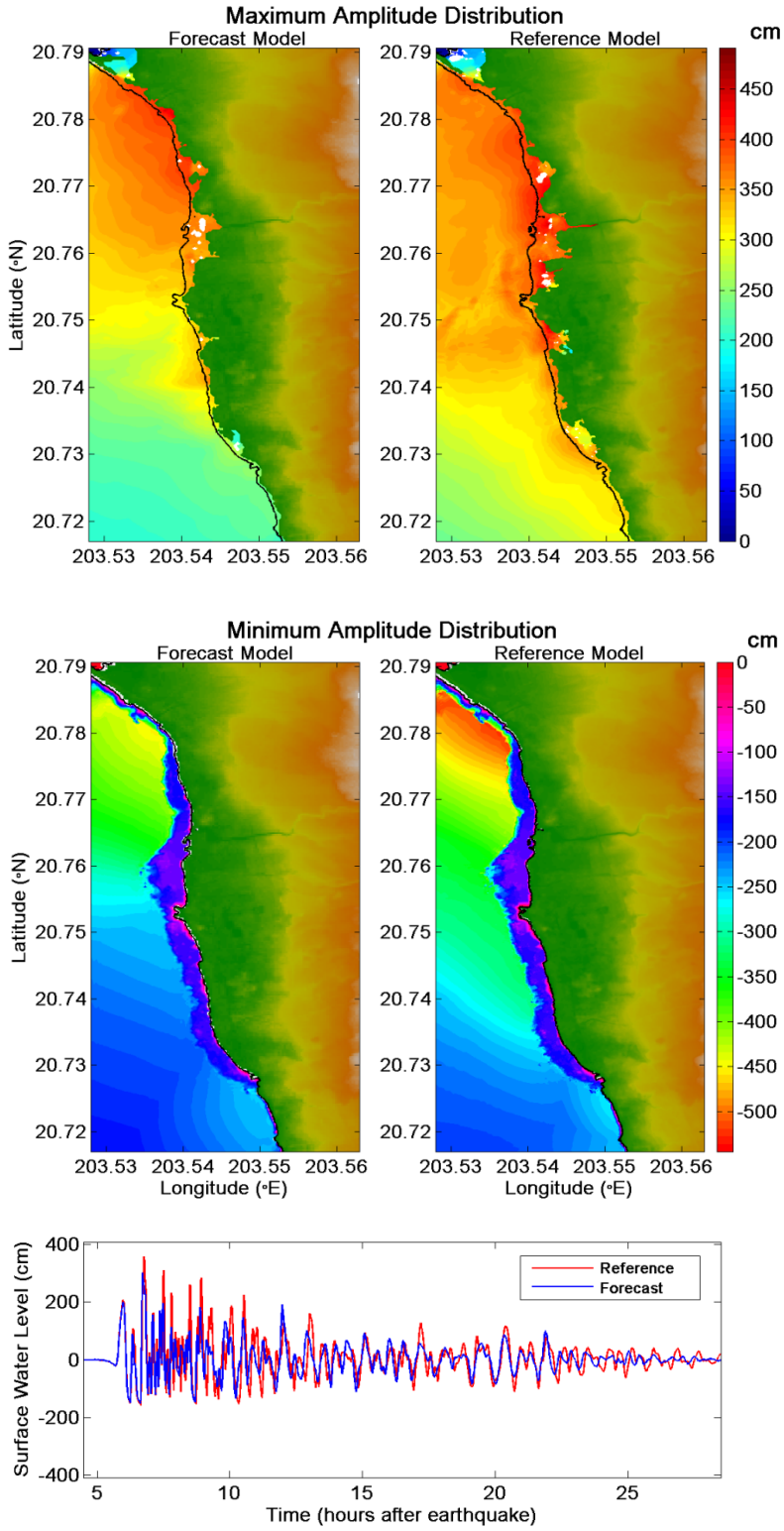

Figure 173. Comparative plot of maximum/minimum tsunami wave amplitude distribution and tsunami time series at C-grid level for synthetic case NTSZ01-10 between forecast and reference models. White areas on land for the top figure indicate non-inundated sections.

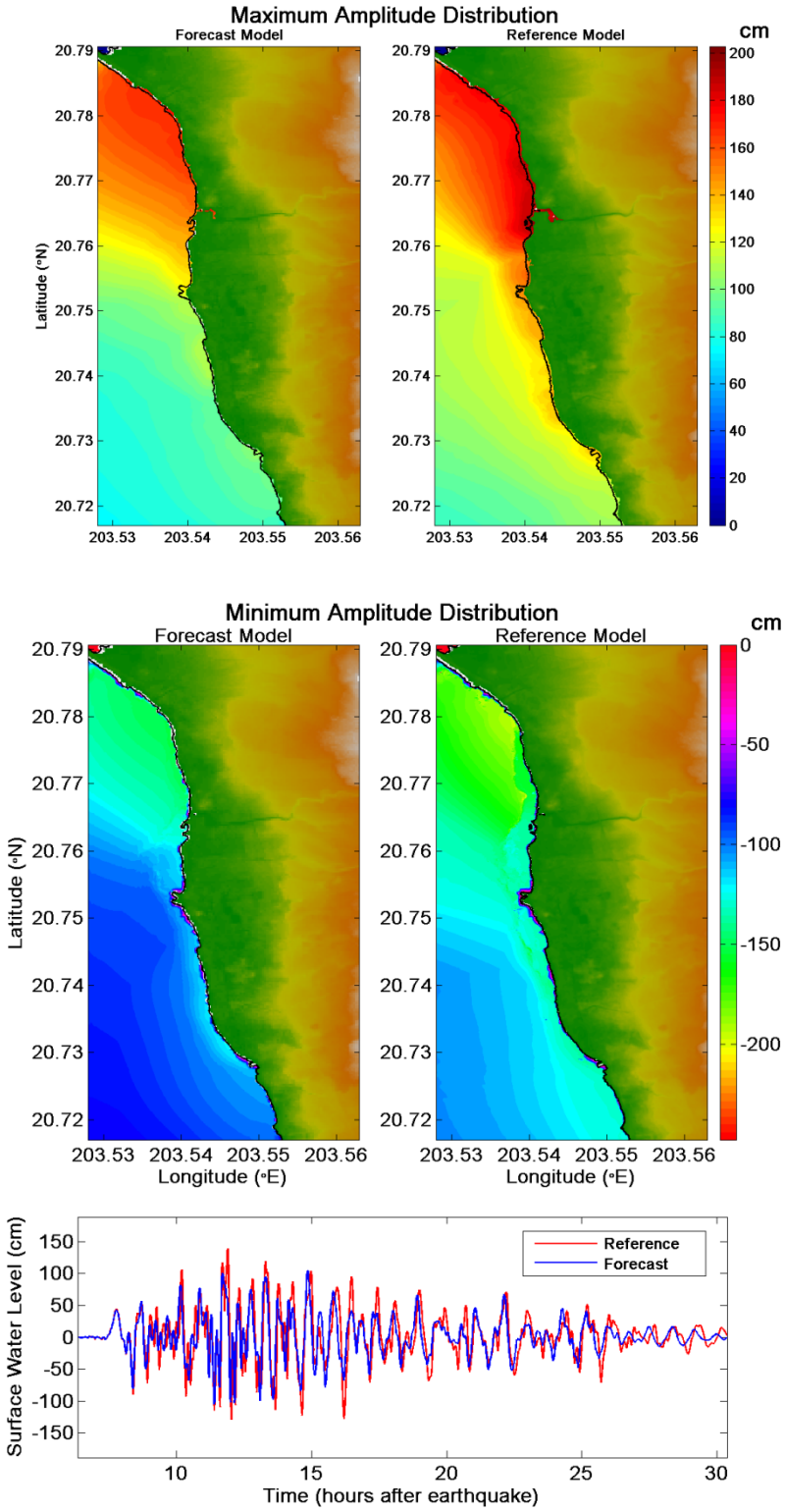

Figure 174. Comparative plot of maximum/minimum tsunami wave amplitude distribution and tsunami time series at C-grid level for synthetic case NTSZ11-20 between forecast and reference models.

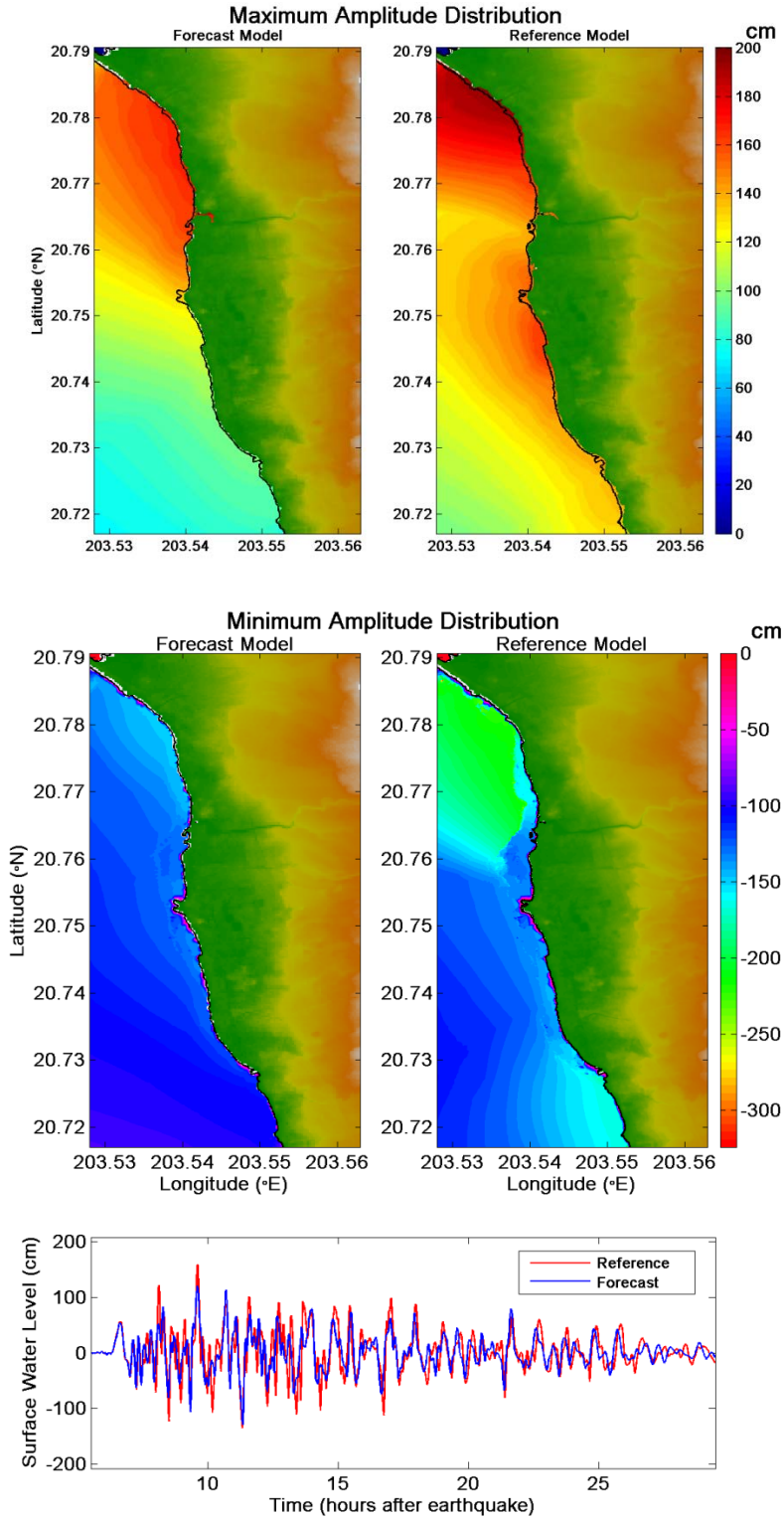

Figure 175. Comparative plot of maximum/minimum tsunami wave amplitude distribution and tsunami time series at C-grid level for synthetic case NTSZ21-30 between forecast and reference models.

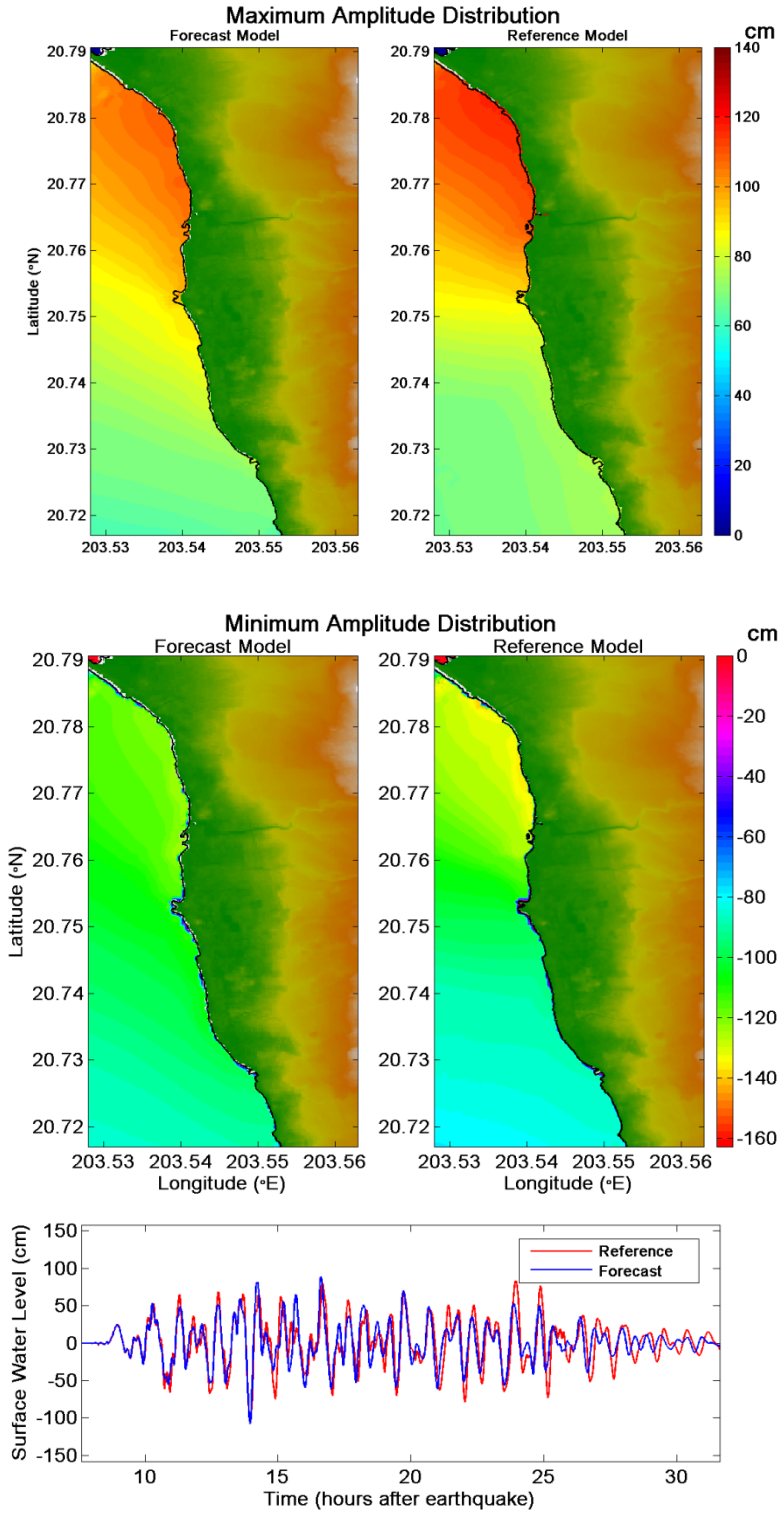

Figure 176. Comparative plot of maximum/minimum tsunami wave amplitude distribution and tsunami time series at C-grid level for synthetic case NTSZ30-39 between forecast and reference models.

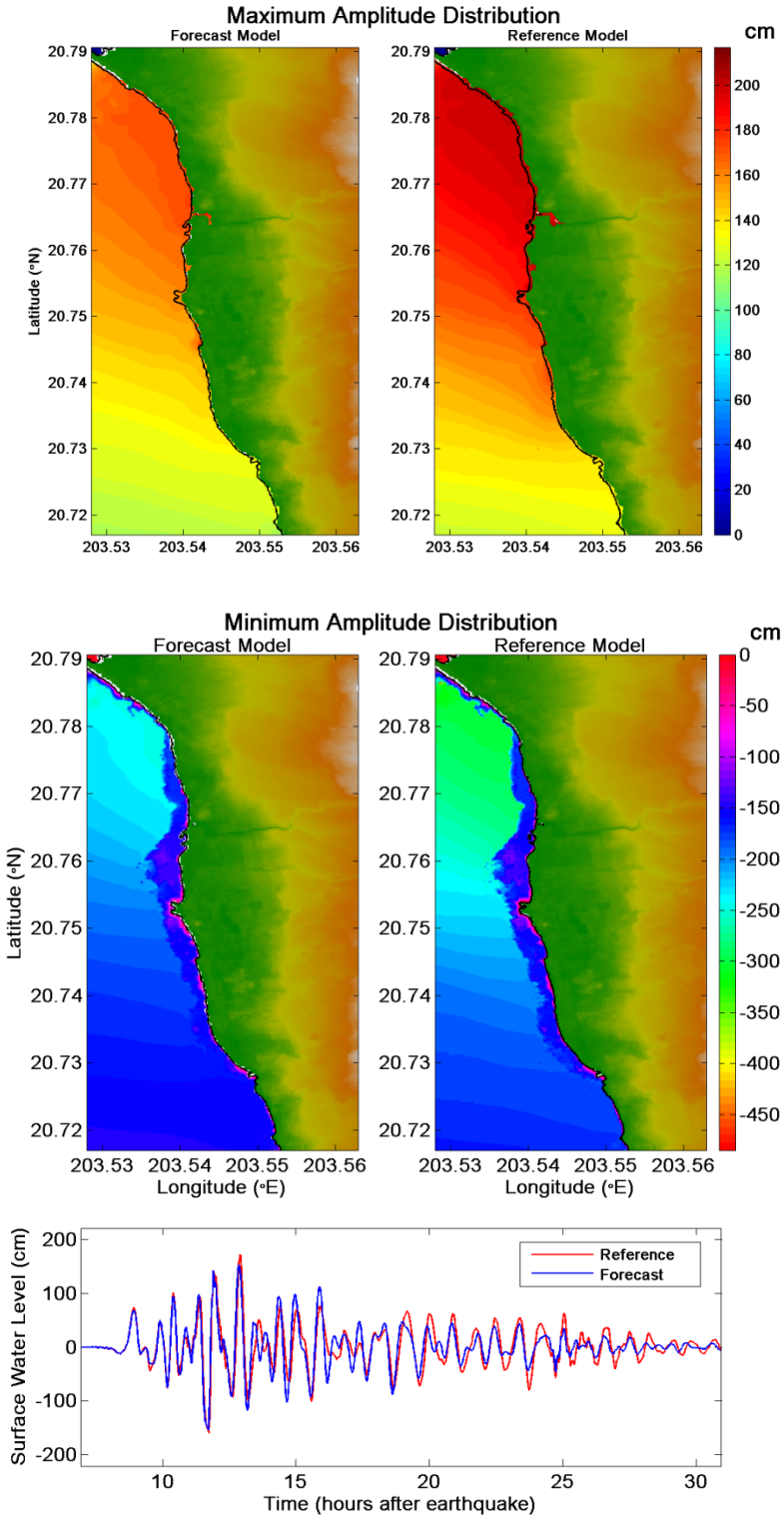

Figure 177. Comparative plot of maximum/minimum tsunami wave amplitude distribution and tsunami time series at C-grid level for synthetic case NVSZ01-10 between forecast and reference models.

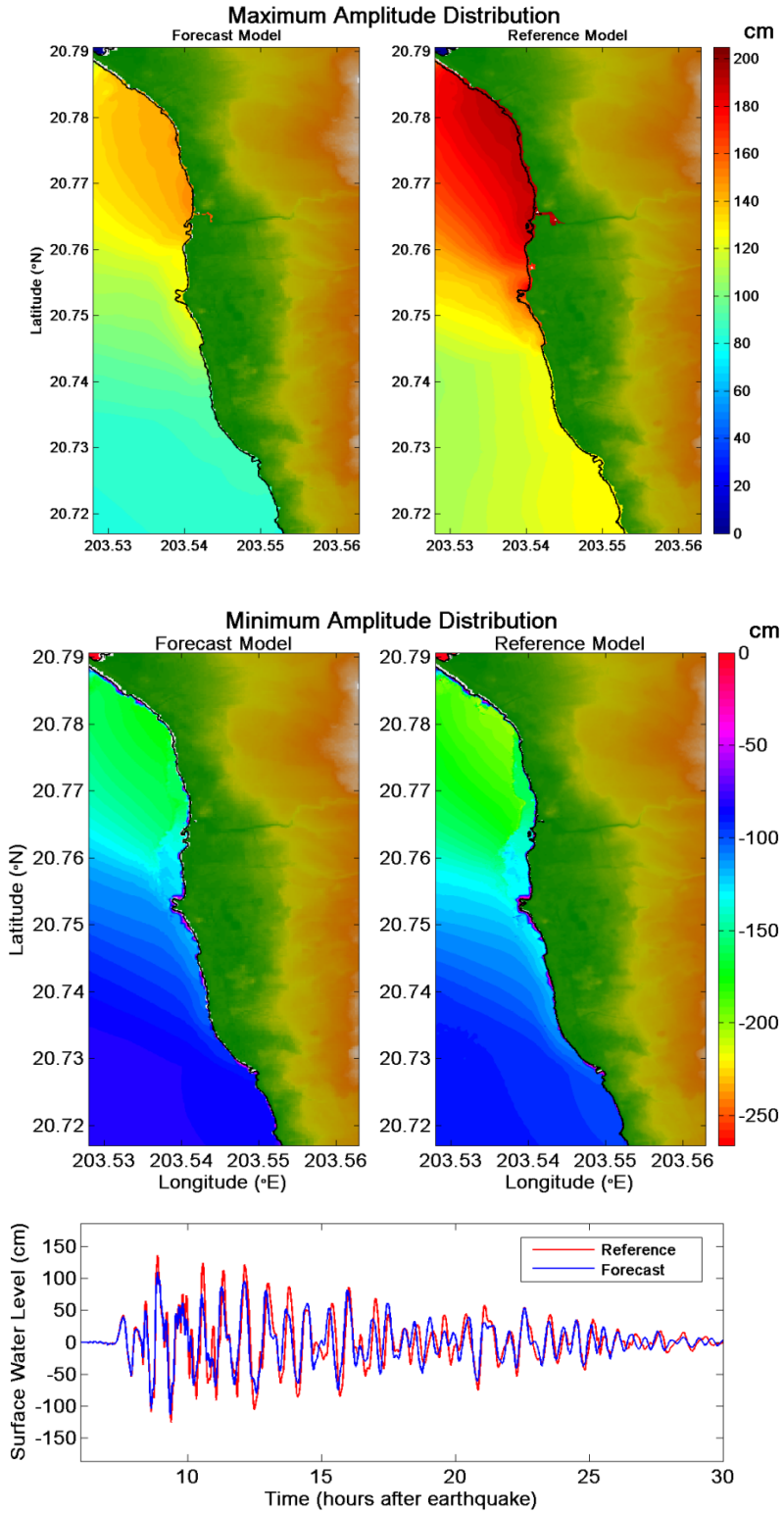

Figure 178. Comparative plot of maximum/minimum tsunami wave amplitude distribution and tsunami time series at C-grid level for synthetic case NVSZ11-20 between forecast and reference models.

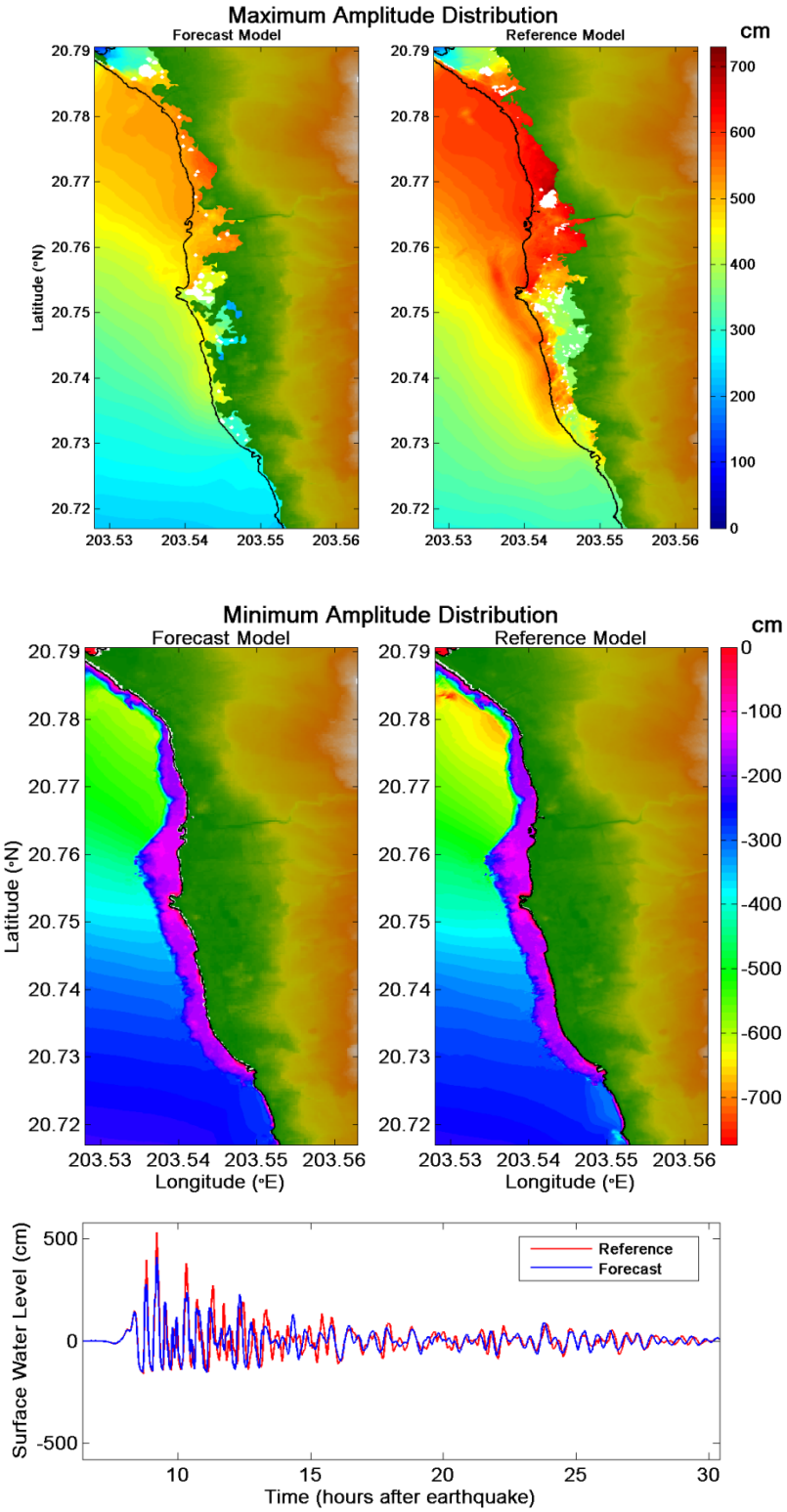

Figure 179. Comparative plot of maximum/minimum tsunami wave amplitude distribution and tsunami time series at C-grid level for synthetic case NVSZ28-37 between forecast and reference models. White areas on land for the top figure indicate non-inundated sections.

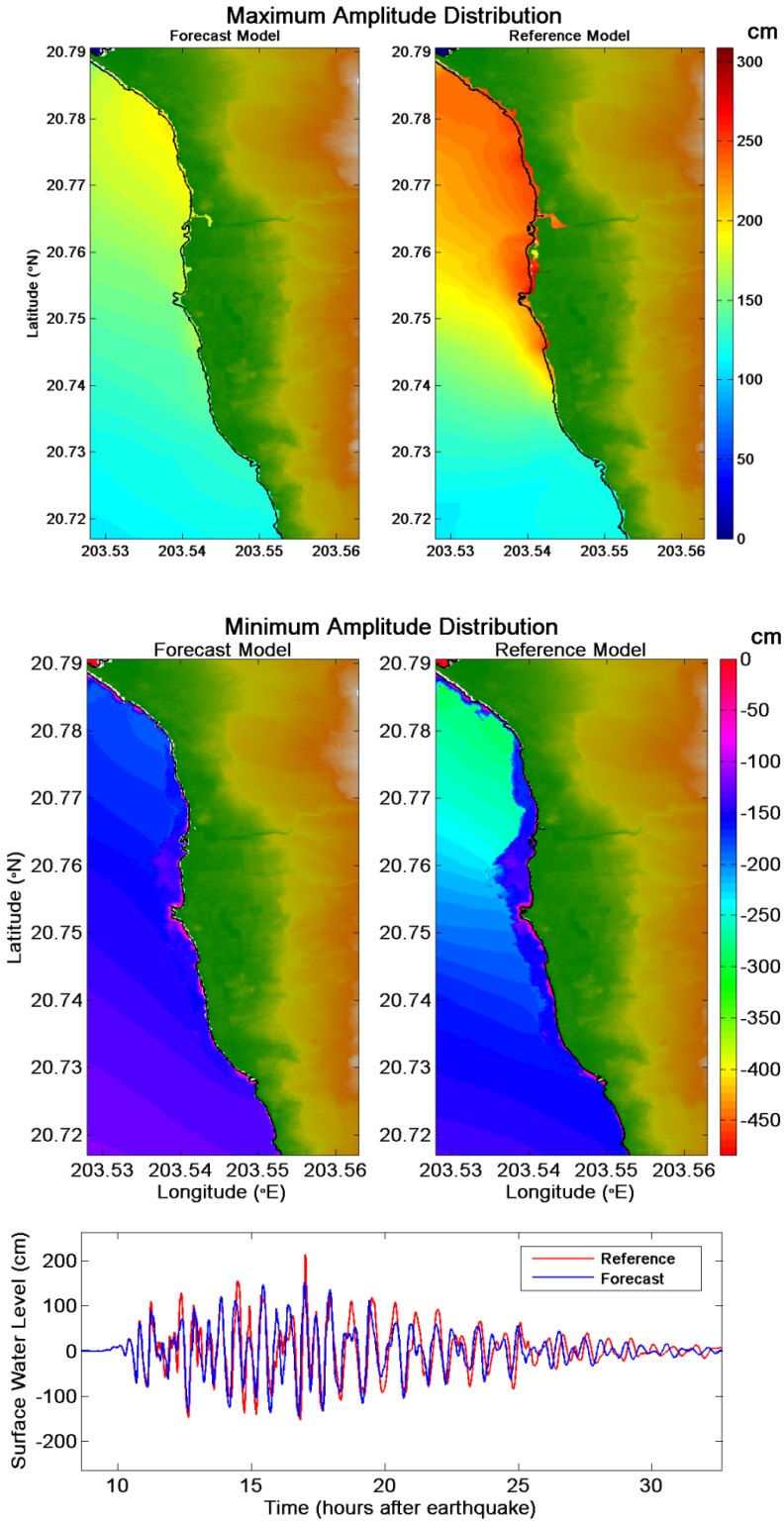

Figure 180. Comparative plot of maximum/minimum tsunami wave amplitude distribution and tsunami time series at C-grid level for synthetic case RNSZ01-10 between forecast and reference models.

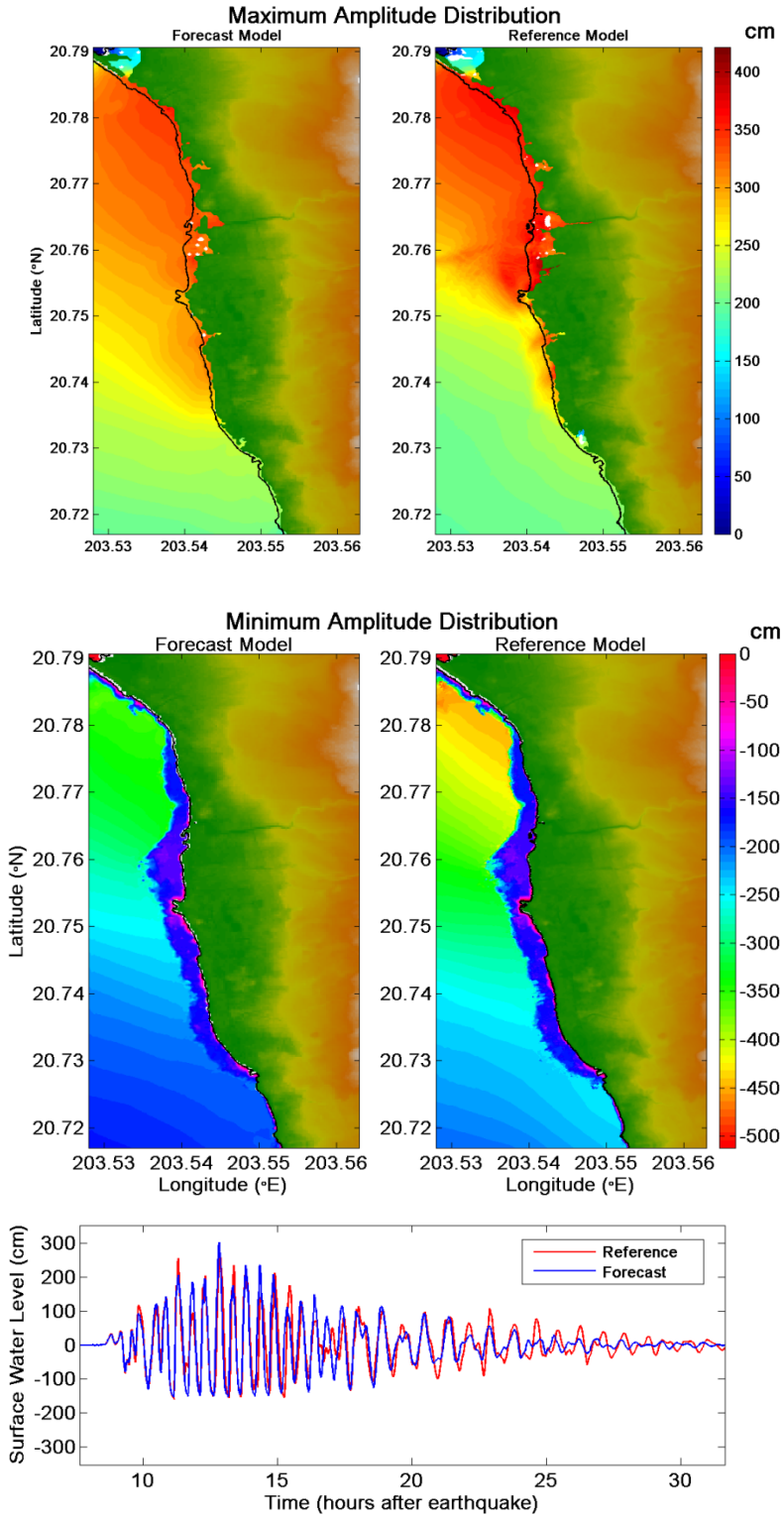

Figure 181. Comparative plot of maximum/minimum tsunami wave amplitude distribution and tsunami time series at C-grid level for synthetic case RNSZ13-22 between forecast and reference models. White areas on land for the top figure indicate non-inundated sections.

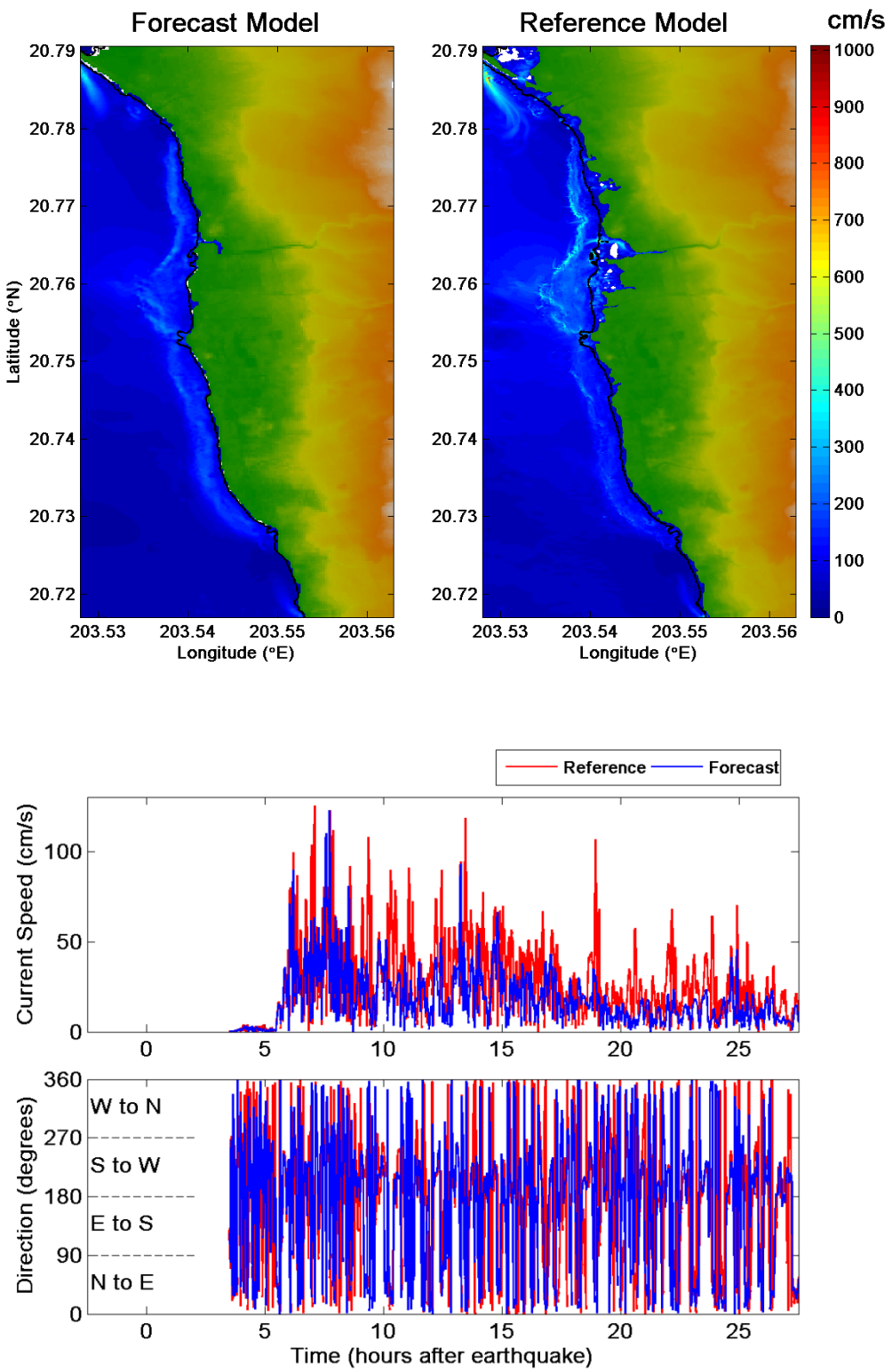

Figure 182. Comparative plot of maximum current distribution, current speed and directionality at the warning point at C-grid level for synthetic case ACSZ01-10 between forecast and reference models. White areas on land for the top figure indicate non-inundated sections.

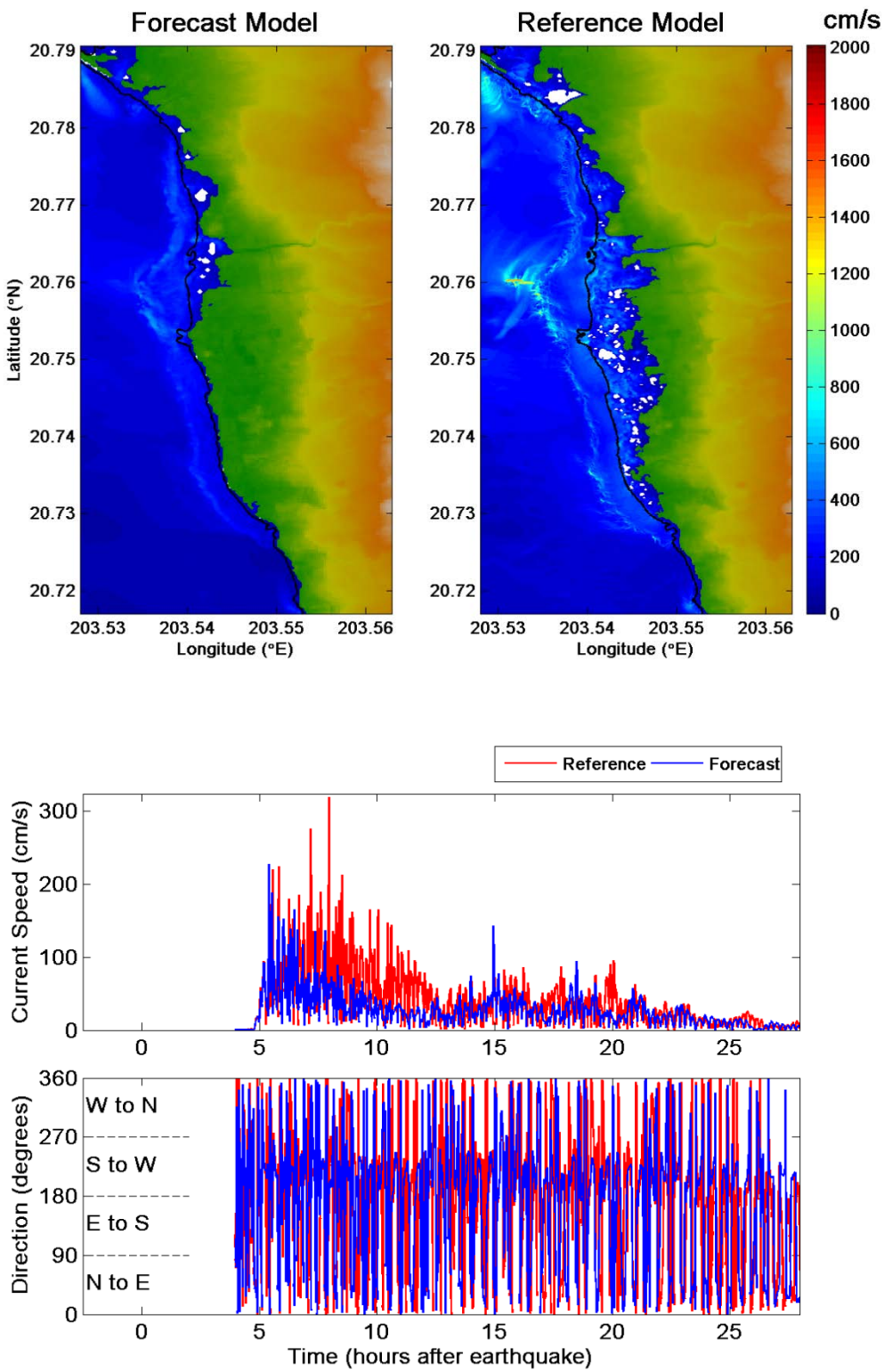

Figure 183. Comparative plot of maximum current distribution, current speed and directionality at the warning point at C-grid level for synthetic case AC11-20 between forecast and reference models. White areas on land for the top figure indicate non-inundated sections.

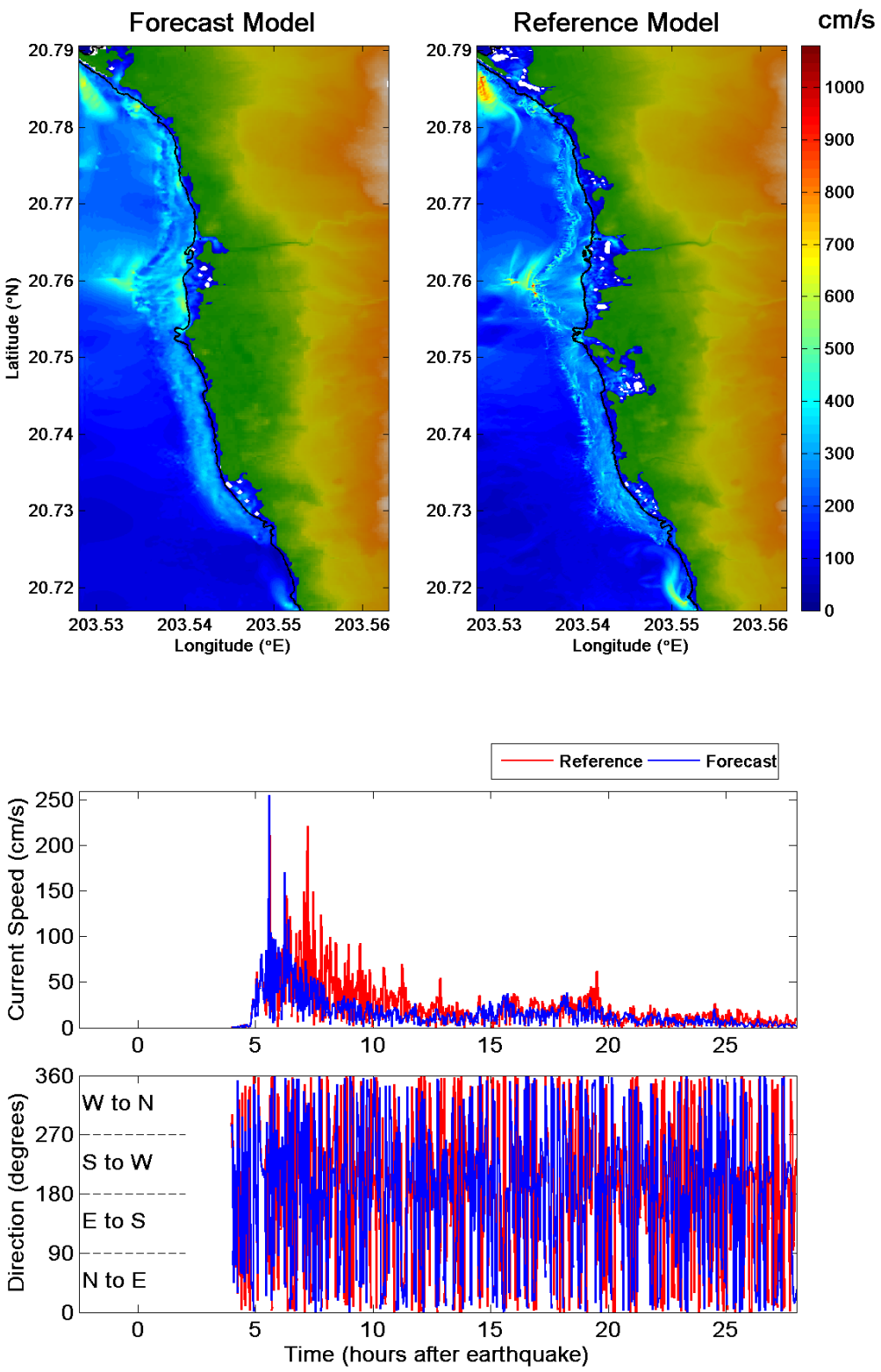

Figure 184. Plot of maximum tsunami wave amplitude distribution for Grids A, B and C and tsunami time series at the warning point for synthetic case AC21-30 between forecast and reference models. White areas on land for the top figure indicate non-inundated sections.

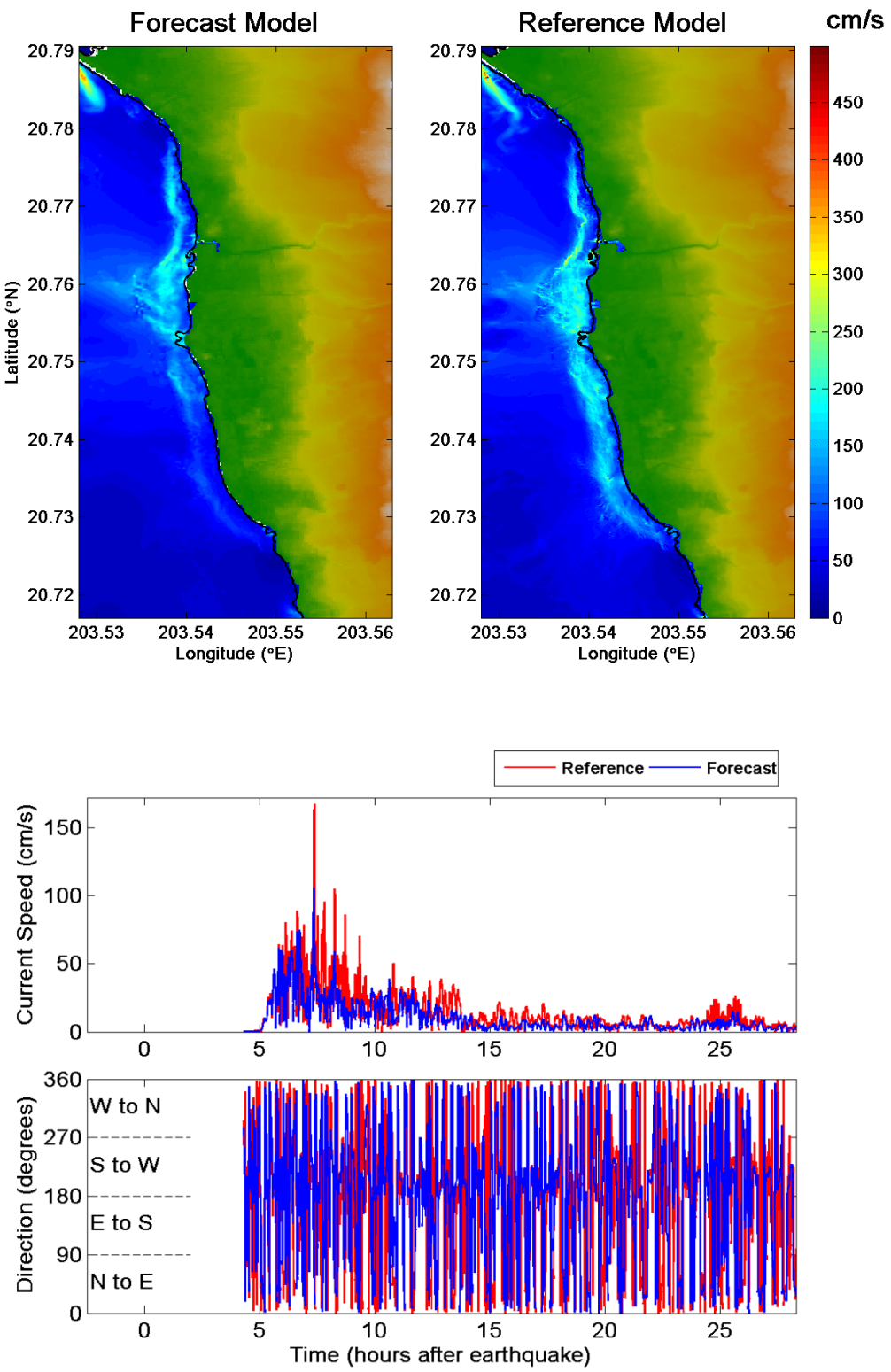

Figure 185. Comparative plot of maximum current distribution, current speed and directionality at the warning point at C-grid level for synthetic case AC31-40 between forecast and reference models.

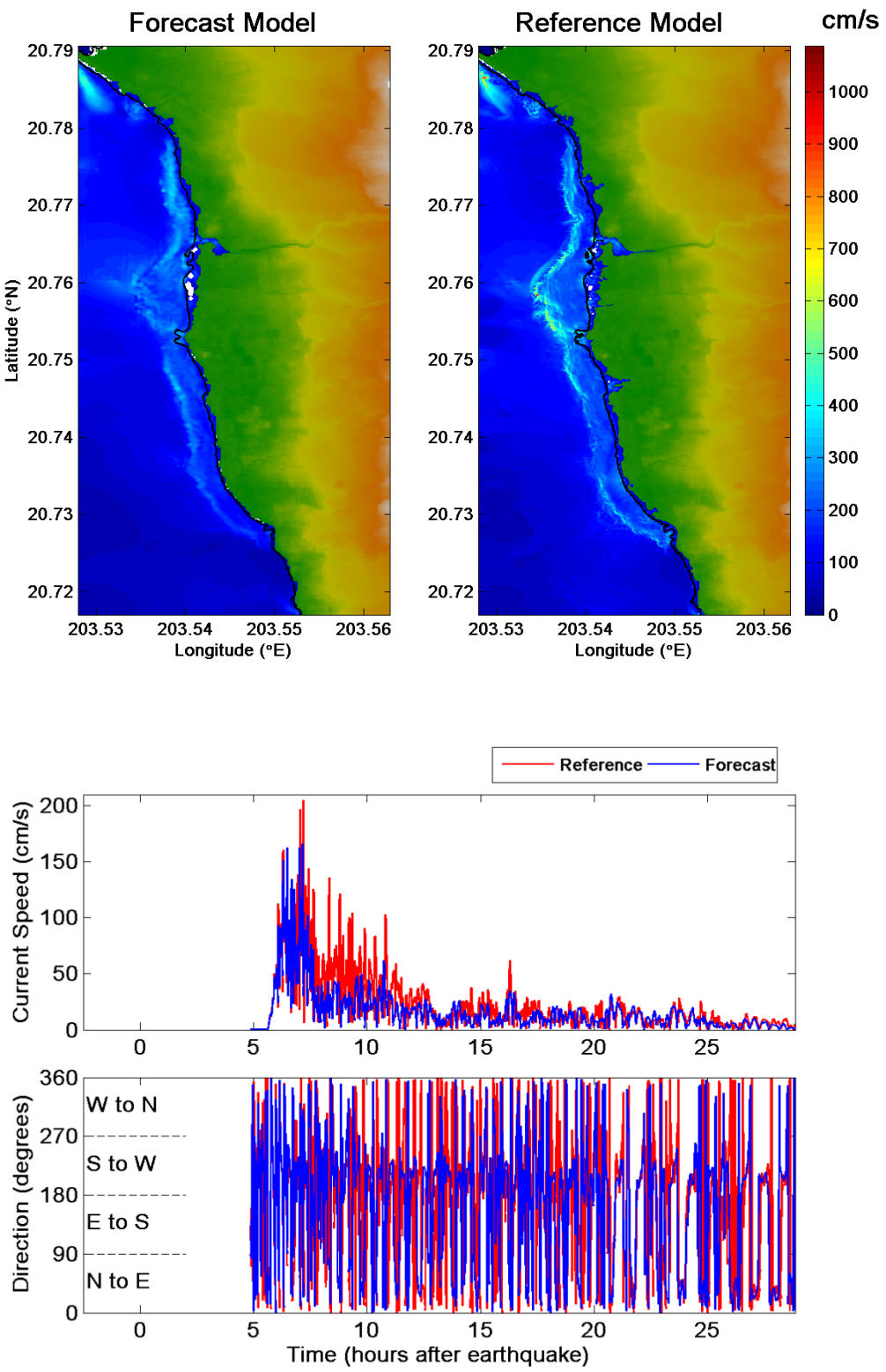

Figure 186. Comparative plot of maximum current distribution, current speed and directionality at the warning point at C-grid level for synthetic case AC41-50 between forecast and reference models. White areas on land for the top figure indicate non-inundated sections.

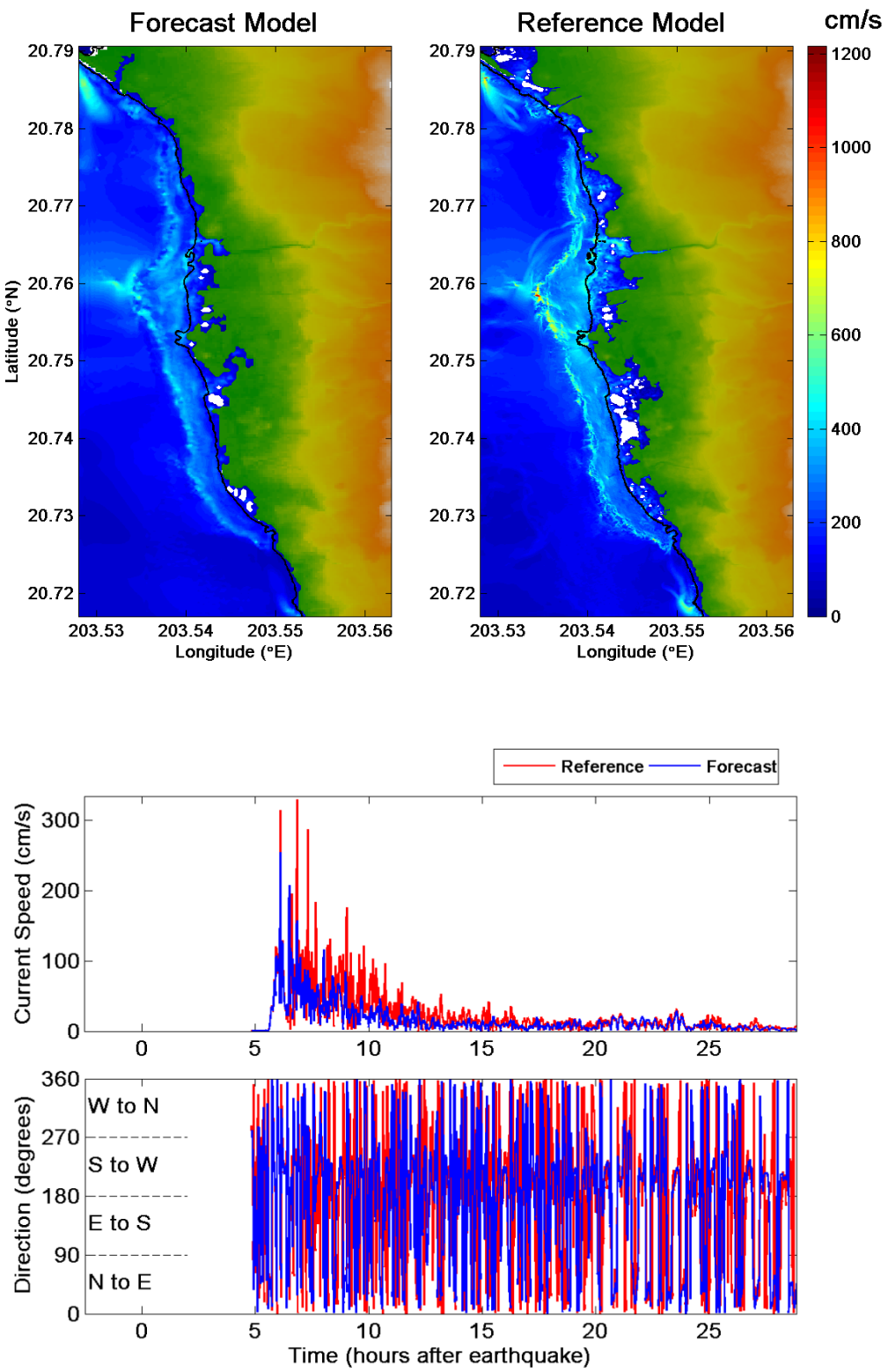

Figure 187. Comparative plot of maximum current distribution, current speed and directionality at the warning point at C-grid level for synthetic case AC46-55 between forecast and reference models. White areas on land for the top figure indicate non-inundated sections.

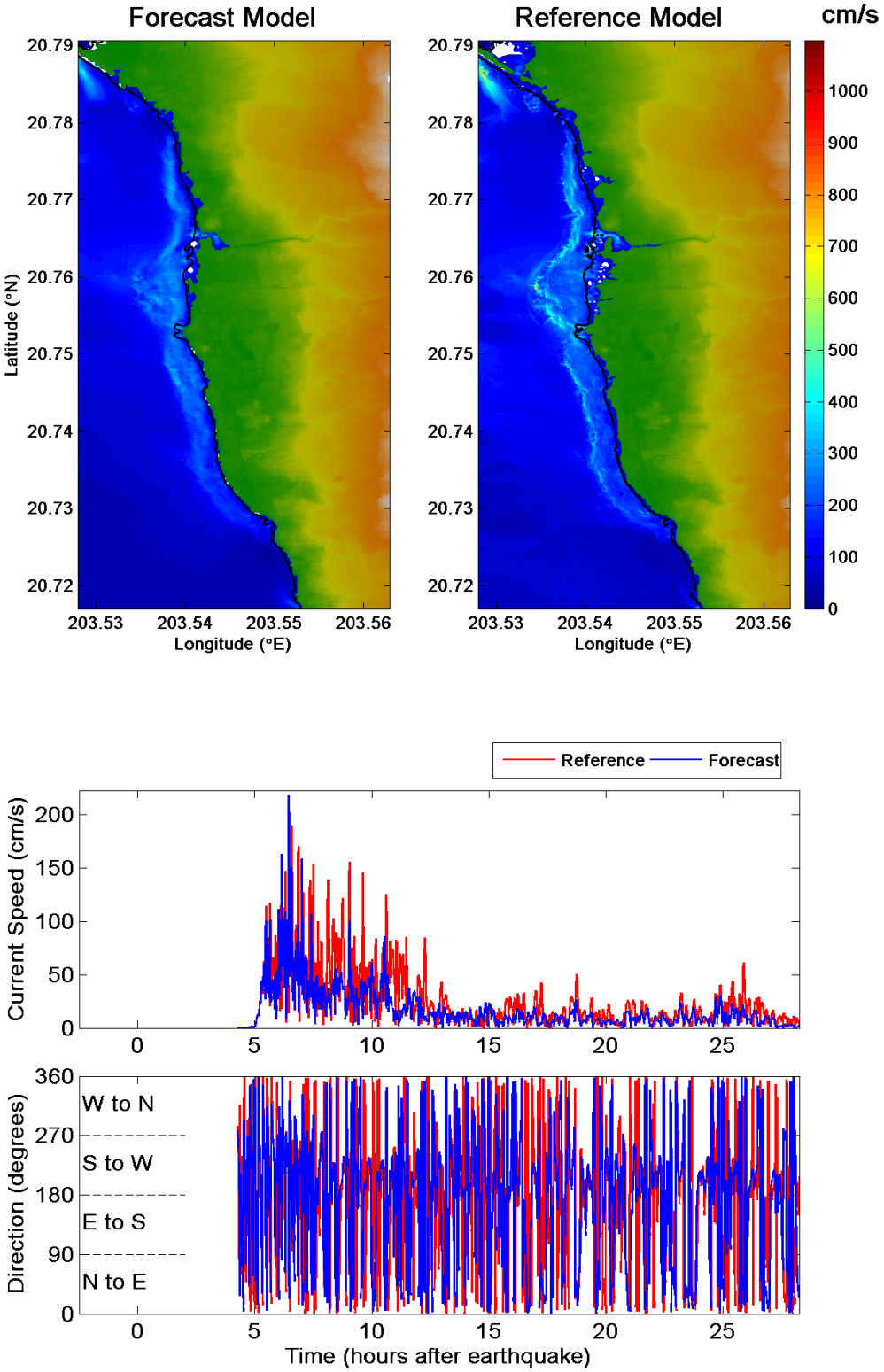

Figure 188. Comparative plot of maximum current distribution, current speed and directionality at the warning point at C-grid level for synthetic case AC56-65 between forecast and reference models. White areas on land for the top figure indicate non-inundated sections.

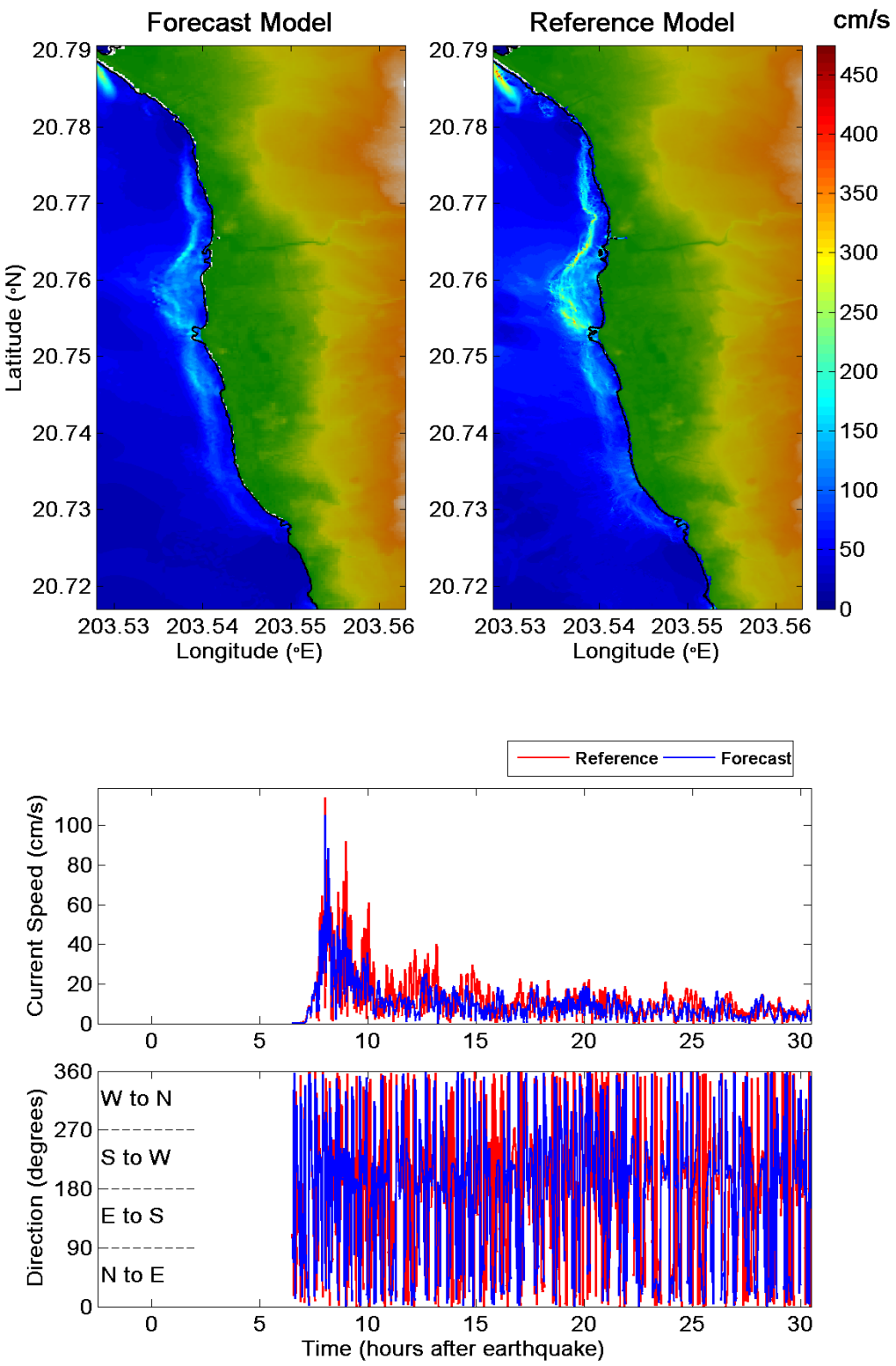

Figure 189. Comparative plot of maximum current distribution, current speed and directionality at the warning point at C-grid level for synthetic case CS01-10 between forecast and reference models.

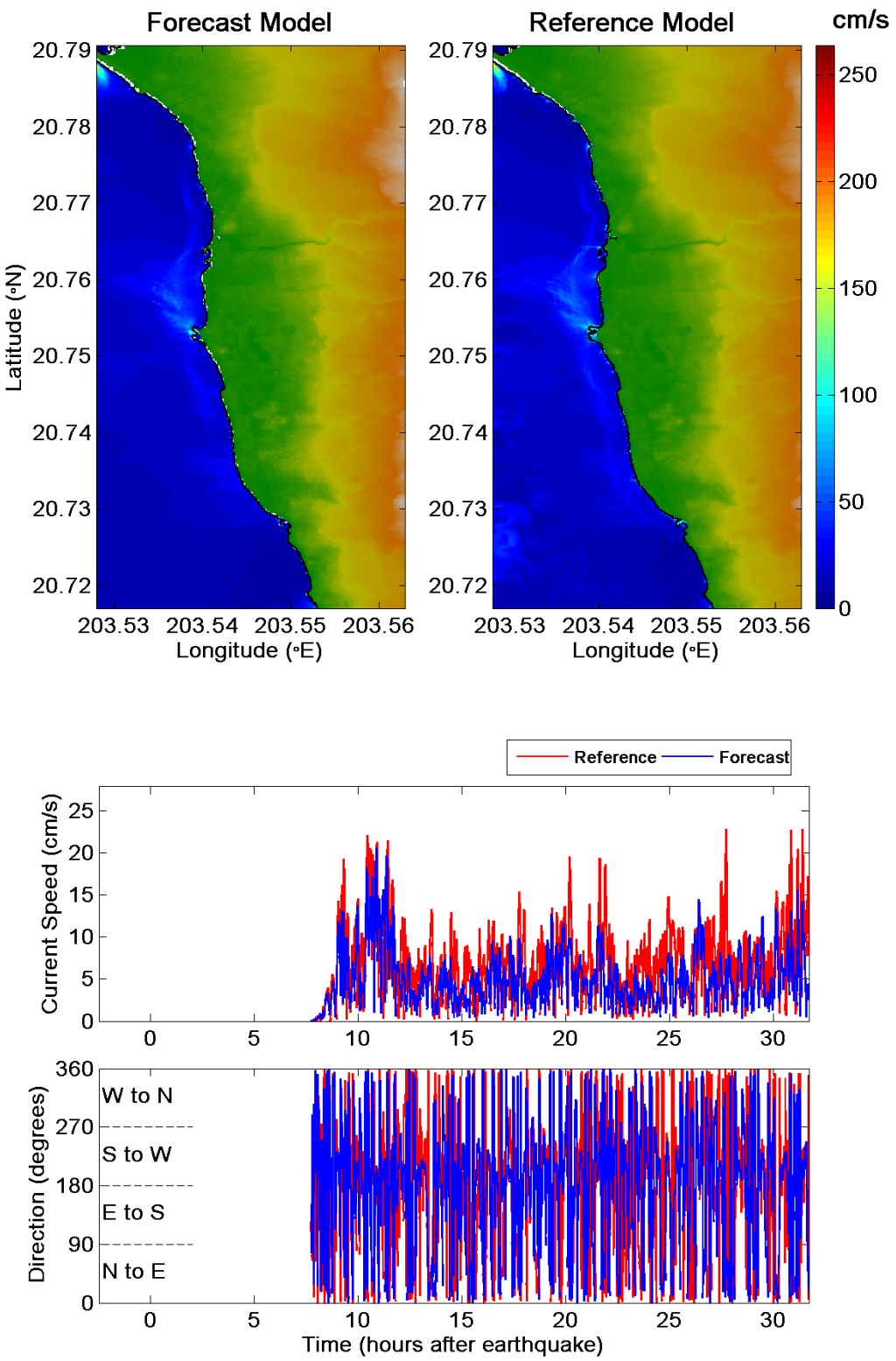

Figure 190. Comparative plot of maximum current distribution, current speed and directionality at the warning point at C-grid level for synthetic case CS11-20 between forecast and reference models.

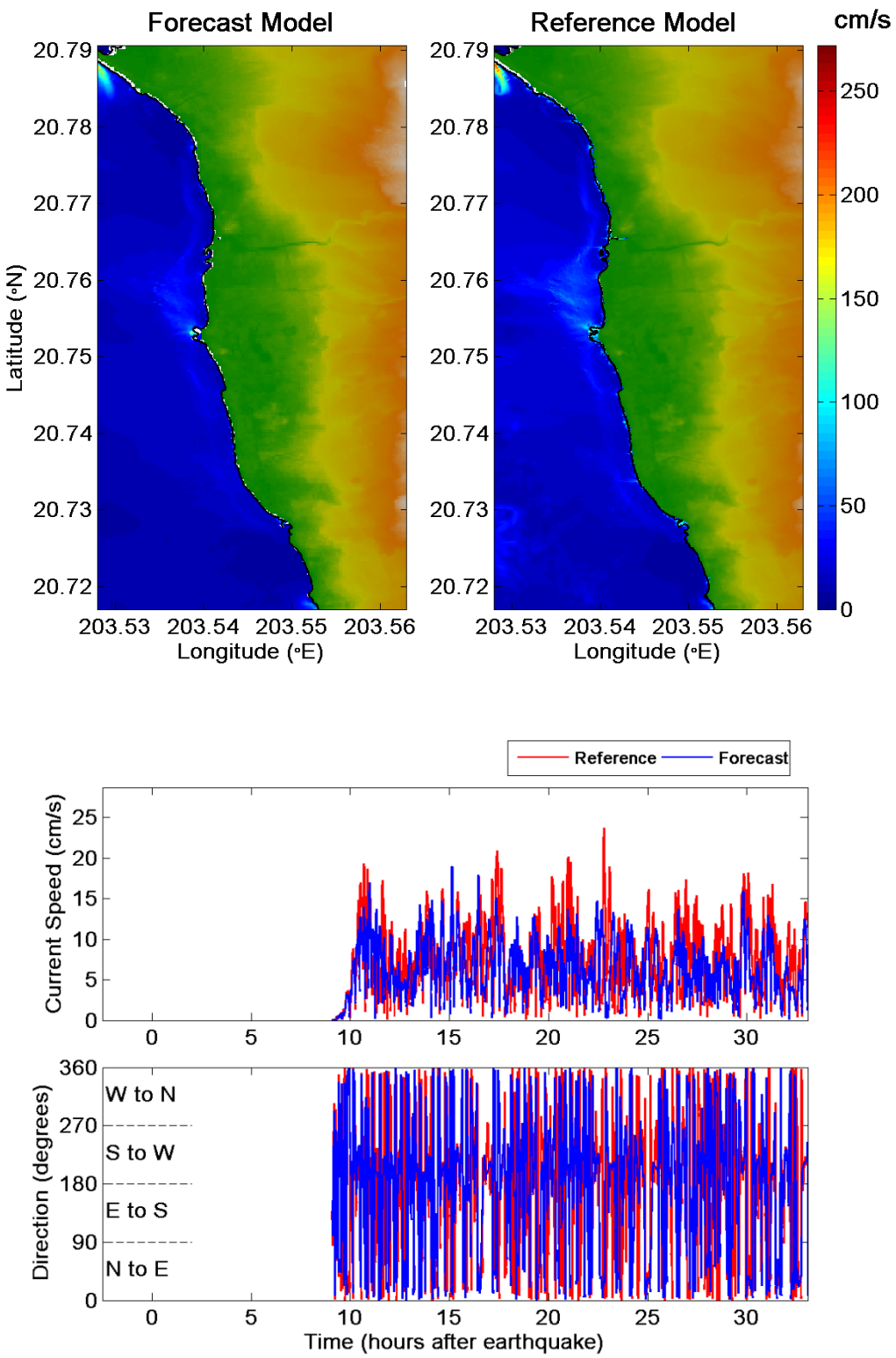

Figure 191. Comparative plot of maximum current distribution, current speed and directionality at the warning point at C-grid level for synthetic case CS21-30 between forecast and reference models.

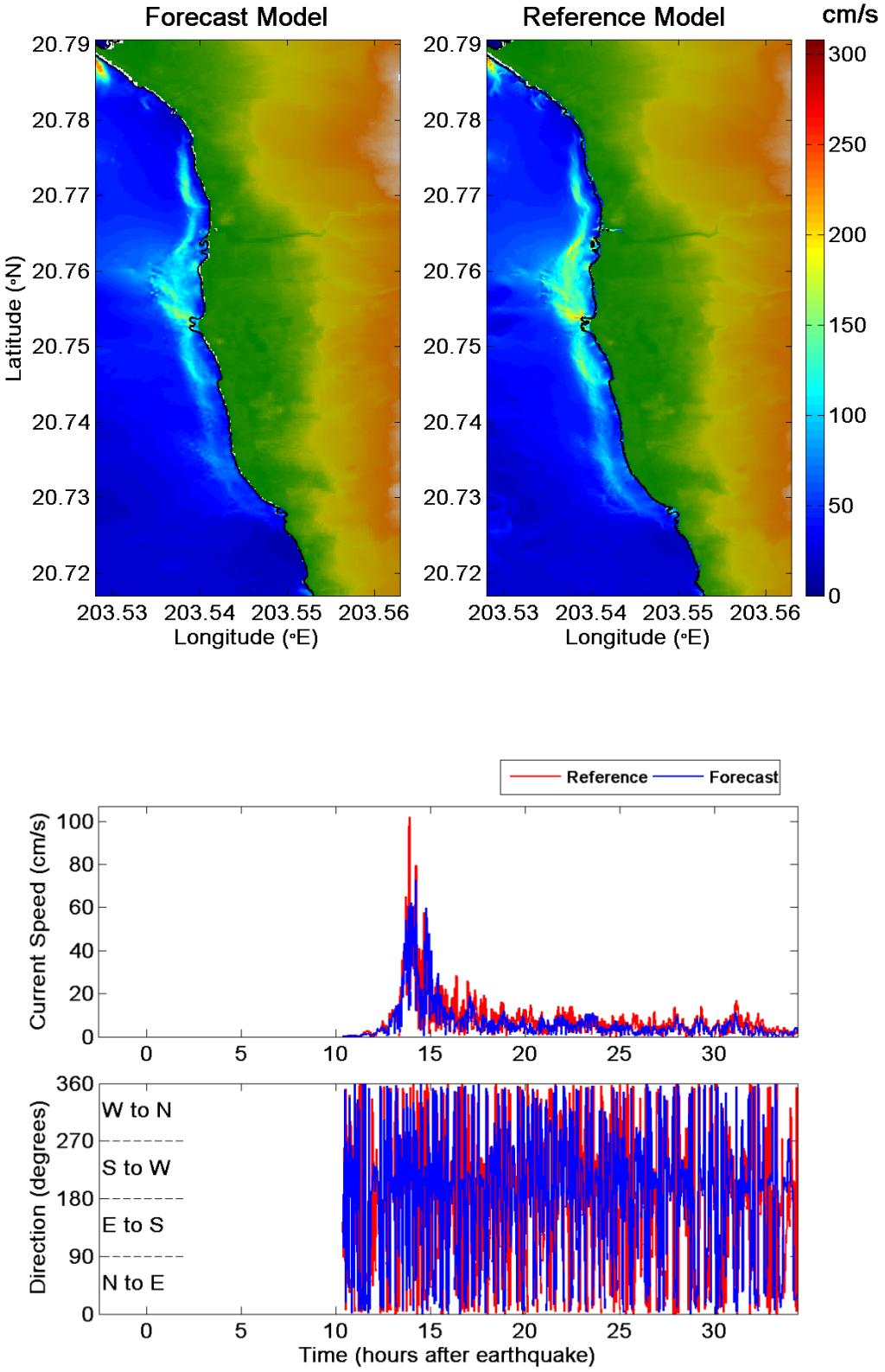

Figure 192. Comparative plot of maximum current distribution, current speed and directionality at the warning point at C-grid level for synthetic case CS31-40 between forecast and reference models.

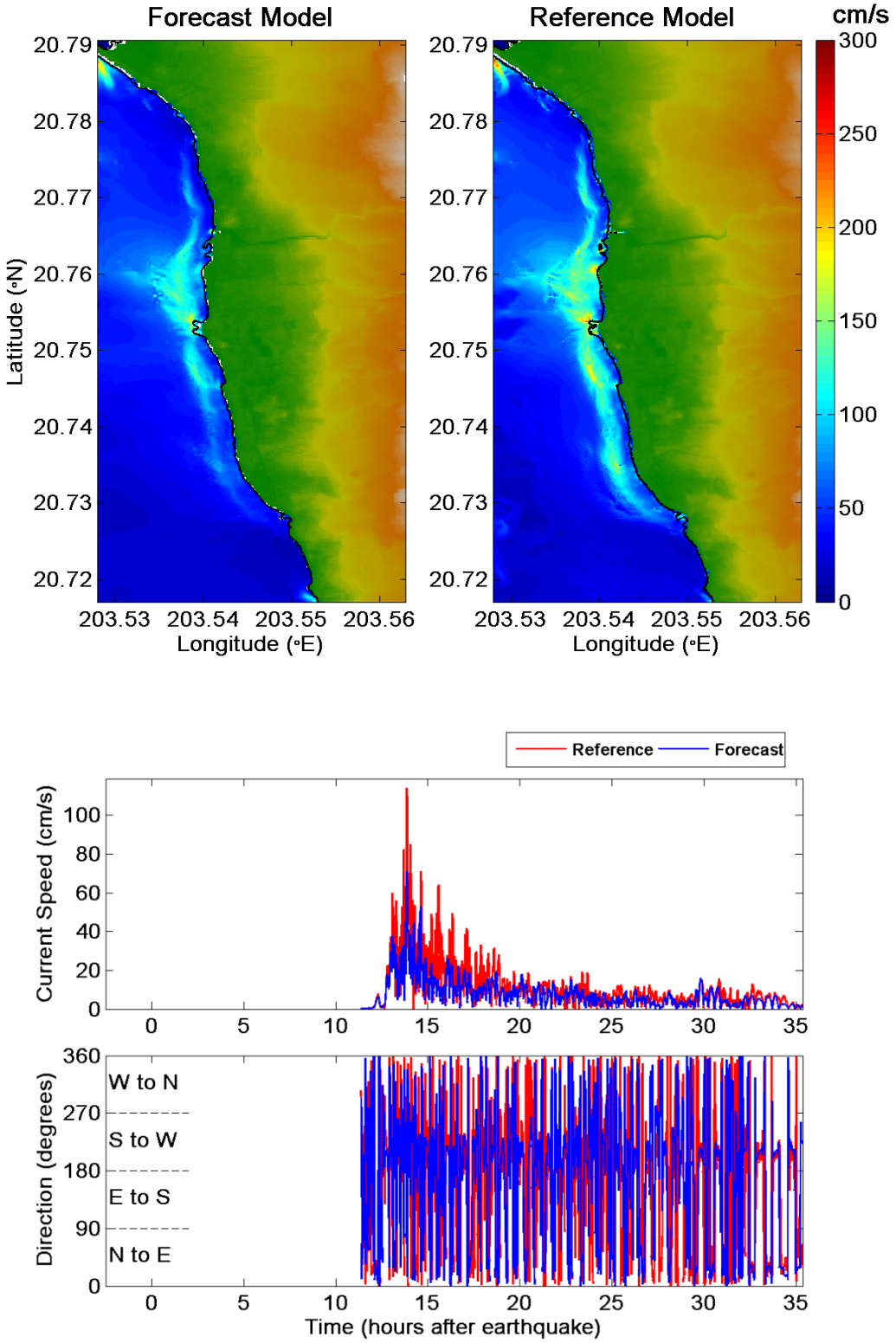

Figure 193. Comparative plot of maximum current distribution, current speed and directionality at the warning point at C-grid level for synthetic case CS41-50 between forecast and reference models.

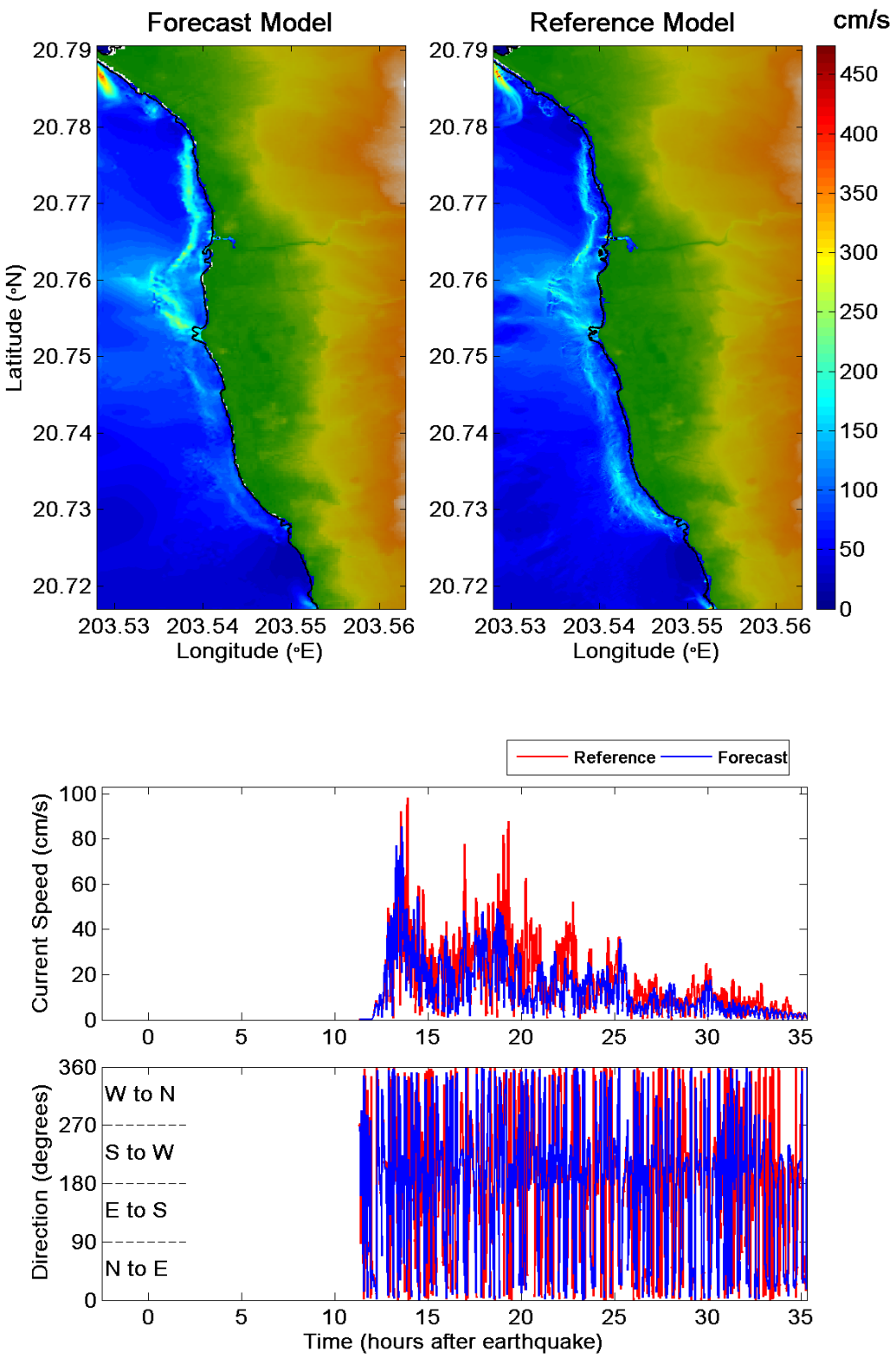

Figure 194. Comparative plot of maximum current distribution, current speed and directionality at the warning point at C-grid level for synthetic case CS51-60 between forecast and reference models.

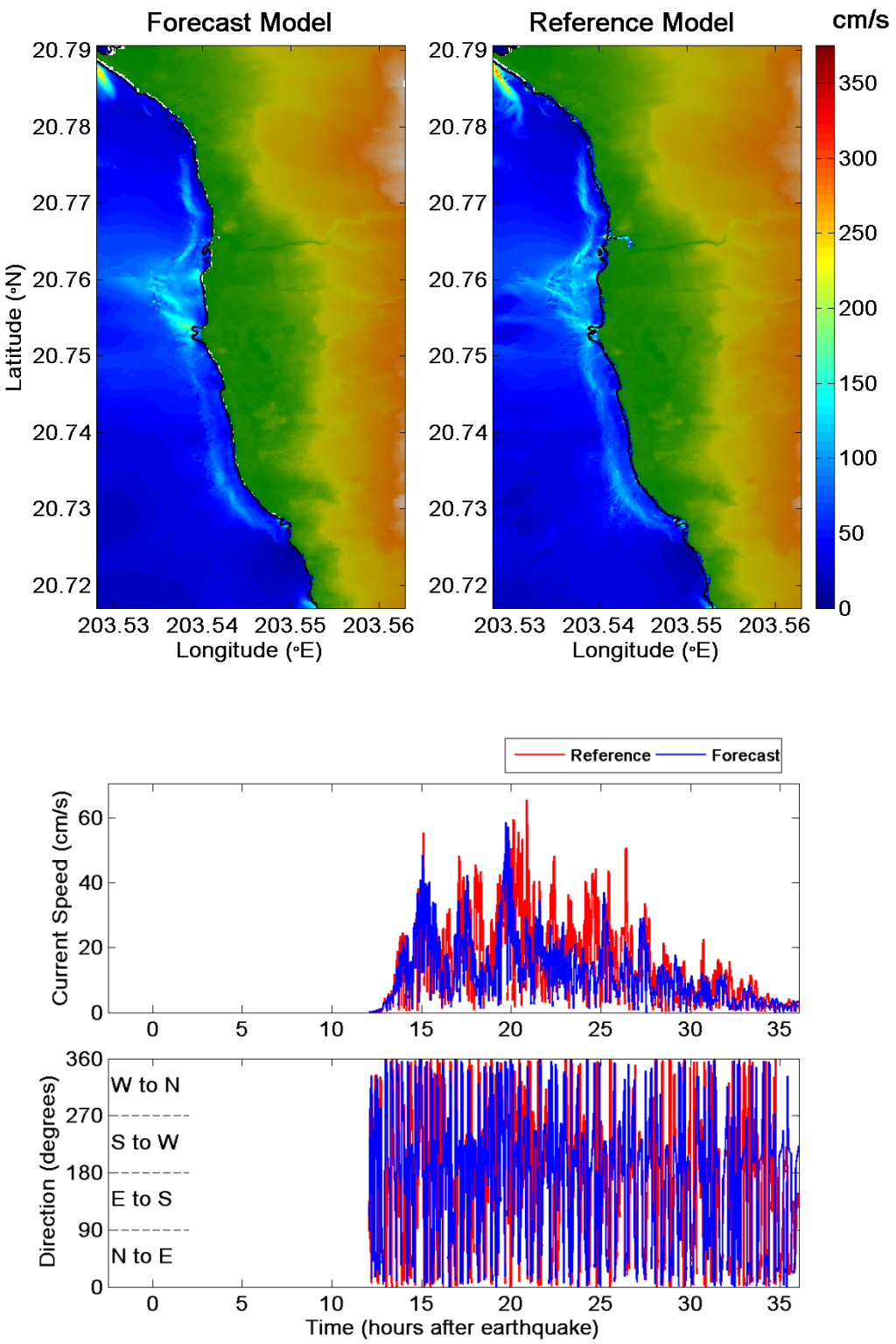

Figure 195. Comparative plot of maximum current distribution, current speed and directionality at the warning point at C-grid level for synthetic case CSSZ 61-70 between forecast and reference models.

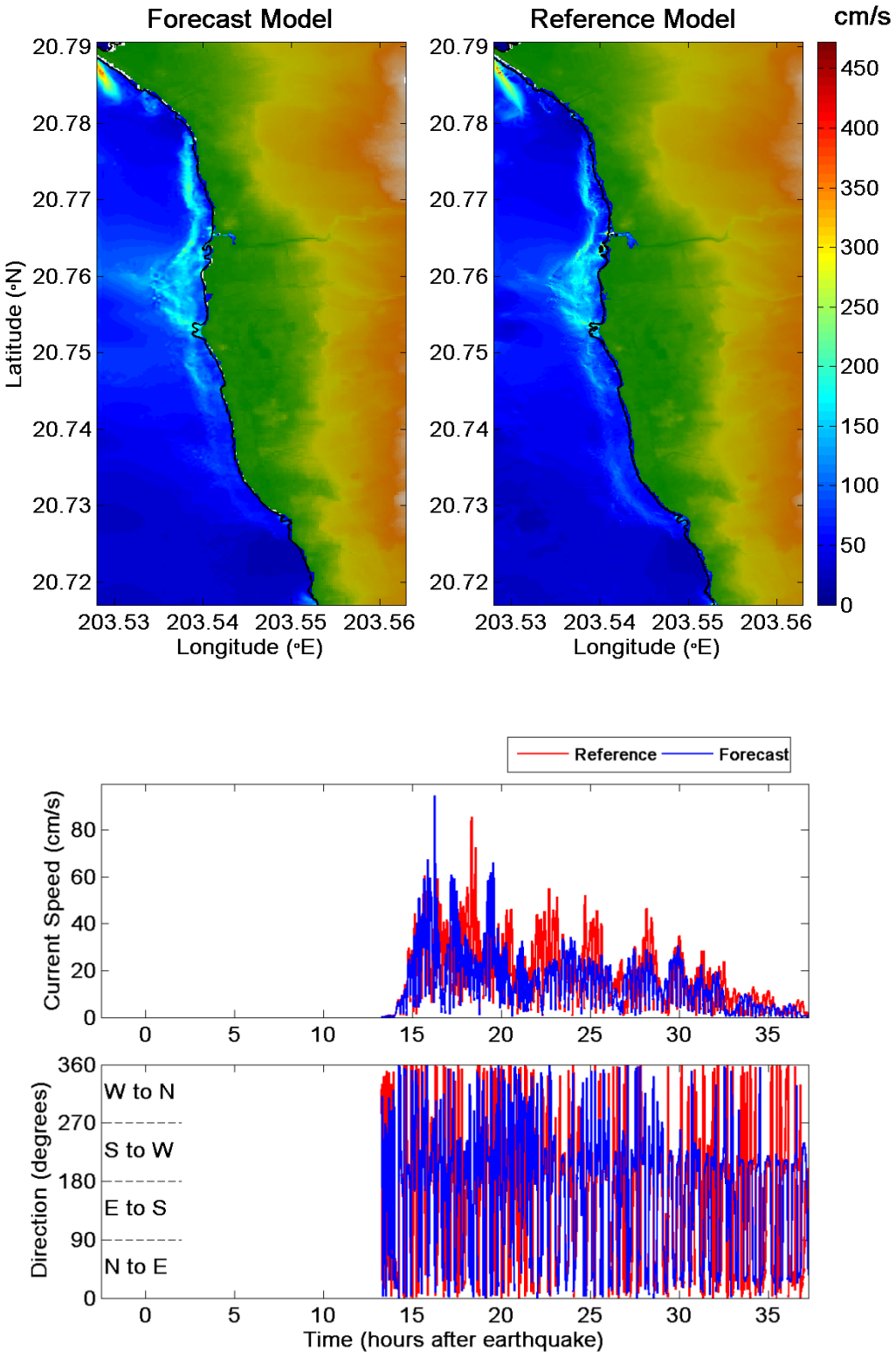

Figure 196. Comparative plot of maximum current distribution, current speed and directionality at the warning point at C-grid level for synthetic case CSSZ 71-80 between forecast and reference models.

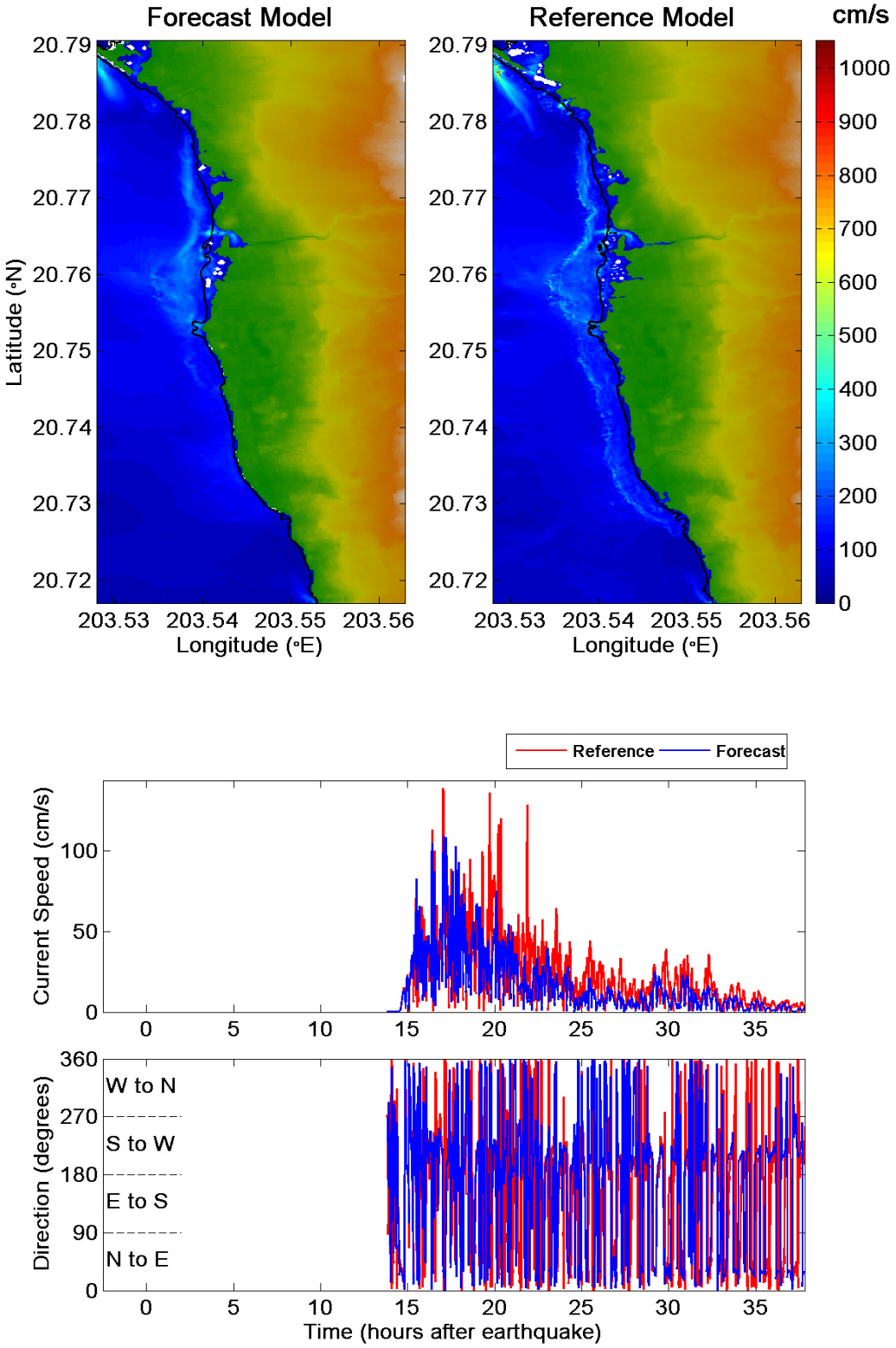

Figure 197. Comparative plot of maximum current distribution, current speed and directionality at the warning point at C-grid level for synthetic case CSSZ 81-90 between forecast and reference models. White areas on land for the top figure indicate non-inundated sections.

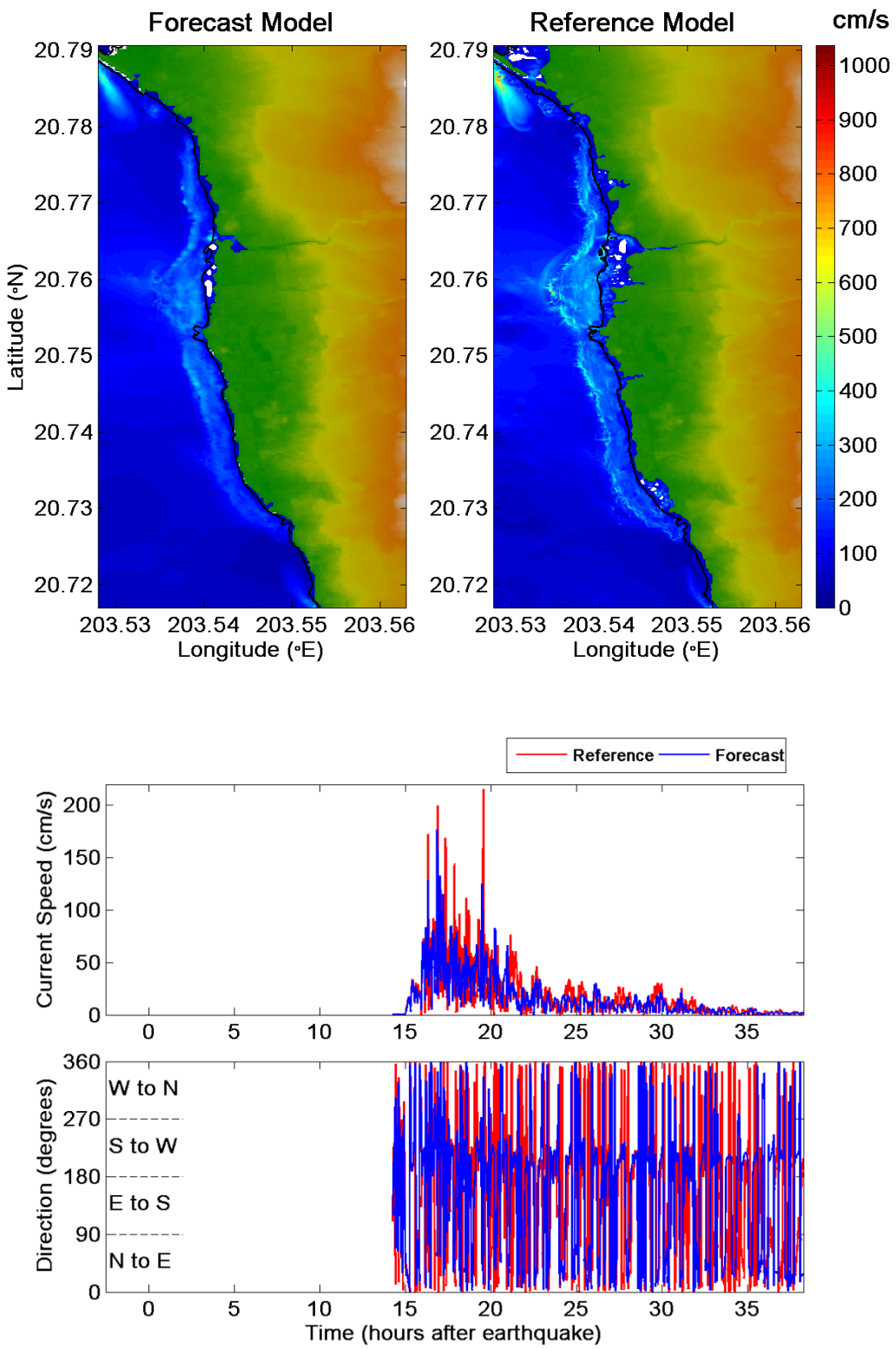

Figure 198. Comparative plot of maximum current distribution, current speed and directionality at the warning point at C-grid level for synthetic case CSSZ 91-100 between forecast and reference models. White areas on land for the top figure indicate non-inundated sections.

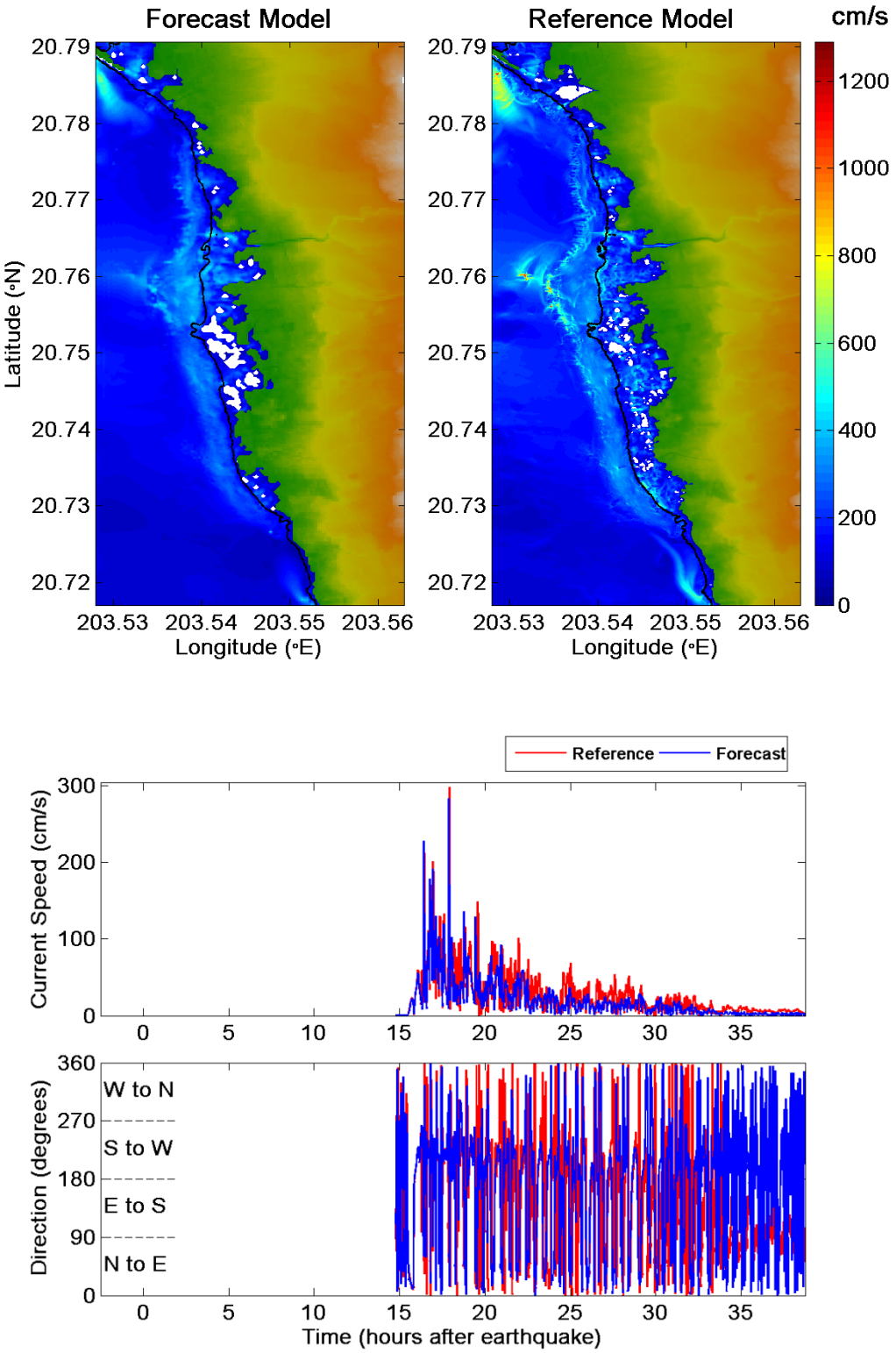

Figure 199. Comparative plot of maximum current distribution, current speed and directionality at the warning point at C-grid level for synthetic case CSSZ 101-110 between forecast and reference models. White areas on land for the top figure indicate non-inundated sections.

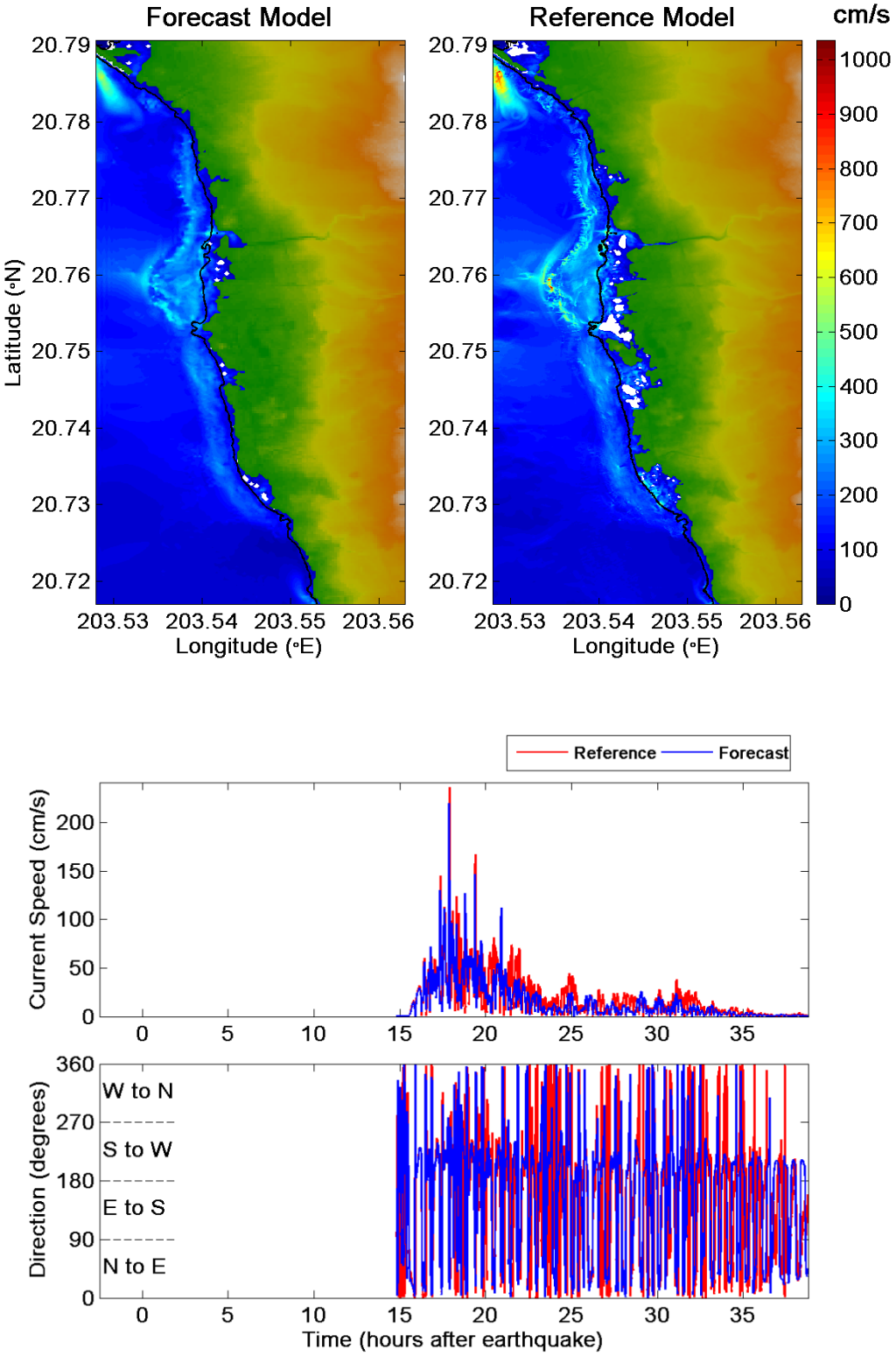

Figure 200. Comparative plot of maximum current distribution, current speed and directionality at the warning point at C-grid level for synthetic case CSSZ 106-115 between forecast and reference models. White areas on land for the top figure indicate non-inundated sections.

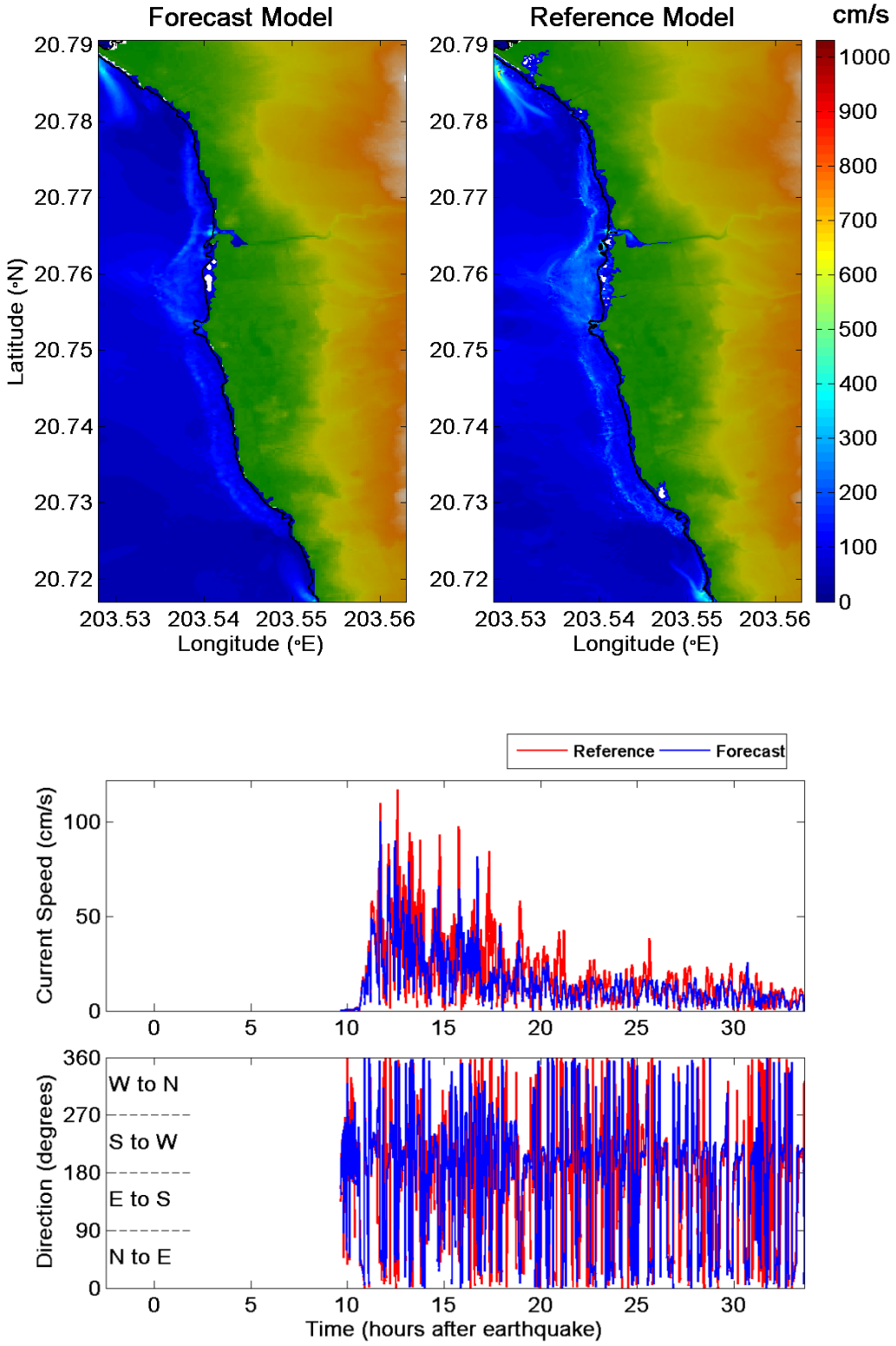

Figure 201. Comparative plot of maximum current distribution, current speed and directionality at the warning point at C-grid level point for synthetic case EPSZ 01-10 between forecast and reference models. White areas on land for the top figure indicate non-inundated sections.

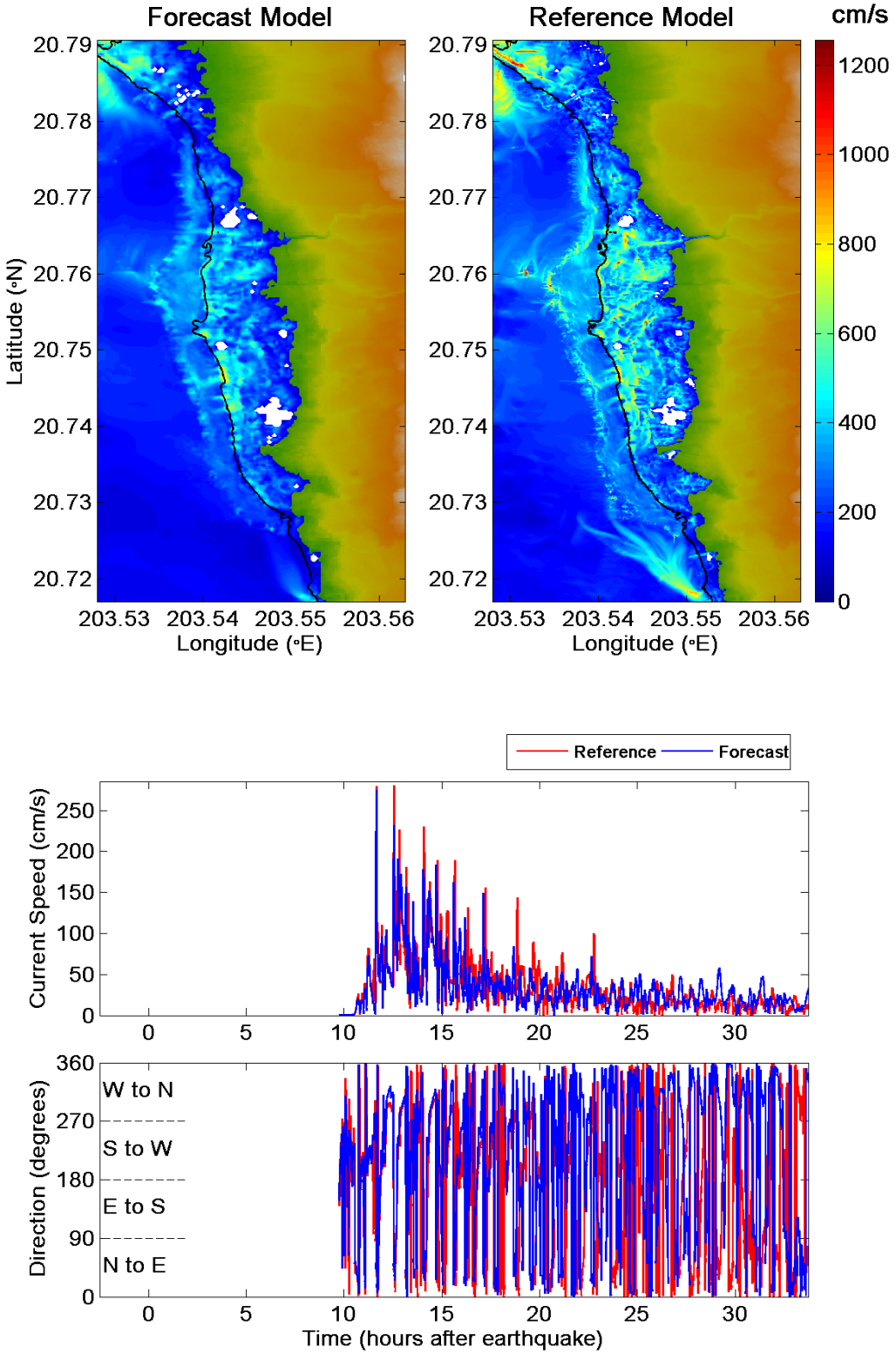

Figure 202. Comparative plot of maximum current distribution, current speed and directionality at the warning point at C-grid level for synthetic case EPSZ 09-18 between forecast and reference models.

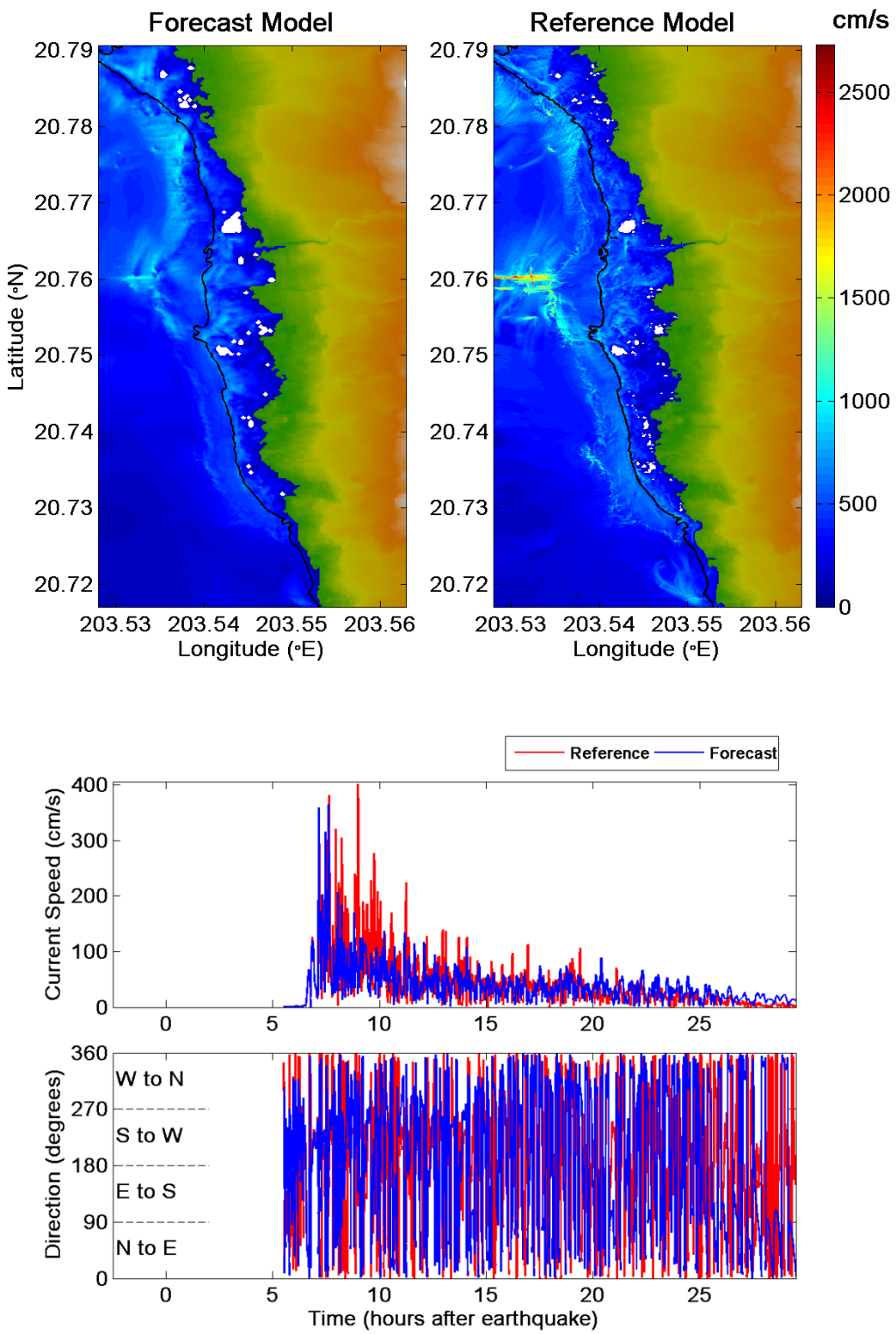

Figure 203. Comparative plot of maximum current distribution, current speed and directionality at the warning point at C-grid level for synthetic case KISZ 01-10 between forecast and reference models. White areas on land for the top figure indicate non-inundated sections.

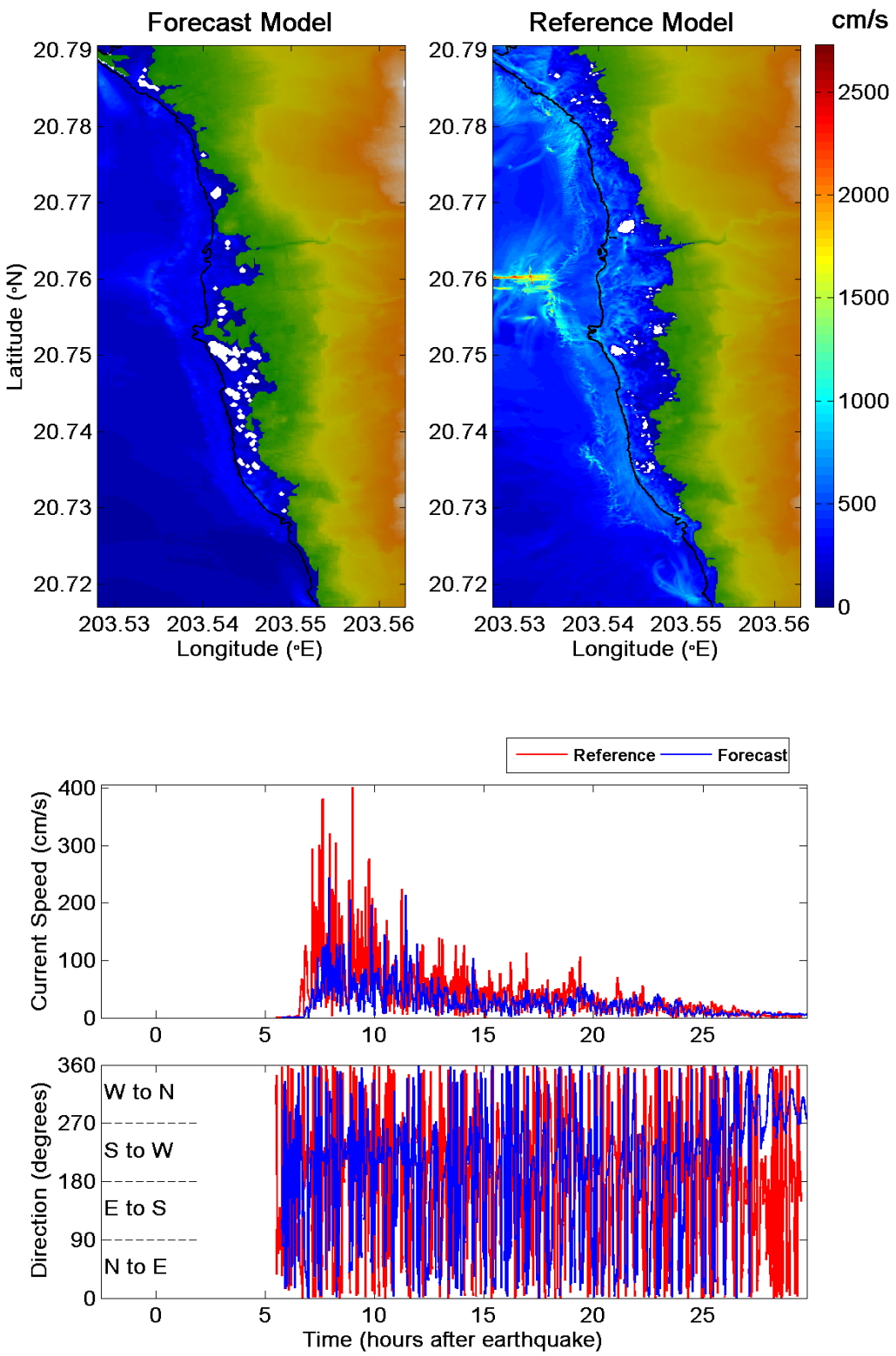

Figure 204. Comparative plot of maximum current distribution, current speed and directionality at the warning point at C-grid level for synthetic case KISZ 11-20 between forecast and reference models. White areas on land for the top figure indicate non-inundated sections.

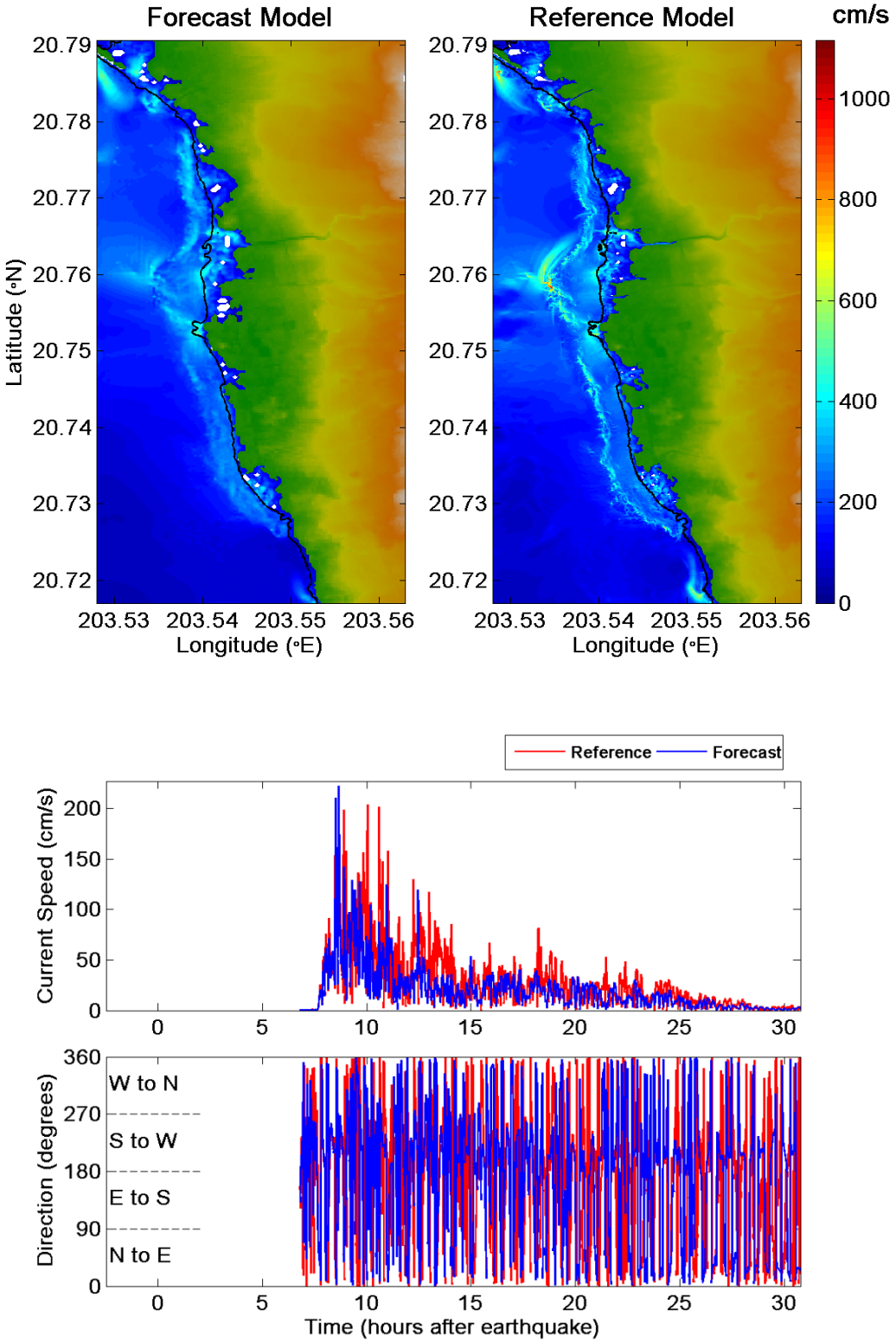

Figure 205. Comparative plot of maximum current distribution, current speed and directionality at the warning point at C-grid level for synthetic case KISZ 32-41 between forecast and reference models. White areas on land for the top figure indicate non-inundated sections.

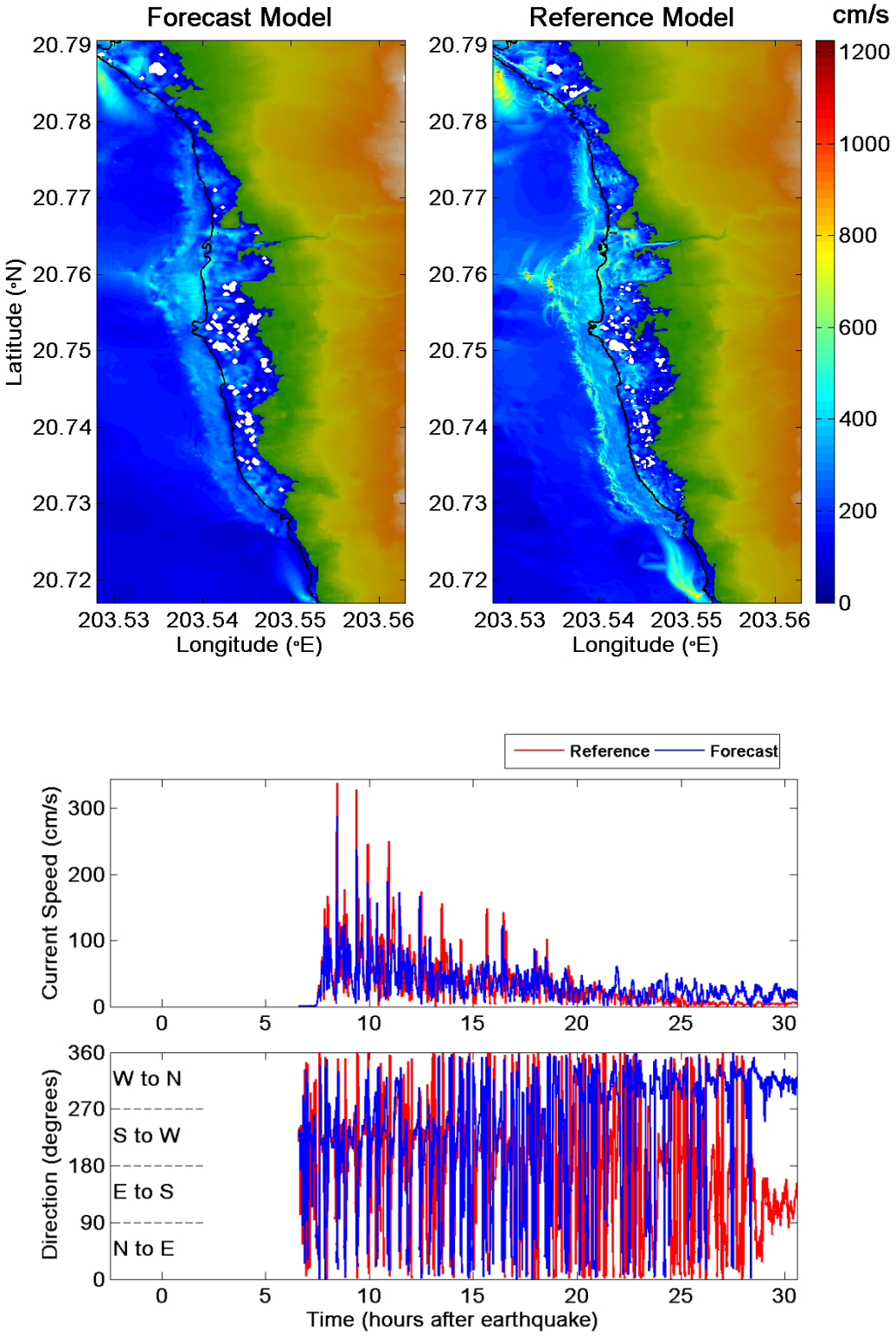

Figure 206. Comparative plot of maximum current distribution, current speed and directionality at the warning point at C-grid level for synthetic case KISZ421-51 between forecast and reference models. White areas on land for the top figures indicate non-inundated sections.

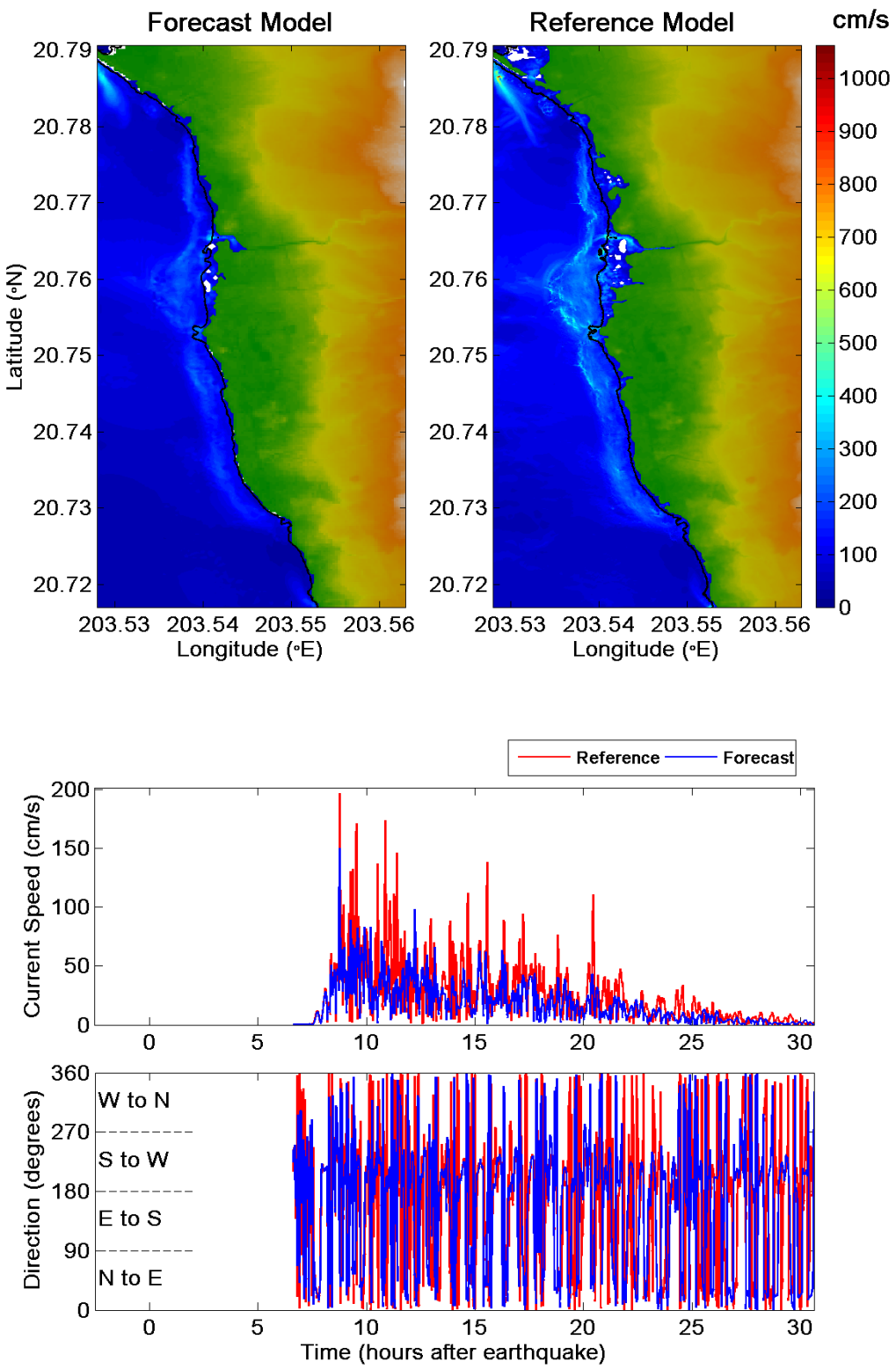

Figure 207. Comparative plot of maximum current distribution, current speed and directionality at the warning point at C-grid level for synthetic case KISZ52-61 between forecast and reference models. White areas on land for the top figure indicate non-inundated sections.

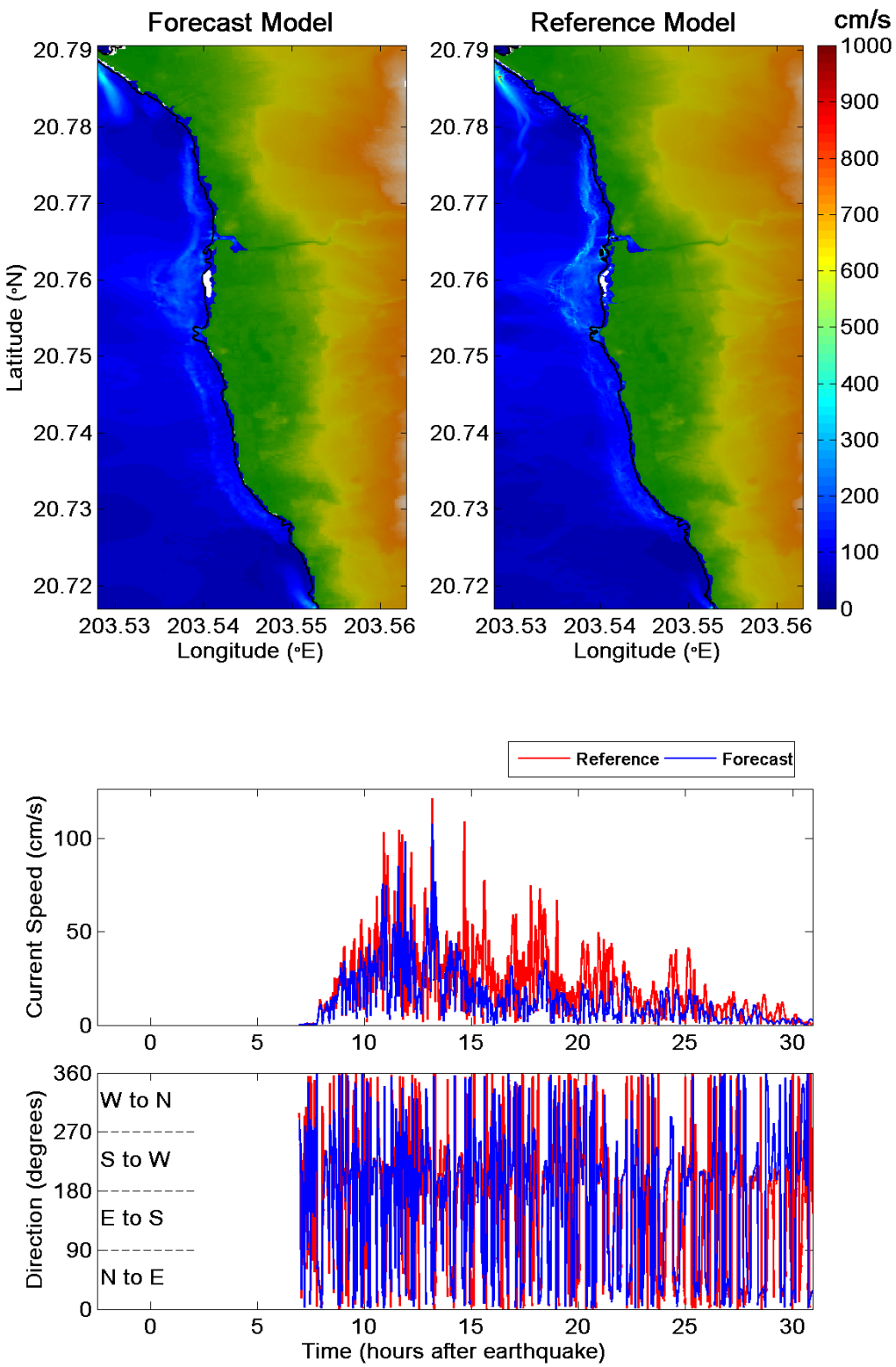

Figure 208. Comparative plot of maximum current distribution, current speed and directionality at the warning point at C-grid level t for synthetic case KISZ56-65 between forecast and reference models. White areas on land for the top figure indicate non-inundated sections.

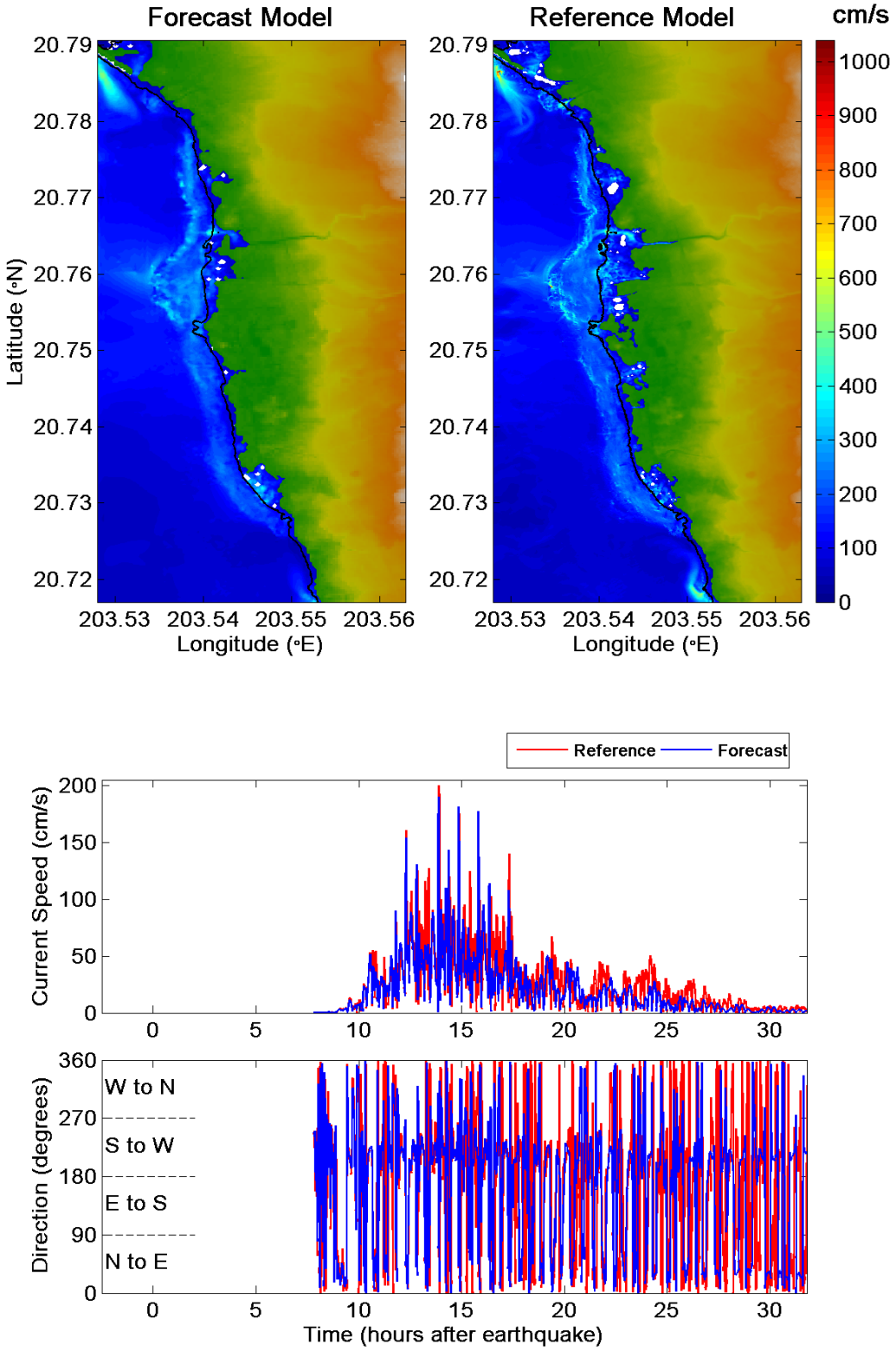

Figure 209. Comparative plot of maximum current distribution, current speed and directionality at the warning point at C-grid level for synthetic case KISZ66-75 between forecast and reference models. White areas on land for the top figure indicate non-inundated sections.

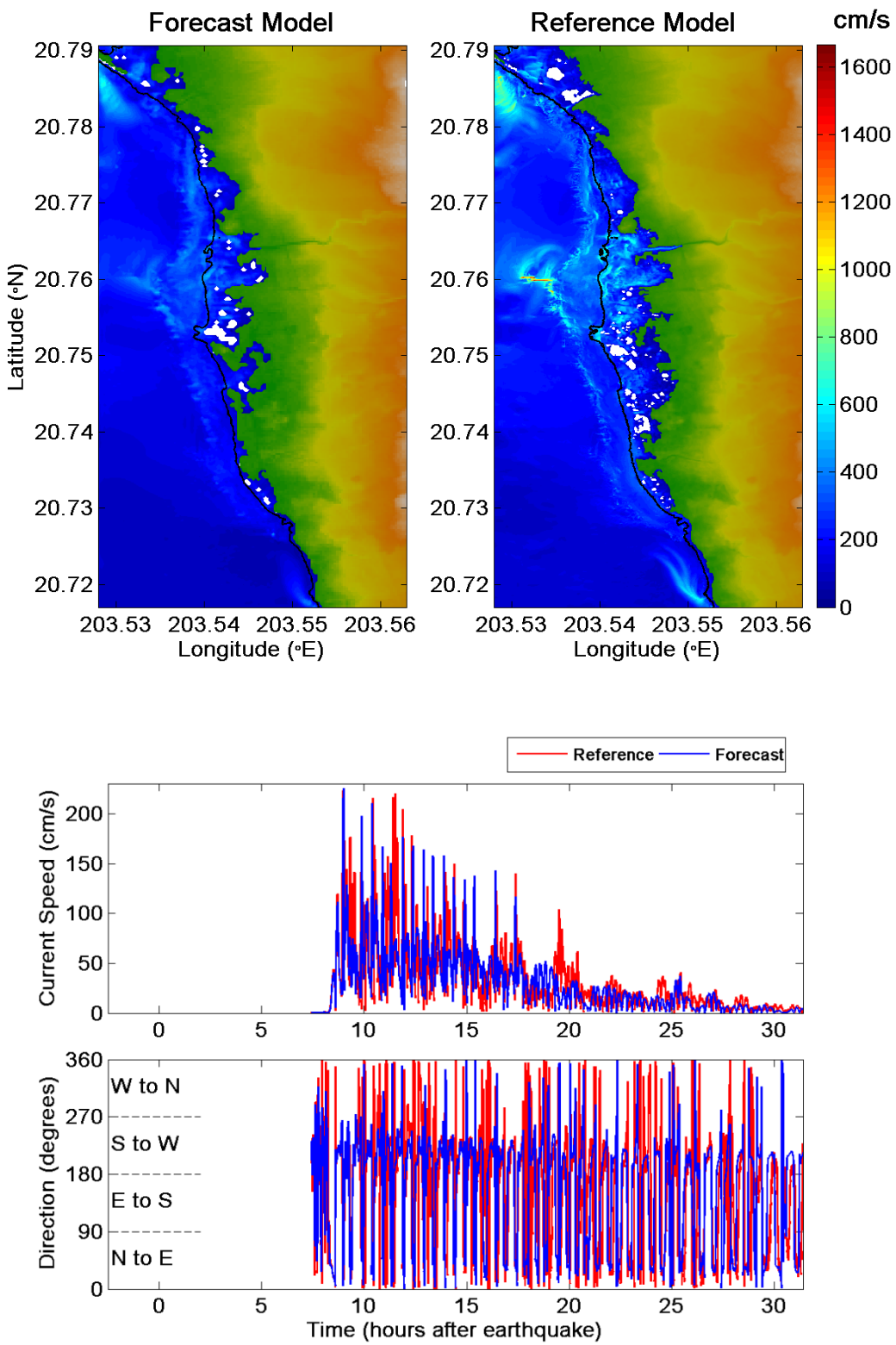

Figure 210. Comparative plot of maximum current distribution, current speed and directionality at the warning point at C-grid level for synthetic case MOSZ01-10 between forecast and reference models. White areas on land for the top figure indicate non-inundated sections.

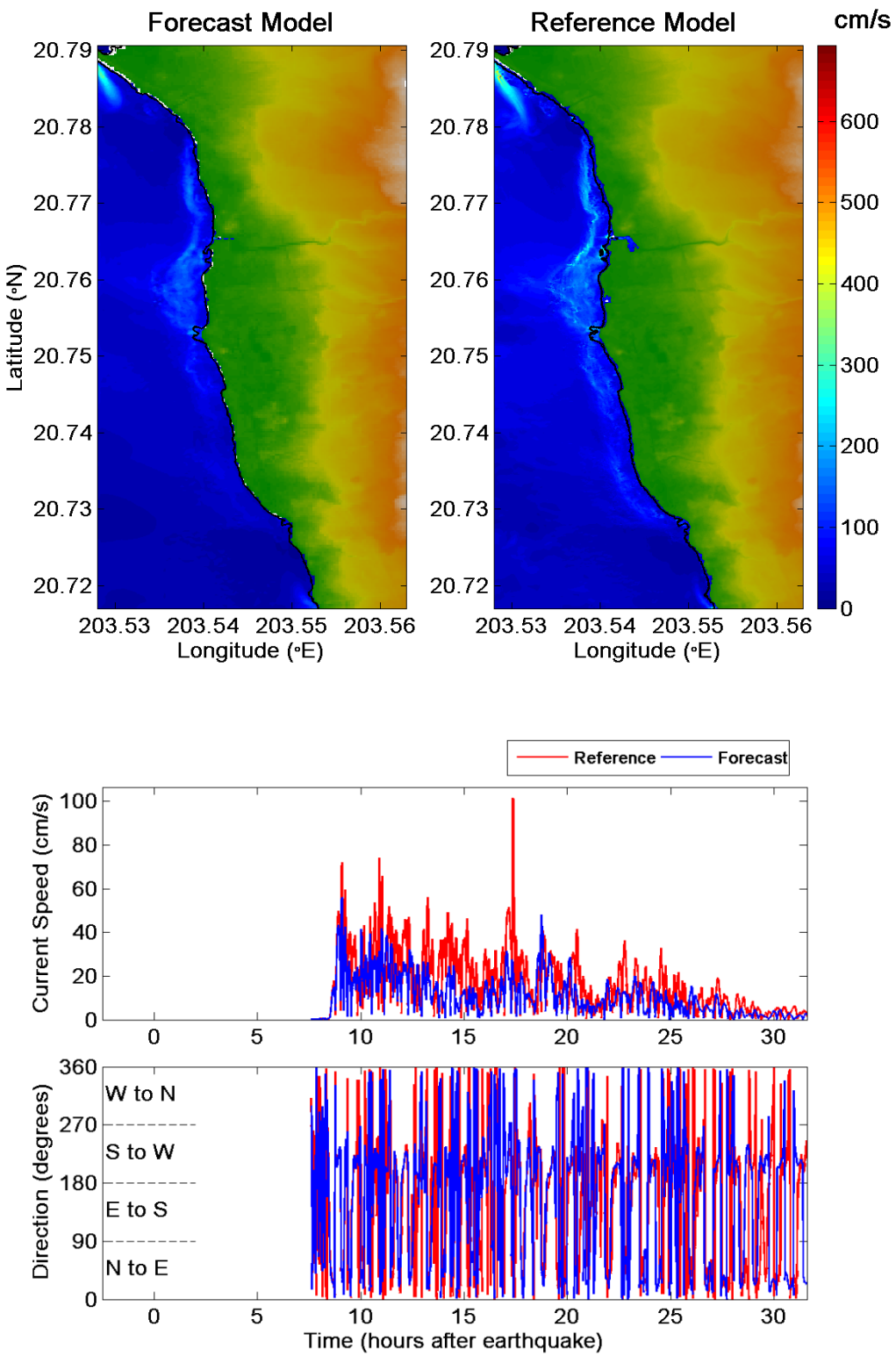

Figure 211. Comparative plot of maximum current distribution, current speed and directionality at the warning point at C-grid level for synthetic case MOSZ08-17 between forecast and reference models.

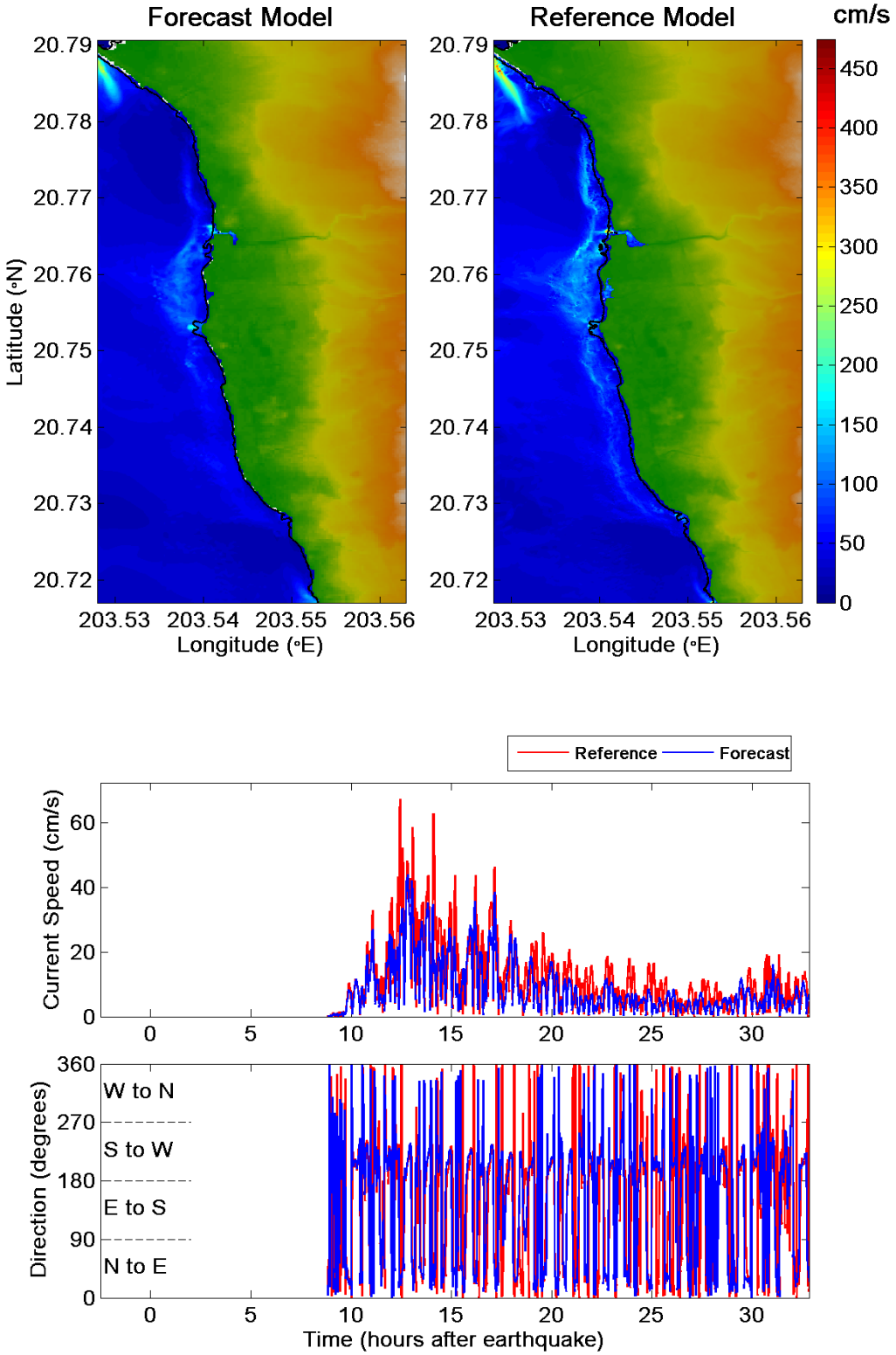

Figure 212. Comparative plot of maximum current distribution, current speed and directionality at the warning point at C-grid level for synthetic case NGSZ01-10 between forecast and reference models.

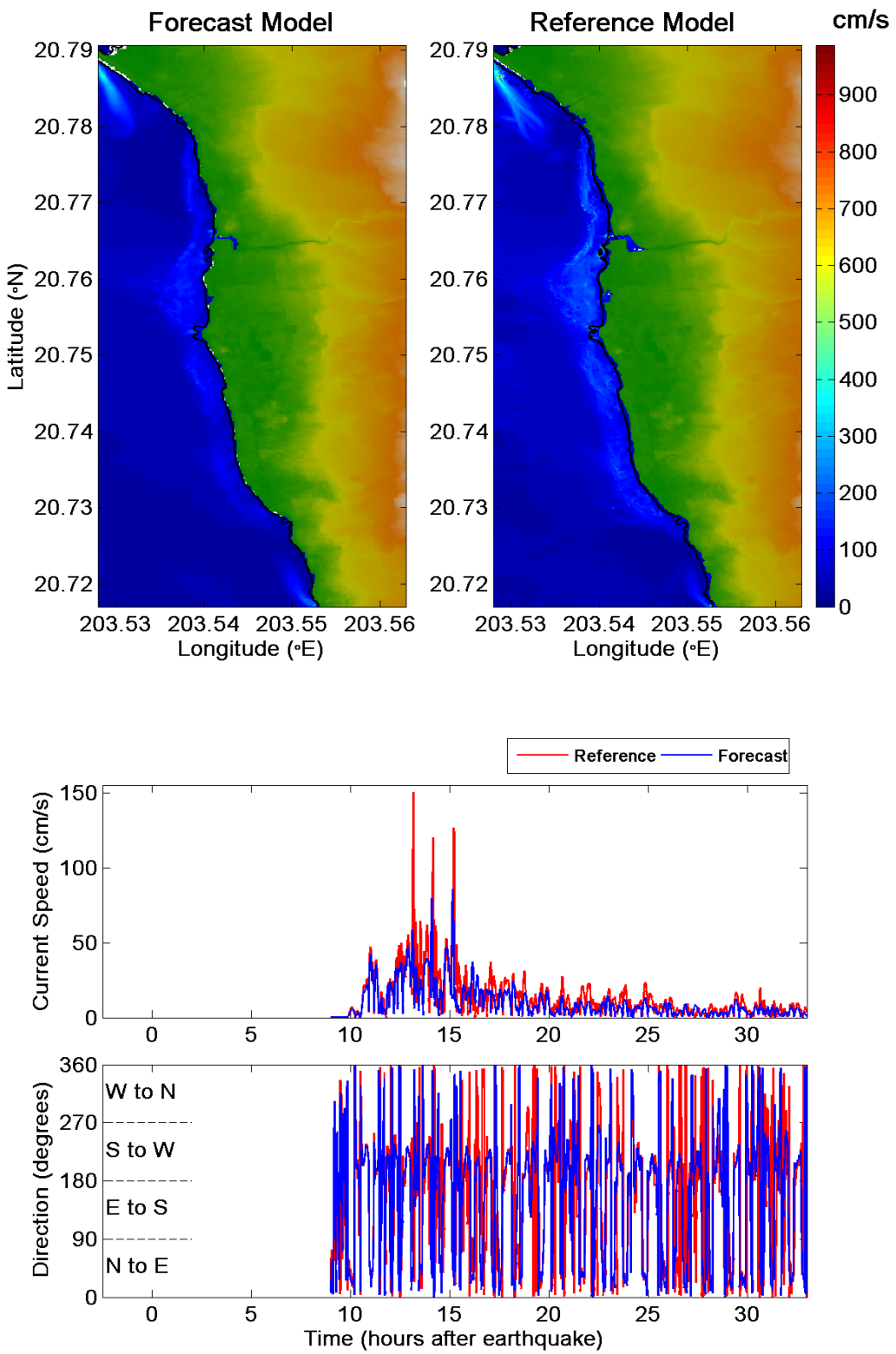

Figure 213. Comparative plot of maximum current distribution, current speed and directionality at the warning point at C-grid level for synthetic case NGSZ06-15 between forecast and reference models.

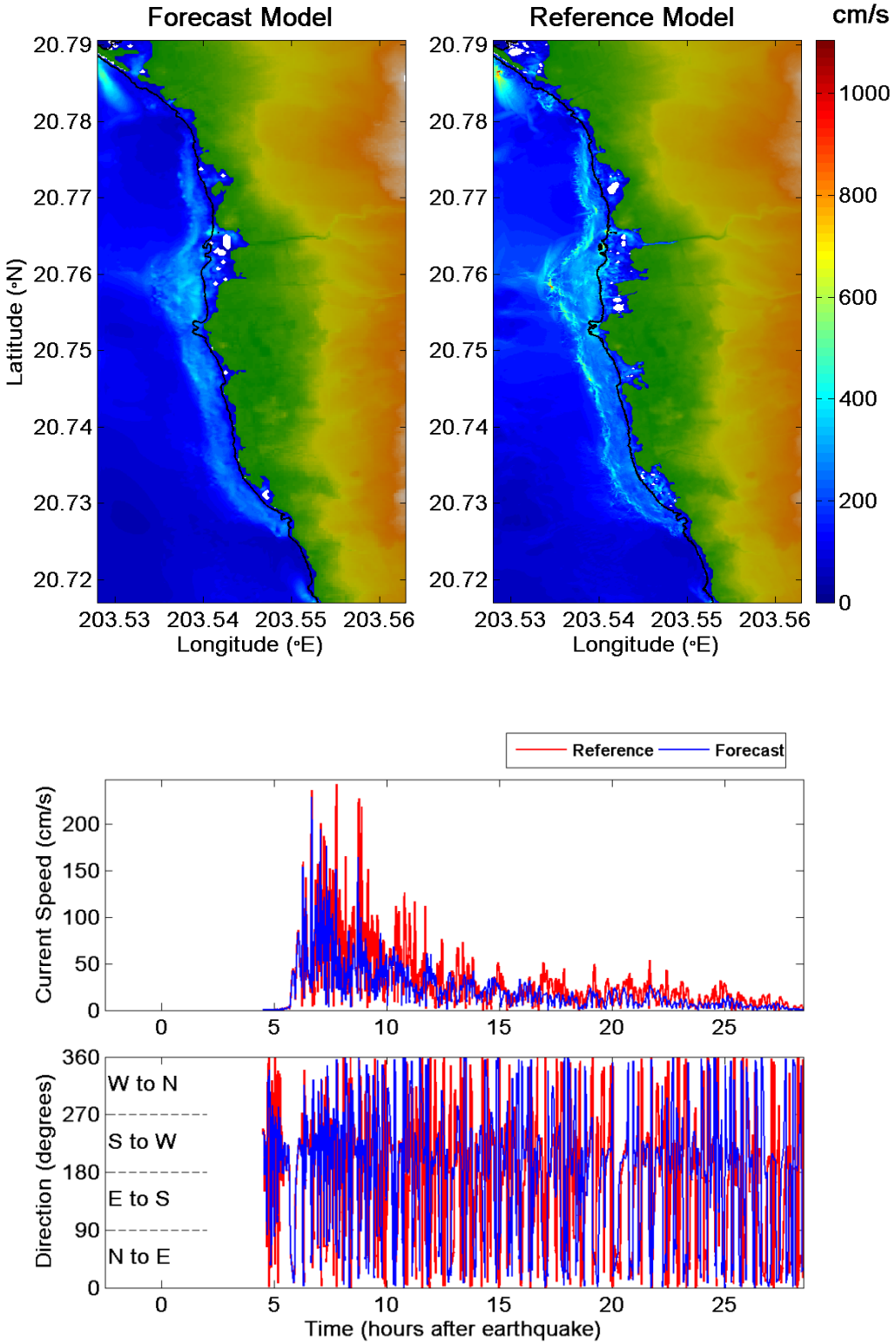

Figure 214. Comparative plot of maximum current distribution, current speed and directionality at the warning point at C-grid level for synthetic case NTSZ01-10 between forecast and reference models. White areas on land for the top figure indicate non-inundated sections.

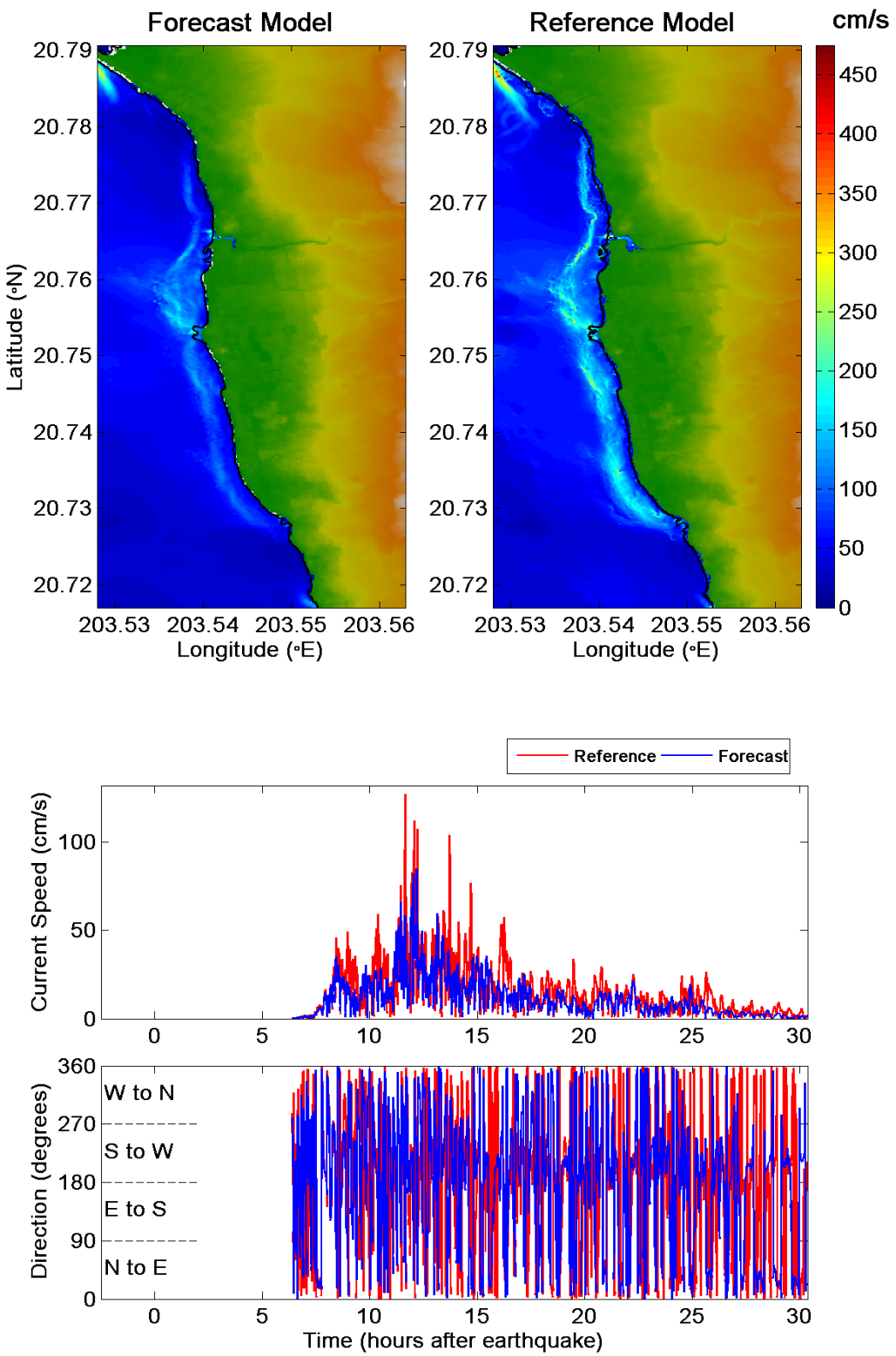

Figure 215. Comparative plot of maximum current distribution, current speed and directionality at the warning point at C-grid level for synthetic case NTSZ11-20 between forecast and reference models.

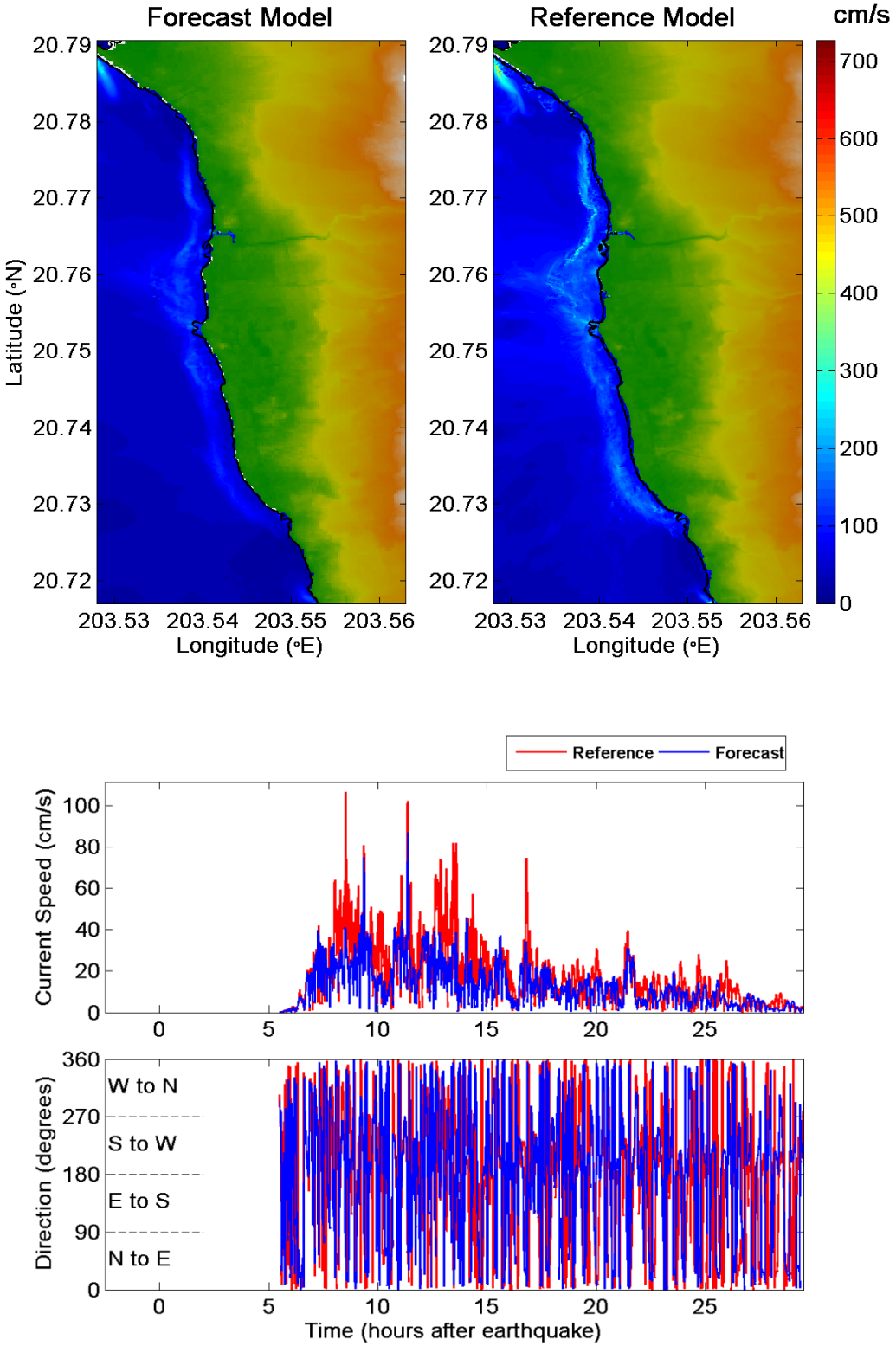

Figure 216. Comparative plot of maximum current distribution, current speed and directionality at the warning point at C-grid level for synthetic case NTSZ21-30 between forecast and reference models.

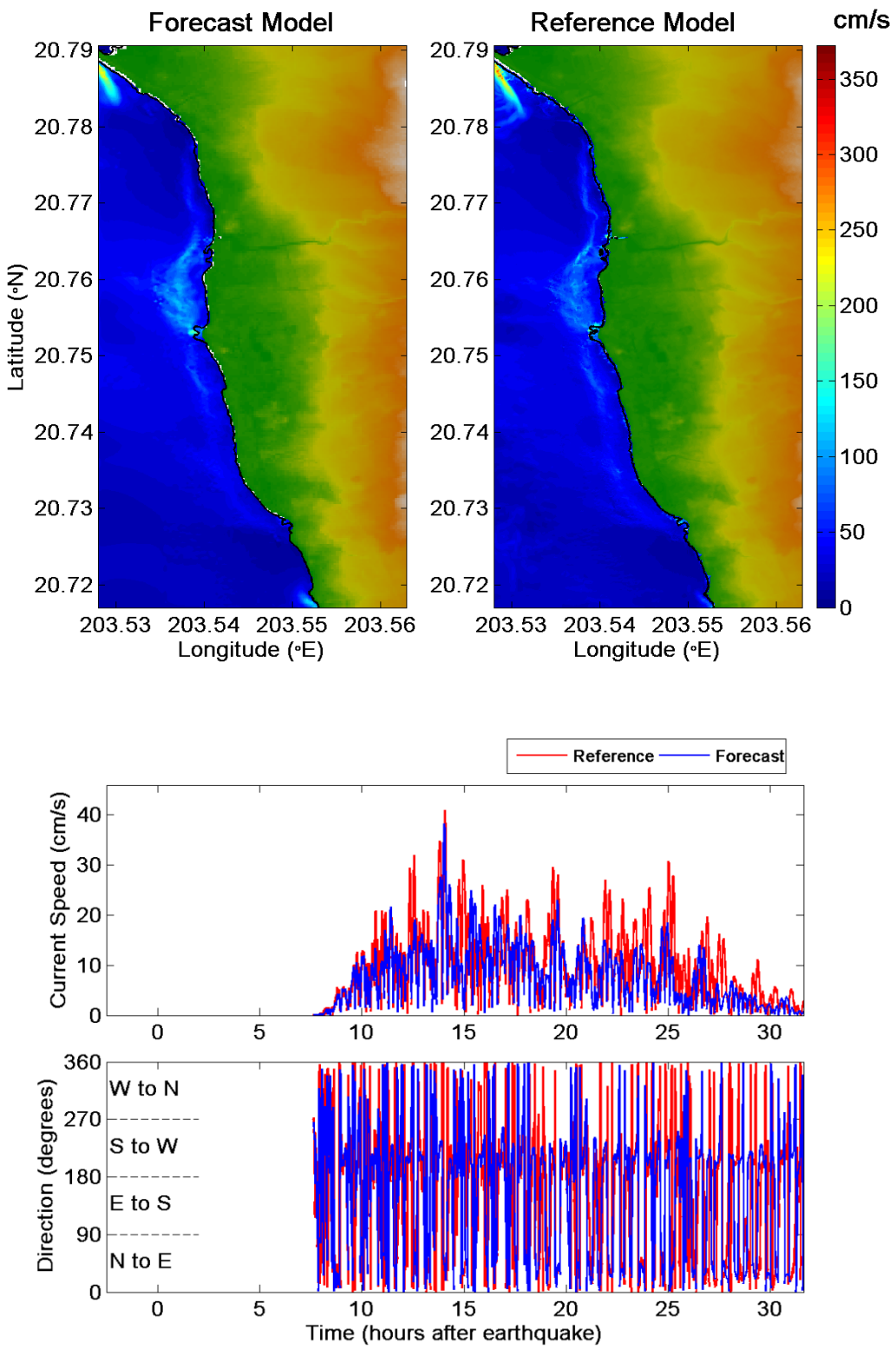

Figure 217. Comparative plot of maximum current distribution, current speed and directionality at the warning point at C-grid level for synthetic case NTSZ30-39 between forecast and reference models.

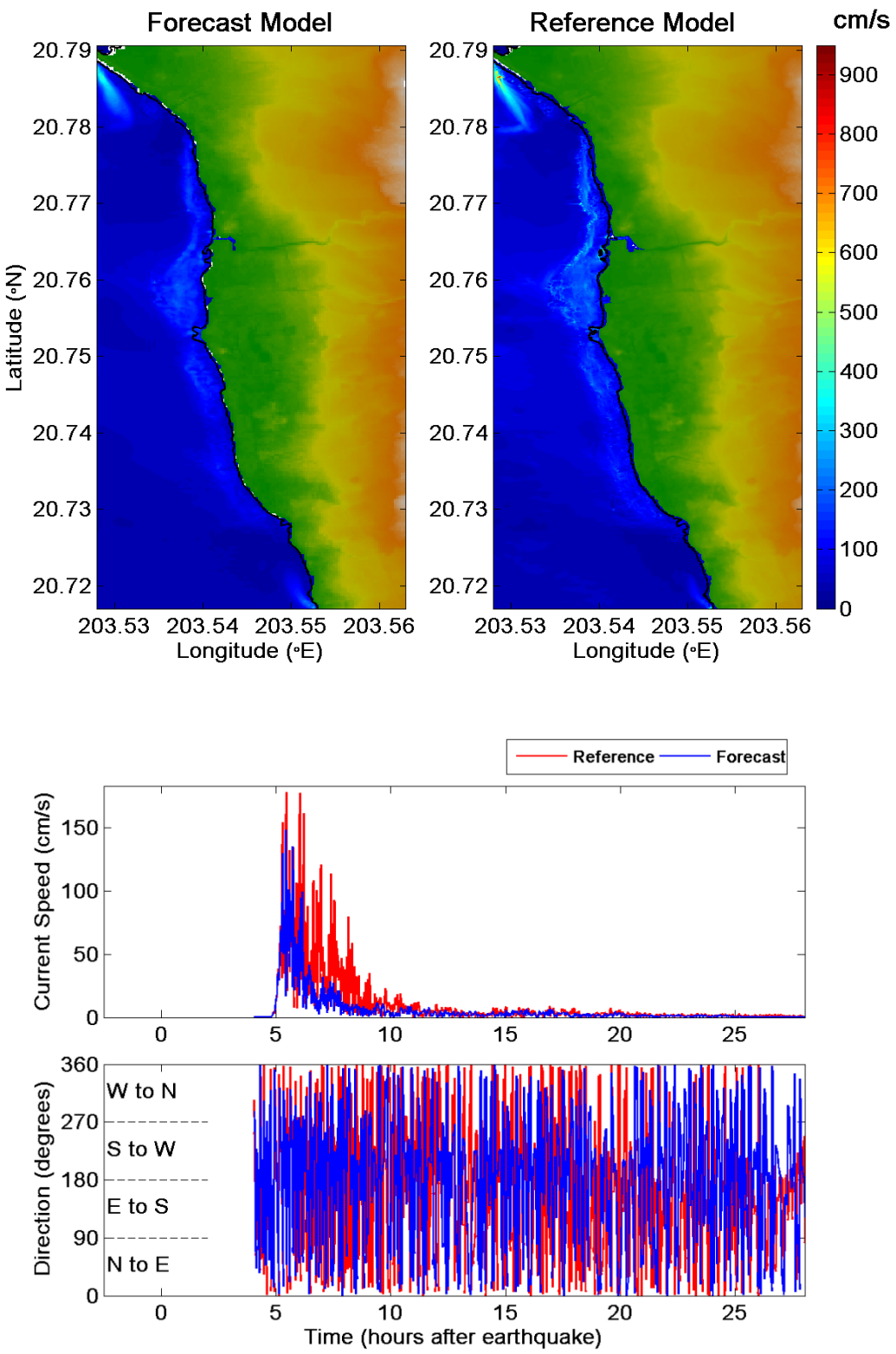

Figure 218. Comparative plot of maximum current distribution, current speed and directionality at the warning point at C-grid level for synthetic case NVSZ01-10 between forecast and reference models.

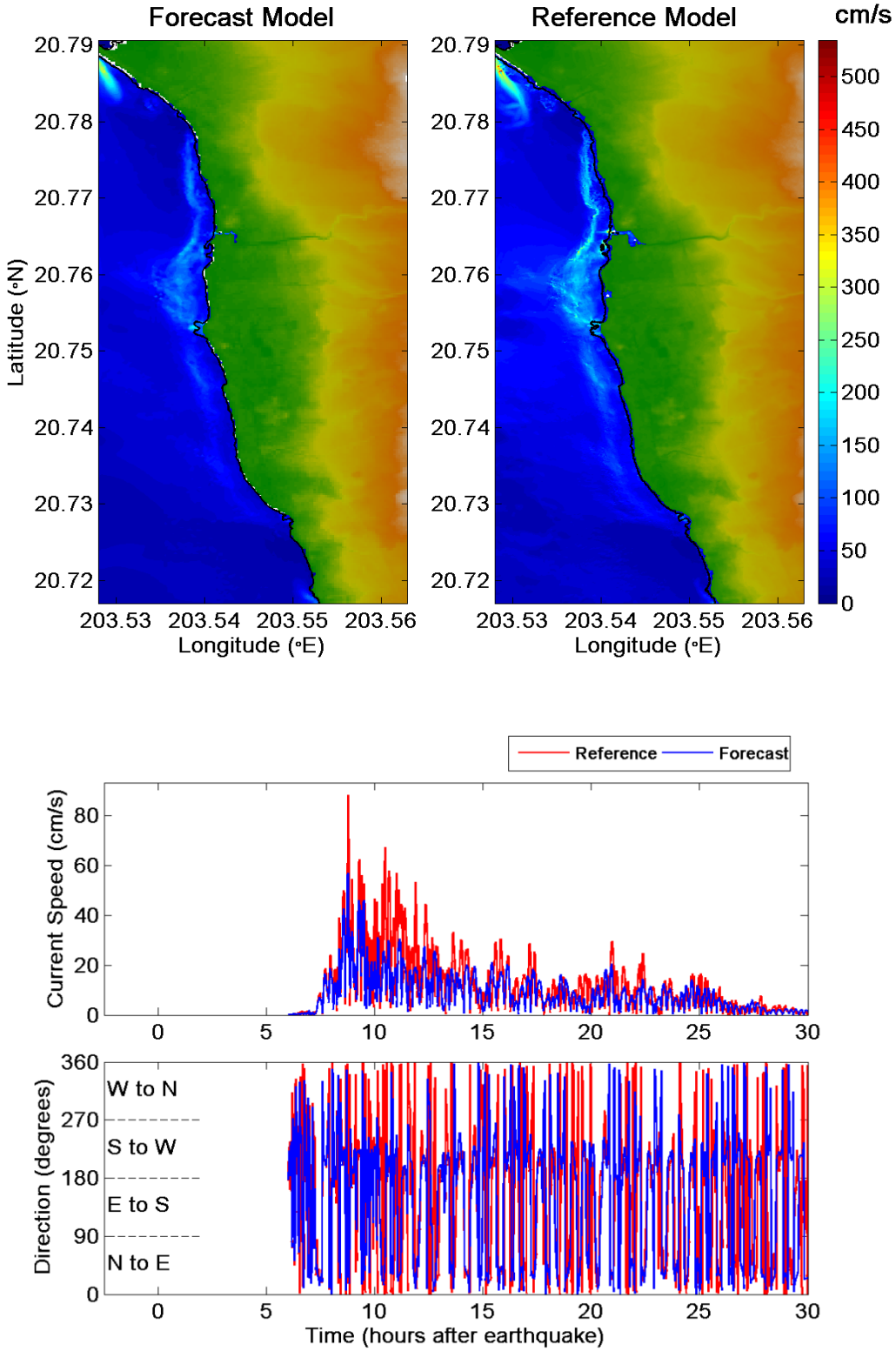

Figure 219. Comparative plot of maximum current distribution, current speed and directionality at the warning point at C-grid level for synthetic case NVSZ11-20 between forecast and reference models.

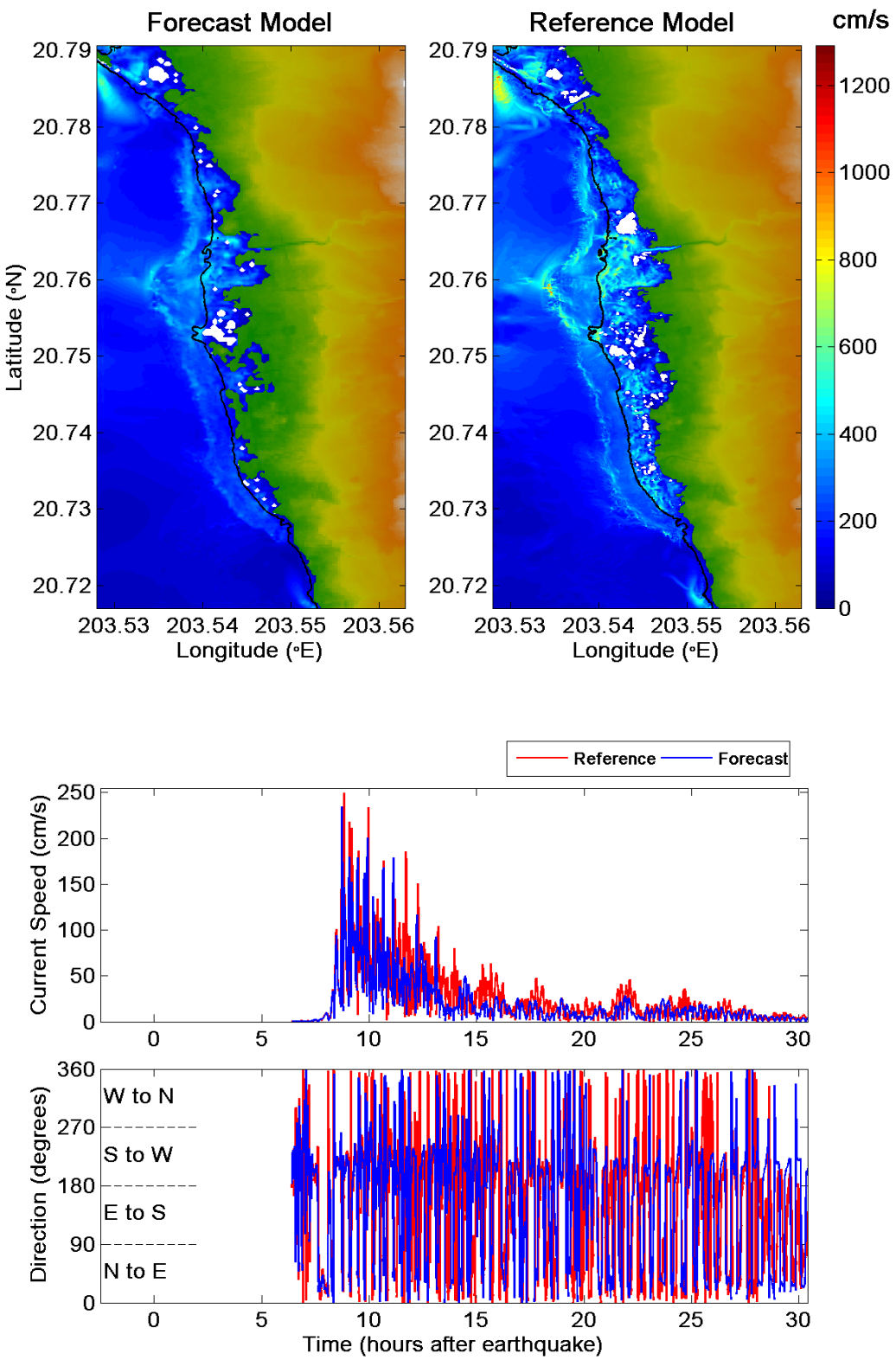

Figure 220. Comparative plot of maximum current distribution, current speed and directionality at the warning point at C-grid level for synthetic case NVSZ28-37 between forecast and reference models. White areas on land for the top figure indicate non-inundated sections.

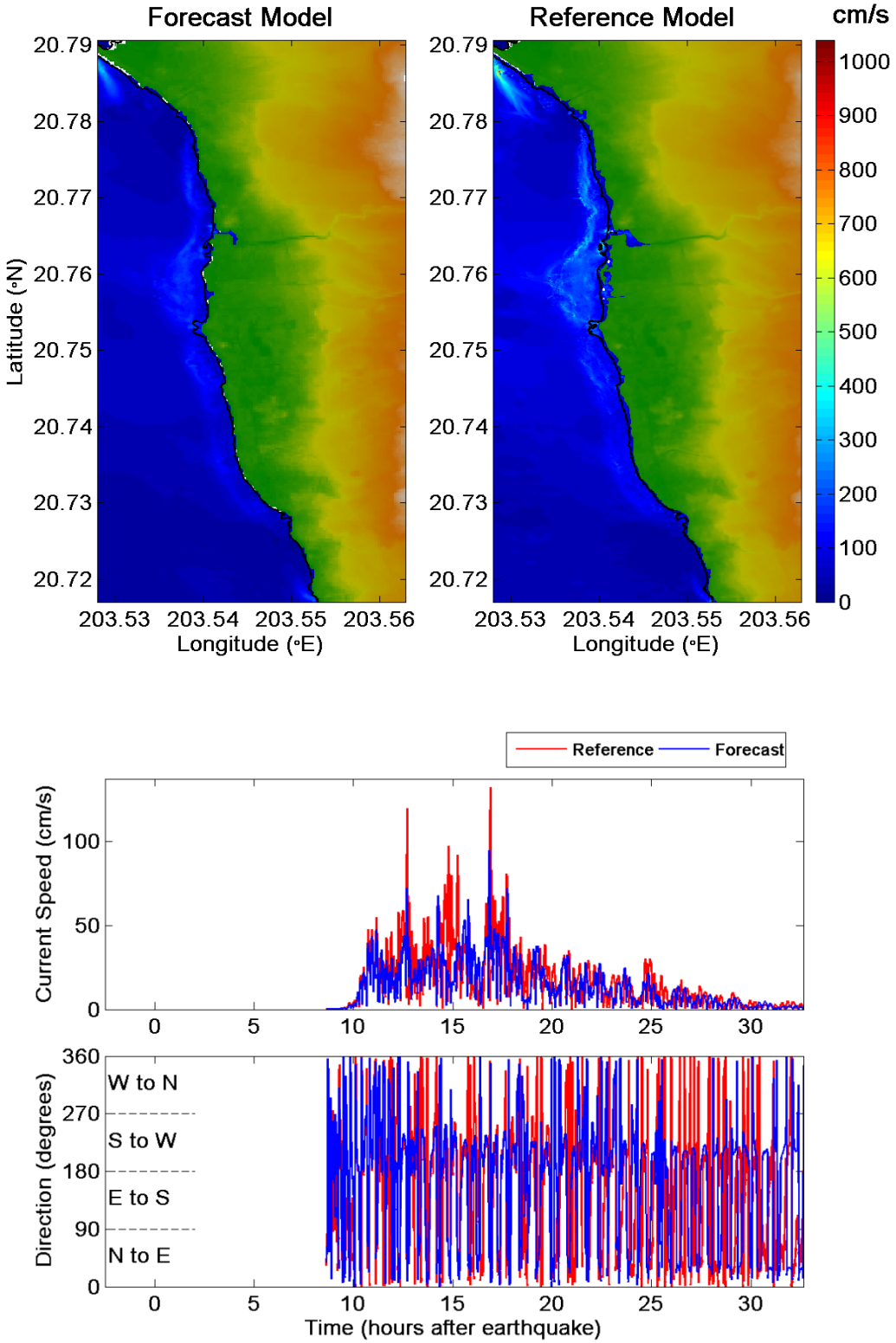

Figure 221. Comparative plot of maximum current distribution, current speed and directionality at the warning point at C-grid level for synthetic case RNSZ01-10 between forecast and reference models. White areas on land for the top figure indicate non-inundated sections.

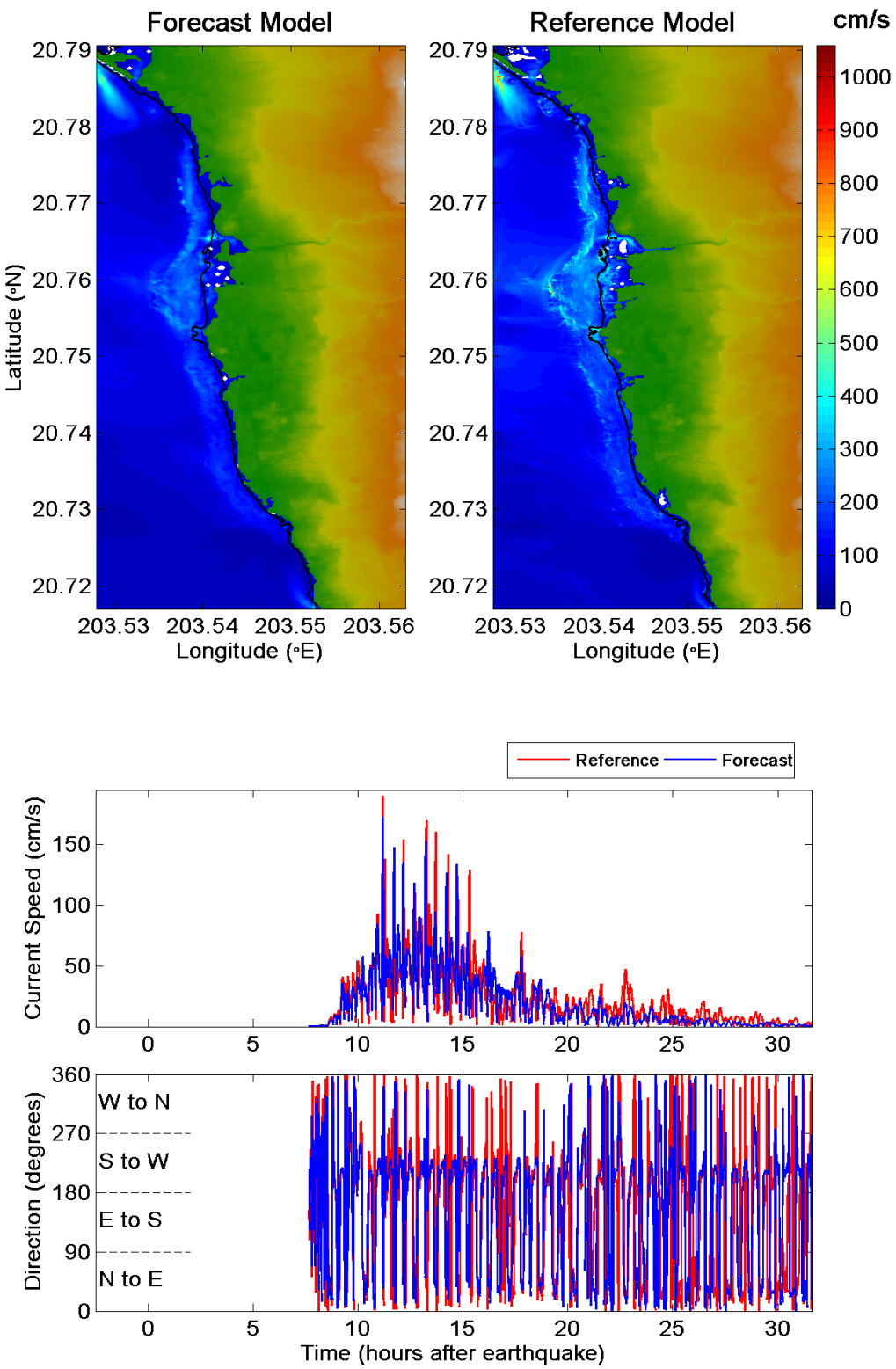

Figure 222. Comparative plot of maximum current distribution, current speed and directionality at the warning point at C-grid level for synthetic case RNSZ13-22 between forecast and reference models. White areas on land for the top figure indicate non-inundated sections.

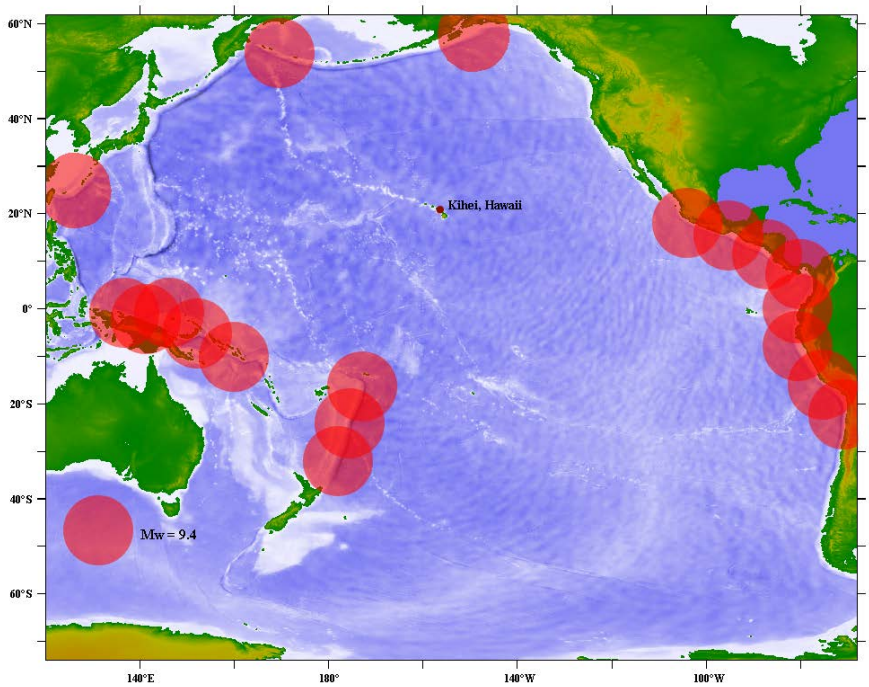

Figure 223. Location of Kihei, Maui, Hawai'i relative to simulated synthetic mega-events that generated low coastal impact.

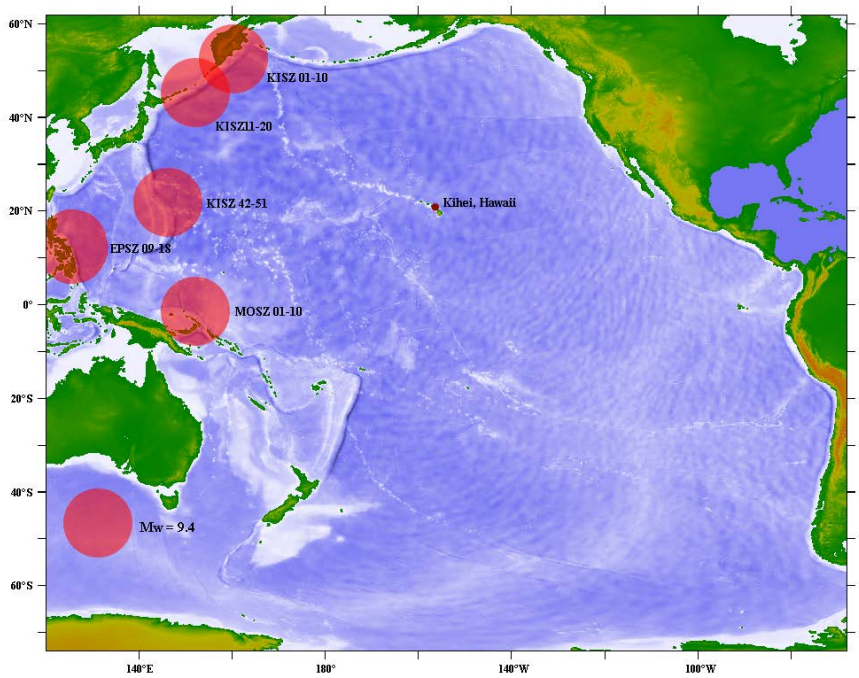

Figure 224. Location of Kihei, Maui, Hawai'i relative to simulated synthetic mega-events that generated extreme coastal impact.

Appendix A

Development of the Kihei, Hawai‘i tsunami forecast model occurred prior to parameter changes that were made to reflect modifications to the MOST model code. As a result, the input file for running both the optimized tsunami forecast model and the high-resolution reference inundation model in MOST have been updated accordingly. Appendix A1 and A2 provide the updated files for Kihei, Hawai‘i.

A1. Reference model *.in file for Kihei, Hawai‘i

0.0001	Minimum amplitude of input offshore wave (m)
1	Input minimum depth for offshore (m)
0.1	Input "dry land" depth for inundation (m)
0.0009	Input friction coefficient (n**2)
1	A & B-grid runup flag (0=disallow, 1=allow runup)
300.0	Blow-up limit (maximum eta before blow-up)
0.3	Input time step (sec)
288000	Input number of steps
12	Compute "A" arrays every n^{th} time step, n=
2	Compute "B" arrays every n^{th} time step, n=
60	Input number of steps between snapshots
1	...Starting from
1	...Saving grid every n^{th} node, n=1

A2. Forecast model *.in file for Kihei, Hawai‘i

0.0001	Minimum amplitude of input offshore wave (m)
1	Input minimum depth for offshore (m)
0.1	Input "dry land" depth for inundation (m)
0.0009	Input friction coefficient (n**2)
1	A & B-grid runup flag (0=disallow, 1=allow runup)
300	Blow-up limit (maximum eta before blow-up)
1	Input time step (sec)
288000	Input number of steps
10	Compute "A" arrays every n^{th} time step, n=
1	Compute "B" arrays every n^{th} time step, n=
30	Input number of steps between snapshots
1	...Starting from
1	...Saving grid every n^{th} node, n=1